

**OPTIMIZING THE COST AND ENERGY PERFORMANCE OF
A DISTRICT COOLING SYSTEM
WITH THE LOW DELTA-T SYNDROME**

by

Anthony Chi-wah LO



A thesis submitted in partial fulfilment of the requirements for the degree of

Doctor of Philosophy

Welsh School of Architecture
Cardiff University

July 2014

DECLARATION AND STATEMENTS



DECLARATION

This work has not been submitted in substance for any other degree or award at this or any other university or place of learning, nor is being submitted concurrently in candidature for any degree or other award.

Signed

Date  19 July 2014

STATEMENT 1

This thesis is being submitted in partial fulfilment of the requirements for the degree of PhD.

Signed

Date  19 July 2014

STATEMENT 2

This thesis is the result of my own independent work/investigation, except where otherwise stated. Other sources are acknowledged by explicit references. The views expressed are my own.

Signed

Date  19 July 2014

STATEMENT 3

I hereby give consent for my thesis, if accepted, to be available for photocopying and for inter-library loan, and for the title and summary to be made available to outside organizations.

Signed

Date  19 July 2014

STATEMENT 4: PREVIOUSLY APPROVED BAR ON ACCESS

I hereby give consent for my thesis, if accepted, to be available for photocopying and for inter-library loans after expiry of a bar on access previously approved by the Academic Standards & Quality Committee.

Signed

Date

❧ ABSTRACT ❧

Almost every chilled water system is affected by the low delta-T syndrome in which the supply and return chilled water temperatures falls short of the design level, particularly at low loads. This results in inefficient chillers and higher energy consumption of the chiller plant. This research is aimed at designing a district cooling system (DCS) that can accommodate the low delta-T problem and minimize its impact on the DCS' energy performance. Methodologies were developed to minimize DCS energy consumption and running cost, particularly those related to the chiller plant and pumping station. A hypothetical urban district and a baseline DCS were set up for simulation of alternative designs to be evaluated and compared. Energy efficiency enhancement measures related to chiller system configuration, pumping station configuration and chilled water temperature were also evaluated.

Moreover, mathematical models that simulate the performance of major DCS components were developed. These models were integrated to become a DCS model for identifying an optimum design. A life cycle cost (LCC) model was also adopted for identifying a cost optimal design solution that would result in the lowest LCC and an optimum energy performance when the DCS was operated under low delta-T conditions.

The variants of DCS design evaluated include five combinations of chiller system configuration, eight chilled water temperature regimes, and 36,192 arrangements of pumping stations. A simple heuristic strategy was adopted to greatly reduce the number of design solutions to be studied. The energy, financial and environmental performances of these possible solutions were then evaluated.

The results show that the optimum design in respect of energy performance, denoted as "Solution E", could save 15.3% of the annual total electricity consumption of DCS₀. After evaluating the LCC of each possible solution, it was found that instead of Solution E, "Solution C" was the most cost-effective. This cost-optimal design was about 7.5% lower in LCC than the baseline case. The LCC saving would amount to HK\$332 million in present value. There were 15 equally-sized variable speed chillers in Solution C. Six pumping stations were located along both the main chilled water supply and return

pipes, with five pumps in each station, and the chilled water supply and return temperatures were 5°C and 13°C respectively. This design could lead to a 14.6% reduction in the electricity consumption of DCS_O. Although this percentage was about 1% lower than that achieved by Solution E, the LCC of Solution C was more financially favourable due to lower initial capital cost, and life-cycle replacement and maintenance cost.

The methods devised in the presented research can help to provide a direction in the search for an integrated DCS design solution that could mitigate the impacts of degrading delta-T on the energy performance of the DCS. The results obtained from this study will enable a DCS owner to evaluate the energy benefits and the associated financial trade-offs. Moreover, the energy-optimal solution identified could lead to fewer impacts on the environment. Had we been able to account for the costs of the environmental impacts as well, the energy-optimal solution could well be the cost-optimal solution as well. This factor should be considered in a selection of the design to adopt in order to help our society achieve a more sustainable future.

❧ ACKNOWLEDGEMENTS ❧

The doctoral journey is often described as an “independent research”, yet I would have never been able to reach the finishing line without the help and support of the most wonderful network of friends and family, to whom I am indebted with deepest gratitude. It is a great honour for me to have this opportunity to extend my appreciation and to acknowledge the contribution of the people who have helped me during this doctoral research.

First and foremost, I would like to express my deepest gratitude to my supervisors Prof. Phil Jones and Dr. Francis Yik. I am grateful to Prof. Phil Jones, who has been very illuminating and supportive to my research. Special thanks also go to Dr. Francis Yik, who has provided excellent guidance and encouragement throughout the entire duration of my research. Without their continuous advice, constructive comments, and kind willingness to share their knowledge with me, I would not have reached where I am today with this work in its present form. I would also like to express my sincere thanks to Ir Colin Chung, who has offered me his expert opinions on the design of district cooling systems. Ir Chung has permanently been of great help, incessant support with the sound knowledge in the field of district cooling.

Furthermore, special appreciation and sincere thanks go to Prof Christopher Underwood and Mr. Simon Lannon, who were willing to participate in my viva voce and give me the valuable suggestions and comments.

My thanks also go to the research office staff, particularly Ms. Katrina Lewis, of the Welsh School of Architecture of Cardiff University, for her administrative support.

I would also like to express my thanks to my friends, Dr. Lee Sze Hung, Mr. Gary Chiang and Mr. Lui Siu Kit for their unflinching support and expert advice.

Last but not least, I am deeply indebted to my parents and parents-in-law for their patience, continuous support and encouragement. Finally, my deepest gratitude goes to my beloved wife for her inspiration, encouragement, endless sacrifices and unconditional support of taking care of my two lovely daughters during the whole period of my study. Without their love and understanding, I would not have been able to reach to where I am now.

∞ TABLE OF CONTENTS ∞

Preface	Declaration and Statements	i
	Abstract	ii
	Acknowledgements	iv
	Table of Contents	v
	List of Figures	xi
	List of Tables	xv
	Nomenclature	xix
	Subscripts	xxi
Chapter 1	INTRODUCTION	1
	1.1 Energy Use in Buildings in Hong Kong and Impacts on Sustainable Development	1
	1.2 Water-Cooled Air-Conditioning Systems and District Cooling Systems	3
	1.3 Chilled Water Systems in DCS	6
	1.4 Impact of Low Delta-T on the Energy Performance of Chilled Water Systems	8
	1.4.1 Bypass Check Valves for P-S Systems	13
	1.4.2 The Controversy between VPF and P-S Systems	14
	1.5 Need for Further Investigation	15
	1.5.1 Chiller System Configuration	16
	1.5.2 Pumping Stations in the Chilled Water Distribution Loop	17
	1.5.3 Chilled Water Temperature in the Distribution Loop	18
	1.5.4 Energy Saving Potentials of P-S and VPF Pumping Systems	22
	1.6 Financial Analysis	23
	1.7 Research Aim and Objectives	23
1.8 Research Methodology	25	
1.9 Scope and Organization of this Thesis	30	
Chapter 2	DEVELOPMENT OF A HYPOTHETICAL DISTRICT AND ENERGY EFFICIENCY ENHANCEMENT MEASURES	33
	2.1 Overview	33

2.2	Development of a Hypothetical District	33
2.2.1	Scale of the Hypothetical District	33
2.2.2	Types of Building	35
2.2.3	Air-Conditioning System Design	37
2.2.4	Cooling Load Simulation	39
2.2.5	Cooling Load of the Hypothetical District	40
2.3	Design of a Baseline DCS	41
2.3.1	Production Loop	42
2.3.2	Distribution Loop	47
2.3.3	Building Loop	49
2.4	Design of Energy Enhancement Measure - Chiller System Configuration	49
2.4.1	Varying the Number of Chiller	50
2.4.2	Unequally-Sized Chillers	50
2.4.3	Variable Speed Chillers	51
2.4.4	Chiller System Configuration	52
2.5	Design of Energy Enhancement Measure - Pumping Station Configuration	54
2.5.1	Multiple pumping stations	55
2.5.2	Multiple pumps in each pumping station	57
2.6	Design of Energy Enhancement Measure - Chilled Water Supply and Return Temperatures	60
2.7	Summary	64
Chapter 3	DEVELOPMENT OF MATHEMATICAL MODELS FOR DCS₀	65
3.1	Overview	65
3.2	Cooling Coil Model	67
3.2.1	Development of Cooling Coil Models	67
3.2.2	Modelling of Cooling Coils Operating under Normal Delta-T Conditions	69
3.2.3	Modelling of Cooling Coils Operating under Low Delta-T Conditions	71
3.3	Heat Exchanger Model	73
3.3.1	Chilled Water Flow at the Secondary Side of the Heat Exchanger	73

3.3.2	Chilled Water Flow at the Primary Side of the Heat Exchanger	74
3.3.3	Flow Rate and Temperature of Chilled Water Returning to the Chiller Plant	76
3.4	Chilled Water Distribution Network Model	77
3.4.1	Characteristics of System Pressure Drop and Flow Rate	77
3.4.2	Differential Pressure Control Setting	80
3.5	Variable Speed Pump Model	82
3.5.1	Normalization of Pump Characteristics	82
3.5.2	Power Demand of Variable Speed Pumps at Part Load	85
3.5.3	Control Strategy	87
3.6	Pumping Station Model	87
3.7	Chiller Model	87
3.7.1	Constant Speed Chillers	87
3.7.2	Variable Speed Chillers	93
3.8	Primary Chilled Water and Seawater Pump Model	93
3.8.1	Flow rate	94
3.8.2	Pump Head	94
3.9	Chiller Plant Model	95
3.9.1	Chiller Plant Control Strategy	97
3.9.2	Part Load Ratio of Chillers	98
3.10	Summary	99
Chapter 4	IMPACTS OF DEGRADING DELTA-T ON THE ENERGY PERFORMANCE OF DCS₀	101
4.1	Overview	101
4.2	A Comparison of the Energy Performance of P-S and VPF Systems	102
4.2.1	Design Considerations	102
4.2.2	Results Discussion	104
4.3	Energy Performance of DCS ₀ under Normal or Low Delta-T Conditions	109
4.3.1	Delta-T of Chilled Water	109
4.3.2	Chilled Water Flow Rate	110
4.3.3	Operating Frequency of Chillers	112

	4.4 Comparison of Electricity Consumption of DCS ₀ under Normal and Low Delta-T Conditions	114
	4.4.1 Electricity Consumption of Secondary Chilled Water Pumps	115
	4.4.2 Electricity Consumption of Chillers	116
	4.4.3 Electricity Consumption of Primary Chilled Water and Seawater Pumps	117
	4.5 Summary	117
Chapter 5	EFFECTS OF CHILLER SYSTEM CONFIGURATION ON THE ENERGY PERFORMANCE OF DCS₀	119
	5.1 Overview	119
	5.2 Comparison of Annual Total Electricity Consumption of DCS ₀ in Different Chiller System Configuration Designs	120
	5.3 Effect of Increasing the Number of Chillers – Case O-B and Case A-D	122
	5.3.1 Electricity Consumption of Chillers	124
	5.3.2 Electricity Consumption of Primary Chilled Water Pumps and Seawater Pumps	126
	5.4 Effects of Uniformity in Chiller Size – Case B-C and Case D-E	127
	5.4.1 Electricity Consumption of Chillers	129
	5.4.2 Electricity Consumption of Primary Chilled Water Pumps and Seawater Pumps	131
	5.5 Effects of Variable Speed Chillers	133
	5.6 Summary	139
Chapter 6	EFFECTS OF PUMPING STATION CONFIGURATION ON THE ENERGY PERFORMANCE OF DCS₀	141
	6.1 Overview	141
	6.2 Multiple Pumping Station Design	142
	6.2.1 Hydraulic Gradient Characteristics of Chilled Water Distribution Network	143
	6.2.2 Identified Combinations of Pumping Station	143
	6.3 Impacts of Changing the Number of Pumps in Each Pumping Station	154
	6.4 Simulation of Electricity Consumption of Pumping Stations	155
	6.5 Results of Simulation	159

	6.5.1 Electricity consumption of the pumping station arrangements with an equal number of pumps in each station	159
	6.5.2 Electricity consumption of the pumping station arrangements with an unequal number of pumps in each station	162
	6.6 Summary	163
Chapter 7	EFFECTS OF CHILLED WATER TEMPERATURE ON THE ENERGY PERFORMANCE OF DCS_O	165
	7.1 Overview	165
	7.2 Effects of Changing the Chilled Water Temperature on the COP of Chillers	166
	7.3 Effects of Changing the Chilled Water Temperature on the Chilled Water Flow Rate	167
	7.3.1 Situation 1 – The design chilled water supply temperature is changed from 4°C to 6°C while the design chilled water return temperature is maintained constant at 11°C, 12°C or 13°C	168
	7.3.2 Situation 2 – The design chilled water return temperature is changed from 11°C to 13°C while the design chilled water return temperature is maintained constant at 4°C, 5°C or 6°C	172
	7.3.3 Situation 3 – The design chilled water supply and return temperatures are changed from 4°C to 6°C and from 11°C to 13°C respectively	174
	7.4 Simulation Results and Analysis	176
	7.4.1 Impacts of the Design Chilled Water Temperature on the Electricity Consumption of the Chiller Plant	178
	7.4.2 Impacts of the Design Chilled Water Temperature on the Electricity Consumption of Secondary Chilled Water Distribution Pumps	183
	7.4.3 Overall Electricity Consumption of DCS _O	184
	7.5 Summary	185
Chapter 8	A TECHNO-ECONOMIC ANALYSIS OF THE INTEGRATED DESIGN SOLUTIONS	187
	8.1 Overview	187
	8.2 Simple Heuristic Strategy for Determining Possible Design Solutions	188
	8.2.1 Selection of Combinations of Chiller System Configuration	188
	8.2.2 Selection of Pumping Station Arrangement	189

	8.2.3 Selection of Chilled Water Temperature Regime	190
	8.3 Simulation of Energy, Financial and Environmental Performances	191
	8.3.1 Simulation of Electricity Consumption and CO ₂ Emissions	192
	8.3.2 The LCC Model	193
	8.4 An LCC Analysis of All Possible Solutions	202
	8.4.1 Comparison of the LCC of all possible design solutions with DCS _O	202
	8.4.2 A Cost-Optimal Design Solution	203
	8.4.3 A Comparative Analysis of the LCC of DCS _O and Solution C	207
	8.5 A Comparative Analysis of Electricity Consumption in DCS _O and Solution C	209
	8.5.1 Electricity Consumption of Chillers	210
	8.5.2 Electricity Consumption of Primary Chilled Water Pumps	211
	8.5.3 Electricity Consumption of Seawater Pumps	212
	8.5.4 Electricity Consumption of Secondary Chilled Water Pumps	212
	8.6 Environmental Benefits of Solution C	214
	8.7 Summary	214
Chapter 9	CONCLUSION AND SUGGESTIONS FOR FUTURE RESEARCH	217
	9.1 Summary of Work Done and Key Findings	217
	9.1.1 Development of a Hypothetical District	218
	9.1.2 Design of a DCS	219
	9.1.3 Development of Mathematical Models for Energy and Cost Simulation	220
	9.1.4 Impact of Low Delta-T on the Energy Performance of DCS _O	220
	9.1.5 Effects of Chiller System Configuration on the Energy Performance of DCS _O	221
	9.1.6 Effects of Pumping Station Configuration on the Energy Performance of DCS _O	222
	9.1.7 Effects of Chilled Water Supply and Return Temperature on the Energy Performance of DCS _O	224
	9.1.8 A Cost-Optimal Integrated Design Solution	225
	9.2 Original Contributions of this Study	227
	9.3 Limitations and Recommendations for Further Research	230
	BIBLIOGRAPHY	232

∞ LIST OF FIGURES ∞

1.1	Total electricity consumption in Hong Kong (2001-2010)	2
1.2	Total electricity consumption in the domestic, transport, commercial and industrial sectors in Hong Kong (2001-2010)	2
1.3	A district cooling system	4
1.4	A three-level chilled water piping system: production, distribution and building loops	7
1.5	Low delta-T characteristic curves of six commercial buildings	10
1.6	A variable primary flow system	15
1.7	Energy consumption of different DCS components	16
1.8	An example of a distribution loop designed with three pumping stations and different number of pumps in each station	18
1.9	Framework of research approach and methodology	26
1.10	Three different energy efficiency enhancement measures for DCS ₀	28
1.11	Organization of the thesis	30
2.1	Typical layout and sections of the four building models	36
2.2	Hourly cooling load profile of the four building models in the design month (July)	39
2.3	Schematic diagram of DCS ₀ designed for the hypothetical district	41
2.4	Schematic of the direct seawater cooling system of the DCS	43
2.5	(a) COP of a typical water-cooled centrifugal chiller of different condenser inlet water temperatures	44
	(b) COP of a typical water-cooled centrifugal chiller with different design cooling capacities	44
2.6	Part load performance of a 2,000 RT constant speed chiller	45
2.7	Potential locations for pumping stations	55
2.8	(a) An example of a combination of three pumping stations with the same number of pumps in each station	57
	(b) An example of a combination of three pumping stations with different number of pumps in each station	58
3.1	An outline of the mathematical models and their outputs for this study	66

3.2	Cooling coil models developed by Yik (1999) and Wang et al. (2012a)	68
3.3	Characteristics of cooling coils of model building A	69
3.4	Characteristics of cooling coils of model building B	70
3.5	Characteristics of cooling coils of model building C	70
3.6	Characteristics of cooling coils of model building D	71
3.7	Normalized cooling load and chilled water flow rate of buildings X and Y	72
3.8	Connection between the chilled water circuit in the building and the distribution loop of the DCS	73
3.9	Hydraulic model of chilled water distribution network	78
3.10	Pressure-distance diagram (with the same variation in the chilled water demands across the branch)	81
3.11	Pressure-distance diagram (no flow from building j to building N)	81
3.12	Characteristic curves of variable speed pump model	84
3.13	Relationship between the total pressure head and chilled water flow rate of the variable speed pump	85
3.14	Two-tail test : Reject null hypothesis	91
3.15	Algorithm for determining the minimum annual electricity consumption of the chiller plant	96
4.1	Operating frequency profile of the pumps in P-S and VPF systems at different flow ratios	105
4.2	Annual energy consumption profile of the P-S and VPF systems at different flow ratios	106
4.3	Variation of the temperature difference between supply and return chilled water under normal or low delta-T conditions	110
4.4	Modelled variation of chilled water delta-T	111
4.5	Chilled water flow rate of different cooling load percentages	111
4.6	Number of operating chillers at different percentages of design cooling load	113
4.7	Frequency of operating additional chillers at low delta-T	114
5.1	Average COP of constant speed chillers in C_O and C_B at different PLR	124
5.2	COP of constant and variable speed chillers with a cooling capacity of 4,000 RT	125
5.3	Average COP of variable speed chillers in C_A and C_D at different PLR	126

5.4	Average COP of constant speed chillers in C_B and C_C at different PLR	130
5.5	Average COP of variable speed chillers in C_D and C_E at different PLR	131
5.6	Part load performance of constant and variable speed chillers with different condenser water entering temperatures	137
5.7	Average COP of the constant and variable speed chillers in C_O and C_A	138
6.1	Examples of a pressure gradient diagram showing: (a) location of one main pumping station and two booster pumping stations; and (b) their pressure gradient in the distribution loop	144
6.2	Situation 1: all six pumping stations are located at the supply side and the minimum differential pressure across the heat exchangers in each branch can be maintained	149
6.3	Situation 2: Equal number of pumping stations at both supply and return sides – (a) and (c) failure cases, (b) successful case in meeting the minimum differential pressure requirement	151
6.4	Situation 3: More pumping stations at the supply side – (a) and (c) failure cases, (b) successful case in meeting the minimum differential pressure requirement	152
6.5	Situation 4: Fewer pumping stations at the supply side – (a) and (c) failure cases, (b) successful case in meeting the minimum differential pressure requirement	153
6.6	Rated power demand of variable speed pumps at different flow rates and pressure heads	156
6.7	Algorithm for calculating the annual electricity consumption of different pumping station combinations	160
6.8	Annual electricity consumption of the pumping station arrangements with 5, 10 or 15 pumps in each station	161
7.1	Part load performance of constant and variable speed chillers of different design chilled water supply temperatures	166
7.2	(a) Connection between the chilled water circuit and the distribution loop of DCS_O via a heat exchanger	169
	(b) Temperature profile of chilled water in a heat exchanger when the design chilled water supply temperature increases from $T_{DCS,i,s}$ to $T_{DCS,i,s}'$	169
7.3	Design chilled water supply and return temperatures in T_1 and T_4	171
7.4	Temperature profile of the chilled water in a heat exchanger where the design chilled water return temperature increases from $T_{DCS,i,r}$ to $T_{DCS,i,r}'$	172
7.5	Design chilled water supply and return temperatures in T_1 and T_2	174

7.6	Temperature profile of chilled water in a heat exchanger where the design chilled water supply and return temperatures, i.e. $T_{DCS,i,s}$ and $T_{DCS,i,r}$, are increased to $T_{DCS,i,s'}$ and $T_{DCS,i,r'}$ but the temperature difference remains the same	175
8.1	Elimination process of achieving an optimum design solution	189
8.2	Algorithm of identifying an energy-optimal design solution with the lowest electricity consumption	193
8.3	Monthly average inflation rate, 2000-2013	196
8.4	Unit cost of the variable speed pump set per pump power	199
8.5	Average COP of constant and variable speed chillers in C_O and C_D at different PLR	210

❧ LIST OF TABLES ❧

1.1	Chiller system configurations of the DCS in the KTD	6
1.2	Design chilled water supply and return temperatures of the DCS in different countries	19
1.3	Range of design supply and return chilled water temperatures of the DCS in Asia, Europe and the United States	21
2.1	Key characteristics of the four building models	35
2.2	Number of storeys occupied by the five functional areas in the four building models	36
2.3	Design criteria for the air-conditioning system in the five functional areas	38
2.4	Cooling load of a hypothetical district housing different combinations of building models	40
2.5	Cooling load distribution of the hypothetical district	41
2.6	Distribution frequency of seawater temperature in a year	46
2.7	Design parameters of C_O and PS_{1-0} in DCS_O	48
2.8	Design parameters of chiller system configurations C_O , C_A , C_B , C_C , C_D and C_E	52
2.9	Design details of chiller system configurations C_O , C_A , C_B , C_C , C_D and C_E	53
2.10	Total number of combinations of pumping stations (PS)	56
2.11	An example showing the different arrangements based on the number of pumps, i.e. with 5, 10 or 15 pumps in each pumping station	58
2.12	Chilled water temperature regimes	62
2.13	Design details of the chiller system configuration and pumping stations under different temperature regimes	63
4.1	Design conditions of the chilled water pumps in P-S and VPF systems	104
4.2	Comparison of the annual electricity consumption of chilled water pumps in the P-S and VPF systems	104
4.3	Annual average chilled water flow rate with different delta-T	112
4.4	Annual electricity consumption of DCS_O under normal and low delta-T conditions	115

4.5	Average PLR and COP when one or two additional chillers are operated under normal or low delta-T conditions	116
5.1	Comparison of the annual total electricity consumption of DCS _O using various chiller system configurations at low delta-T	121
5.2	Selection of cases for comparing the energy impact of each design parameter	122
5.3	Configuration of chiller systems in cases O-B and A-D	123
5.4	Case O-B: Percentage of electricity saving after addition of chillers in C _B	123
5.5	Case A-D: Percentage of electricity saving after addition of chillers in C _D	123
5.6	Operating chiller hours of chillers and electricity saving of the primary chilled water and seawater pumps in case O-B	127
5.7	Operating chiller hours and electricity saving of the primary chilled water and seawater pumps in case A-D	127
5.8	Configuration of chiller systems in cases B-C and D-E	128
5.9	Case B-C: Percentage of annual electricity saving after using unequally-sized chillers in C _C	129
5.10	Case D-E: Percentage of annual electricity saving after using unequally-sized chillers in C _E	129
5.11	Distribution of average PLR of the chillers operating around the 8760 hours of a year in cases B-C and D-E	130
5.12	Chiller hours and electricity saving of the primary chilled water and seawater pumps in case B-C	133
5.13	Chiller hours and electricity saving of the primary chilled water and seawater pumps in case D-E	133
5.14	Configuration of chiller systems in cases O-A, B-D, and C-E	134
5.15	Electricity saving resulting from using variable speed chillers in case O-A	135
5.16	Electricity saving resulting from using variable speed chillers in case B-D	135
5.17	Electricity saving resulting from using variable speed chillers in case C-E	135
5.18	Difference in COP between constant and variable speed chillers with different condenser water entering temperatures	138
5.19	Operating hours of chillers in case C-E	139
6.1	Number of pumping station combinations that are technically feasible in meeting the minimum pressure differential requirement	145
6.2	Combination of pumping station (PS) location that is technically feasible	146

6.3	Total number of arrangements for the 140 combinations that are technically feasible in meeting the minimum pressure differential requirement	154
6.4	Comparison of pump power and annual electricity consumption between PS ₁₋₀ and PS ₆₋₃₅₄₆₄	162
6.5	Difference in annual electricity consumption of DCS ₀ adopting the design of PS ₁₋₀ or PS ₆₋₃₅₄₆₄	163
7.1	Annual average chilled water flow rate in different temperature regimes	167
7.2	Change in the annual average chilled water flow rate due to an increase in the design chilled water supply temperature:	
	(a) Return temperature is maintained at 11°C	170
	(b) Return temperature is maintained at 12°C	170
	(c) Return temperature is maintained at 13°C	170
7.3	Comparison of the hourly chilled water flow rate of T ₁ and T ₄ in the distribution loop at design or part load	171
7.4	Change in the annual average chilled water flow rate due to an increase in the design chilled water return temperature:	
	(a) Supply temperature is maintained at 4°C	173
	(b) Supply temperature is maintained at 5°C	173
	(c) Supply temperature is maintained at 6°C	173
7.5	Comparison of the hourly chilled water flow rate in T ₁ and T ₂ in the distribution loop at design or part load	175
7.6	Change in the annual average chilled water flow rate due to an increase in the chilled water supply and return temperature:	
	(a) Temperature difference remains at 6°C	176
	(b) Temperature difference remains at 7°C	176
	(c) Temperature difference remains at 8°C	176
7.7	Comparison of annual electricity consumption of DCS ₀ in nine different temperature regimes at low delta-T	177
7.8	Percentage of electricity saving of chillers in different temperature regimes	179
7.9	Percentage of electricity saving of the primary chilled water pumps in different temperature regimes	180
7.10	Percentage of electricity saving of seawater pumps in different temperature regimes	182
7.11	Percentage of electricity saving of the chiller plant in different temperature regimes	183
7.12	Percentage of electricity saving of the secondary chilled water distribution pumps in different temperature regimes	184
8.1	Percentage of annual electricity saving with different chiller system configurations	189

8.2	Percentage of annual total electricity saving with different pumping station arrangements	190
8.3	Percentage of annual electricity saving in different temperature regimes	190
8.4	Life span and number of replacement of equipment	194
8.5	Different costs of the constant speed and variable speed chillers	197
8.6	Capital costs of variable speed chilled water pumps with different operational characteristics	198
8.7	Percentage of average LCC saving of the solutions designed with different chiller system configurations, C_A , C_D and C_E with reference to DCS_O	203
8.8	Percentage of average LCC saving of the solution designed with different number of pumping stations with reference to DCS_O	203
8.9	Percentage of average LCC saving of the solution designed with temperature regimes T_4 , T_5 , T_6 and T_7 with reference to DCS_O	203
8.10	Ranking of the 434,268 design solutions based on the LCC saving achieved in comparison with DCS_O	204
8.11	Comparison of system details of DCS_O and Solution C	205
8.12	Comparison of the annual electricity consumption of Solutions C and E	206
8.13	Comparison of the LCC of Solutions C and E	207
8.14	Comparison of the LCC of DCS_O and Solution C	208
8.15	Comparison of the annual electricity consumption of DCS_O and Solution C	209
8.16	Comparison of the operating pump hour, power demand and electricity consumption of the primary chilled water pumps in DCS_O and Solution C	211
8.17	Comparison of power demand and electricity consumption of the seawater pumps in DCS_O and Solution C	212
8.18	Comparison of power demand and electricity consumption of the secondary chilled water pumps in DCS_O and Solution C	213
8.19	Annual and life-cycle greenhouse gas emissions from DCS_O and Solution C	214

∞ NOMENCLATURE ∞

<i>AHU</i>	Air-handling unit
<i>AU</i>	Overall heat transfer coefficient of heat exchanger, kW/°C
<i>C</i>	Chiller system configuration
<i>c</i>	Specific heat capacity, kJ/kg°C
<i>CC</i>	Cooling capacity of chiller, kW
<i>COP</i>	Coefficient of performance of chiller
<i>CSP</i>	Constant speed pump
<i>D</i>	Internal diameter of pipe, m
<i>d</i>	Real discount rate, %
<i>DCS</i>	District cooling system
<i>Dd</i>	Depth of DCS plant room, m
ΔP	Pressure drop, Pa
ΔT	Difference between chilled water supply and return temperature, °C
<i>e</i>	Real escalation rate of electricity price, %
<i>FCU</i>	Fan coil unit
<i>f</i>	Friction factor
<i>g</i>	Gravitational acceleration, m/s ²
<i>H</i>	Pressure head, m
<i>h</i>	Normalized pump head
<i>k</i>	Flow resistance of pipe, Pa / (l/s) ²
<i>L</i>	Length of pipe, m
<i>LCC</i>	Life-cycle cost
<i>LCC(E)</i>	Life-cycle electricity cost
<i>LCC(L)</i>	Life-cycle license cost

$LCC(M)$	Life-cycle maintenance cost
$LMTD$	Log mean temperature difference
LS	Life span
M	Chilled water flow rate, m^3/s
m	Normalized chilled water flow rate
N	Number
n	Speed of pump
PAU	Primary air-handling unit
PLR	Part load ratio
PS	Pumping station
$P-S$	Constant Primary and variable secondary pumping system
Q	Cooling output, kW
q	Normalized cooling output
T	Temperature, °C
$USPWF$	Uniform series present worth factor
VFD	Variable frequency drive
VPF	Variable primary flow
VSP	Variable speed pump
W	Electrical power, kW
w	Normalized power
Wd	Width of DCS plant room, m
v	Average velocity, m/s
η	Efficiency
π	Normalized efficiency
ρ_w	Density of chilled water, kg/m^3

∞ SUBSCRIPTS ∞

<i>bldg</i>	Building
<i>c</i>	Critical branch of chilled water distribution network
<i>ch</i>	Chiller
<i>comb</i>	Combination
<i>con</i>	Condenser water entering chiller
<i>const</i>	Constant speed
<i>cwp</i>	Chilled water pump
<i>ch</i>	Chiller
<i>hx</i>	Heat exchanger
<i>i</i>	Building <i>i</i>
<i>j</i>	Location of pumping station in a building <i>zone</i>
<i>k</i>	Number of arrangement of pumping station
<i>min</i>	Minimum
<i>o</i>	Rated condition
<i>PS</i>	Pumping station
<i>pf</i>	Pump fitting
<i>R</i>	Replacement of equipment
<i>r</i>	Chilled water return
<i>s</i>	Chilled water supply
<i>swp</i>	Seawater pump
<i>TR</i>	Total replacement
<i>w</i>	Water
<i>var</i>	Variable speed
<i>z</i>	Building zone number

Chapter 1

Introduction

1.1 Energy Use in Buildings in Hong Kong and Impacts on Sustainable Development

Buildings are the major source of demand for energy in modern cities. Situated south of the tropic of Cancer, Hong Kong has a humid subtropical climate, with an annual mean temperature around 23°C. Summer is the longest season, with a mean temperature exceeding 25°C for the months of May to October (Ho, 2003). It has been expected that the annual mean temperature in the decade 2090-2099 will rise by 4.8 °C (Leung et al., 2007). Under such climate, air-conditioning becomes the dominant energy end-use in buildings. As air-conditioning systems in the buildings in Hong Kong are predominantly powered by electricity, their energy consumption incurs emissions of carbon dioxide, nitrogen oxides, sulphur dioxide, and other pollutants from the power stations. Besides global warming, such emissions have also led to poor air quality, which has become a significant concern of the local people and the government.

As shown in Figure 1.1, the annual electricity consumption in Hong Kong increased steadily from 134,138 TJ in 2001 to 150,895 TJ in 2010, i.e. by 12.5% over the 10-year period (EMSD, 2012b). In this period, the commercial sector, which is the dominant electricity consumer, had further increased its electricity consumption by 21% (Figure 1.2).

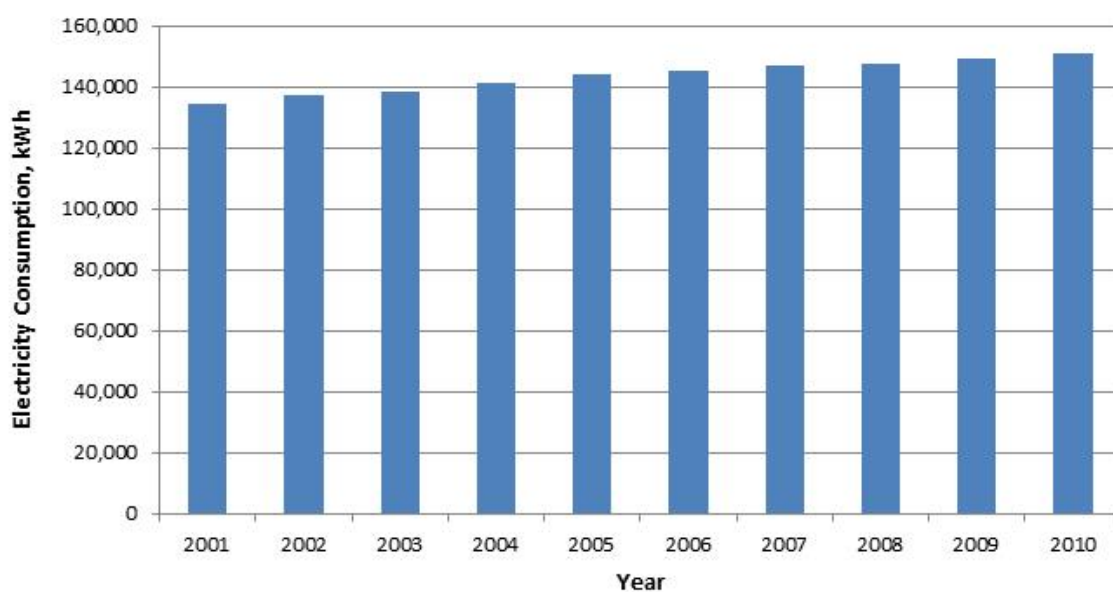


Figure 1.1 Total electricity consumption in Hong Kong (2001-2010)
(Source: EMSD, 2012b)

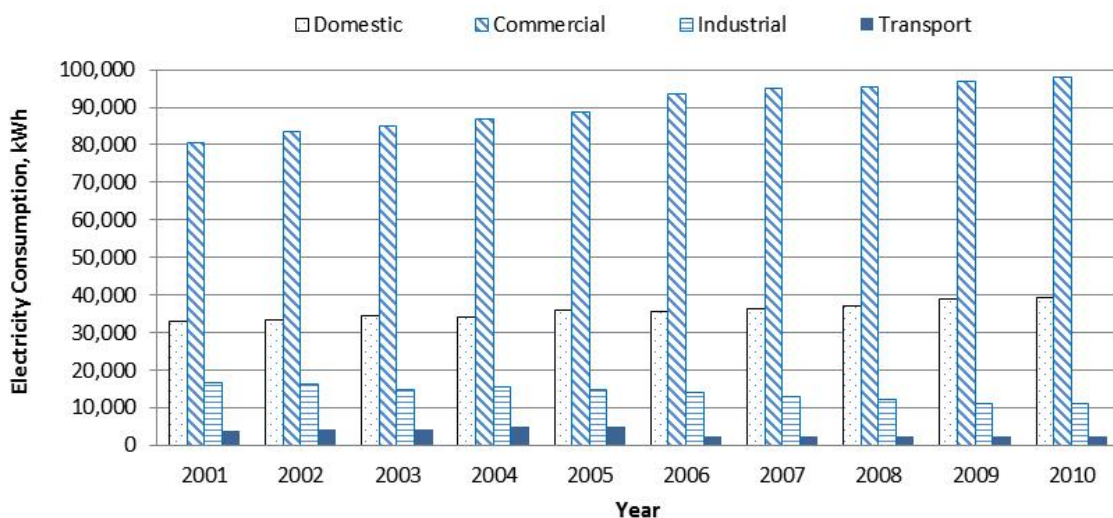


Figure 1.2 Total electricity consumption of the domestic, transport, commercial and industrial sectors in Hong Kong (2001-2010)
(Source: EMSD, 2012b)

On average, 75% of the total amount of electricity is consumed by non-domestic buildings in Hong Kong, of which about 30% is used for air-conditioning, which is equivalent to 23% of the total electricity consumed. Air-conditioning energy use is expected to grow further in Hong Kong in view of the growing population and

economic activities. In order to reduce greenhouse gas emissions from power plants, improving the efficiency of energy use in buildings, in particular that for air-conditioning, is a key measure that the Hong Kong government should continuously undertake.

1.2 Water-Cooled Air-Conditioning Systems and District Cooling Systems

Hong Kong has been relying on mainland China for fresh water supply. This has been a critical concern of the people and the government before Hong Kong's return to China in 1997. To minimize the use of this vulnerable public utility for less essential purposes, the Waterworks Regulations has prohibited the use of potable water from government town mains to make up water losses in evaporative cooling towers for comfort air-conditioning. Consequently, the majority of the air-conditioned buildings in Hong Kong have been equipped with air-conditioning systems that utilize outdoor air for condenser heat rejection. These are commonly referred to as air-cooled air-conditioning systems (AACS) (Yik et al., 2001b).

In Hong Kong, air-cooled chillers used in AACS are typically rated at an outdoor temperature of 35°C and the coefficient of performance (COP, which is the ratio of cooling output to power input) of chillers, taking into account the condenser fan power, ranges from 2.6 to 2.9. However, for a direct seawater-cooled chiller plant with seawater entering at a temperature of 27°C, the COP of the chiller plant can be 4 to 5, or even higher (EMSD, 2012a; Yik et al., 2001a).

Aimed at reducing the environmental impacts due to air-conditioning energy use, the Hong Kong Electrical and Mechanical Services Department (EMSD) launched a pilot scheme in 2000. Under this scheme, permission can be obtained to use fresh water for replenishing water losses in cooling towers, making it possible to use the more energy efficient water-cooled air-conditioning systems (WACS) in buildings (EMSD, 2000; EMSD, 2004). This has become a standing scheme since 2008.

The EMSD also commissioned several consultancy studies on a territory-wide application of different types of WACS. One of the studies looked into the potentials of

implementing a district cooling system (DCS) in the former airport site - the South East Kowloon Development (SEKD).

A DCS is basically a large centralized chiller plant that can meet the chilled water demands of multiple buildings in a district (Figure 1.3). Chilled water is produced in the centralized chiller plant and distributed to a group of buildings through a chilled water distribution network. The overall system efficiency is higher than that of the discrete chiller plants installed in individual buildings because the chilled water is mass-produced by much larger chillers with higher efficiency (Chan et al., 2007). This will also result in reduced primary fuel consumption and environmental emissions (Wu and Rosen, 1999).

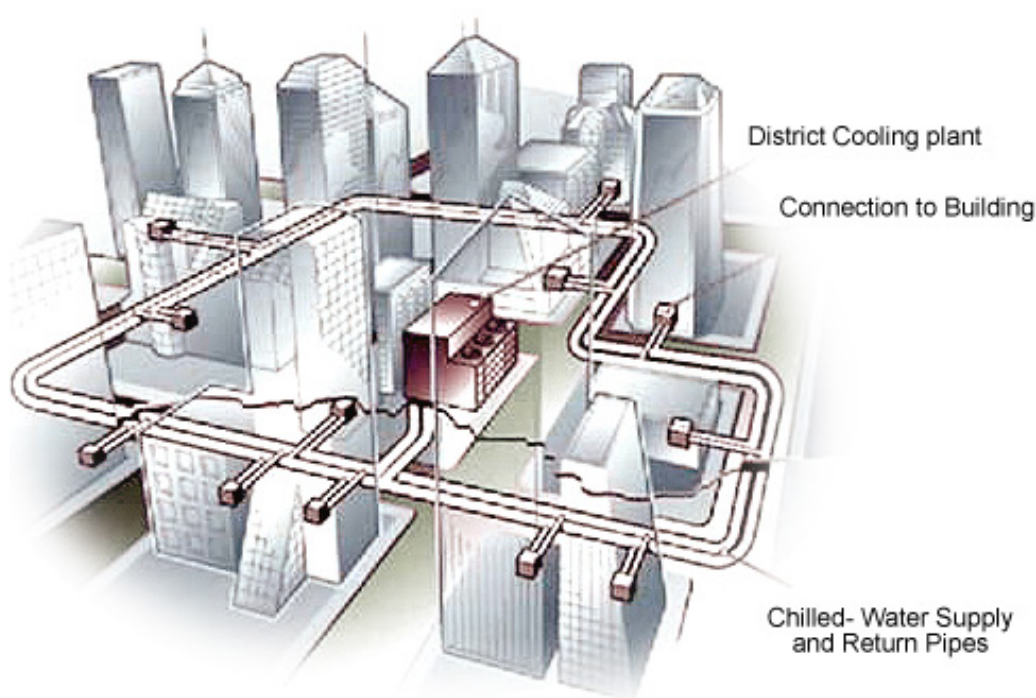


Figure 1.3 A district cooling system
(Source: EMSD, 2013)

In addition to the economy of scale, a DCS can take the advantage of diversity of cooling demands from the different buildings it serves so that the installed cooling capacity of the DCS plant can be lower than the sum of peak cooling demands of the buildings. Without a central chiller plant in the building, the DCS users can utilize building space more effectively.

DCS have already been used for a long time in different parts of the world ([Helsinki Energy, 2006](#)), such as Sweden, France and the United States ([Delbes, 1999](#)). They can also be found in some Asian countries, including Japan ([Japan for Sustainability, 2009](#)), Malaysia ([Shiu, 2000](#)) and Singapore ([EMA, 2002](#)). In November 2013, Pearl-Qatar in the Arabian Gulf became the world's largest district cooling plant with a cooling capacity of around 450 MW ([Wikipedia, 2013](#)).

In a consultancy study commissioned by the EMSD, it was found that application of DCS in the SEKD could lead to an energy saving of up to 35%, as compared to using independent AACS in individual buildings ([EMSD, 2002](#)). Further studies were also conducted to explore whether DCS or centralized piped seawater supply for condenser cooling could be implemented in the Wan Chai and Causeway Bay districts. Based on these findings, the EMSD considered the SEKD to be a suitable location for setting up a DCS. To start with, a large piece of land, to be made available by land reclamation from the harbour, was needed to house the DCS plant. However, land reclamation from the Victoria Harbour turned into a controversial issue among the general public and delayed the development plan.

Eventually in 2010, the government commenced with the development of Hong Kong's first DCS in the Kai Tak Development (KTD, formerly the SEKD), to meet the demand of public and private non-domestic developments for chilled water for air-conditioning. The proposed DCS will provide air-conditioning for a total floor area of about 1.73 million square meters, with about one-third being government buildings and the rest being hotels, offices and retail outlets. The estimated maximum cooling demand would amount to 80,000 RT (about 280 MW, as 1 RT = 3.517 kW) when all buildings served by the DCS are occupied ([Environment Bureau, 2013](#)). There will be two chiller plants in this DCS. Altogether there will be 26 chillers with cooling capacities of 5,000 RT, 2,500 RT (8,793 kW), 1,250 RT (3,946 kW), 600 RT (2,110 kW) and 400 RT (1,407 kW) ([Tam, 2014](#)). [Table 1.1](#) summarizes the chiller system configuration and cooling capacities of the chillers to be installed. The variable primary flow (VPF) chilled water system is adopted and all chillers have constant speed compressors, except those four with smaller cooling capacities (i.e. 400 RT (1,407 kW) and 600 RT (2,110 kW)).

Table 1.1 Chiller system configurations of the DCS in the KTD

Location	Year	Chiller system configuration			
		Cooling capacity, RT/kW	No.	Type	Total installed capacity, RT/kW
Southern chiller plant	2013 (Package A)	1,250 / 3,946	3	VPF	4,950 / 17,409
		600 / 2,110	2	VPF +VSD	
	2017 (Package B)	5,000 / 17,585	2	VPF	10,000 / 35,170
	2021 (Package C)	2,500 / 8,793	2	VPF	20,000 / 70,340
		5,000 / 17,585	3	VPF	
Total			12		34,950 / 122,919
Northern chiller plant	2013 (Package A)	1,250 / 3,946	2	VPF	3,300 / 11,606
		400 / 1,407	2	VPF +VSD	
	2017 (Package B)	2,500 / 8,793	2	VPF	5,000 / 17,585
	2021 (Package C)	5,000 / 17,585	8	VPF	40,000 / 140,680
	Total			14	

Moreover, to further promote energy efficiency and conservation, the Hong Kong government plans to implement DCS in some new development areas. Two new areas - the West Kowloon Cultural District and the North East New Territories Development - have been identified as the potential sites for the implementation of DCS. Public consultation about these two projects is tentatively to be completed by 2014 (Arup, 2014).

1.3 Chilled Water Systems in DCS

For many years, the design of chilled water systems in buildings has been dominated by the constant primary-variable secondary (P-S) configuration as it is simple and familiar to engineers (Severine, 2004). There is no exception for the large scale chilled water systems in various DCS. In this system, chilled water is circulated between the central chiller plant and the buildings via a three-level chilled water piping system that comprises a production loop, a distribution loop and building loops (see Figure 1.4).

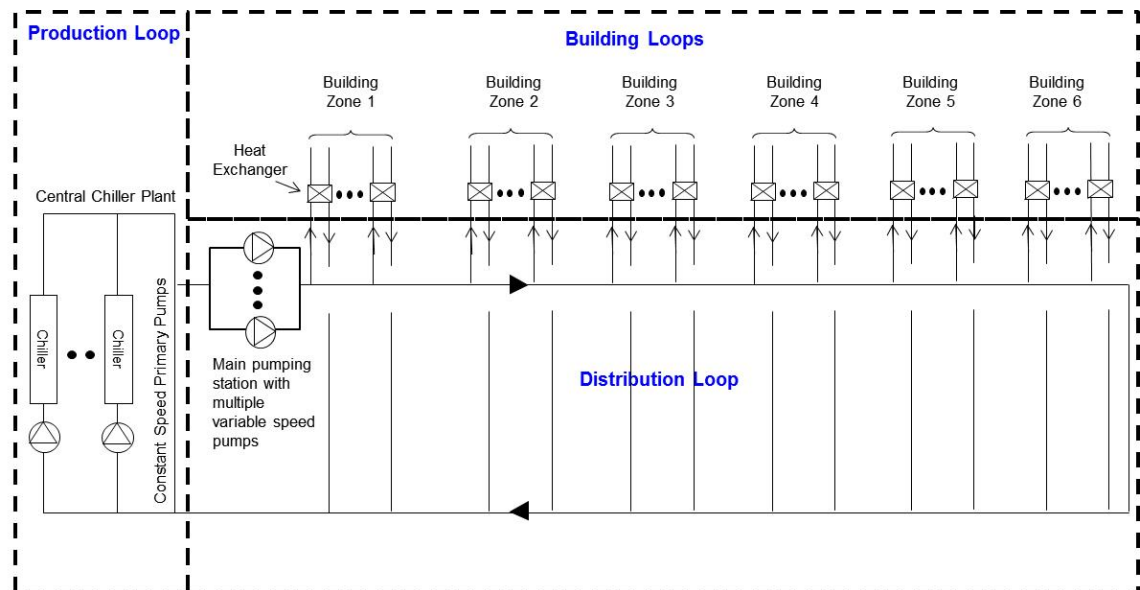


Figure 1.4 A three-level chilled water piping system: production, distribution and building loops

The following is a more detailed description of this system.

- i. The production loop comprises the chillers in the central plant and primary chilled water pumps, which are constant speed and constant flow pumps.
- ii. The distribution loop is connected to the production loop and comprises secondary chilled water distribution pumps that deliver chilled water from the central chiller plant to the heat exchanger in each building via a distribution piping network. The pumps are variable speed and variable flow pumps, responsible for overcoming pressure losses incurred by the chilled water flow around the network.
- iii. There is a building loop in each building, which typically includes a heat exchanger that acts as an interface between the distribution loop and the user's building loop. In each building loop, there is a group of chilled water pumps that distribute chilled water from the heat exchanger to the air-side equipment inside the buildings.

The production and distribution loops are two hydraulically de-coupled piping systems, which share a common pipe section referred to as the decoupler bypass pipe. This can prevent the flow rates in the primary and the secondary loops from influencing each other. As this pumping system provides a stable and simple operation of chillers and the distribution system, it is widely adopted in large scale chilled water systems (Ma and Wang, 2011; Chang et al., 2011).

Under design conditions, the chilled water supplied by the DCS to different buildings is expected to return at the same temperature, i.e. the difference between the chilled water supply and return temperatures, delta-T (ΔT), across the supply and return connections to each building should be constant. The flow rate of the chilled water passing through each building, m , is adjusted to meet its cooling demand as follows.

$$Q = m\rho_w c_w \Delta T$$

where Q is the cooling load, c_w is the specific heat capacity of water and ρ_w is the density of chilled water.

Ideally, if the chilled water flow rate can be varied to match with the changes in the cooling demand, the ΔT value can be kept at the design value. However, this is seldom possible.

1.4 Impacts of Low Delta-T on the Energy Performance of Chilled Water Systems

In reality, in nearly every large scale chilled water distribution system, the temperature of the chilled water returning from the building is lower than the design value and hence delta-T often falls well short of the design level, particularly at low load. This is called the “low delta-T syndrome”. In the last few decades, a number of researchers (Kirsner, 1996; Avery, 1998; Kirsner, 1998; Mcquay, 2002; Taylor, 2002a; Hyman and Little, 2004; Durkin, 2005) have reported the occurrence of the low delta-T syndrome in many P-S pumping systems.

When the low delta-T syndrome occurs in the user's buildings served by a DCS, delta-T in the chilled water distribution network will decrease and thus the required chilled water flow rate will become larger. This may call for a more than required number of chillers to be run to cope with the total cooling demand. Otherwise, deficit flow, i.e. chilled water returning from the building flows back through the decoupling bypass and mixes with the supply water from the chiller, will arise which is undesirable. Under such circumstances, the chillers will all operate at part load, possibly under an inefficient condition. Energy consumption of the chiller plant, including the pumps, increases accordingly. Low delta-T continues to be a problem confronting DCS ([Moe, 2005a](#)).

There are many causes of the low delta-T syndrome ([Fiorino, 1999](#); [Taylor, 2002a](#); [Durkin, 2005](#); [Taylor Engineering, 2009](#)). The most common cause is improper set point on controllers controlling the supply air temperature of cooling coils such as VAV systems and other central fan systems. When the set point of a cooling coil is too low, the controller will cause the chilled water valve to open fully since it is unable to attain the set point irrespective of the amount of chilled water flowing through the coil. In this case, the delta-T significantly drops. Moreover, some building operators typically reset the chilled water temperature at a higher level at low loads to minimize the electricity consumption of the chiller. It is because chillers are more energy efficient at higher leaving chilled water temperature. However, high chilled water temperature will reduce coil performance and hence coils will demand more chilled water and lower the delta-T. The energy saved in the chiller may offset by the additional energy consumption in the coil.

For a conservative design, some designers oversize the control valve with direct digital controls using proportional-integral-derivative control loops and variable speed drives to control the chilled water system pressure in a building. However, grossly oversized control valves can cause the controller to "hunt", alternatively opening and closing the valve, over- and under-shooting the set point. The overall average chilled water flow is higher than desired, and thus the delta-T is reduced. Some causes are inevitable. Typically, it is because the heat transfer effectiveness of the cooling coil is reduced by water fouling due to slime, scale or corrosion on the inside of the coil tube. Any

reduction in coil effectiveness will increase the water flow rate in order to attain the desired leaving water temperature, thus resulting in a low delta-T.

To understand the relationship between the cooling load and chilled water flow rate under low delta-T conditions in details, [Cai et al. \(2012\)](#) studied six commercial buildings in Hong Kong and Shenzhen that suffered from the low delta-T problem. They found that the cooling output required high demand of chilled water flow rate, i.e. higher than the design chilled water flow (Figure 1.5). In this regard, the actual delta-T under operation will be lower than the design value.

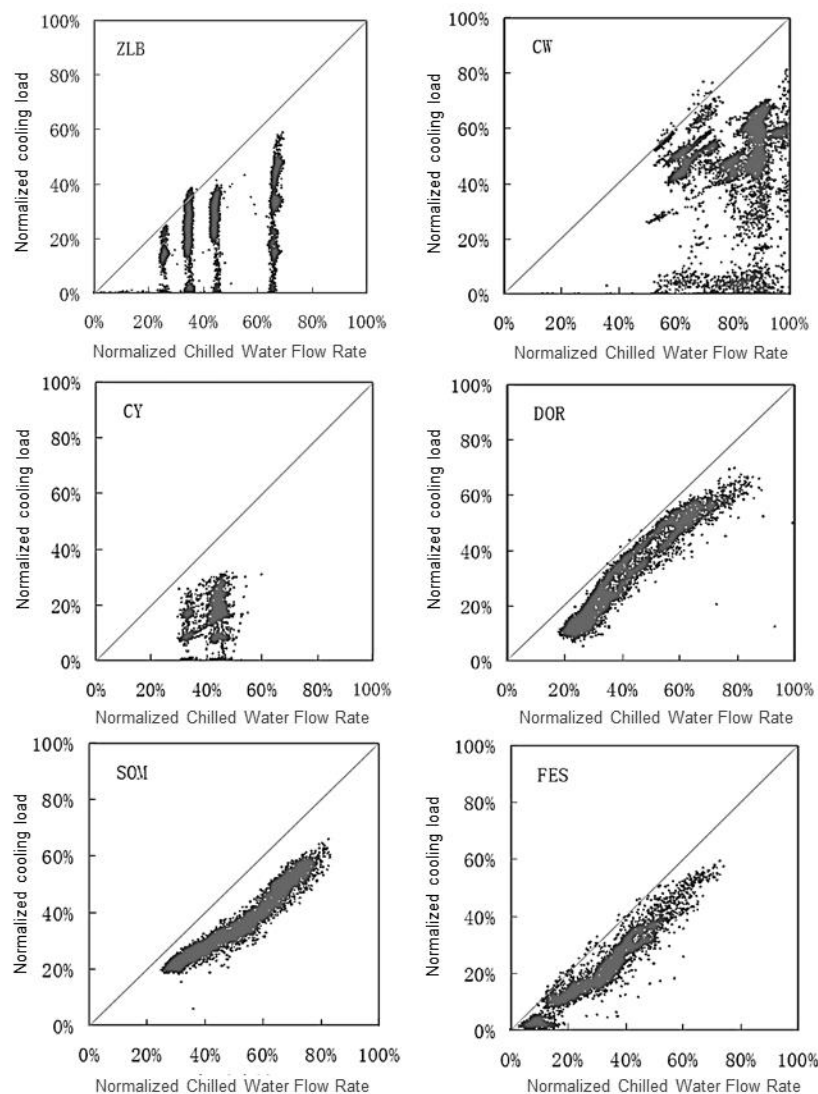


Figure 1.5 Low delta-T characteristic curves of six commercial buildings (Source: [Cai et al., 2012](#))

Over the last two decades, many methods have been proposed for overcoming the low delta-T syndrome in chilled water systems (Ma and Wang, 2011). Taylor (2002a) summarized the potential solutions to deal with the low delta-T problem as a result of different possible causes. Fiorino (1999) recommended 25 “best practices” for achieving a high chilled water delta-T, from component selection criteria to distribution system configuration guidelines. These recommendations were meant to be applicable to new installations as well as retrofit projects.

One common cause of low delta-T is improper selection of control valves for cooling coils. Many designers and manufacturers would oversize control valves and some believed that the chilled water system with direct digital controls using proportional-integral-derivative controller and variable speed pumps could help to control system pressure (Taylor, 2002a; Taylor Engineering, 2009). This is partly true, but cannot compensate for a grossly oversized valve. Oversized control valves cause the controller to “hunt”, alternately opening and closing the valve, over- and under-shooting the set point. The overall average flow is higher than desired, and thus delta-T is reduced.

In this regard, Durkin (2005) and Moe (2005b) recommended to use pressure independent control valves (PICV) to replace the conventional two-way control valves to keep delta-T across the coils in the user’s building close to the design delta-T at part load. As cooling load varies on a chilled water system, the differential pressures across any given coil control valve changes continuously. Dynamic pressure fluctuations can be absorbed by the diaphragm and spring within the PICV. The PICV automatically balances the system regardless of the amount or location of the system load because the pressure regulating part of the valve absorbs any excess pressure across the valve. As long as the differential pressures across the PICV are within their specified ranges, the PICV can help to maintain a relatively constant differential pressure across the valve so that flow rate remains steady.

Nevertheless, there are some demerits of these valves, which have their specified flow rates and must be installed in the correct location. Furthermore, the springs inside the valves would fail or deteriorate over time. Strainers are needed for each valve to prevent

clogging. This will result in a higher pump head and energy for overcoming pressure drop of the strainers. The main hindrance to wider use of PICV is its high initial cost, which is about four to five times greater than that of the pressure dependent valve with a comparable size (Siemens, 2006).

Another attempt to overcome the low delta-T problem was the use of two control logics in a P-S chilled water pumping system in a large shopping mall in Hong Kong (Chan, 2006). In the original design, additional chillers would be staged on when there was a deficit flow where the flow rate exceeded 25% of the rated flow rate of a 1,600 RT (5,627 kW) chiller and when the temperature of chilled water in the rising main exceeded 10°C. Under such circumstances, however, additional chillers were switched on even when the actual cooling load demand was far less than the cooling capacity of the operating chillers. This could result in hunting of chillers due to insufficient loadings. Moreover, the chillers would operate at a low percentage of loading that is outside the optimum range for high energy efficiency.

In the first control logic proposed by Chan (2006), only one additional chilled water pump was switched on to satisfy the flow demand when the deficit flow exceeded the pre-set limit. The second logic was to switch on an additional chiller when a true cooling load was detected according to different criteria such as the percentage full load ampere of the running chillers, average temperature of the chilled water leaving the chiller, the amount of deficit flow at the bypass, actual building load, and running average of the building load. These two control strategies could save the electricity consumption by 435,000 kWh and significantly reduce the frequency of chiller hunting. However, the capital investment required for changing the control logic and adding the associated equipment was not mentioned and thus an assessment of the cost effectiveness has not been possible.

There has been a lot of discussion on the low delta-T issue in the P-S pumping system. Most of these issues can be mitigated by a proper design and component selection, and proper operation and maintenance. However, there are still factors such as degradation of coil effectiveness due to aging system or valve leakage that will result in a degrading delta-T. These factors are inevitable, particularly at low load (Taylor, 2002a).

Taylor (2002a) proposed some methods for designing a chiller plant so that chiller energy would not be affected by low delta-T. The first is the use of variable speed chillers, which could help to improve the chiller's low-load performance and prevent premature staging from affecting energy use. The other four were suggested to provide more flow through operating chillers, so that they might be more fully loaded before another chiller must be staged on. These four techniques included: adoption of a VPF pumping scheme, installation of a check valve in the decoupling bypass, use of unequally-sized chillers or pumps, and adoption of low design delta-T in the primary loop. Among these five recommendations, the bypass check valve and the VPF pumping system have received great attention and opened up further discussion.

1.4.1 Bypass Check Valves for P-S Systems

Some researchers (Avery, 1998; Kirsner, 1998; Taylor, 2002a; Severini, 2004; Bahnfleth and Peyer, 2004; Wang et al., 2010) have extolled the use of a check valve in the decoupling bypass. This valve always keeps the chilled water flow rate in the production loop greater than or equal to the flow rate in the distribution loop. This can prevent chilled water supplied from the chiller plant from mixing with the chilled water returning to the chiller plant. Otherwise, the temperature of chilled water supplied from the chiller plant will increase. Additional chillers may activate to provide additional primary flow for the undue rise in temperature. Bahnfleth and Peyer (2004) and Wang et al. (2010) conducted a parametric study and an experimental test respectively and proved that this method could save 4% and 9.2% of the total plant energy.

However, some practitioners and designers have concerns that the use of a bypass check valve would destroy the decoupling philosophy of the P-S design, i.e. forcing the primary and secondary pumps into series operation and increasing the chilled water flow rate in the chiller. Additional chillers have to be switched on if flow rate is beyond the maximum flow of the operating chiller. Therefore, the inclusion of a bypass check valve is not recommended for the P-S system (McQuay, 2002; Luther, 2002). Moreover, Ma and Wang (2011) have pointed out that secondary pumps might be shut off when all primary pumps are turned off in order to avoid the secondary pumps from operating with no chilled water flowing inside. In this situation, the rotating impeller will continue

to agitate the same volume of water. As the water rotates, frictional forces cause its temperature to rise to a point where it vaporizes. The vapor disrupts cooling of the pump and may cause excessive wear and tear to its bearings. This indicates that the use of a bypass check valve may lead to problems in the chiller plant and may not be helpful in tackling the low delta-T issue. Hence, some researchers have proposed the use of VPF pumping systems. This will be further elaborated in the following section.

1.4.2 The Controversy between VPF and P-S Systems

Following the advancement of chiller technology in the 1990's, chillers can operate with variable chilled water flow through their evaporators as long as the flow can be maintained not to fall below a minimum level, typically at 50% to 60% of the rated flow rate (Brasz and Tetu, 2008; Yang and Lin, 2012; Trane Hong Kong, 2013). In this regard, some researchers (Kirsner, 1996; Avery, 1998; Hartman, 2001) and manufacturers (Schwedler and Bradley, 2000) have advocated the use of the VPF system to replace the P-S system to solve the low delta-T problem. A VPF system (Figure 1.6) consists of a single variable volume chilled water loop within which the chilled water circulates between the chiller plant and buildings. The primary pumps are equipped with variable frequency drives so that the chilled water flow rate round the distribution loop can be varied to meet different operating conditions. This eliminates the need for secondary variable speed pumps, but requires varying the flow through the chiller's evaporator. The decoupler bypass in the P-S system is replaced by a bypass with a normally closed control valve that opens only to maintain a minimum flow through active chillers.

The major benefit of the VPF system is that both the capital cost and the required plant space can be reduced by eliminating the secondary pumps in the chilled water distribution network. However, for the chilled water distribution pumps, Taylor (2002a) and Rishel (2000) pointed out that the P-S system consumes more pumping energy than the VPF system because the primary constant speed pumps selected for a lower pressure head in the P-S system are generally less energy efficient. The efficiency of the primary pump is about 70%, which is about 10% less than that of the secondary pump (Bahnfleth and Peyer 2004).

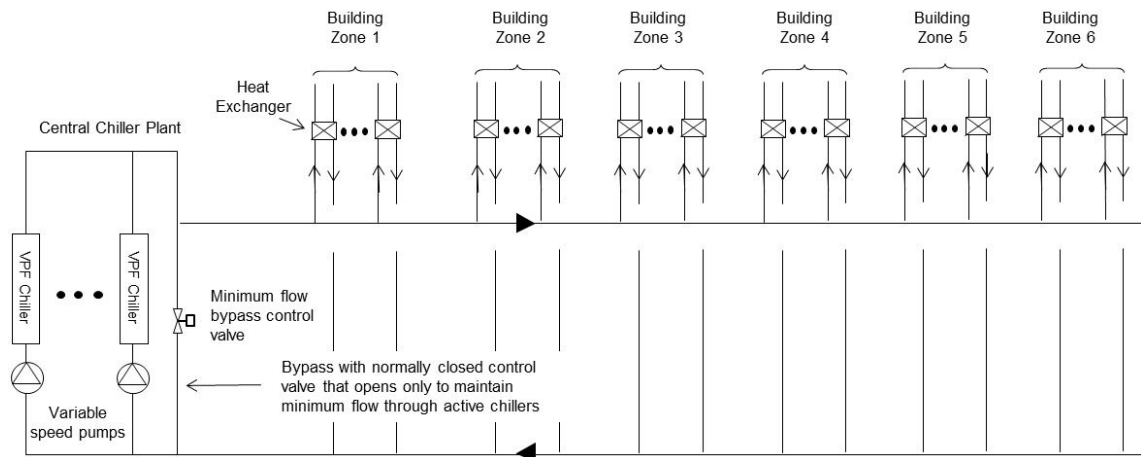


Figure 1.6 A variable primary flow system

This inherently less efficient characteristic has made the comparison of the two systems unfair. Nowadays, with the advancement in technology, the efficiency of the primary pump with a lower pressure head can be designed as high as 85% (PACO, 2014), which is comparable to the efficiency of pumps with a higher pressure head and the same design chilled water flow rate. Moreover, there is no energy consumption benefit as to whether or not the chiller is designed as constant or variable chilled water flow through the evaporator. Studies (Schwedler and Bradley, 2000; Bahnfleth and Peyer, 2006; Bullet, 2007) showed that the power demand of a chiller is the same whether the system's primary flow is constant or variable. It is because the VPF system, having less chilled water flow via the chiller, tends to reduce the water-side heat transfer coefficient. This would cause a drop in the evaporator's saturation temperature, and thus increase the pressure head that the compressor has to deliver and the power demand of the compressor. However, for a constant primary flow chiller in the P-S system, the entering evaporator temperature and log mean temperature difference reduce as cooling load decreases. The convective heat transfer coefficient remains constant despite of the reduction in cooling load. Hence, there is no difference in the electricity consumption of the chillers in these two systems.

1.5 Need for Further Investigation

From the above mentioned studies, it can be seen that there is a lack of consensus on which solution can help to entirely mitigate the impacts of low delta-T on the energy

performance of a DCS. More detailed simulation or in-depth case study of the recommendations given by Taylor (2002a) is still lacking, in particular for DCS. A comprehensive review of the design of DCS would be very useful for practitioners in designing a DCS that can operate efficiently when low delta-T is inevitable and can help owners save the long-term operating energy cost.

1.5.1 Chiller System Configuration

Yik et al. (2001a) studied the energy consumption of a hypothetical DCS using the P-S system. The cooling capacity of this DCS ranged from 40 MW to 200 MW. Among the major DCS components, they found that the chillers were responsible for 76-81% of the total energy consumption of the DCS, while the secondary pumps were responsible for 13-18% (Figure 1.7). This indicates that the performance of chillers has the most significant impact on a DCS' energy consumption. The optimization of chiller system configuration such as the number, cooling capacity and chiller type (constant or variable speed) is one of the effective ways to enhance the DCS' energy efficiency.

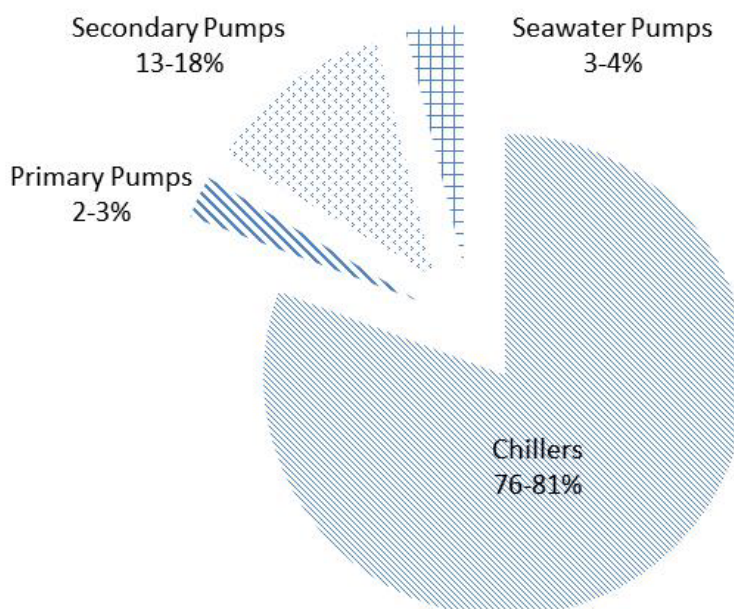


Figure 1.7 Energy consumption of different DCS components

1.5.2 Pumping Stations in the Chilled Water Distribution Loop

Owing to the long distance that chilled water needs to be transported through the piping network, the secondary chilled water pumps are the second largest electricity consuming equipment among all major equipment in a DCS. At low delta-T, the additional chilled water flow in the distribution loop will further increase the energy consumption of the secondary chilled water pumps. It is imperative to have an energy efficient design for the secondary pumping system in order to reduce energy consumption and hence increase the energy efficiency of the DCS.

In a typical P-S pumping system of a DCS, the secondary chilled water pumps are installed either inside the chiller plant room or in a pumping station immediately downstream of the chiller plant. One of the benefits of this design is that the primary pumps in the production loop do not need to be designed with a high pressure head to overcome pressure drops along the extensive distribution pipework. However, the secondary pumps may impose greater water pressure to the nearby heat exchangers. The pressure head is much higher than required to overcome pressure drops in heat exchangers, pipes and fittings. A pressure reducing valve or some other mechanical devices must be incorporated to throttle off the excessive pressure. This over-pressure may force the use of high-pressure or industrial grade control valves at the primary side of the heat exchangers.

Hence, one single pumping station may not be desirable for a large scale chilled water pumping system in DCS. It may be advantageous to place a second pumping station, and perhaps even a third one or more, in different locations along the chilled water supply and return routes of the distribution loop. This can avoid imposing high pressure on the equipment close to the discharge end of the first pumping station and reduce the differential pressure drops in the distribution network. Moreover, unequal number of pumps in each pumping station can be explored to achieve an optimum pumping station design. [Figure 1.8](#) shows an example of a distribution loop designed with a three-pumping station combination having different number of pumps in each station.

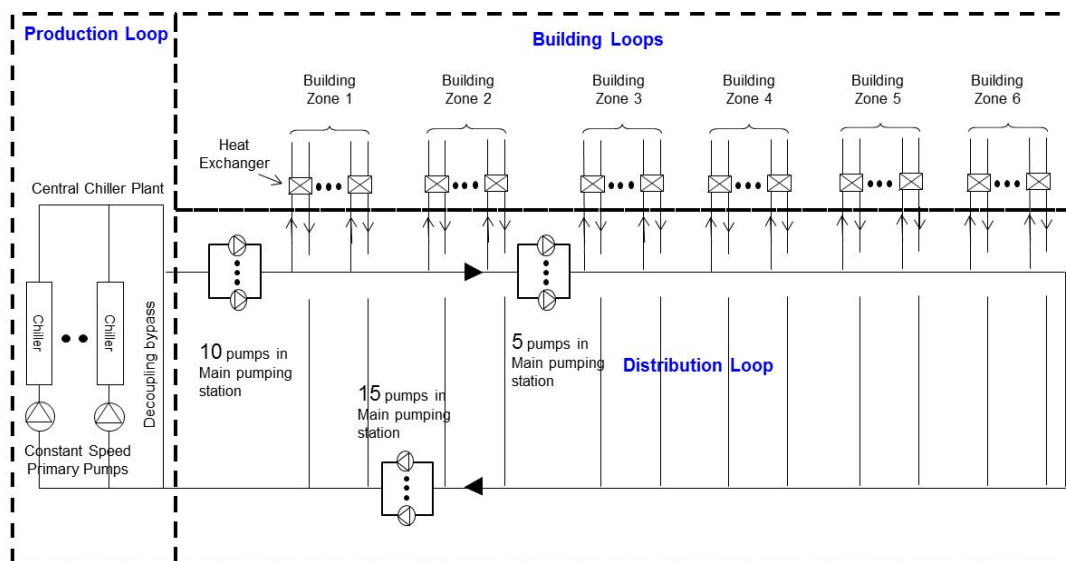


Figure 1.8 An example of a distribution loop designed with three pumping stations and different number of pumps in each station

1.5.3 Chilled Water Temperature in the Distribution Loop

A successful implementation of the DCS also depends greatly on the ability of the chilled water system to obtain a large difference between the supply and return chilled water temperatures in the distribution loop. Increasing the temperature difference is an effective way to improve efficiency of the chilled water system and save the chiller plant's operating cost (Zhang et al., 2012) because this allows minimizing pumping energy requirement for distributing chilled water to the buildings within the district. For a centrifugal chiller, the typical design chilled water supply temperature ranges from 4°C to 6°C and the return temperature ranges from 12 °C to 15°C (Skagestad and Mildenstein, 1999; IEA, 2002).

Table 1.2 lists out the design chilled water supply and return temperatures, and the temperature difference of different DCS projects in different countries. A summary of the design temperature range in different continents is given in Table 1.3. It can be seen that the temperature difference in DCS ranges from 5.4-10.5°C and is relatively higher than that in the conventional chilled water system in buildings, i.e. 5°C. The operating efficiency of the chilled water system can be increased with an increased temperature difference due to the reduced pumping requirement caused by a reduced flow rate in the distribution system.

Table 1.2 Design chilled water supply and return temperatures of the DCS in different countries

	Continent	Country	City/ State	Location of DCS	Supply floor area, m ²	Supply temp, °C	Return temp, °C	Delta-T, °C	Total cooling capacity, kW	Source of information
1	Asia	Japan	Chiba	Chiba Newtown Center	467,000	7	14	7	29,183	www.nt-cnc.co.jp/netu/index3.html
2	Asia	Japan	Fukuoka	Fukuoka Seaside Momochi District	691,812	6	12	6	55,201	www.jdhc.or.jp/area/kyushu/06.html www.fukuoka-es.co.jp/area/momochi.html
3	Asia	Japan	Kobe	Southern District of Sannomiya Station	78,200	7	14	7	11,075	www.ores-dhc.co.jp/system/sannomiya.html
4	Asia	Japan	Osaka	Kinki	238,109	7	14	7	39,000	www.ores-dhc.co.jp/system/konohana.html
5	Asia	Japan	Osaka	Nanko	750,000	6.5	13	6.5	62,233	www.ores-dhc.co.jp/system/nankou.html
6	Asia	Japan	Osaka	Rinku Town	245,634	6	13.5	7.5	23,206	www.ores-dhc.co.jp/system/rinku.html
7	Asia	Japan	Tokyo	Downtown Waterfront District	2,132,953	7	14	7	221,860	www.jdhc.or.jp/area/tokyo/47.html www.tokyo-rinnetu.co.jp/?page_id=11
8	Asia	Japan	Tokyo	Ikebukuro	605,257	5	14	9	71,023	www.jdhc.or.jp/area/tokyo/04.html www.ikenetu.co.jp/area/index.html
9	Asia	Japan	Yokohama	Minato Mirai 21	2,793,900	6	13	7	130,795	www.jdhc.or.jp/area/kanto/01.html www.mm21dhc.co.jp/english/owner/erea_center.php
10	Asia	Japan	Tokyo	Shinjyuku Shin-toshin District	2,222,630	4	12	8	207,444	www.hitachi-ap.com/products/business/chiller_heater/district/shinjyuku.html
11	Asia	Japan	Tokyo	Shinjuku South	241,000	7	14	7	36,813	www.jdhc.or.jp/area/tokyo/52.html www.sesdhc.co.jp/dhc/equipment_outline.html
12	Asia	Japan	Tokyo	Shiodome Kita	719,777	4	14.5	10.5	95,973	www.jdhc.or.jp/area/tokyo/63.html www.shiodome-ue.co.jp/index4.html
13	Asia	Malaysia	Kuala Lumpur	Kuala Lumpur City Centre	604,000	4.4	14.4	10	128,000	Majid et al., 2008
14	Asia	Malaysia	Kuala Lumpur	Kuara Lumpur International Airport	605,320	7.5	14.5	7	123,060	Majid et al., 2008
15	Asia	Malaysia	Perak	University Technology Petronas	104,000	6	13	7	48,520	Majid et al., 2008

Table 1.2 Design chilled water supply and return temperatures of the DCS in different countries (Con't)

	Continent	Country	City/ State	Location of DCS	Supply floor area, m ²	Supply temp, °C	Return temp, °C	Delta-T, °C	Total cooling capacity, kW	Source of information
16	Asia	Singapore	Buona Vista	One-North	185,000	7	14	7	87,900	www.keppeldhcs.com.sg/singapore_plants.html www.keppeldhcs.com.sg/file/DHCS_Technical_Specs.pdf
17	Asia	Singapore	Changi	Changi Business Park	1,000,000	7	14	7	105,480	www.keppeldhcs.com.sg/singapore_plants.html www.keppeldhcs.com.sg/file/DHCS_Technical_Specs.pdf
18	Asia	Singapore	Marina Bay	Marina Bay	8,000,000	6	14	8	157 (Plant 1) 180 (Plant 2)	Tey, 2010
19	Asia	Singapore	Woodlands Wafer Fab Park	Woodlands Wafer Fab Park	485,000	7	14	7	38,676	www.keppeldhcs.com.sg/singapore_plants.html www.keppeldhcs.com.sg/file/DHCS_Technical_Specs.pdf
20	Europe	Czech Republic	Ostrava	Ostrava and Dothan Regional Airport	2,000,000	6	14	8	24,500	Dalkia, 2009
21	Europe	Netherlands	Amsterdam	Zuidas	2,500,000	6	16	10	60,000	Nuon, 2013
22	Europe	Sweden	Solna	Norrenergi AB Plant	u/a	6	16	10	50,000	Evans, 2006
23	Europe	Sweden	Stockholm	Nimrod Plant	u/a	5	11	6	43,300	Friotherm, 2013
24	USA	USA	Washington	The Pentagon	u/a	6	12	6	132,000	Delbes, 1999
25	USA	USA	Colorado	Denver International Airport	u/a	4.4	13.3	8.9	42,000	Delbes, 1999
26	USA	USA	Texas	Texas Medical Centre	1,900,000	4.4	11.7	7.3	112,512	Clark et al., 2011
27	USA	USA	Texas	Johnson Space Centre in NASA	u/a	5.5	12.7	8.2	21,000	Delbes, 1999
28	USA	USA	New York	Cornell University	1,300,000	7.2	15.6	8.4	56,256	Dalin, 2012
29	USA	USA	Texas	The University of Texas at Austin	1,416,401	4	9.4	5.4	61,000	Kuretich, 2010
30	USA	USA	Minnesota	Saint Paul	2,000,000	5.6	13.3	7.7	101,964	www.district.energy.com

Table 1.3 Range of design supply and return chilled water temperatures of the DCS in Asia, Europe and the United States

Continents	Chilled water temperature, °C		
	Supply	Return	Delta-T
Asia (Japan, Singapore and Malaysia)	4-7.5	12-14.5	6-10.5
Europe (Sweden, Netherlands and Czech Republic)	5-6	11-16	6-10
United States	4-7.2	9.4-15.6	5.4-8.9

In 2009, the Energy Market Authority (EMA) of Singapore issued an Energy Service Supply Code for DCS service providers. Under this code, the operator undertakes to regulate the chilled water supply temperature within $6^{\circ}\text{C} \pm 0.5^{\circ}\text{C}$ and the consumer has to ensure that the chilled water return temperature should be 14°C or higher (EMA, 2009).

In Hong Kong, researchers such as Yik et al. (2001b) and Chow et al. (2004b) have selected 5°C and 12.5°C to be the design chilled water supply and return temperatures respectively in their research study. These temperatures are typically used for buildings in Hong Kong and are within the range of chilled water temperatures of the DCS in other countries. In 2012, the Hong Kong EMSD (2012c) issued a draft technical guideline for setting up DCS. Under this guideline, chilled water pipes in the distribution network shall be connected to the plate type heat exchangers installed inside the user's premises. The design chilled water supply and return temperatures in the distribution loop are $5^{\circ}\text{C} (\pm 1^{\circ}\text{C})$ and 13°C . The design chilled water supply and return temperatures at the building's chilled water side under normal operating conditions are $6^{\circ}\text{C} (\pm 1^{\circ}\text{C})$ and 14°C . Both the operator and the consumer have the obligations to fulfil these design conditions to ensure energy efficiency and that all consumers are supplied with high quality chilled water.

However, there is still no universal standard for determining an optimum chilled water supply and return temperature and hence the temperature difference for optimizing energy performance of DCS at low delta-T. Changing this temperature will have a significant impact on the energy performance of chillers and chilled water pumps as the COP of chillers and chilled water flow rate in the distribution network are affected.

This has led to the need to conduct a detailed investigation and find out an optimum chilled water temperature that can strike a good balance between chiller power and chilled water pump power to minimize the overall electricity consumption of DCS.

1.5.4 Energy Saving Potentials of P-S and VPF Pumping Systems

For the Hong Kong KTD project, a P-S system was originally proposed in the consultancy reports (Yik et al. 2001a; Chow et al., 2004a). However, a VPF system was later adopted during the tendering stage in 2010 (see Table 1.1). VPF system configuration requires installation of one group of variable speed primary pumps with a higher pressure head in the chiller plant instead of using one set of primary constant speed and one set of secondary variable speed pumps in the P-S system. Moreover, almost all the chillers (except those four with a small cooling capacity) are constant speed. This may help to save the initial capital cost incurred by variable speed chillers and additional secondary chilled water pumps for the P-S system.

However, as explained in section 1.4.2 of this chapter, with the advancement in technology, the efficiency of the primary pump with a lower pressure head can be designed as high as 85%, which is comparable to the efficiency of pumps with a higher pressure head and the same design chilled water flow rate. And, the use of variable chilled water flow chillers in the VPF system does not bring any benefit in energy consumption as compared to using constant chilled water flow chillers in the P-S system.

In this regard, VPF systems may not be a good choice for DCS. There has been a lack of detailed quantitative analysis regarding the energy savings resulting from application of P-S and VPF systems in the chilled water pumping system of a large scale DCS, which is similar to the one in the present study. A comparative analysis of the energy performance of the pumping systems in the P-S and VPF schemes is given in Chapter 4.

1.6 Financial Analysis

In view of the huge capital investment and the lengthy payback period required by a large scale infrastructural development like DCS, adoption of measures that can improve the system's energy efficiency may increase the capital cost and subsequent replacement, operating and maintenance costs. The DCS owner may have concerns over these additional costs. To the system designer, there is always a budgetary constraint in selecting or designing an optimum set of energy efficiency enhancement measures. Therefore, to help these parties gain more insights about the real costs and ultimate energy benefits, a financial analysis of the cost effectiveness of various energy efficiency enhancement measures is indispensable.

A life cycle cost (LCC) approach is the most widely used method in cost-effectiveness analysis for comparing the economic viability of various types of energy efficiency enhancement measures (Master and Ela, 1998; Field and Field, 2009). The technique is based on discounting, or reducing, all costs to current values or representing them as an annual cost. The smaller the LCC value, the more worthwhile the option is to be taken in comparison with other options.

1.7 Research Aim and Objectives

Most research studies have focused on only a few design measures to mitigate the impacts of low delta-T in the existing chilled water systems in buildings. There is a lack of comprehensive review and in-depth research on the design of DCS, with an aim to minimizing the impacts of low delta-T on its energy performance.

As a result, this research is aimed at finding out a cost-optimal design that can enable the chiller plant and pumping station in a DCS to achieve a satisfactory energy performance and the minimum long term LCC under the influence of the low delta-T problems. This aim can be achieved through the following objectives.

- i. To construct a hypothetical district model to represent the high-rise buildings in a commercial district in Hong Kong and design a typical DCS for providing

chilled water to the district. As the first DCS in Hong Kong is still at a burgeoning stage, field data about its energy performance, in particular that related to the impacts of low delta-T, is not yet available. In this regard, a model-based approach is the most practical and cost effective evaluation method. Together with a design DCS for the hypothetical district, they provide a vital simulation environment for this study.

- ii. To tailor design mathematical models for a hydraulic distribution network and all major equipment of a DCS, including constant and variable speed chillers, variable speed chilled water pumps, heat exchangers and cooling coils of buildings. These models can act as an effective tool for energy simulation and an evaluation of the impacts of low delta-T on the DCS' energy performance.
- iii. To propose and evaluate the effectiveness of various energy efficiency enhancement measures that can mitigate the impacts of low-delta T on the DCS' energy performance.

In order to achieve these objectives, it is necessary to examine and find out an optimum design, which is derived from a combination of the following three energy efficiency enhancement measures:

- a. chiller system configuration – this can be done by changing the major influential design parameters such as the number and cooling capacity of chillers, and application of constant and variable speed chillers;
- b. pumping station – this can be done by analyzing the application of multiple pumping stations in different locations of the chilled water supply and return network, and the use of different number of pumps in each pumping station; and
- c. design chilled water supply and return temperatures – this can be done by conducting a sensitivity analysis of different temperature regimes.

- iv. To devise a cost-optimal design solution that can integrate the various measures in item (iii), and lead to the lowest LCC and an optimum energy performance when the DCS is operating under low delta-T conditions.

1.8 Research Methodology

As the development of Hong Kong's first DCS was still at an early stage when the present study was conducted, records of its operating energy performance were unavailable. Therefore, a model-based approach was the only practical and feasible methodology to be taken. Besides, it is a flexible method that can allow different scenarios to be studied. To provide a basis for the study, it was necessary to set up a hypothetical district that could represent the typical urban districts in Hong Kong and a DCS model had to be designed for this district. The model was first incorporated with typical design parameters and was taken as the base case. The effectiveness of different energy efficient measures was then evaluated by modifying the base case model. Moreover, mathematical models were tailor-made for analyzing the DCS' performance under various operating conditions.

[Figure 1.9](#) outlines the approach and methodology adopted for identifying the optimum design solution for DCS.

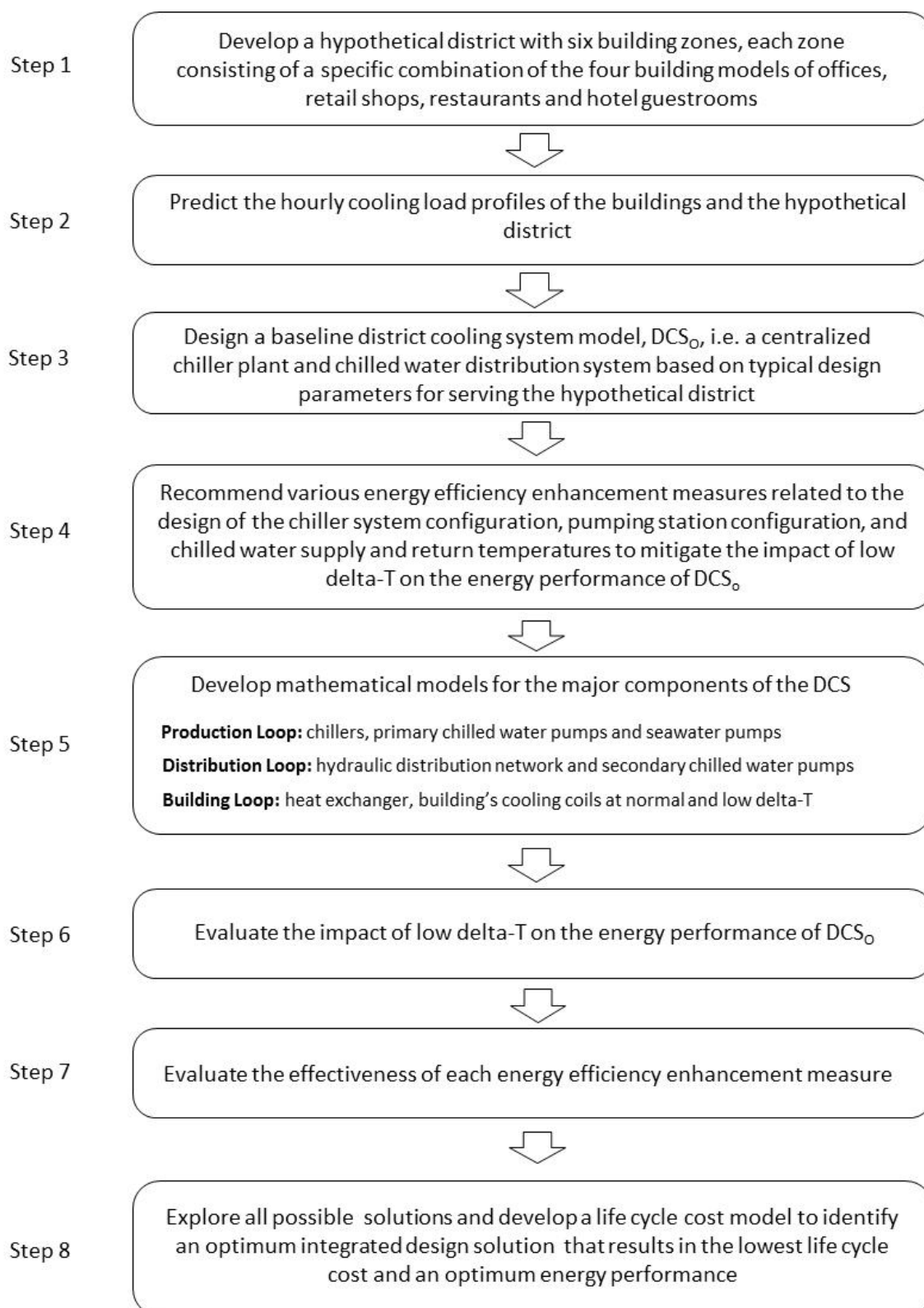


Figure 1.9 Framework of research approach and methodology

The following is a detailed explanation of each step.

Step 1 – Develop a hypothetical district model

A hypothetical district model was established on the basis of the building models developed by [Yik et al. \(2001b\)](#). In their study, four building models comprising a range of combinations of offices, retail shops, restaurants and hotel guestrooms were formulated to represent the densely populated high-rise buildings in typical commercial districts in Hong Kong. The hypothetical district model for the present study was made up of six building zones, each comprising of a group of these four building models.

Step 2 – Simulate the hourly cooling load profile

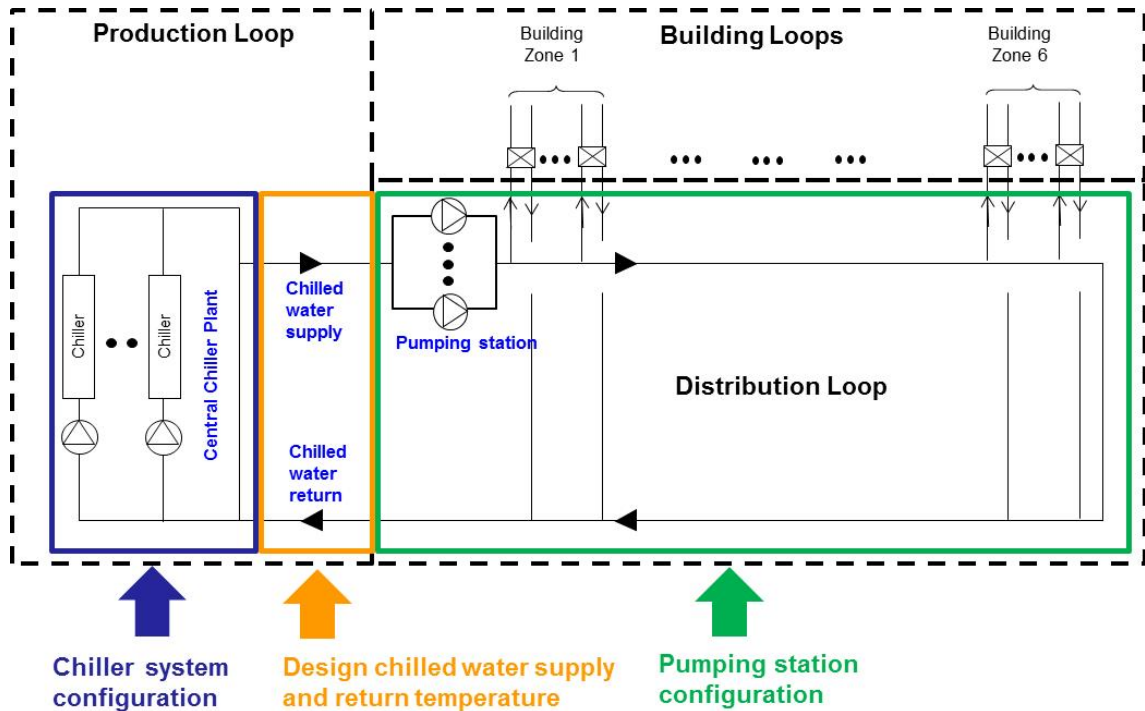
Two simulation programs, namely HTB2 ([Alexander, 1996](#)) and BECON, ([Yik, 1996](#)) were used to predict the cooling loads of the four building models at different times of the year and the hourly power demand of air conditioning equipment. The cooling capacity required of the DCS serving the group of buildings, and the simultaneous hourly cooling loads on the DCS in the year were determined on this basis.

Step 3 – Develop a baseline DCS model for the hypothetical district

Based on the cooling load data obtained from Step 2, a baseline DCS, named as “DCS₀”, was designed to serve the hypothetical district. This DCS was used as a reference base for an evaluation of the effectiveness of various energy efficiency enhancement measures that can further improve the energy efficiency of the system.

Step 4 – Recommend the energy efficiency enhancement measures for DCS₀

To improve the overall energy performance of DCS₀ under low delta-T conditions, measures can be taken in the following areas ([Figure 1.10](#)).



Integrated design solution to optimize the energy performance of DCS

Figure 1.10 Three different energy efficiency enhancement measures for DCS₀

- chiller system configuration – this can be done by changing the major influential design parameters such as the number, cooling capacity and type (constant or variable speed) of chillers;
- chilled water supply and return temperatures – this can be done by conducting a sensitivity analysis of different design chilled water supply and return temperatures; and
- pumping station configuration – this can be done by analyzing the application of multiple pumping stations at different locations of the chilled water supply and return network, and the use of different number of pumps in each pumping station.

Step 5 – Develop mathematical models for the DCS

There are many well-developed mathematical models for air-conditioning equipment and chilled water systems for application in buildings. They, however, cannot be applied directly to modelling a DCS. For the present study, specific mathematical models were developed for simulation of the major DCS components, including constant and variable speed chillers, variable speed pumps, heat exchangers, the hydraulic distribution network and the cooling coils in buildings.

Step 6 – Evaluate the impacts of low delta-T

This baseline DCS and the system and equipment models provided a vital simulation platform for conducting a comparative analysis of the energy performance of DCS₀ with and without the low delta-T syndrome.

Step 7 – Evaluate the effectiveness of the energy efficiency enhancement measures in three areas ([Figure 1.10](#))

To evaluate the effectiveness of various combinations of measures in these three areas, DCS₀ was modified by changing its design parameters. The objective was to find out the feasible measures that can improve the energy performance of DCS₀.

Step 8 – Determine a cost-optimal design solution

Based on the results of Step 7, many possible design solutions integrated with different energy efficiency enhancement measures were identified. A simple heuristic algorithm was developed to select the effective solutions for a more detailed evaluation of their energy, financial and environmental performances. For evaluation of the financial viability of these possible solutions, an LCC model was established and used to find out the ultimate solution, which should lead to the lowest LCC.

1.9 Scope and Organization of this Thesis

This thesis is organized into nine chapters, which are grouped under six primary sections. A graphical representation of the relationship between the chapters is given in [Figure 1.11](#).

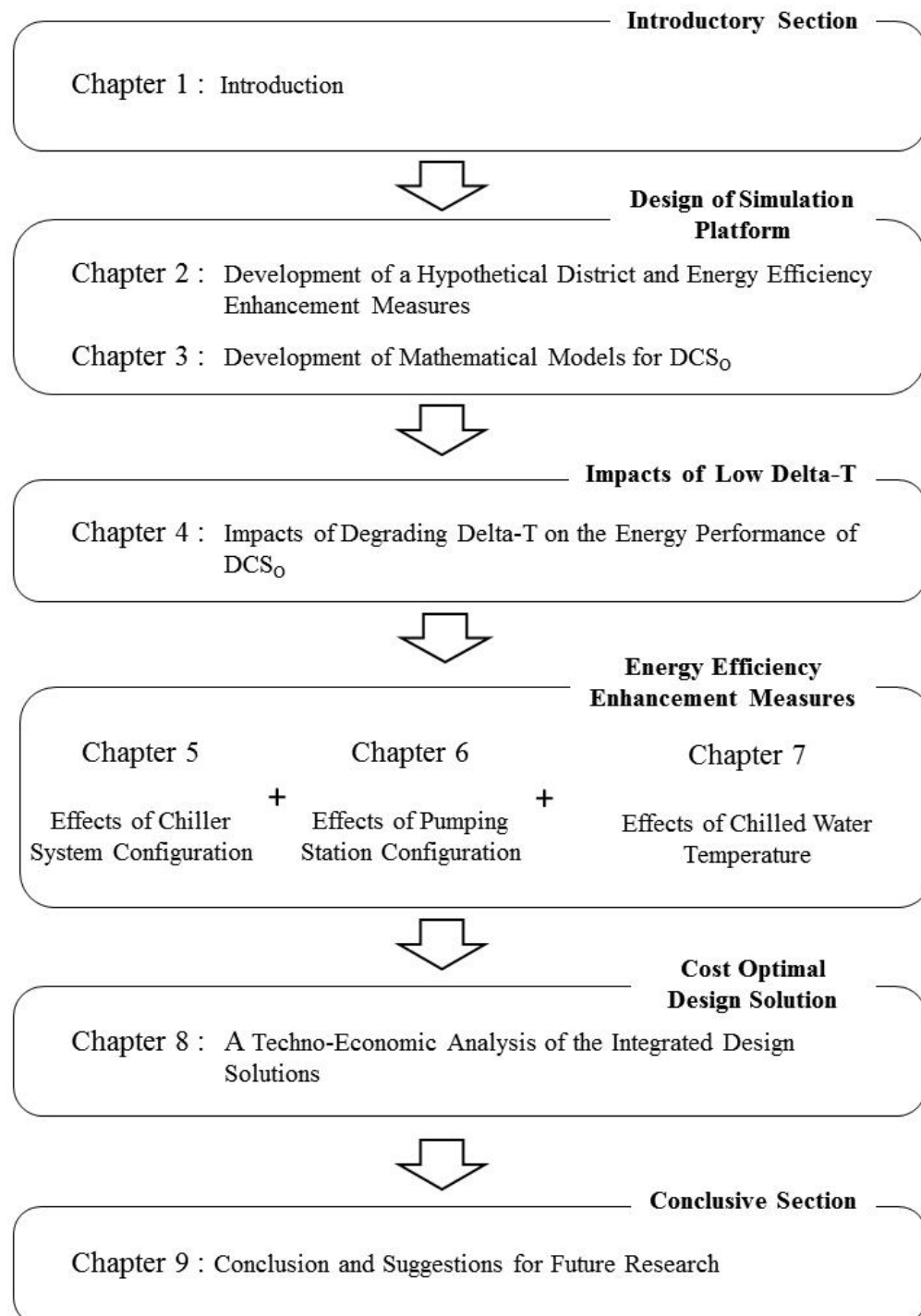


Figure 1.11 Organization of the thesis

[Chapter 2](#) presents the design of a hypothetical district comprising different combinations of buildings with a total cooling load of around 200 MW. A district cooling system, DCS_O, was designed to provide centralized chilled water to the buildings in the district. Three energy efficiency enhancement measures related to chiller system configuration, pumping station configuration, and chilled water temperature were proposed. DCS_O was treated as a base case for a comparative analysis of the effectiveness of these three measures.

In [Chapter 3](#), mathematical models were tailor-designed for all the major DCS equipment such as constant and variable speed chillers, variable speed chilled water pumps, heat exchangers, a hydraulic distribution network and the building's cooling coils. These models were used to simulate the energy performance of DCS_O designed with the energy efficiency enhancement measures mentioned in [Chapter 2](#).

[Chapter 4](#) presents the findings of a comparative analysis of the pumping energy performance of P-S and VPF systems at low delta-T and the impacts of low delta-T on the energy performance of DCS_O.

In [Chapter 5](#), the effects of changing the chiller system configuration on the energy performance of DCS_O at low delta-T via a study of the key design parameters such as the number, cooling capacity and type of chillers are evaluated. The aim was to find out an optimum combination of these parameters, which could improve the energy performance of DCS_O.

[Chapter 6](#) presents the results of an evaluation of the impacts of changing the pumping station's configuration on the energy performance of DCS_O. The measures included the use of multiple pumping stations and an unequal number of pumps in each station. In view of the vast number of pumping station combinations possible for analysis, a hydraulic gradient evaluation method was adopted to assist a quick assessment and exploration of those combinations that would be technically feasible. Furthermore, the energy performance of all these technically feasible combinations was evaluated to identify an optimum design that would lead to the lowest electricity consumption.

Chapter 7 gives a comparison of the effects of changing the design chilled water temperature on the energy performance of DCS₀. Different chilled water temperature regimes were designed and compared to find out an optimum range that could minimize the overall electricity consumption of DCS₀.

In Chapter 8, all the possible design solutions were identified, as a result of combining the energy efficiency enhancement measures mentioned in Chapters 5, 6 and 7. To reduce the number of possible solutions, a simple heuristic algorithm was developed. In addition, an LCC model was established to compare the LCC and understand the financial viability of these possible solutions. The results could also be used for determining an ultimate solution that could achieve the least long term total cost of an ownership and an optimum energy performance.

Chapter 9 concludes this thesis with a summary of the key findings reported in all preceding chapters, and is followed by some recommendations for further research that would help to design a more energy efficient DCS for Hong Kong.

Chapter 2

Development of a Hypothetical District and Energy Efficiency Enhancement Measures

2.1 Overview

This chapter consists of six sections. [Section 2.2](#) presents the design of a hypothetical district that was made up of office buildings, commercial complexes and hotels to represent the commercial districts in Hong Kong. The configuration of a hypothetical DCS for serving this district is illustrated in [Section 2.3](#). Three energy efficiency enhancement measures related to chiller system configuration, pumping station configuration and chilled water temperature are proposed in [Sections 2.4, 2.5 and 2.6](#). [Section 2.7](#) gives a summary of this chapter.

2.2 Development of a Hypothetical District

2.2.1 Scale of the Hypothetical District

A number of consultancy and research studies ([EMSD, 1999](#); [Yik et al., 2001a](#); [Yik et al., 2001b](#); [EMSD, 2003a](#); [EMSD, 2003b](#); [Chow et al., 2004b](#); [EMSD, 2005](#)) were conducted to analyze the energy benefits of adopting DCS in Hong Kong and predict the impacts of using different heat rejection methods for DCS. For example, based on

the results of energy simulation, [Chow et al. \(2004b\)](#) concluded that once-through direct seawater cooling scheme using variable flow seawater pumps was the most suitable for the South East Kowloon Development Project in Hong Kong from an economic point of view. However, these studies did not address in detail the issue of finding an optimum scale of DCS so that it could be the most cost effective in terms of initial capital investment and operating costs.

[Lo et al. \(2006\)](#) carried out a techno-economic analysis for optimization of DCS application to a large city such as Hong Kong. They studied into adopting DCS as an alternative to air-cooled air-conditioning systems (AACS) or water-cooled air-conditioning systems (WACS) in individual buildings in a district. Six hypothetical district models consisting of different types of premises were established to represent the district, which had a peak total cooling demand that ranged from 10 MW to 200 MW. The energy simulation results showed that adoption of direct seawater-cooled DCS could significantly reduce the annual electricity consumption of the water-side air-conditioning system. The savings were 20-25% and 9-15% when compared to equipping individual buildings in a district with their own AACS and WACS respectively. In that study, a cost model was also established to evaluate the economic viability of the DCS. The results showed that the energy cost saving of using DCS was high enough to compensate for the additional capital cost investment in comparison with AACS or WACS. DCS was found to be the lowest in terms of its annualized unit cost (AUC), i.e. the present value of life cycle cost per unit cooling output per annum, thus making it economically favourable.

Moreover, the DCS exhibited the effect of economy of scale. It was also found that the AUC of energy for producing chilled water decreased as the scale of the DCS increased. However, this levelled off when the cooling capacity reached 200 MW. On the other hand, the AUC of a small scale DCS, i.e. less than 20 MW, was found to be not competitive against individual buildings using WACS. In this regard, in the present study, the cooling capacity of a DCS was set at 200 MW, which is close to the scale of the biggest single DCS in Japan - the Shinjuku District Heating and Cooling Centre. This centre has a cooling capacity of 208 MW for a total service floor area of 2.2 million square meters ([EMSD, 2013](#)).

2.2.2 Types of Building

In Hong Kong, buildings in commercial districts, for example, Central, Wan Chai and Causeway Bay, are dominated by premises such as offices, retail shops, restaurants and hotels. For the KTD, the gross floor area of these premises attributes over 70% of that of the entire project (Chow et al., 2004a). Hence, these premises were used to represent the commercial district in this study. In 2001, Yik et al. (2001a) studied 23 office/commercial buildings and 16 hotels, and developed four different building models with different combinations of these premises. These four models are denoted as buildings A to D in this study (see Table 2.1). The survey data that Yik et al. (2001a) collected also provided information for the patterns of occupancy, appliance loads and lighting loads to be used in the current simulation study.

Table 2.1 Key characteristics of the four building models

	Unit	Building A	Building B	Building C	Building D
Type of building		Office	Commercial complex	Commercial complex	Hotel
No. of storey		40	32	17	26
Gross floor area:					
Office	m ²	91,000	54,600	31,850	0
Retail	m ²	0	13,650	4,550	22,750
Restaurant	m ²	0	4,550	2,275	6,825
Guestroom	m ²	0	0	0	29,575
Total	m ²	91,000	72,800	38,675	59,150
On each floor:					
Floor-to-floor height	m	3.2	3.5	3.5	3.5
Construction floor area	m ²	2,500	2,500	2,500	2,500
Air-conditioned area	m ²	2,275	2,275	2,275	2,275
Operating period:					
Weekday		0800 - 2000	0600 - 2300	0600 - 2300	0000 - 2400
Saturday		0800 - 1600	0600 - 2300	0600 - 2300	0000 - 2400
Sunday		Off	0600 - 2300	0600 - 2300	0000 - 2400

Building A represents an office-only building, whereas buildings B and C represent building complexes comprising a combination of different functional areas such as single-tenanted offices, multi-tenanted offices, retail shops and restaurants. The fourth model, i.e. building D, represents a hotel block comprising guestrooms and commercial units. In Hong Kong, the ground floors of commercial buildings or hotels are often used as entrance lobby and some commercial buildings may consist of communal podiums

above the ground floor. For simplicity, entrance lobbies and podiums were not included in the design of the four building models in this study. Figure 2.1 shows the typical floor plans and elevations of these building models and Table 2.2 shows the mixes of the five functional areas in buildings A to D.

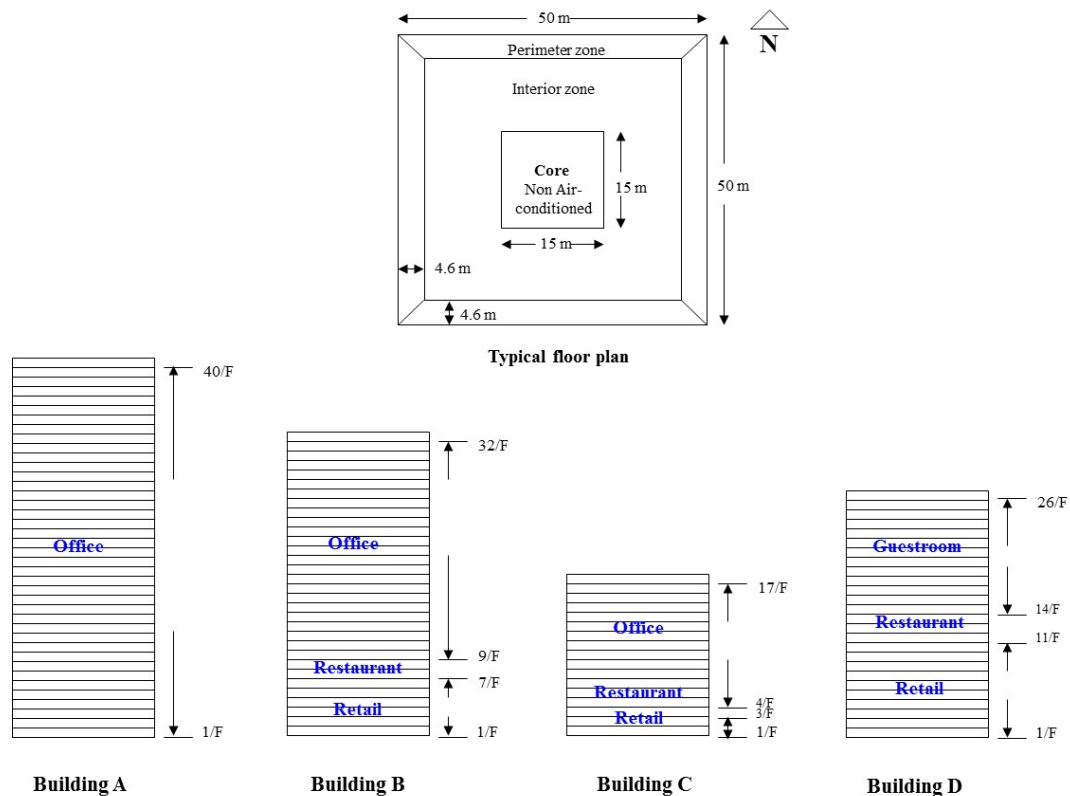


Figure 2.1 Typical layout and sections of the four building models

Table 2.2 Number of storeys occupied by the five functional areas in the four building models

Model building	Building A	Building B	Building C	Building D
Type	Office	Commercial complex	Commercial complex	Hotel
Office (single-tenanted)	40	0	0	0
Office (multi-tenanted)	0	24	14	0
Retail	0	6	2	10
Restaurant	0	2	1	3
Guestroom	0	0	0	13
Total no. of storey	40	32	17	26

2.2.3 Air-Conditioning System Design

2.2.3.1 Offices

A typical office building in Hong Kong adopts either a primary air fan-coil system or a variable air volume (VAV) system, depending on the specific usage characteristics of the individual air-conditioned space. For either system, there is typically a central primary air system supplying treated fresh air to the air-conditioned spaces.

There are two major types of office buildings in Hong Kong: multi-tenanted and single-tenanted office buildings. Fan coil units (FCU) are widely used in multi-tenanted office buildings, which may be leased or sold. The system design is relatively simple in comparison with other air-side systems. They provide more flexibility in partitioning and leasing to different tenants on the same floor.

VAV systems, which are more common among single-tenanted offices, are more energy efficient as compared to constant air volume (CAV) systems (Yang and Ting, 2000; Wei and Zmeureanu, 2009). VAV systems are increasingly equipped with variable speed fans for the much greater fan energy saving achievable. Their energy performance can be further improved through the use of an economizer cycle, which eliminates or reduces refrigeration cooling by utilizing the free cooling capacity of the ambient environment.

This, however, is rare in Hong Kong due to the large outdoor air intake and exhaust ducts and grilles or louvers required. In a VAV system, the air handling unit (AHU) treats and distributes conditioning air at a constant temperature to multiple VAV boxes placed above the false ceiling of the air-conditioned spaces. Control of air distribution is accomplished through the pressure independent VAV boxes that control the amount of supply air to the space according to the temperature of the space fed back by the indoor temperature sensor. The speed of the supply air fan inside the AHU will be controlled to regulate the flow rate of supply air to the air-conditioned spaces.

To ensure that the hypothetical building models can well represent the situation of Hong Kong, both multi-tenanted and single-tenanted offices were covered in this study. A

VAV system was designed for the single-tenanted offices in building A, while a FCU system was designed for the multi-tenanted offices in buildings B and C.

2.2.3.2 Restaurants and Retail Shops

CAV systems were designed to serve locations where a high rate of air infiltration would arise due to frequent movement of people. A constant high air flow rate is desirable to lower the space temperature and humidity when there is an in-rush of warm and humid air. The control of zone temperature is accomplished by varying the supply air temperature in response to the feedback signal from the indoor temperature sensor.

2.2.3.3 Hotel Guestrooms

Primary air fan coil systems are the most typical design for guestrooms in hotels. Their arrangement is similar to the design used for the multi-tenanted offices. A thermostat with a three-speed fan switch is provided for each FCU to control the temperature and air flow rate. The system type and design criteria of the air-conditioning system for an individual area are given in [Table 2.3](#).

Table 2.3 Design criteria for the air-conditioning system in the five functional areas

Functional area	Air-side system	Design condition ⁽¹⁾		Fresh air flow rate ⁽²⁾
		Summer	Winter	
Office (multi-tenanted)	PAU + FCU	23°C DB	22°C DB	10 l/s/person
Office (single-tenanted)	AHU + PAU (VAV)	23°C DB	22°C DB	10 l/s/person
Restaurant	AHU + PAU (CAV)	22°C DB	22°C DB	10 l/s/person
Retail shop	AHU + PAU (CAV)	22°C DB	24°C DB	1 l/s/m ²
Hotel guestroom	PAU + FCU	22°C DB	24°C DB	15 l/s/room

Remarks:

1. From [EMSD, 2012c](#).
2. From [ASHRAE, 2001](#).

2.2.4 Cooling Load Simulation

Two simulation programs, namely HTB2 (Alexander, 1996) and BECON (Yik, 1996), were used. HTB2 is a detailed building heat transfer simulation program for predicting the realistic cooling loads of buildings at different times of the year. BECON is an air-conditioning system simulation program that can predict the hourly power demand of air-conditioning equipment on the basis of the cooling loads predicted by HTB2. The weather data used in the simulation was actual hourly weather data of Hong Kong in 1989, which was identified to be a representative year (Wong and Ngan, 1993). A number of research studies verified that HTB2 and BECON could yield acceptable predictions of electricity use in commercial buildings (Lomas et al., 1997; Wong, 1997; Wan, 1998; Yik and Lam, 1998; Sat and Yik, 2003).

With the aid of these two simulation programs, the annual hourly cooling load data of all the buildings can be obtained. Figure 2.2 shows the hourly cooling load profile of the four building models in a hot summer day. Yik et al. (1999) found that the peak cooling load determined by this detailed simulation approach could be used as the basis for sizing chiller plant equipment in Hong Kong with a sufficiently high degree of confidence.

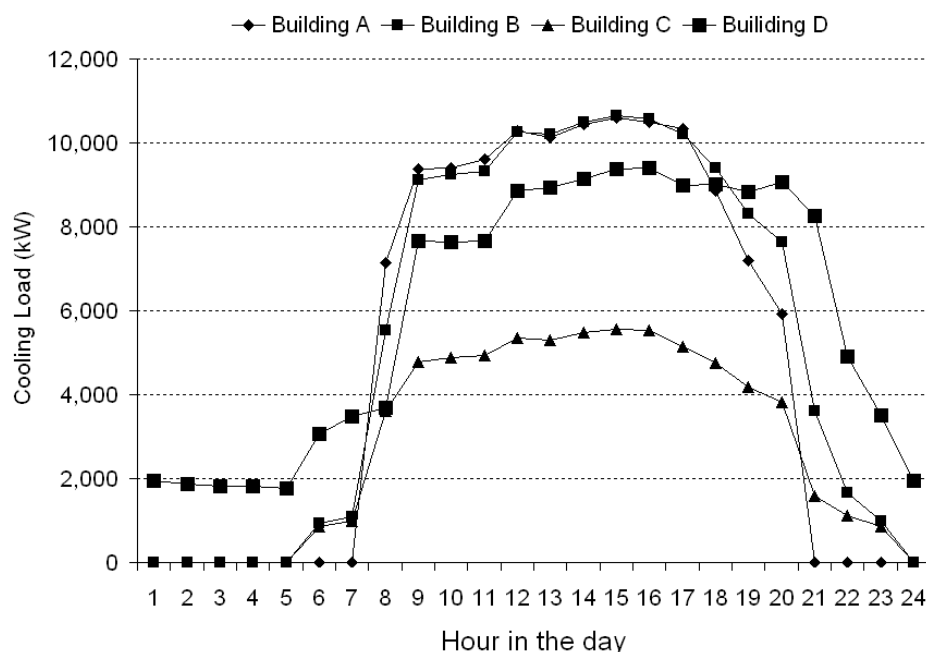


Figure 2.2 Hourly cooling load profile of the four building models in the design month (July)

2.2.5 Cooling Load of the Hypothetical District

There were six building zones in the hypothetical district. Each zone consisted of different number of building models A to D, as listed in [Table 2.4](#).

Table 2.4 Cooling load of a hypothetical district housing different combinations of building models

Building zone	No. of building model				Total no. of building
	A	B	C	D	
1	2	1	1	1	5
2	2	1	1	1	5
3	1	1	1	1	4
4	1	1	1	1	4
5	1	1	0	0	2
6	1	1	0	0	2

Due to the difference in building types, cooling loads of the four building models do not peak at the same time. As a result, the DCS plant may experience a lower peak cooling load than the sum of the buildings' individual peak cooling loads. This phenomenon is referred to as diversity. A diversity factor may be defined as the ratio of the simultaneous peak cooling load of a district to the arithmetic sum of the peak cooling loads of individual buildings in the district.

Based on the cooling load profile of each building, the simultaneous hourly cooling load to be handled by the district cooling plant can be determined. The peak cooling load of the district was estimated to be about 204.3 MW. This is less than the total peak cooling loads of all individual buildings, which is 224.5 MW, and the diversity factor value is 0.91. This reflects a reduction in the total plant cooling capacity required to serve the district when the DCS is used in lieu of discrete plants in individual buildings.

[Table 2.5](#) shows the cooling load distribution of the hypothetical district. Peak cooling capacity is needed for only a few hours in a year. For system load that is greater than 0.9, it accounts for less than 1% of the total operating hours. For the rest of the year, light to medium loads dominate the chiller plant's operating landscape. The percentage of

system load that is less than 50% accounts for 77% of the total operating hours. This suggests that the chiller system needed to be operated under part load conditions for most of the time.

Table 2.5 Cooling load distribution of the hypothetical district

% of design cooling load	% of operating hour
<10	34
$10 < L \leq 20$	12
$20 < L \leq 30$	13
$30 < L \leq 40$	12
$40 < L \leq 50$	6
$50 < L \leq 60$	4
$60 < L \leq 70$	5
$70 < L \leq 80$	6
$80 < L \leq 90$	7
$90 < L \leq 100$	1

2.3 Design of a Baseline DCS

Figure 2.3 shows a schematic diagram of the basic design of a DCS for the hypothetical district.

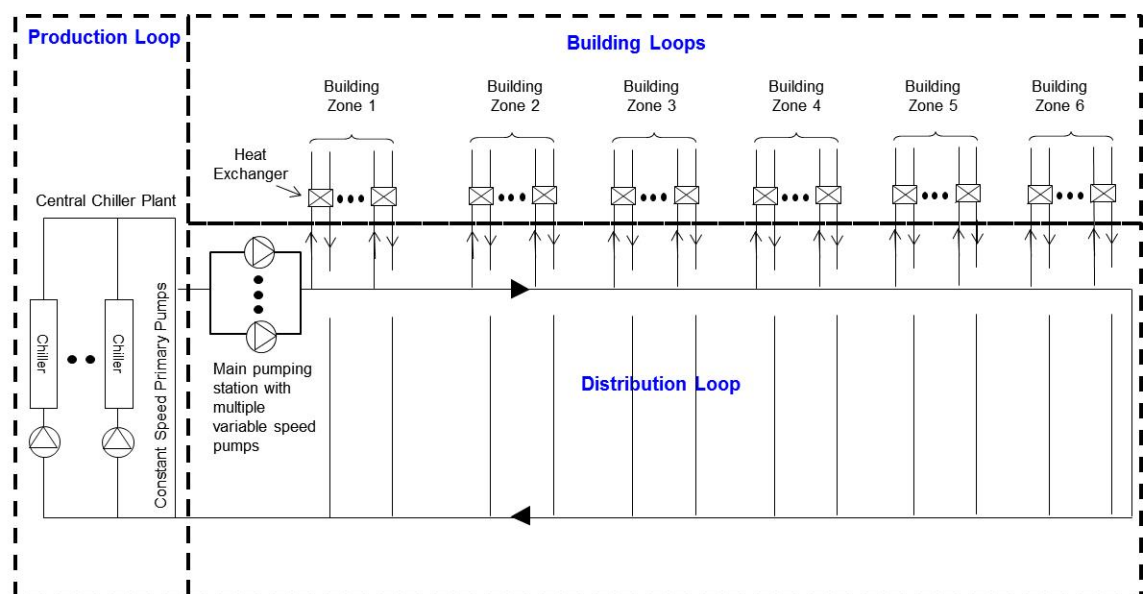


Figure 2.3 Schematic diagram of DCS₀ designed for the hypothetical district

This DCS, denoted as DCS_O, consisted of a production loop, a distribution loop and building loops. It adopted a constant primary-variable secondary scheme for chilled water distribution instead of a variable primary flow pumping scheme, because the latter is not an energy efficient chilled water pumping system in DCS. A detailed comparative analysis of the energy performance of the two schemes that justifies this selection is given in [Chapter 4](#).

The chilled water distribution system comprises constant speed primary pumps in the production loop and variable speed secondary pumps in the distribution loop. A constant chilled water flow rate is maintained in the production loop which prevents the temperature from dropping too low to impair the evaporator and avoid frequent shutdown of chillers. The variable flow in the distribution loop can maximize the difference between the supply and return chilled water temperatures, and minimize pumping system energy in the distribution loop. A decoupler by-pass pipe hydraulically decouples the production and distribution pumps so that they can each operate at a different flow rate independent of each other.

2.3.1 Production Loop

2.3.1.1 Heat rejection method is a crucial factor that affects the energy efficiency of chillers. WACS are widely adopted in DCS as they are more energy efficient than AACS. In a WACS, seawater or fresh water may be used as a cooling medium for removal of the rejected heat from the condensers of the DCS' chillers. In the absence of major rivers in Hong Kong, only those districts that are situated near the harbour can adopt seawater cooling. A study conducted by [Yik et al. \(2001b\)](#) showed that direct seawater-cooled system was the most energy efficient (COP = 5.2) in comparison with fresh water-cooled systems with cooling towers and indirect seawater-cooled systems (COP = 4.7). [Figure 2.4](#) shows a direct seawater-cooled system, which uses seawater to absorb the rejected heat from the chiller condensers in a DCS. This system is applied in large centralized air-conditioning installations where sufficient cooling water is available, such as the areas along the seafront of Victoria

Harbour. In Hong Kong, over 25 million cubic meters of seawater is used for cooling purpose everyday (Ma et al., 1998).

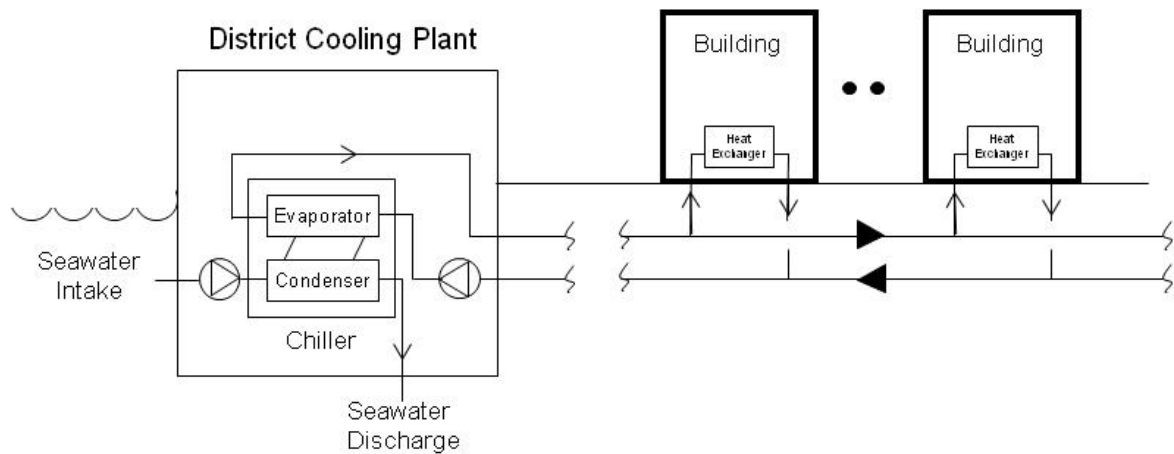


Figure 2.4 Schematic of the direct seawater cooling system of the DCS

For a direct seawater cooling scheme, the temperature of the intake seawater affects the chiller's performance significantly. Chow et al. (2004a) showed that the COP of a typical centrifugal chiller with a large cooling capacity increased by about 20% when the temperature of cooling water at the condenser inlet decreased from 30°C to 20°C (Figure 2.5). Moreover, a chiller's COP increased significantly with its design capacity, to up to 5.5 MW (or 1,500 RT). There was a significant increase in the COP if the chiller's cooling capacity was above 1,500 RT. Beyond this capacity, no significant increase in COP could be observed. They remarked that the largest R-134a type of vapour-compression chiller currently available on the market would be 22.1 MW (6,000 RT).

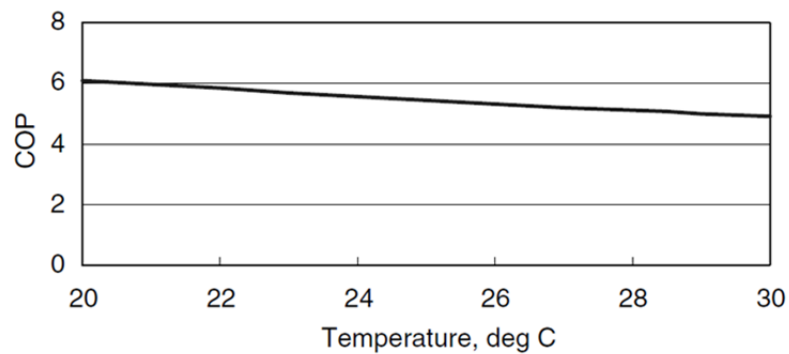


Figure 2.5 (a) COP of a typical water-cooled centrifugal chiller of different condenser inlet water temperatures

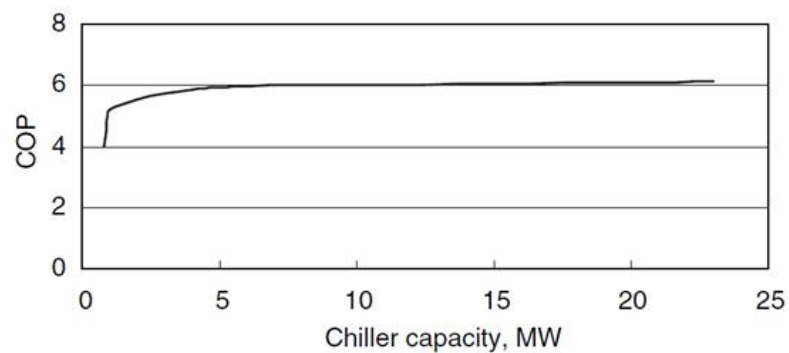


Figure 2.5 (b) COP of a typical water-cooled centrifugal chiller with different design cooling capacities
(Source: [Chow et al., 2004a](#))

2.3.1.2 Once-through direct seawater cooling was taken as the heat rejection method for all DCS analyzed in this study. The temperature of the condenser water (seawater) entering the chiller is dependent on the temperature of surface seawater available, which affects the chiller's performance significantly. To investigate the impact of entering condenser water temperature, performance data of a 2000 RT (7,034 kW) constant speed chiller with a rated chilled water supply temperature of 5°C were collected from various manufacturers for aggregation and normalisation, which is shown in [Figure 2.6](#).

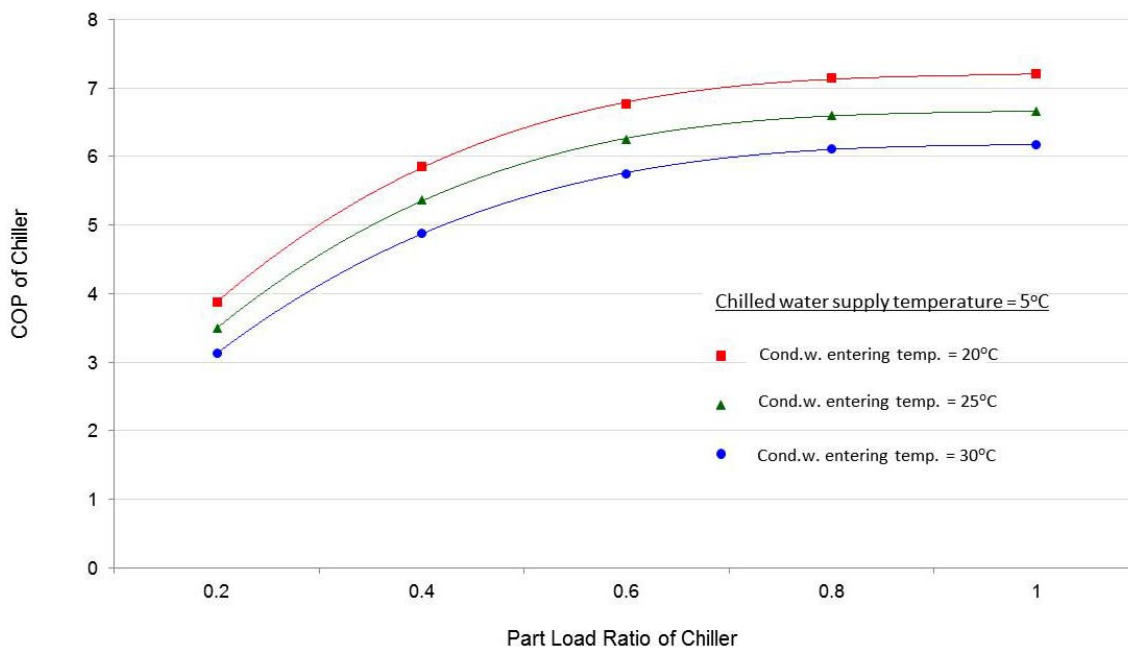


Figure 2.6 Part load performance of a 2,000 RT (7,034 kW) constant speed chiller

The COP of the chiller with a condenser water entering temperature of 20°C is about 9% higher than that of a chiller with a condenser water temperature of 25°C. Similarly, when the temperature is 25°C, the COP of the chiller is also about 9% higher than that with a condenser water temperature of 30°C.

Table 2.6 shows the statistics of the annual seawater temperatures generated by the model embedded in BECON for prediction of the year round seawater temperature. Periods in which the seawater temperature is below 25°C occupy 52% of the total operating hours in a year. This illustrates the key advantage of using direct seawater cooling for heat rejection, as chillers can run at a higher COP at almost all times throughout the year.

Table 2.6 Distribution frequency of seawater temperature in a year (Yik, 1996)

Seawater temperature, °C	% of occurrence in a year
≤ 16	0
$16 < T_{con} \leq 17$	9
$17 < T_{con} \leq 18$	6
$18 < T_{con} \leq 19$	4
$19 < T_{con} \leq 20$	5
$20 < T_{con} \leq 21$	5
$21 < T_{con} \leq 22$	4
$22 < T_{con} \leq 23$	5
$23 < T_{con} \leq 24$	6
$24 < T_{con} \leq 25$	8
$25 < T_{con} \leq 26$	12
$26 < T_{con} \leq 27$	16
$27 < T_{con} \leq 28$	20

2.3.1.3 Besides the cooling load profile, there are many factors to consider in designing the configuration of a chiller system. For example, a large number of combinations and mixes of chiller types and capacities may be considered but evaluating the performance of each of them to inform selection of the optimum one is very time consuming.

A simple approach to take is to use equally-sized chillers for a multiple-chiller system and pump, which will make it much easier to implement optimized control strategies (e.g. chiller sequencing controls) and provide greater flexibility for operation and maintenance.

In this study, a chiller plant with multiple, equally-sized and constant speed centrifugal chillers was first designed to serve as the base case for comparison with different design options (as will be described in the following chapters).

2.3.1.4 According to the information given by the manufacturers, the maximum cooling capacity of centrifugal seawater-cooled chillers that are currently available on the market is about 6,000 RT (21,102 kW). It is a normal practice to reserve about 10% as a spare cooling capacity for contingency purposes (Yu, 2001). Based on this consideration, the chiller plant taken as the base

case in this study was designed to consist of 10 x 6,000 RT (21,102 kW) chillers to meet the peak load of the hypothetical district.

- 2.3.1.5 Each chiller is equipped with a dedicated primary chilled water pump and seawater pump. All are interlocked with one another, i.e. the three would be switched on and off at the same time. The primary chilled water pump and seawater pump are constant speed and constant flow pumps.
- 2.3.1.6 To comply with the EMSD's technical guidelines for DCS ([EMSD, 2012c](#)), the DCS taken as the base case in this study was designed to supply chilled water at the temperature of 5°C. The temperature of the return chilled water was taken as 12°C. The design temperatures of the supply and return chilled water within the building loop were 7°C and 14°C respectively.

2.3.2 Distribution Loop

- 2.3.2.1 A pumping station with 10 variable speed pumps was designed downstream of the chiller plant to circulate chilled water between the DCS and the buildings.
- 2.3.2.2 The distribution loop is hydraulically de-coupled from the production loop by the decoupler bypass pipe between the two loops. All secondary pumps in the distribution loop are variable speed and variable flow pumps.
- 2.3.2.3 The diameter of the main chilled water supply and return pipes is about 1,500 mm, based on the following distribution pipe sizing criteria.
- i. Pressure drop ranges from 220 to 400 Pa per unit length ([Yik et al., 2001a ; ASHRAE, 2009](#)).
 - ii. A velocity limit of 1.2 m/s is designed for 50mm pipe and smaller. A higher velocity of up to 3 m/s ([ASHRAE, 2009](#)) was designed for pipes immediately downstream of the secondary pump so as to ensure that pipe size would not exceed 1.5 m. Since the pipes are buried underground,

noise generated as a result of high velocity flow should not be a problem (Yik et al., 2001a).

iii. The difference between the chilled water supply and return temperature of the system was designed to be 7°C (Yik et al, 2001a).

2.3.2.4 The total design pipe run of the distribution network is 2,500 km, which is close to the pipe run in the Kai Tak Development DCS project.

2.3.2.5 C_O and PS₁₋₀ denote the base chiller system and pumping station configuration, respectively. Their details are shown in Table 2.7.

Table 2.7 Design parameters of C_O and PS₁₋₀ in DCS_O

Chiller system configuration C _O		
a. Direct seawater-cooled chiller		
Type	Constant speed	
Rated cooling capacity per chiller, kW/RT	21,102 / 6,000	
Total no.	10	
Rated compressor power, kW	3,419	
COP at full load	6.17	
Integrated part load value	6.57	
Chilled water supply/return temp., °C	5 / 12	
Chilled water flow rate, l/s	718	
Condenser water entering/leaving temp., °C	29.4 / 35.4	
Condenser water flow rate, l/s	973	
b. Primary chilled water pump		
Total no.	10	
Rated flow rate, l/s	718	
Pump head, m	16.8	
Rated power, kW	164.4	
c. Seawater pump		
Total no.	10	
Rated flow rate, l/s	973	
Pump head, m	16.8	
Rated power, kW	223.3	
Pumping station configuration PS ₁₋₀		
d. Secondary chilled water pump		
Total no.	10	
Rated flow rate, l/s	718	
Pump head, m	56.9	
Rated power, kW	576.0	

2.3.3 Building Loop

- 2.3.3.1 An energy transfer station is the interface between the building's cooling system and the DCS. Each station consists of heat exchangers, isolation and control valves, controllers, measurement equipment and energy meters. The building's chilled water is cooled to the design supply temperature by the heat exchanger with chilled water of the distribution loop flowing at the other side. The energy transfer station is located at the perimeters of the building to ensure ease of installation and operation and maintenance. Only one energy transfer station will be provided for each building.
- 2.3.3.2 Heat exchangers are the key components that separate the building's chilled water network from the DCS' distribution network and facilitate heat transfer from the former to the latter. It is vital to minimize the log mean temperature difference of the heat exchanger, which requires the use of a close temperature approach, i.e. within 1°C (EMSD, 2012b). Plate type heat exchanger is the only type of heat exchanger that can serve this purpose (Skagestad and Mildenstein, 1999).
- 2.3.3.3 Each building in the building loop has its own variable speed pumps to circulate chilled water through the air-side equipment, i.e. FCU and AHU. Two-way control valves are used in the air-side equipment to modulate the chilled water flow rate according to the cooling loads on them. At light load, the valves are closed (partially or fully), resulting in a pressure rise in the building loop. A differential pressure sensor measures the pressure rise and this signal is transmitted to the pump speed controller which alters the speed and hence the chilled water flow rate of the variable speed pumps.

2.4 Design of Energy Enhancement Measure - Chiller System Configuration

The energy performance of a chiller plant can be affected by varying the major influential system parameters, such as the number, cooling capacity and type of chillers. This section reviews the impacts of varying each parameter to inform selection of the

range of these parameters to be considered in the attempt to find out an optimum chiller system configuration.

2.4.1 Varying the Number of Chiller

Lee and Lee (2007) pointed out that most chillers in commercial buildings had an optimum operating point that corresponds to the peak energy efficiency, which would occur at a specific part load ratio. This optimum operating point of typical chillers is about 80% of the maximum capacity (Trane, 1989; Lee and Lee, 2007). Hence, running more chillers than the minimum number that can marginally meet the load may reduce the energy use of the chillers. On the other hand, other factors also need to be considered, such as spatial requirement, capital cost investment and energy consumption of other associated equipment, including the chilled and condenser water pumps. More chillers in operation means that more energy will be consumed by the pumps because the chilled water pump and the seawater pump are interlocked with the chiller, and will also be operated whenever their associated chiller is run. Whether the energy consumption of the extra pumps may be fully offset by the energy saving due to operating those chillers needs to be evaluated in detail when an optimized sequencing control strategy is formulated.

No concrete guidelines can be found in the open literature for determining the optimum number of chillers for a DCS. This deserves further exploration. Reference was made to the DCS plant in Japan's Shinjyuku Shin-toshin, which has more or less the same design cooling capacity as the DCS for the hypothetical district in this study. This Japanese chiller plant consists of 12 turbo and absorption chillers, including 3 x 10,000 RT (35,170 kW), 2 x 7,000 RT (24,619 kW), 1 x 4,000 RT (14,068 kW), 1 x 2,870 RT (10,094 kW), 1 x 2,000 RT (7,034 kW), 2 x 2,065 RT (7,263 kW) and 2 x 1,000 RT (3,517 kW) chillers. The total installed cooling capacity is 59,000 RT (208 MW). To avoid complicating the present study, the maximum number of chillers was set to be 15.

2.4.2 Unequally-Sized Chillers

It is a common practice to use equally-sized chillers in designing a chiller system

(Mcquay International, 2001; Lee and Lee, 2007). This has merits because pumps or cooling towers are of the same size and are interchangeable, and these are more flexible to operate and maintain. On the other hand, Landman (1996) and Chan and Yu (2004) advocated the use of unequally-sized chillers for a chiller plant, as this could prolong their operation at near full load and reduce electricity consumption of the chiller plant. It is because unequally-sized chillers allow selection of the most suitable combination of chillers, which can match more closely the cooling load demand at different operational periods and achieve the best energy performance.

Therefore, multiple chillers of unequal sizes were considered in this study to see whether they could help alleviate the adverse impacts of the low delta-T problem. Traditionally, this can be accomplished by using the rule of thumb, i.e. the size of the small chiller is one-third or two-thirds of the size of the largest chiller in a plant. Given that the largest cooling capacity of available direct seawater-cooled chiller is 6,000 RT, which is also the largest chiller designed for DCS on the commercial market, the chiller plant in the present hypothetical DCS model was thus designed with three different sizes: 2,000 RT, 4,000 RT and 6,000 RT. Within the limit of 15 chillers at maximum, the combinations of chillers are: 5 x 6,000 RT, 5 x 4,000 RT and 5 x 2,000 RT, which together would provide a total of 60,000 RT (about 210 MW) (Hitachi Appliance Inc., 2013). This allows flexibility for running different combinations of chillers to meet the variable load, in particular, during low load conditions.

2.4.3 Variable Speed Chillers

Over the last two decades, the cost of variable speed drives has come down significantly due to advances in technology and expansion of market size. This technology has also been applied to chillers. Qureshi and Tassou (1996) conducted a review of the use of variable speed chiller, and confirmed that variable speed drives had been applied successfully to perform capacity modulation for chiller compressors. The variable speed chillers bring about superior part load efficiency, as compared to chillers using multiple constant speed compressors with cycling control.

As degrading delta-T occurs most often when the cooling load drops to about two-thirds

to one-half of the design cooling load (Taylor, 2002a), variable speed chillers were adopted in this study to assess their effectiveness in mitigating the impacts of low delta-T on the electricity consumption of the chiller plant.

2.4.4 Chiller System Configuration

The base case chiller system configuration, C_O , consisted of 10 x 6,000 RT (21,102 kW) constant speed chillers. With reference to the three design parameters described above, five additional chiller system configurations, denoted as C_A , C_B , C_C , C_D and C_E , were formed, as summarized in Table 2.8. Their total installed cooling capacities still remained the same as that of C_O , i.e. 60,000 RT (21,1020 kW). The effectiveness in enhancing the energy performance of DCS_O at low delta-T, by replacing C_O with one of these chiller system configurations is evaluated in this study. However, the same design of chilled water distribution system, including the number of pumping stations and the chilled water temperatures, was applied to all these alternative chiller plants.

Table 2.8 Design parameters of chiller system configurations C_O , C_A , C_B , C_C , C_D and C_E

Chiller system configuration	C_O	C_A	C_B	C_C	C_D	C_E
No. of chiller	10	10	15	15	15	15
Size	Equal	Equal	Equal	Unequal	Equal	Unequal
Cooling capacity	10 x 6,000 RT	10 x 6,000 RT	15 x 4,000 RT	5 x 2,000 RT 5 x 4,000 RT 5 x 6,000 RT	15 x 4,000 RT	5 x 2,000 RT 5 x 4,000 RT 5 x 6,000 RT
Type	Constant speed	Variable speed	Constant speed	Constant speed	Variable speed	Variable speed

The design details of the chillers and the associated primary chilled water pumps and seawater pumps in these six chiller system configurations, including those of the base case, are summarized in Table 2.9. A detailed evaluation of their effectiveness in improving the energy performance over that of DCS_O at low delta-T is presented in Chapter 5.

Table 2.9 Design details of chiller system configurations C_O, C_A, C_B, C_C, C_D and C_E

Chiller system configuration	C _O	C _A	C _B	C _C			C _D	C _E		
1. Seawater-cooled chiller										
Type	Constant speed	Variable speed	Constant speed	Constant speed	Constant speed	Constant speed	Variable speed	Variable speed	Variable speed	Variable speed
Rated cooling capacity per chiller kW (RT)	21,096 (6,000)	21,096 (6,000)	14,064 (4,000)	7,032 (2,000)	16,174 (4,000)	21,096 (6,000)	14,064 (4,000)	7,032 (2,000)	16,174 (4,000)	21,096 (6,000)
Total no.	10	10	15	5	5	5	15	5	5	5
Rated compressor power, kW	3,419	3,419	2,279	1,140	2,279	3,419	2,279	1,140	2,279	3,419
COP at full load	6.17	6.17	6.17	6.17	6.17	6.17	6.17	6.17	6.17	6.17
Integrated part load value	6.57	9.76	6.57	6.57	6.57	6.57	9.76	9.76	9.76	9.76
Chilled water supply/return temp, °C	5/12	5/12	5/12	5/12	5/12	5/12	5/12	5/12	5/12	5/12
Chilled water flow rate, l/s	718	718	478	239	478	718	478	239	478	718
Condenser water entering/leaving temp, °C	29.4/35.4	29.4/35.4	29.4/35.4	29.4/35.4	29.4/35.4	29.4/35.4	29.4/35.4	29.4/35.4	29.4/35.4	29.4/35.4
Condenser water flow rate, l/s	973	973	649	324	649	973	649	324	649	973
2. Primary chilled water pump										
Total no.	10	10	15	5	5	5	15	5	5	5
Rated flow rate, l/s	718	718	478	239	478	718	478	239	478	718
Pump head, m	16.8	16.8	16.8	16.8	16.8	16.8	16.8	16.8	16.8	16.8
Rated power, kW	164.4	164.4	109.6	56.9	109.6	164.4	109.6	56.9	109.6	164.4
3. Seawater pump										
Total no.	10	10	15	5	5	5	15	5	5	5
Rated flow rate, l/s	973	973	649	324	649	973	649	324	649	973
Pump head, m	16.8	16.8	16.8	16.8	16.8	16.8	16.8	16.8	16.8	16.8
Rated power, kW	223.3	223.3	149.1	75.3	149.1	223.3	149.1	75.3	149.1	223.3

2.5 Design of Energy Enhancement Measure - Pumping Station Configuration

In the base case DCS_O, only one main pumping station, PS₁₋₀, was located immediately downstream of the chiller plant. Ten identical variable speed distribution pumps were designed to simplify maintenance and provide interchangeability of parts.

However, a single pumping station designed for a large district may not be the most cost-effective design. It is because the design pump head and flow rate are very large so as to ensure that the chilled water can be distributed to the far end of the district. Under such circumstances, the building near the pumping station will be over-pressurized. The pressure is much more than that required in these buildings for overcoming the internal piping and cooling coil losses. Pressure reducing valves or other energy consuming mechanical devices have to be installed to prevent over-pressurizing the buildings, hence making the pumping station not energy efficient. Moreover, there is a large variation of distribution friction among the buildings in the district. Balance valves have to be installed to overcome this problem.

Hence, two design initiatives were investigated in this study to optimize the energy performance of the pumping station. These include the use of:

- i. multiple pumping stations – In addition to the main pumping station, additional booster pumping stations were adopted at different locations along the main chilled water supply or return pipes of the distribution loop to assist circulation of chilled water. This can help reduce the pressure head, and hence the power demand of the main station, while those pumping stations downstream will only need to handle a smaller chilled water flow rate, which will also help reduce the pumping energy use; and
- ii. multiple pumps in each pumping station – To further optimize the design of the pumping stations(s), different number of pumps for each station will be explored. For simplicity, however, this number was limited to 5, 10 or 15.

2.5.1 Multiple pumping stations

As shown in Figure 2.7, excluding that of the main pumping station, a total of 11 locations along the main chilled water supply or return pipes were identified to be possible sites for the booster pumping stations for distributing chilled water to all the buildings and returning it to the central plant.

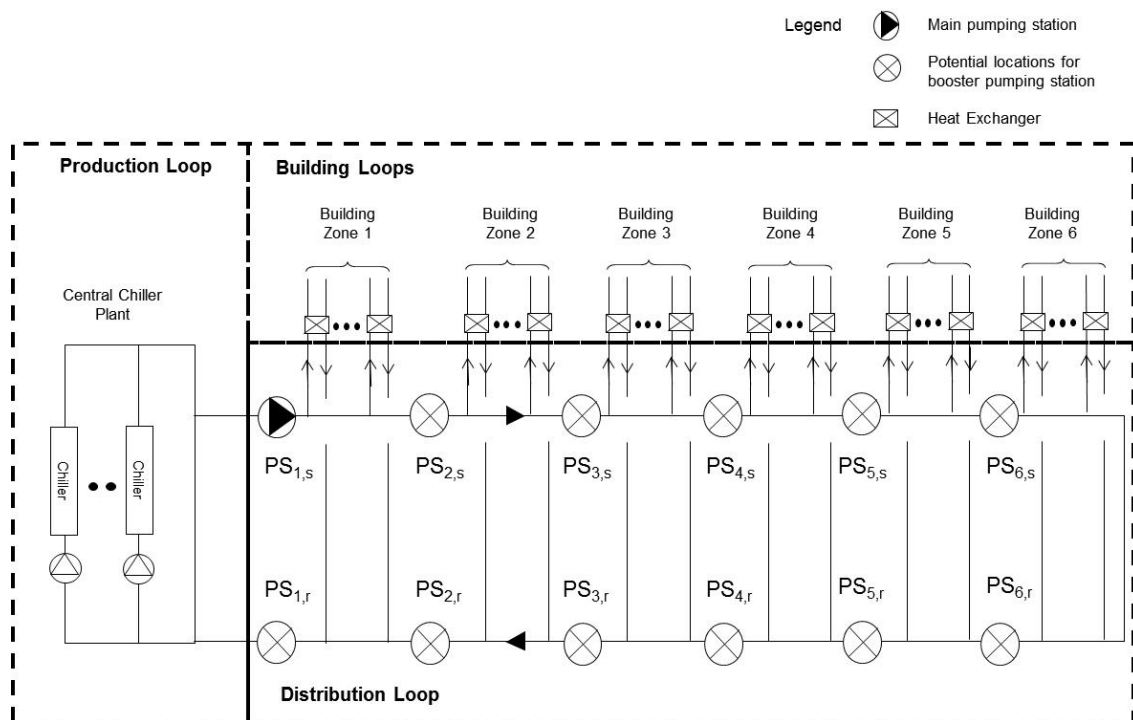


Figure 2.7 Potential locations for pumping stations

As an example, for the case with two pumping stations in the distribution loop, one main pumping station must be located before the connection to the first served building, and one booster pumping station may be at any one of the 11 locations. Therefore, there are 11 possible combinations of location for these two pumping stations. Similar arrangement can be made in designing three, four, five or six pumping stations. According to the calculation in Table 2.10, there were 55, 165, 330 and 462 possible combinations of locations for placing three, four, five and six pumping stations in the distribution loop. As a result, there were a total of 1,024 possible combinations for cases with one to six pumping stations.

Table 2.10 Total number of combinations of pumping stations (PS)

No. of PS	Possible combination of PS at chilled water supply and/or return sides	No. of combination	Total no. of combination
1	Main PS	1	1
2	Main PS plus <ul style="list-style-type: none"> • 1 PS at the supply side • 1 PS at the return side 	5 ($= {}_5C_1$) 6 ($= {}_6C_1$)	11
3	Main PS plus <ul style="list-style-type: none"> • 2 PS at the supply side • 2 PS at the return side • 1 PS at the supply and 1 PS at the return side 	10 ($= {}_5C_2$) 15 ($= {}_6C_2$) 30 ($= {}_5C_1 \times {}_6C_1$)	55
4	Main PS plus <ul style="list-style-type: none"> • 3 PS at the supply side • 3 PS at the return side • 1 PS at the supply and 2 PS at the return side • 2 PS at the supply and 1 PS at the return side 	10 ($= {}_5C_3$) 20 ($= {}_6C_3$) 75 ($= {}_5C_1 \times {}_6C_2$) 60 ($= {}_5C_2 \times {}_6C_1$)	165
5	Main PS plus <ul style="list-style-type: none"> • 4 PS at the supply side • 4 PS at the return side • 1 PS at the supply and 3 PS at the return side • 3 PS at the supply and 1 PS at the return side • 2 PS at the supply and 2 PS at the return side 	5 ($= {}_5C_4$) 15 ($= {}_6C_4$) 100 ($= {}_5C_1 \times {}_6C_3$) 60 ($= {}_5C_3 \times {}_6C_1$) 150 ($= {}_5C_2 \times {}_6C_2$)	330
6	Main PS plus <ul style="list-style-type: none"> • 5 PS at the supply side • 5 PS at the return side • 1 PS at the supply and 4 PS at the return side • 4 PS at the supply and 1 PS at the return side • 3 PS at the supply and 2 PS at the return side • 2 PS at the supply and 3 PS at the return side 	1 ($= {}_5C_5$) 6 ($= {}_6C_5$) 75 ($= {}_5C_1 \times {}_6C_4$) 30 ($= {}_5C_4 \times {}_6C_1$) 150 ($= {}_5C_3 \times {}_6C_2$) 200 ($= {}_5C_2 \times {}_6C_3$)	462
		Total	1,024

2.5.2 Multiple pumps in each pumping station

Additionally, the number of pumps in each pumping station may be 5, 10 or 15. Taking the design shown in Figure 2.8 as an example, it is one of the combinations using three pumping stations in a distribution loop. It consists of one main pumping station at location $PS_{1,s}$ and two booster pumping stations at locations $PS_{3,s}$ and $PS_{2,r}$. Figure 2.8 (a) shows a design with the same number of pumps in all three stations, and Figure 2.8 (b) represents an arrangement of different number of pumps in each station.

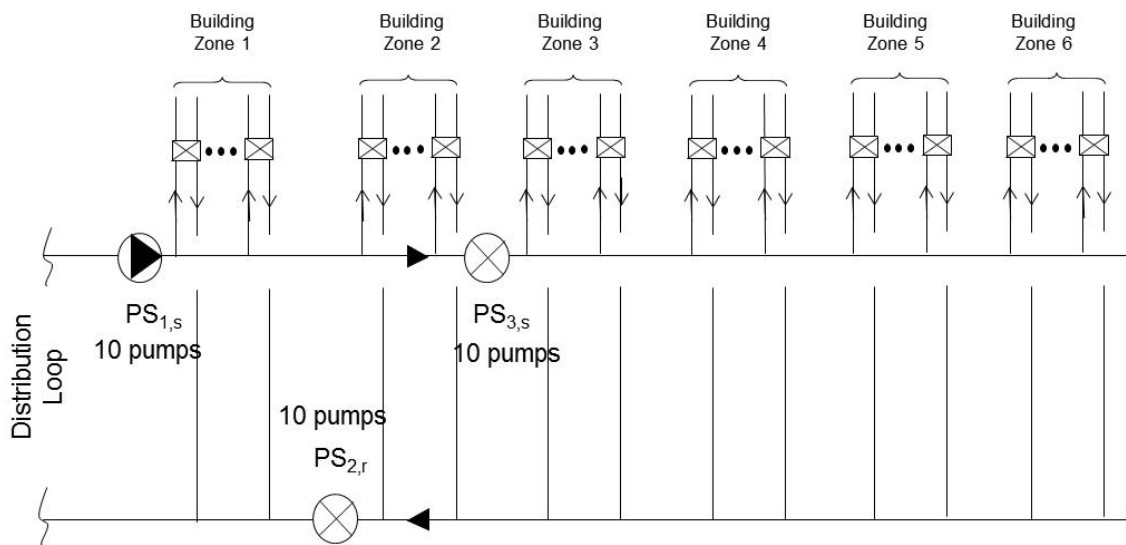


Figure 2.8 (a) An example of a combination of three pumping stations with the same number of pumps in each station

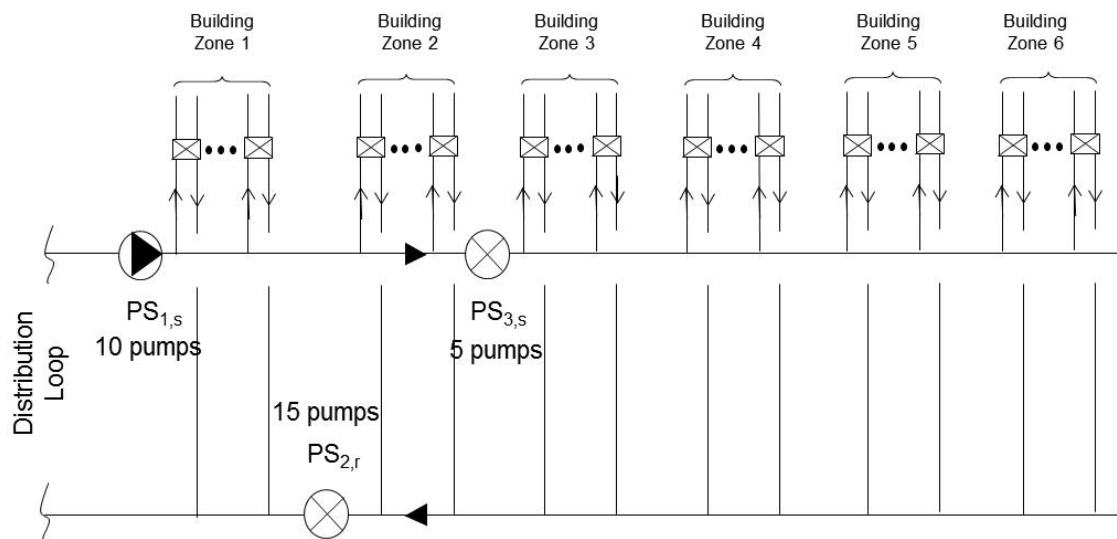


Figure 2.8 (b) An example of a combination of three pumping stations with different number of pumps in each station

Using this approach, a total of 27 (i.e. = 3^3) “arrangements” based on the variation in pump number can be identified for this particular three-pumping station combination, as shown in Table 2.11. In this chapter, the phrase “pumping station arrangement” specifically refers to the grouping of pumping station based on the number of pumps.

Table 2.11 An example showing the different arrangements based on the number of pumps, i.e. with 5, 10 or 15 pumps in each pumping station

Arrangement	No. of pump in each pumping station		
	PS _{1,s}	PS _{3,s}	PS _{2,r}
1	5	5	5
2	5	5	10
3	5	5	15
4	5	10	5
5	5	10	10
6	5	10	15
•	•	•	•
•	•	•	•
•	•	•	•
27	15	15	15

} 27 arrangements

As shown in [Table 2.10](#), there are 55 combinations of using three pumping stations. Hence, there are 1,485 (= 27 arrangements x 55 combinations) pumping station arrangements that are using three pumping stations.

The above principle was applied to determine the total number of pumping station arrangement for using N_{ps} number of pumping stations. For a chilled water distribution network designed with N_{ps} number of pumping stations, there are N_{comb} number of combinations. For each combination of N_{ps} number of pumping stations, there are $3^{N_{ps}}$ number of pumping station arrangements. Hence, the total number of pumping station arrangements of using N_{ps} number of pumping stations that have N_{comb} number of combination is $N_{comb} \times 3^{N_{ps}}$.

As shown in [Table 2.10](#), there are 1, 11, 55, 165, 330 and 462 combinations of one, two, three, four, five and six pumping stations respectively. The number of pumping station arrangement for each combination of one, two, three, four, five and six pumping stations would be 3 ($=3^1$), 9 ($=3^2$), 27 ($=3^3$), 81 ($=3^4$), 243 ($=3^5$) and 729 ($=3^6$) respectively.

Hence, this led to 3 (= 1 x 3), 99 (= 11 x 9), 1,485 (= 55 x 27), 13,365 (= 165 x 81), 80,190 (= 330 x 243) and 336,798 (= 462 x 729) arrangements that used one, two, three, four, five and six pumping stations.

There are a total of 431,940 “arrangements” (= 3 + 99 + 1,485 + 13,365 + 80,190 + 336,798).

A detailed evaluation of the effectiveness of these pumping station arrangements for improving the energy performance of DCS_0 is presented in [Chapter 6](#).

2.6 Design of Energy Enhancement Measure - Chilled Water Supply and Return Temperatures

In a chiller plant, changes in the design chilled water supply and return temperatures will affect the energy performance of the chiller, secondary chilled water pumps, seawater pumps and heat losses, which are discussed as follows.

For a chiller, its energy performance, typically gauged by its COP, will increase by raising the design chilled water supply temperature. A higher design chilled water supply temperature will lead to a higher evaporating temperature of the refrigerant in the evaporator. This will result in a reduced pressure difference between the evaporator and the condenser and hence a reduction in the power demand of the compressor. As a result, the COP of the chiller will increase when it is outputting the same rate of cooling.

For every 1°C drop in the chilled water supply temperature, there will be an increase of about 2.4% in the energy input (Wulfinghoff, 2004). However, changing the chilled water return temperature has no significant impact on the COP and hence the power demand of chillers (Taylor, 2011). This is because most chillers are equipped with an output capacity control system that utilizes the chilled water supply temperature as the feedback of cooling demand rather the chilled water return temperature. According to the data provided by a number of manufacturers regarding the COP of a 1,000 RT (3,517 kW) variable speed chiller, the COP of the chiller will only vary by less than 0.1% if the chilled water return temperature changes from 11°C to 12°C, given that the chilled water supply temperature is fixed at either 4°C, 5°C, 6°C or 7°C.

For secondary pumps, their energy consumption is proportional to the product of pressure head and chilled water flow rate. The chilled water flow rate at a given load is inversely proportional to the difference between the supply and return chilled water temperatures, denoted as a “temperature difference”. Halving the temperature difference at a given load would effectively double the flow requirements. The energy required to pump chilled water throughout the district will be most immediately and directly increased by decreasing the temperature difference. This will increase the energy

consumption of the secondary pumps in the pumping station, which are the second largest energy consuming component in DCS.

Regarding the seawater pump, its power demand depends on the pressure head and seawater flow rate. If the seawater pump configuration is not changed, there is no change in the pressure head of the pump. Estimation of the seawater flow rate for once-through condenser cooling is determined on the basis of the heat rejection rate of chillers. It is taken as the sum of cooling capacity and the rated power demand of the chiller. Hence, the flow rate of seawater pumps can be expressed by [Equation 2.1](#).

$$\text{Flow Rate} = \frac{\text{Chiller Cooling Capacity}}{\rho_{condw} c_{condw} \Delta T_{condw}} \times \left(1 + \frac{1}{\text{COP}} \right) \quad (2.1)$$

where c_{condw} is the specific heat capacity of condensing water, ρ_{condw} is the density of condensing water and ΔT_{condw} is the difference of condensing water entering and leaving temperatures.

Regarding heat loss, it is the most common method to build the DCS by laying the chilled water pipe underground. The difference between the typical supply and return temperatures of chilled water and the soil is so low that it is possible to build a DCS without cold insulation ([International Energy Agency, 2002](#)). In Hong Kong, it is typical to insulate the chilled water pipe by phenolic foam. Hence, heat loss of the pipework with insulation in the earth is minimal and was taken into account in the energy simulation.

According to the above analysis, changing the chilled water supply and return temperatures will mainly affect the energy performance of chillers, secondary chilled water pumps and seawater pumps. It is worth investigating the impacts of different temperature regimes to find out an optimum chilled water temperature that can balance the power demand of chillers and pumps and minimize the impacts of low delta-T on the DCS.

The design chilled water supply temperature of DCS_O was 5°C. The design temperature of the chilled water returning from the building loop was 12°C. To simulate the effects of changing these two design temperatures, the base chilled water supply and return temperatures were increased or decreased by ±1°C to form eight temperature regimes. The resulting combinations are listed in [Table 2.12](#).

Table 2.12 Chilled water temperature regimes

Temp regime	Chilled water temp, °C		
	Supply	Return	Delta-T
T ₀ [#]	5	12	7
T ₁	4	11	7
T ₂	4	12	8
T ₃	4	13	9
T ₄	5	11	6
T ₅	5	13	8
T ₆	6	11	5
T ₇	6	12	6
T ₈	6	13	7

Remark:

- This is the base temperature regime of DCS_O.

[Table 2.13](#) shows the technical details of base DCS_O under different temperature regimes. A detailed evaluation of the effectiveness of these eight temperature regimes in improving the energy performance of DCS_O is presented in [Chapter 7](#).

Table 2.13 Design details of the chiller system configuration and pumping stations under different temperature regimes

Temp regime	T ₀	T ₁	T ₂	T ₃	T ₄	T ₅	T ₆	T ₇	T ₈
1. Seawater-cooled chiller									
Type	Constant speed								
Rated cooling capacity per chiller, kW / RT	21,102/6,000								
Total no.	10								
Rated compressor power, kW	3,419								
Condenser water entering/leaving temp, °C	29.4/35.4								
Condenser water flow rate (l/s)	973	975	975	975	973	973	971	971	971
COP at full load	6.17	6.07	6.07	6.07	6.17	6.17	6.26	6.26	6.26
Integrated part load value	6.57	6.41	6.41	6.41	6.57	6.57	6.73	6.73	6.73
Chilled water supply/return temp, °C	5/12	4/11	4/12	4/13	5/11	5/13	6/11	6/12	6/13
Chilled water flow rate (l/s)	718	718	628	558	837	628	1005	837	718
2. Primary chilled water pump									
Total no.	10								
Pump head, m	16.8								
Flow rate, l/s	718	718	628	558	837	628	1005	837	718
Rated power, kW	164.4	164.4	144.6	128.3	191.4	144.6	230.7	191.4	164.4
3. Seawater pump									
Total no.	10								
Pump head, m	16.8								
Flow rate, l/s	973	975	975	975	973	973	971	971	971
Rated power, kW	223.3	223.9	223.9	223.9	223.3	223.3	222.9	222.9	222.9
4. Secondary chilled water pump									
Total no.	10								
Flow rate, l/s	718	718	628	558	837	628	1005	837	718
Pump head, m	56.9	56.9	54.4	52.7	60.7	54.4	67	60.7	56.9
Rated power, kW	576.0	576.0	481.2	423.7	709.4	481.2	920.2	709.4	576.0

2.7 Summary

This chapter describes the establishment of a hypothetical district, which comprised different types of buildings to represent the typical commercial districts in Hong Kong. The design cooling load of this hypothetical district was about 200 MW, which is close to the scale of the biggest single DCS in Japan.

Moreover, a district cooling system, DCS_O , was designed to provide centralized chilled water supply to buildings in the district. This DCS comprised a production loop, a distribution loop and as many building loops as there were buildings in the district. In the primary loop, inside the centralized chiller plant C_O , there were 10 constant speed chillers, each with a dedicated primary chilled water pump and a seawater pump. In the distribution loop, there was one pumping station, PS_{1-0} , which comprised 10 variable speed chilled water pumps for distributing chilled water to each building served by the DCS. The design chilled water supply and return temperatures were 5°C and 12°C respectively. Heat exchangers were used for heat transfer from the chilled water in the building loops to the chilled water in the distribution loop.

Variations in the design parameters were introduced to form: five combinations of chiller system configuration, eight temperature regimes and 431,490 arrangements of pumping station. DCS_O was taken as a base case for comparing the effectiveness of these variations. The results will be further discussed in [Chapters 5, 6 and 7](#).

Chapter 3

Development of Mathematical Models for DCS_O

3.1 Overview

After the configuration of the reference DCS (denoted as DCS_O) is determined, mathematical models for its major components have to be developed for prediction of annual energy consumption of the centralized chiller plant and pumping station such that the effects of applying various energy efficiency enhancement measures to DCS_O can be compared. These components include constant and variable speed chillers, primary chilled water and seawater pumps, secondary chilled water distribution pumps, chilled water distribution network, heat exchangers and cooling coils of buildings.

A review of literature has shown that mathematical models for most of the abovementioned components have been developed but nearly all of them are for application to systems in buildings rather than a DCS. However, the operating conditions of these components in a system serving a single building are different from those of the components in a DCS. For example, the chilled water supply temperature of a DCS can be set as low as 4°C instead of 7°C, which is widely applied to buildings. For the present study, it was of practical importance to limit the complexity of the component models, as long as they could predict the performance of the components to an acceptable degree of accuracy. Moreover, mathematical models of the chilled water distribution network had to be tailor-made to suit the purpose of this study.

The mathematical models developed are discussed in [Sections 3.2 to 3.9](#), which include models for cooling coils of buildings, heat exchangers, chilled water distribution network, secondary variable speed pumps, constant and variable speed chillers, and primary chilled water and seawater pumps. [Figure 3.1](#) outlines the mathematical models developed for this study.

	Model	Application	Output of Model
Building Loops	Cooling load simulation model HTB2 + BECON	Offices, restaurants, retail shops and hotel guestrooms in buildings	Hourly cooling load of each building model and the hypothetical district
	Cooling coil models	Cooling coil	Hourly chilled water flow rate of each building model
	Heat exchanger model	Heat exchanger	Hourly chilled water flow rate in the distribution network
Distribution Loop	Chilled water distribution network model	Distribution network	Hourly pressure head of the distribution network
	Variable speed pump model	Secondary chilled water pump	Hourly power demand of secondary pumps
	Pumping station model	Pumping station configuration	Annual electricity consumption of various pumping station configurations
Production Loop	Constant & variable speed chiller models	Chiller in DCS	Hourly power demand of chillers
	Constant speed pump model	Primary chilled water pump Seawater pump	Hourly power demand of pumps
	Chiller plant model	Chiller system configuration	Annual electricity consumption of chillers, primary chilled water pumps and seawater pumps

Figure 3.1 An outline of the mathematical models and their outputs for this study

3.2 Cooling Coil Model

3.2.1 Development of Cooling Coil Models

Over the last 30 years, different types of cooling coil models have been developed for predicting the performance of cooling coils operating at different air and chilled water flow rates and entering states. They can be classified into theoretical and empirical models (Wang et al., 2004).

A theoretical model is typically developed on the basis of energy balance and heat transfer principles and it takes into account the cooling coil construction and geometry, and the physical properties of the composing materials and working fluids. Such models are usually composed of a set of rather complex equations and are used to provide a basis for the design of cooling coils or detailed performance simulation (Brandemuehl, 1993; Lebrun, 1999; Underwood and Yik, 2004).

Empirical models are typically developed based on a specific coil or family of coils of similar configuration. However, their applications are limited to the specific coil design based upon which they were developed, and may be restricted to a limited range of operating conditions. Taking the empirical model developed by Stoecker (1975) as an example, as the transport properties are not included in the equations, a given set of empirical constants can only be used to predict the performance of a coil provided the coil is handling the same fluid as that used when data was obtained for developing the coil model (Wang et al., 2004). Separate sets of empirical constants need to be established for different fluids (Rabehl, 1999). Moreover, in order to estimate the values of these empirical constants, a large number of data points are required, often more than those given in a typical product catalogue.

For use in building energy simulation, Yik (1999) developed a quadratic regression model (see Equation 3.1) that relates the cooling output of a cooling coil to the chilled water flow rate, based on prior research study on cooling coil modelling (Yik, 1996).

$$q = 1.2709m^3 - 2.6609m^2 + 2.4169m \quad (3.1)$$

where

q = normalized cooling output

m = normalized chilled water flow rate of the cooling coil

Moreover, Wang et al. (2012a) modelled a sample of cooling coils from a manufacturer's catalogue. Figure 3.2 shows the normalized simulation results with the total cooling output plotted against the chilled water flow rate. These results are more or less the same as those predicted by the cooling coil model developed by Yik (1999).

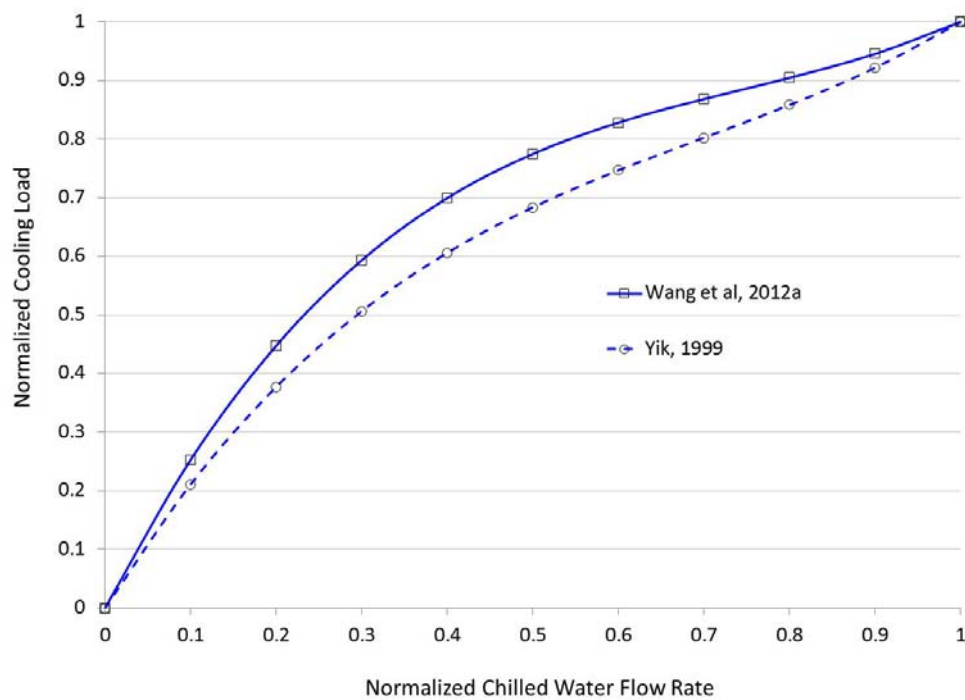


Figure 3.2 Cooling coil models developed by Yik (1999) and Wang et al. (2012a)

As shown in Figure 3.2, the cooling output of a chilled water cooling coil does not bear a linear relationship with the chilled water flow rate through the coil. When flow rate is reduced, assuming that the supply temperature remains unchanged, the temperature difference between the inlet and outlet chilled water will become larger. It is because the water will stay inside the tubes of the coil for a longer time. The longer detention time allows each unit mass of water to absorb or reject more heat from or to the air. This coil output-flow rate relationship can be well represented by Equation 3.1.

3.2.2 Modelling of Cooling Coils Operating under Normal Delta-T Conditions

In this study, the hourly cooling load and chilled water flow rate predicted by using HTB2 and BECON were normalized and plotted in Figures 3.3 to 3.6 to present the cooling coil characteristics of the four model buildings. These buildings are an office, a low and a high rise commercial complex, and a hotel respectively.

The Solver program in Excel was used to determine a polynomial regression equation, which could fit for the normalized data, and points (0,0) and (1,1) with the maximum determination coefficient R^2 . Results indicate that R^2 was at a higher value. The blue curves in Figures 3.3 to 3.6 are the regression curves of the four model buildings. The curves are similar to the results as predicted by the cooling coil models developed by Yik (1999) and Wang et al. (2012), as shown in Figure 3.2. These regression curves were used to model the cooling coil output and the chilled water flow rate of each building under design conditions.

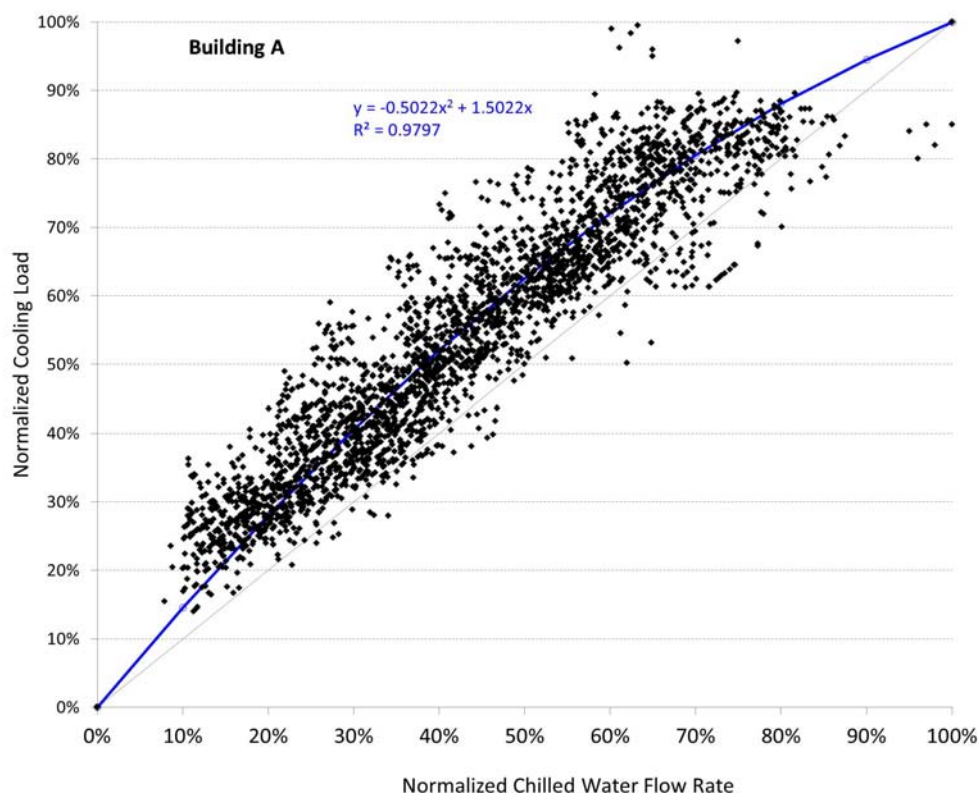


Figure 3.3 Characteristics of cooling coils of model building A

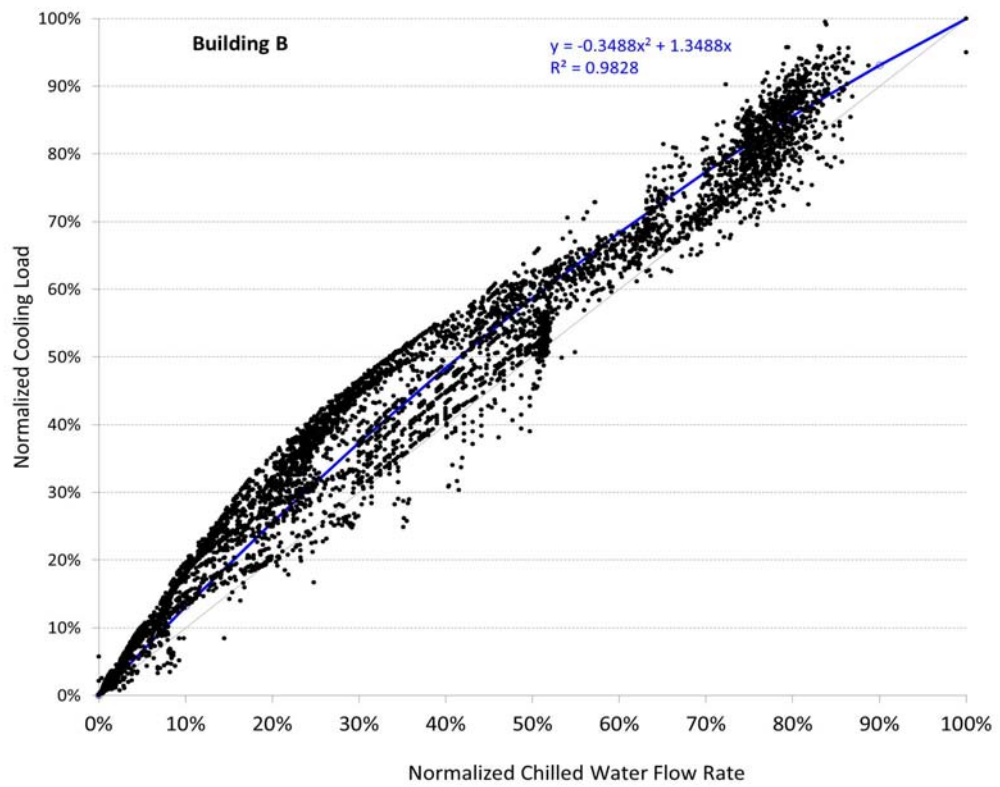


Figure 3.4 Characteristics of cooling coils of model building B

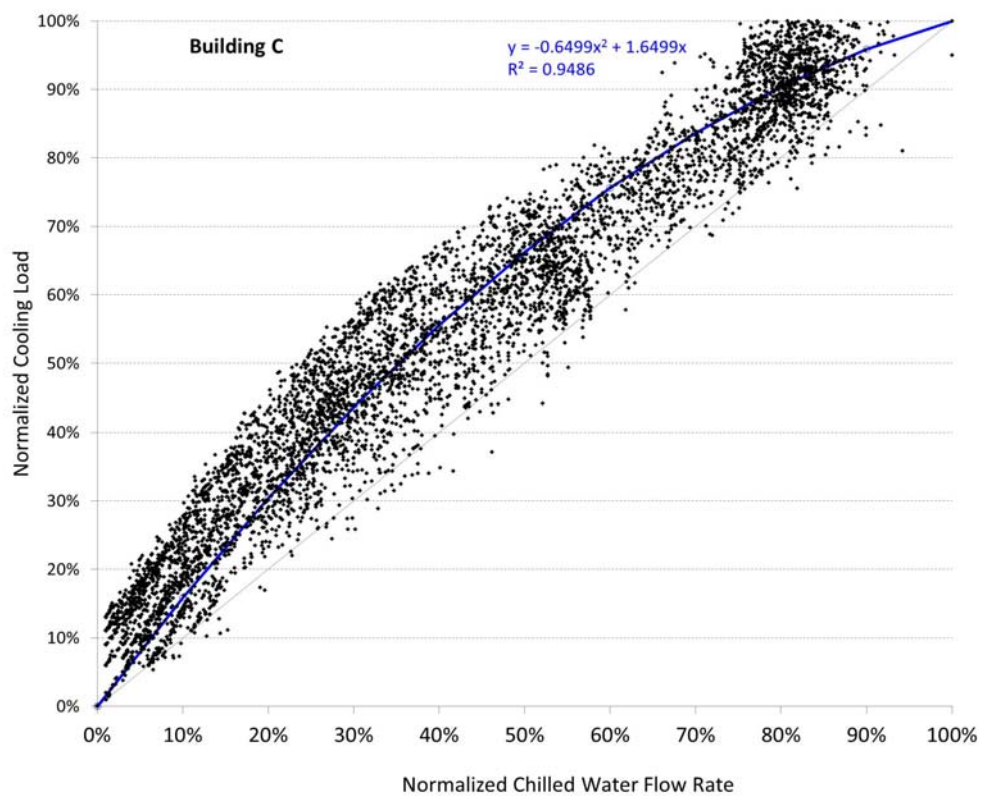


Figure 3.5 Characteristics of cooling coils of model building C

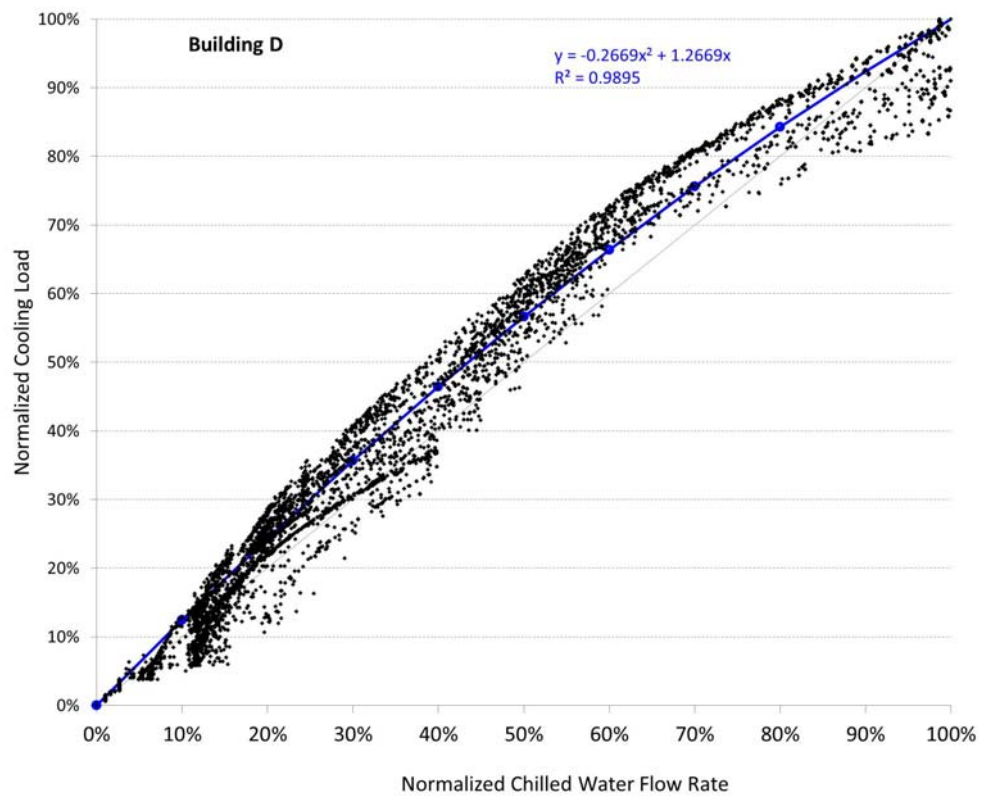


Figure 3.6 Characteristics of cooling coils of model building D

3.2.3 Modelling of Cooling Coils Operating under Low Delta-T Conditions

Strictly speaking, no in-depth study could be found in the open literature on the relationship between the chilled water flow rate and the cooling load of a building when the air-conditioning system in buildings is exhibiting the low delta-T syndrome. To overcome this challenge, effort has been made in this study to collect data to provide a basis for developing a pseudo cooling coil model that exhibits the low delta-T syndrome for use in this study. However, most buildings did not have a comprehensive record of their air-conditioning system operating data, making it difficult to gather sufficient data to support the analysis. Actual performance data, including cooling loads and the corresponding chiller water flow rates of only two commercial buildings, denoted as buildings X and Y, with the low delta-T syndrome was obtained from the property management companies that operated the buildings.

Buildings X and Y are two commercial complexes which consist of offices, retail shops, and restaurants. Their characteristics are similar to those of the model buildings A, B and C in this study. Figure 3.7 shows a scatter plot of these two buildings' annual cooling loads and chilled water flow rates, which had been normalized by the total rated cooling capacity and chilled water flow rate of the chillers installed in the respective buildings. The figures demonstrate the same pattern that percentage reduction in chilled water flow rate is smaller than the corresponding percentage reduction in total cooling load. As a result, the temperature difference between the supply and return chilled water in the building loop is significantly smaller than that under the normal condition. This characteristic is similar to the data presented by Cai et al. (2012) for six commercial buildings with the low delta-T syndrome, as shown in Figure 1.5 in Chapter 1.

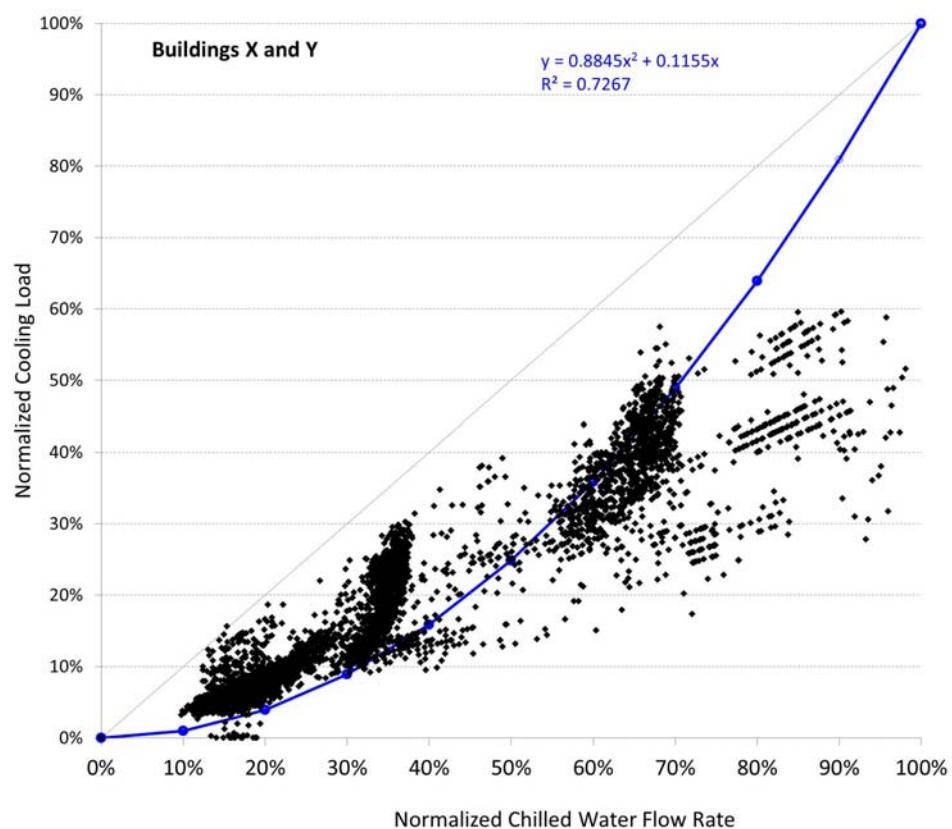


Figure 3.7 Normalized cooling load and chilled water flow rate of buildings X and Y

Although the data available is limited, these two real cases were taken as the basis for developing a model for building loops operating at low delta-T. A polynomial was obtained by a regression analysis, as shown in Equation 3.2 and compared graphically

with the non-linear and the normalized cooling loads and flow rates data of buildings X and Y, as shown in Figure 3.8. This equation will be used for simulation of the characteristics of the building loops with the low delta-T syndrome.

$$q = 0.8845m^2 + 0.1155m \quad (3.2)$$

where q and m in Equation 3.2 denote the normalized cooling output and the normalized chilled water flow rate of the building loop respectively.

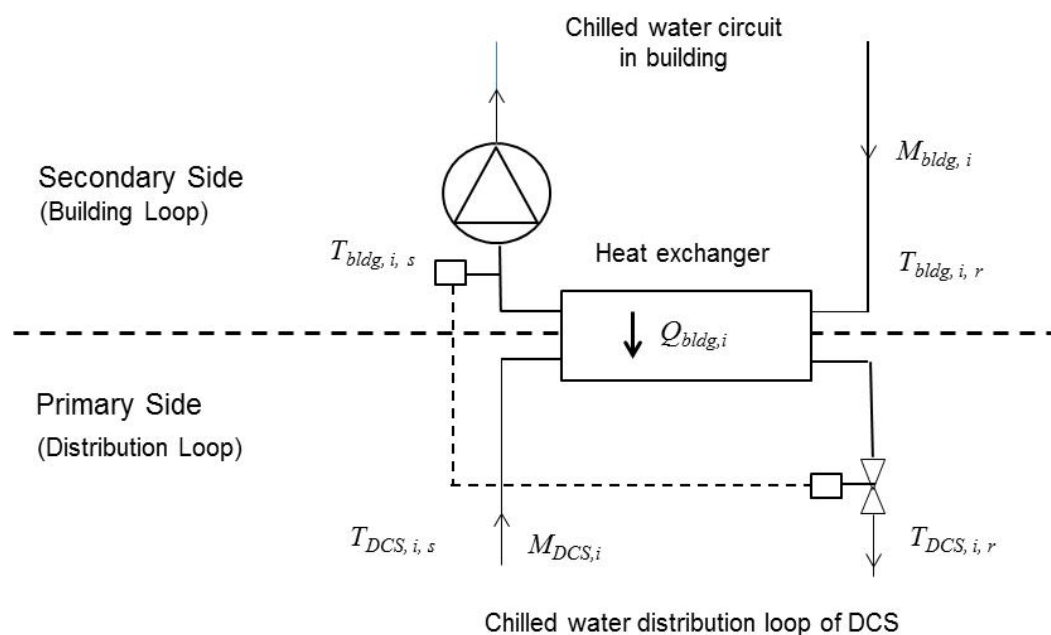


Figure 3.8 Connection between the chilled water circuit in the building and the distribution loop of the DCS

3.3 Heat Exchanger Model

3.3.1 Chilled Water Flow at the Secondary Side of the Heat Exchanger

Buildings served by a DCS are equipped with a heat exchanger, which acts as an interface between the chilled water distribution loop of the DCS and the chilled water circuit in the building, as shown in Figure 3.8. A temperature control system regulates the chilled water flow rate from the DCS through the heat exchanger ($M_{DCS,i}$), i.e. at the primary side of the heat exchanger, so that the temperature of the chilled water of the

building loop leaving the heat exchanger of building i , i.e. secondary side, will stay steady at the set-point level of $T_{bldg,i,s}$. The rate of heat transfer from the chilled water in the building circuit through the heat exchanger to the chilled water in the distribution loop of the DCS equals the building's cooling load, $Q_{bldg,i}$.

The chilled water flow rate in the chilled water circuit of building i , $M_{bldg,i}$, depends not only on the cooling load of the building, $Q_{bldg,i}$, but also on the characteristics of the chilled water system in the building, including the cooling coils in the air-side systems in the building and the type of control system used for regulating chilled water flow rate. The relationship between $M_{bldg,i}$ and $Q_{bldg,i}$ under normal and low delta-T conditions can be represented by the cooling coil models presented in [Section 3.2](#).

It should be noted that return chilled water temperature in the building, under the rated condition ($T_{bldg,i,r,o}$) and under a general condition ($T_{bldg,i,r}$), can be evaluated by [Equations 3.3](#) and [3.4](#).

$$T_{bldg,i,r,o} = T_{bldg,i,s} + \frac{Q_{bldg,i,o}}{M_{bldg,i,o} c_w} \quad (3.3)$$

$$T_{bldg,i,r} = T_{bldg,i,s} + \frac{Q_{bldg,i}}{M_{bldg,i} c_w} \quad (3.4)$$

where c_w is the specific heat capacity of water, which is assumed to be 4.19 kJ/kg°C.

3.3.2 Chilled Water Flow at the Primary Side of the Heat Exchanger

Similarly, the design temperature of the chilled water returning from the heat exchanger to the DCS' distribution loop ($T_{DCS,i,r,o}$) can be evaluated on the basis of the temperature of the rated chilled water supply ($T_{DCS,i,s,o}$), which is assumed to be maintained steadily at the set point level at all times. The design return temperature of the chilled water returning from the heat exchanger is expressed by [Equation 3.5](#). [Equation 3.6](#) can be

used to calculate the temperature of the chilled water returning from the heat exchanger at the primary side in a general condition.

$$T_{DCS,i,r,o} = T_{DCS,i,s} + \frac{Q_{bldg,i,o}}{M_{DCS,i,o}c_w} \quad (3.5)$$

$$T_{DCS,i,r} = T_{DCS,i,s} + \frac{Q_{bldg,i}}{M_{DCS,i}c_w} \quad (3.6)$$

The performance of the heat exchanger in building i is characterized by its heat transfer area (A_i) and the overall heat transfer coefficient (U_i). The value of the product of these terms, A_iU_i , can be determined by [Equations 3.7](#) and [3.8](#) at rated conditions.

$$A_iU_i = \frac{Q_{bldg,i,o}}{LMTD_o} \quad (3.7)$$

$$LMTD_o = \frac{(T_{bldg,i,r,o} - T_{DCS,i,r,o}) - (T_{bldg,i,s} - T_{DCS,i,s})}{\ln\left(\frac{T_{bldg,i,r,o} - T_{DCS,i,r,o}}{T_{bldg,i,s} - T_{DCS,i,s}}\right)} \quad (3.8)$$

Furthermore, assuming that the value of A_iU_i will not change significantly under the entire range of operating conditions of the heat exchanger, the chilled water temperatures at the primary and secondary sides of the heat exchanger can be related by applying the log mean temperature difference (LMTD) model ([Equations 3.9](#) and [3.10](#)).

$$Q = (AU) \cdot LMTD \quad (3.9)$$

$$LMTD = \frac{(T_{bldg,i,r} - T_{DCS,i,r}) - (T_{bldg,i,s} - T_{DCS,i,s})}{\ln\left(\frac{T_{bldg,i,r} - T_{DCS,i,r}}{T_{bldg,i,s} - T_{DCS,i,s}}\right)} \quad (3.10)$$

Therefore, once $T_{bldg,i,r}$ is obtained from Equation 3.4, the temperature of the chilled water returning to the distribution loop from the building, $T_{DCS,i,r}$, can be found by solving Equation 3.11, which is obtained by combining Equations 3.9 and 3.10.

$$Q_{bldg,i} = (A_{bldg,i} U_{bldg,i}) \frac{(T_{bldg,i,r} - T_{DCS,i,r}) - (T_{bldg,i,s} - T_{DCS,i,s})}{\ln\left(\frac{T_{bldg,i,r} - T_{DCS,i,r}}{T_{bldg,i,s} - T_{DCS,i,s}}\right)} \quad (3.11)$$

Then, by substituting $T_{DCS,i,r}$ into Equation 3.12, the required chilled water flow rate at the primary side of the heat exchanger, $M_{DCS,i}$, can be obtained.

$$M_{DCS,i} = \frac{Q_{bldg,i}}{c_w (T_{DCS,i,r} - T_{DCS,i,s})} \quad (3.12)$$

3.3.3 Flow Rate and Temperature of Chilled Water Returning to the Chiller Plant

The chilled water flow rate at the primary side of each heat exchanger installed in building i , i.e. $M_{DCS,i}$, can be determined using Equation 3.12 once $T_{DCS,i,r}$ has been evaluated by solving the LMTD model. The total flow rate of the chilled water returning to the centralized chiller plant at time t , $M_{DCS,r}(t)$, can be determined by Equation 3.13.

$$M_{DCS,r}(t) = \sum_{i=A}^D N_{bldg,i} M_{DCS,i}(t) \quad (3.13)$$

The temperature of the chilled water returning from all buildings to the centralized chiller plant at time t , $T_{DCS,r}(t)$, equals the temperature of the chilled water resulted from mixing of the chilled water returning from the primary side of each heat exchanger, $T_{DCS,i,r}(t)$. $T_{DCS,r}(t)$ can be determined by Equation 3.14

$$T_{DCS,r}(t) = \frac{\sum_{i=A}^D N_{bldg,i} M_{DCS,i}(t) T_{DCS,i,r}(t)}{\sum_{i=A}^D N_{bldg,i} M_{DCS,i}(t)} \quad (3.14)$$

3.4 Chilled Water Distribution Network Model

3.4.1 Characteristics of System Pressure Drop and Flow Rate

For the distribution loop, it comprises a variety of components, including heat exchangers, pumps, pipes, valves and other accessories. A change in the chilled water flow rate in the loop would also affect pressure loss along the distribution network. This exhibits a non-linear characteristic between flow and pressure loss. To facilitate a simulation of the chilled water flow and pressure drop in the distribution loop of a DCS, a hydraulic chilled water distribution network model was developed.

The model couples the chilled water pressure-flow relationships in the hydraulic network with the hourly thermal loads of the buildings in the hypothetical district. This model was employed in this study to calculate the year-round hourly pumping energy use corresponding to the hourly chilled water flow rate and pumping pressure requirement in the distribution network. The model can be considered as a collection of flow elements connected together to form a network of flow paths. Pressure drop due to fluid flow inside a pipe is described by the Darcy-Weisbach equation, as shown in [Equation 3.15 \(Douglas, 1985\)](#). The Darcy-Weisbach equation with friction factors obtained from the Moody chart or the Hazen-Williams equation allows the pressure drop through the pipes in the chilled water piping system to be evaluated.

$$\Delta P = f \left(\frac{L}{D} \right) \left(\frac{v^2}{2g} \right) \quad (3.15)$$

where

ΔP = pressure drop, Pa

f = friction factor, dimensionless

L = length of pipe, m

- D = internal diameter of pipe, m
 v = average velocity, m/s
 g = gravitational acceleration, m/s²

Assuming there is a turbulent flow regime, the pressure drop across any fixed flow element, including pipe section, fittings and various equipment, is proportional to the square of the flow rate, Q , which can be expressed by Equation 3.16.

$$\Delta P = kQ^2 \quad (3.16)$$

where

- k = flow resistance of an element, which can be obtained from the ASHRAE Fundamentals Handbook (ASHRAE, 2009)

Figure 3.9 shows a hydraulic network with a number of heat exchangers that equals the number of buildings (N_{bldg}) connected to the DCS and one pumping station equipped with N_{pump} number of pumps.

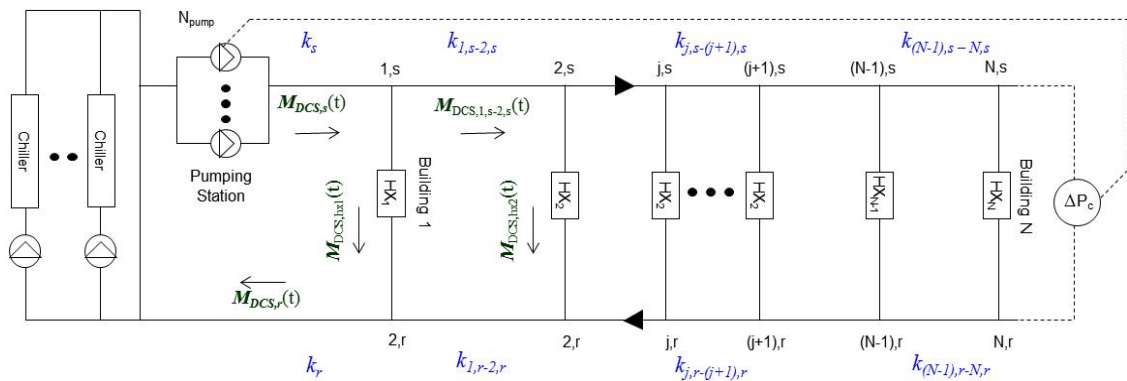


Figure 3.9 Hydraulic model of chilled water distribution network

The overall pressure drop in the distribution network equals the sum of pressure drops through the pump fittings (including the pressure drop through the header that directs the flow into and from each pump, and the pressure drop through the valves in the pump headers), and through each pipeline section along the supply and return pipelines and the heat exchanger at the farthest branch.

Pressure drop across the pump fittings at time t can be expressed by [Equation 3.17](#).

$$\Delta P_{pf}(t) = k_{ft} \left(\frac{M_{DCS,s}(t)}{N_{pump}} \right)^2 \quad (3.17)$$

Pressure drop across each pipeline section, i.e. j,s to $(j+1),s$ and j,r to $(j+1),r$, along the supply and return pipelines can be expressed by [Equation 3.18](#).

$$\begin{aligned} \Delta P_{pipeline}(t) = & k_s (M_{DCS,s}(t))^2 \\ & + \sum_{r=1}^N [k_{j,r-(j+1),r} (M_{DCS,j,r-(j+1),r}(t))^2] + [k_{j,s-(j+1),s} (M_{DCS,j,s-(j+1),s}(t))^2] \\ & + k_r (M_{DCS,r}(t))^2 \end{aligned} \quad (3.18)$$

Pressure drop across the heat exchanger at the remote end at time t can be expressed by [Equation 3.19](#).

$$\Delta P_{hx}(t) = k_{hx} (M_{DCS,N}(t))^2 \quad (3.19)$$

The total pressure drop, $\Delta P(t)$, of the network for the corresponding flow rate at time t can therefore be expressed by [Equation 3.20](#).

$$\Delta P(t) = \Delta P_{pf}(t) + \Delta P_{pipeline}(t) + \Delta P_{hx}(t) \quad (3.20)$$

In [Equations 3.17](#) to [3.20](#), k is the flow resistance along the pipework, and N is the node number. Subscripts pf , hx , s and r denote the pump fitting, heat exchanger, supply pipeline and return pipeline, respectively.

3.4.2 Differential Pressure Control Setting

In the chilled water distribution system, the operating points (flow rate and pressure head) of the secondary chilled water pumps are consistently regulated by varying their running speed to match the changes in chilled water demand and the consequential changes in pressure losses across the flow elements in the system.

A differential pressure transmitter is installed across the critical path, typically the farthest branch, so that any change in the flow rate demand, which is reflected by a change in the differential pressure across the critical branch, can be detected and used as a reference signal for controlling pump speed. With this control system, the differential pressure across the critical branch, ΔP_c , could be maintained within a small range about the set-point level.

As system flow rate reduces, less pressure drop will be incurred by the chilled water circulating in the main supply and return pipes. As the pressure difference is held constant at ΔP_c across the critical branch, pumping pressure will be reduced to a level just sufficient to maintain this pressure difference at the critical branch, and to overcome the pressure drop along the main pipes between the pump and the critical branch.

Figure 3.10 shows a pressure-distance diagram of the chilled water system in a distribution loop, under both design and part-load conditions. An assumption has been made in constructing this diagram that the rate of pressure drop per unit length of the pipe run remains unchanged along the main supply and return pipes. The pressure variations along these pipes therefore appear as slopping straight lines. Furthermore, reduction in the flow rates is assumed to take place uniformly across all the branches.

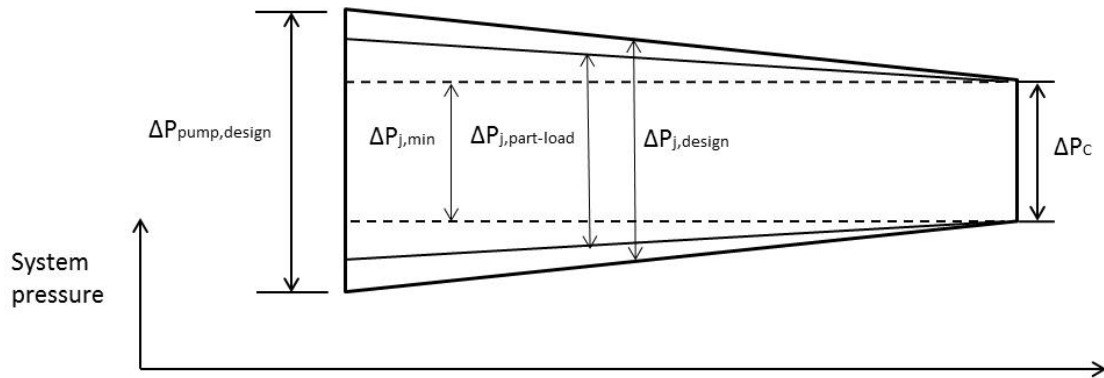


Figure 3.10 Pressure-distance diagram (with the same variation in the chilled water demands across the branch) (Yik, 1999)

Figure 3.11 shows that as system flow rate decreases, the pressure difference across each intermediate branch, ΔP_j , will become smaller than the maximum level that will exist under design conditions ($\Delta P_j = \Delta P_{j,part-load} < \Delta P_{j,design}$). If the flow rate demand becomes very small, the differential pressure across the branches will approach the setting of the differential pressure control system of the critical branch ($\Delta P_{j,part-load} \rightarrow \Delta P_{j,min} \approx \Delta P_c$).

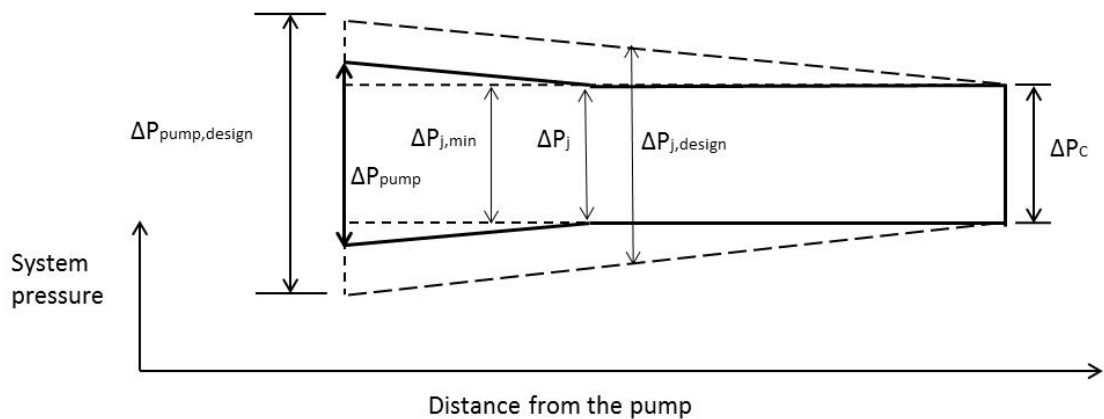


Figure 3.11 Pressure-distance diagram (no flow from building j to building N) (Yik, 1999)

When there is no chilled water flow from building j to all other buildings downstream, the differential pressure across branch j will drop to ΔP_c , irrespective of whether water flow is maintained in other branches upstream (Figure 3.11).

It can be seen that the choice of differential pressure control setting, ΔP_c , will affect the amount of chilled water that can flow through all the buildings in the DCS. A necessary condition to be fulfilled in making this decision is that, when being subjected to a differential pressure ΔP_c , each branch (building) should remain capable of maintaining the design flow rate for the building concerned. Otherwise, the heat exchanger in the building will be unable to attain a full cooling output.

This condition imposes a requirement that the total pressure drop in each building should not exceed the differential pressure set-point ΔP_c when chilled water flow rate equals the design flow rate. Any building that will incur a design flow pressure drop exceeding this should in fact be chosen as the critical building with the differential pressure transmitter installed across the branch for pump speed control.

3.5 Variable Speed Pump Model

3.5.1 Normalization of Pump Characteristics

An individual pump's performance at its rated speed can be expressed by third order polynomials as depicted by [Equations 3.21 and 3.22 \(Underwood and Yik, 2004\)](#), which represent the relationship between flow rate (M_{pump}) and the total system pressure head (H_{pump}) and power (W_{pump}) respectively. The polynomial coefficients $a_0, a_1, a_2, a_3, b_0, b_1, b_2$ and b_3 can be determined by using regression based on the performance data for a given pump obtained from the manufacturers.

$$H_{pump} = a_0 + a_1 M_{pump} + a_2 M_{pump}^2 + a_3 M_{pump}^3 \quad (3.21)$$

$$W_{pump} = b_0 + b_1 M_{pump} + b_2 M_{pump}^2 + b_3 M_{pump}^3 \quad (3.22)$$

For prediction of the year-round hourly electricity consumption of the variable speed pumps in the distribution loop under the possible operating conditions, enormous effort is required to source for the characteristic curves of thousands of pumps.

In order to widen the use of the above equations for modelling pumps of similar design but different design flow rates and pressure heads, the characteristic curves of 63 different pumps were collected. This range of pumps can cover the operating range of the variable speed pumps (with pump flow rates ranging between 144 and 4,968 m³/hr and pump heads between 1.1 and 63.3 m) used in this study. On the basis of this set of pump performance data, a set of normalized pump characteristic curves were developed such that the normalized curves can be applied to predict the performance of all the pumps used in this study, instead of using a specific set of pump curve for each pump.

The normalized pump head h and power w are defined by using the design pump head $H_{pump,o}$ and power $W_{pump,o}$.

$$h \equiv \frac{H_{pump}}{H_{pump,o}}, \quad w \equiv \frac{W_{pump}}{W_{pump,o}}$$

The normalized pump curves derived from [Equations 3.23 and 3.24](#) were then used to formulate the characteristic curves of all other pumps by inputting their respective design pump head and power.

$$\begin{array}{l} \text{Pressure} \\ \text{head} \end{array} : \quad \frac{H_{pump}}{H_{pump,o}} = a_0 + a_1 \left(\frac{M_{pump}}{M_{pump,o}} \right) + a_2 \left(\frac{M_{pump}}{M_{pump,o}} \right)^2 + a_3 \left(\frac{M_{pump}}{M_{pump,o}} \right)^3 \quad (3.23)$$

$$\text{Power} : \quad \frac{W_{pump}}{W_{pump,o}} = b_0 + b_1 \left(\frac{M_{pump}}{M_{pump,o}} \right) + b_2 \left(\frac{M_{pump}}{M_{pump,o}} \right)^2 + b_3 \left(\frac{M_{pump}}{M_{pump,o}} \right)^3 \quad (3.24)$$

Data of the normalized pump head and power of 63 centrifugal pumps was collected from the manufacturers and the least-square error curve fitting technique was used to evaluate the coefficients of the third order polynomials to represent the h - m and w - m relationship. These characteristics can be expressed by [Equations 3.25 and 3.26](#) respectively and the characteristic curves were plotted in [Figure 3.12](#).

The pressure head-flow relationship can be expressed by Equation 3.25.

$$h = -0.0612m_{pump}^3 - 0.1143m_{pump}^2 - 0.2996m_{pump} + 1.4657 \quad (3.25)$$

The power-flow relationship can be expressed by Equation 3.26.

$$w = -0.3839m_{pump}^3 + 0.8015m_{pump}^2 - 0.1943m_{pump} + 0.7769 \quad (3.26)$$

where

$$m_{pump} = \frac{M_{pump}}{M_{pump,o}}$$

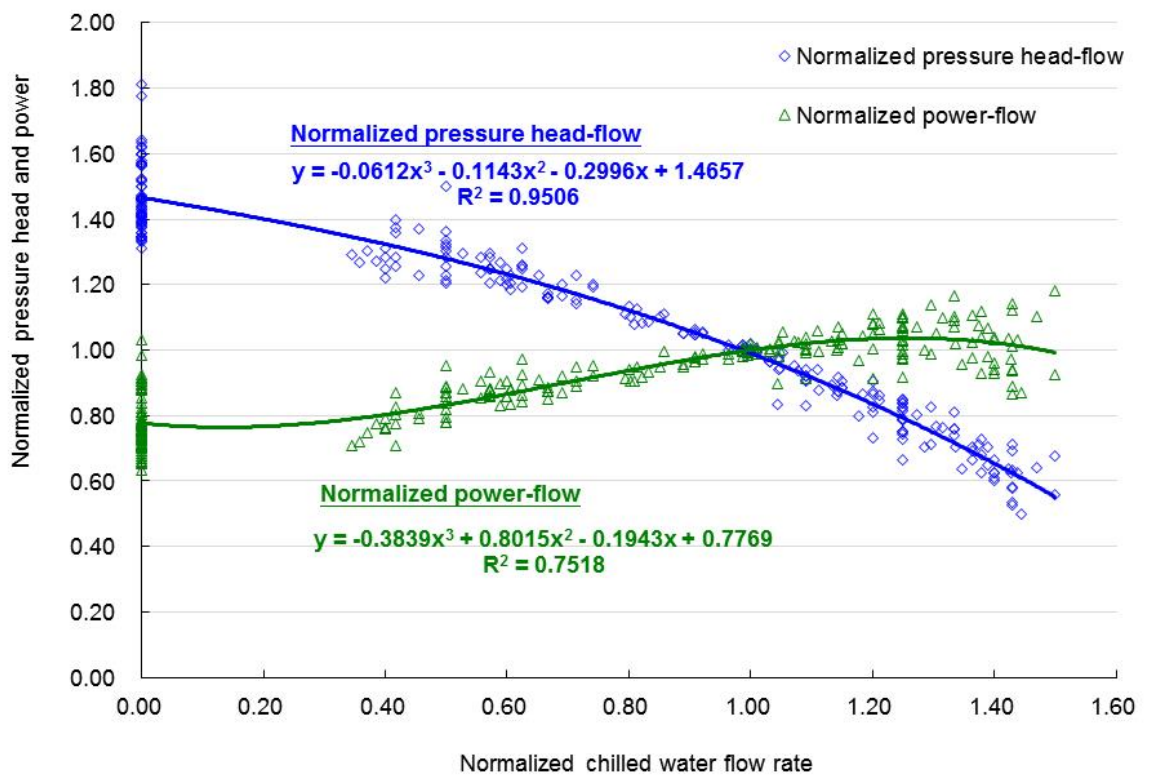


Figure 3.12 Characteristic curves of variable speed pump model

3.5.2 Power Demand of Variable Speed Pumps at Part Load

As is the case in nearly all DCS, variable speed distribution loop pumps were adopted for the DCS analysis in this study. Figure 3.13 shows the pressure-flow rate curve (1) of a variable speed pump running at rated speed n_o and the system characteristic curve (2) at design condition. The operating point of the variable speed pump is the intersection point O of curves (1) and (2).

Since the pump pressure requirement includes the differential pressure to be maintained across the critical branch and the pressure loss round the network, a system curve representing the pumping pressure requirement at different flow rates at time t can be plotted, as shown by curve (2') in Figure 3.13. Moreover, the corresponding pump curve of the variable speed pump can be represented by curve (1'). The operating point of the variable speed pump at time t is the intersection point A of curves (1') and (2').

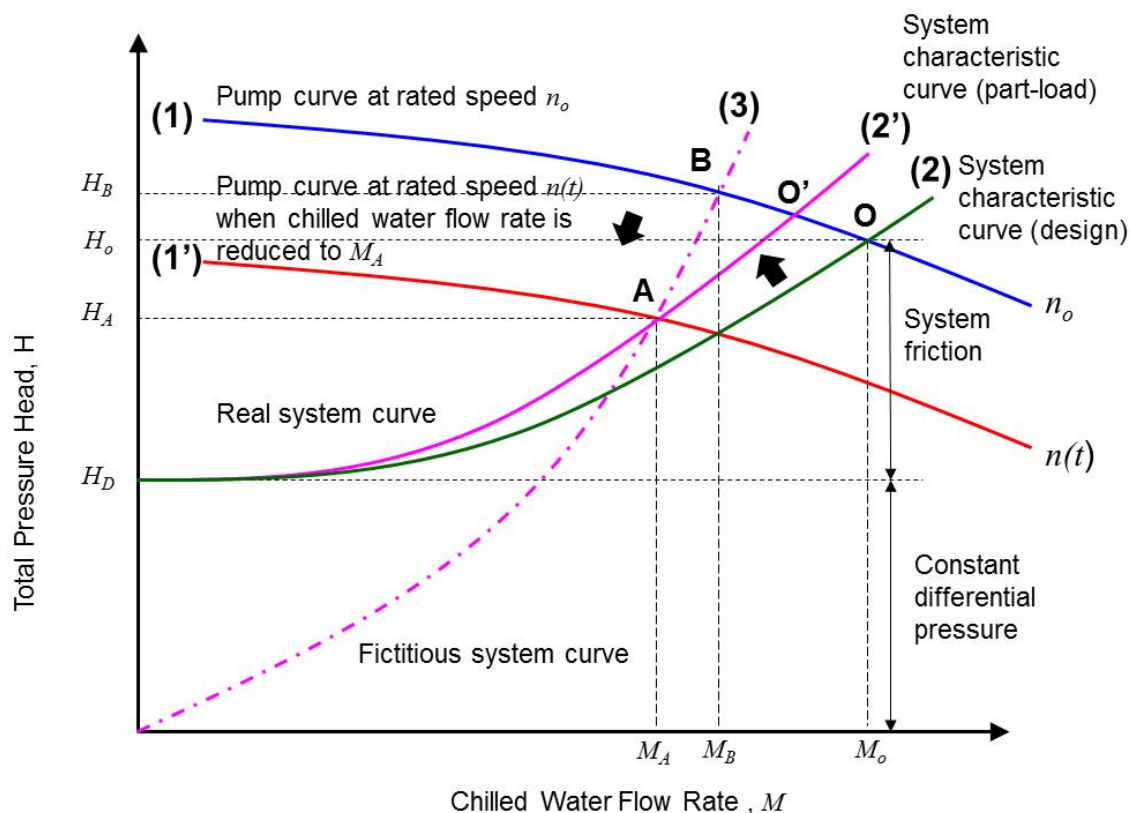


Figure 3.13 Relationship between the total pressure head and chilled water flow rate of the variable speed pump

However, if the DCS is at part load, the chilled water flow rate will be lower than M_o (Figure 3.13). The speed of the variable speed pump will in fact be reduced to match the required flow rate M_A . The pressure head and power demand of a variable speed pump at a reduced operating speed, $n(t)$, at time t can be modelled by Equations 3.27 and 3.28 respectively, which were derived based on the pump affinity laws (Underwood and Yik, 2004).

$$\frac{H_{pump}}{H_{pump,o}} = a_0 \left(\frac{n(t)}{n_0} \right)^2 + a_1 \left(\frac{n(t)}{n_0} \right) \left(\frac{M(t)}{M_o} \right) + a_2 \left(\frac{M(t)}{M_o} \right)^2 + a_3 \left(\frac{n_0}{n(t)} \right) \left(\frac{M(t)}{M_o} \right)^3 \quad (3.27)$$

$$\frac{W_{pump}}{W_{pump,o}} = b_0 \left(\frac{n(t)}{n_0} \right)^3 + b_1 \left(\frac{n(t)}{n_0} \right)^2 \left(\frac{M(t)}{M_o} \right) + b_2 \left(\frac{n(t)}{n_0} \right) \left(\frac{M(t)}{M_o} \right)^2 + b_3 \left(\frac{M(t)}{M_o} \right)^3 \quad (3.28)$$

According to the pump affinity law, the ratio of speed at part load, $n(t)$, to the rated speed n_o , $\frac{n(t)}{n_o}$, is proportional to the ratio of chilled water flow rates at the two speeds.

However, the affinity law applies only to two operating points that are dynamically similar. To find the operating point on the curve for the rated speed that is dynamically similar to the actual operating point, a fictitious system curve which is a parabola as shown in Figure 3.13 can be used, because the parabola preserves the affinity law for

the relation between pumping pressure and flow rate ratios, i.e. $\frac{H_A}{H_B} = \left(\frac{n(t)}{n_o} \right)^2$. This

system curve (3) passes through operation point A at part load and intersects with pump curve (1) at point B, and points A and B are indeed dynamically similar. The ratio of speed at part load, $n(t)$, to the rated speed, can be expressed by Equation 3.29.

$$\frac{n(t)}{n_o} = \frac{M_A(t)}{M_B(t)} \quad (3.29)$$

By solving Equations 3.28 and 3.29, the hourly power demand of the variable speed pump can be determined and summing their values over the year yields the annual energy consumption of the variable speed pump. Electricity consumption data of the

pumping station can thus be calculated by summing up the energy consumption figures of each variable speed pump in the pumping station.

3.5.3 Control Strategy

A multi-pump system, comprising identical pumps sets, was designed for each pumping station in DCS_O. This can facilitate easier implementation of control strategy and more flexible operation and maintenance. For a pumping system with pumps of equal capacity, a commonly used approach is to switch the pumps on and off sequentially according to the actual demand flow rate. The total chilled water flow demand is shared by each operating pump.

3.6 Pumping Station Model

One of the energy efficiency enhancement measures in this study was to optimize the design of pumping station configuration via the application of multiple pumping stations in different locations along the chilled water supply and return pipes, and use of different number of pumps in each pumping station.

Based on the mathematical model developed for variable speed chilled water pumps, an optimization program was written using Excel VBA for calculating the annual electricity consumption of different combinations of pumping stations that are equipped with different number of pumps in each station. An algorithm of this pumping station model is presented in [Figure 6.8](#) of [Chapter 6](#).

3.7 Chiller Model

3.7.1 Constant Speed Chillers

3.7.1.1 Bi-Quadratic Regression

A number of researchers have developed models for water-cooled chillers ([Lam, 1997](#); [Hydeman et al., 2002](#); [Lee and Lee, 2007](#); [Yu, 2009](#)). However, these models can only

be used for chillers in typical air-conditioning systems in buildings because the rated chilled water supply temperature is not an explicit independent variable in those models, which were established based on the typical supply temperature of 7°C. In a DCS, however, the chilled water supply temperature can be set at a level lower than 7°C. Therefore, a new mathematical model for chillers had to be developed for this study. [Gordon et al. \(1995\)](#) and [ASHRAE \(2011\)](#) suggested that the power demand of a chiller (W_{ch}) depends mainly on the following three variables.

1. Cooling load on the chiller, Q_{ch}
2. Temperature of the chilled water is set to supply, $T_{ch,s}$
3. Temperature of the cooling medium supplied to the condenser of the chiller, T_{con} , i.e. the temperature of the seawater entering the chiller condenser, as direct seawater cooling was assumed in this study

A mathematical model was built to relate the power demand of chillers to these influencing variables so that the electricity consumption of the chiller plant could be predicted by computer simulation.

Instead of relating the actual value of the power demand of a chiller to the value of the corresponding cooling load, the model developed in this study relates the normalized power demand ($w_{ch, const}$) to the part load ratio (PLR) of a constant speed chiller. These normalized values can be evaluated by dividing the part-load power and the load by their respective rated full-load values for a given chiller. The use of normalized values can make the model applicable to similar chillers of different rated capacities. The supply temperatures of the chilled water ($T_{ch,s}$) and the cooling medium, i.e. seawater (T_{con}) in °C, were used in the model without any conversion. [Equation 3.30](#) was adopted as the mathematical form of the chiller model for relating the power consumption of a chiller to the independent variables. This model form was chosen because it could account for the non-linear dependence of chiller power on the cooling load and the cooling medium temperature, and yet would be relatively simple.

$$\begin{aligned}
w_{ch,const} = & c_0 + c_1(PLR) + c_2(T_{ch,s}) + c_3(T_{con}) + c_4(PLR^2) + c_5(T_{ch,s}^2) + c_6(T_{con}^2) + c_7 \\
& (PLR \cdot T_{ch,s}) + c_8(PLR \cdot T_{con}) + c_9(T_{ch,s} \cdot T_{con}) + c_{10}(PLR^2 \cdot T_{ch,s}) + c_{11} \\
& (PLR^2 \cdot T_{con}) + c_{12}(T_{ch,s}^2 \cdot PLR) + c_{13}(T_{ch,s}^2 \cdot T_{con}) + c_{14}(T_{con}^2 \cdot PLR) \\
& + c_{15}(T_{con}^2 \cdot T_{ch,s}) + c_{16}(PLR \cdot T_{ch,s} \cdot T_{con}) \quad (3.30)
\end{aligned}$$

where

$w_{ch,const}$ = the normalized power of constant speed chiller at different PLRs, typically at 20%, 40%, 60%, 80% and 100%

c_0 to c_{16} = regression coefficient

Full and part load performance data of 1,000 RT (3,517 kW) and 800 RT (2,814 kW) constant speed direct seawater-cooled centrifugal chillers with different condenser water entering temperatures, i.e. 20°C, 25°C and 30°C, and different chilled water supply temperatures, i.e. 4°C, 5°C, 6°C and 7°C was obtained from the manufacturers for developing the chiller models.

On the basis of this set of chiller performance data, the model coefficients (c_0 to c_{16}) were evaluated by using the regression function available in Excel. The regression method used assures that, for the given mathematical form of the model, the resulting set of coefficients would lead to the least sum of squared deviations between the model predictions and the chiller performance data.

The normalized power demand of the constant speed chiller, $w_{ch,const}$, can be expressed by Equation 3.31. There are 16 regression variables and the determination coefficient, R^2 is 0.9295. This means that the normalized power of chiller can be estimated by the model with reasonably high accuracy.

$$\begin{aligned}
w_{ch,const} = & 1.095 - 0.101(T_{ch,s}) + 0.45(T_{con}) - 0.0167(PLR^2) + 0.003(T_{ch,s}^2) + \\
& 0.443(T_{con}^2) + 0.008(PLR \cdot T_{ch,s}) - 0.059(PLR \cdot T_{con}) - \\
& 0.0056(T_{ch,s} \cdot T_{con}) + 0.0007(PLR^2 \cdot T_{ch,s}) + 0.0055(PLR^2 \cdot T_{con}) - \\
& 0.0004(T_{ch,s}^2 \cdot PLR) + 0.00017(T_{ch,s}^2 \cdot T_{con}) - 0.037(T_{con}^2 \cdot PLR) + \\
& 0.0047(T_{con}^2 \cdot T_{ch,s}) + 0.0005(PLR \cdot T_{ch,s} \cdot T_{con}) \quad (3.31)
\end{aligned}$$

3.7.1.2 Stepwise Regression

Although the chiller model in Equation 3.31 can well represent the performance of constant speed chillers, the equation consists of 16 terms of which some may be less significant as compared to the others. To find out the best combination of independent variables for achieving an accurate prediction of the performance of chillers, stepwise regression can be used, as it is a widely used regressor variable selection procedure and an efficient approach in finding the regression equation with only significant regression coefficients (Campbell, 2001; Montgomery and Runger, 2010; Shanableh and Assaleh, 2010). Stepwise regression is usually used for handling a large number of independent variables, which are generally more than 15 (NCSS, 2013).

Stepwise regression is a step-by-step method for determining a model equation that begins with no independent variable in the equation. It proceeds forward by adding one variable (i.e. forward adding approach) at a time based on statistical criteria. The stepping criteria employed for entry is based on the significance level, which is measured in terms of a probability (i.e. P-value) of the independent variable related to the output variable.

Assuming an output variable, y , has to correlate a potentially independent variable, x , the modelling equation can be expressed as $E(y) = \beta_0 + \beta_1 x$. P-value is to test the null hypothesis $H_0: \beta_1 = 0$, i.e. the coefficient of x is equal to ZERO (no effect) against the alternative hypothesis $H_a: \beta_1 \neq 0$. Since P is a probability, it is a number between 0 and 1. The significance level of P-value, α , is usually set at 0.05 (Cevik et al., 2010; Ssegane et al., 2012; Zhan et al., 2013). P-value is considered to be small if it is less than 0.05.

If the P-value is less than 0.05, the probability of getting $\beta_1 = 0$ is low. Therefore, the null hypothesis can be rejected in favour of the alternative hypothesis. It indicates that β_1 is NOT equal to 0, i.e. the output variable, y , is associated with changes in the independent variable x . The P-value can be obtained by using t -test (Dielman, 2005). The test statistic Z , which is used in the test, can be calculated as follows.

$$Z = \frac{\bar{m}}{\sigma/\sqrt{n}} \quad (3.32)$$

where \bar{m} and σ are the sample mean and standard deviation of a sample of size n .

The P-value corresponding to the value of Z can be obtained from the table of standard normal distribution (Onyiah, 2009). As the above alternative hypothesis is a two-tail test, the null hypothesis can be rejected if the P-value is smaller than $\sigma/2 = 0.025$. Figure 3.14 shows the two-tail test of rejecting the null hypothesis.

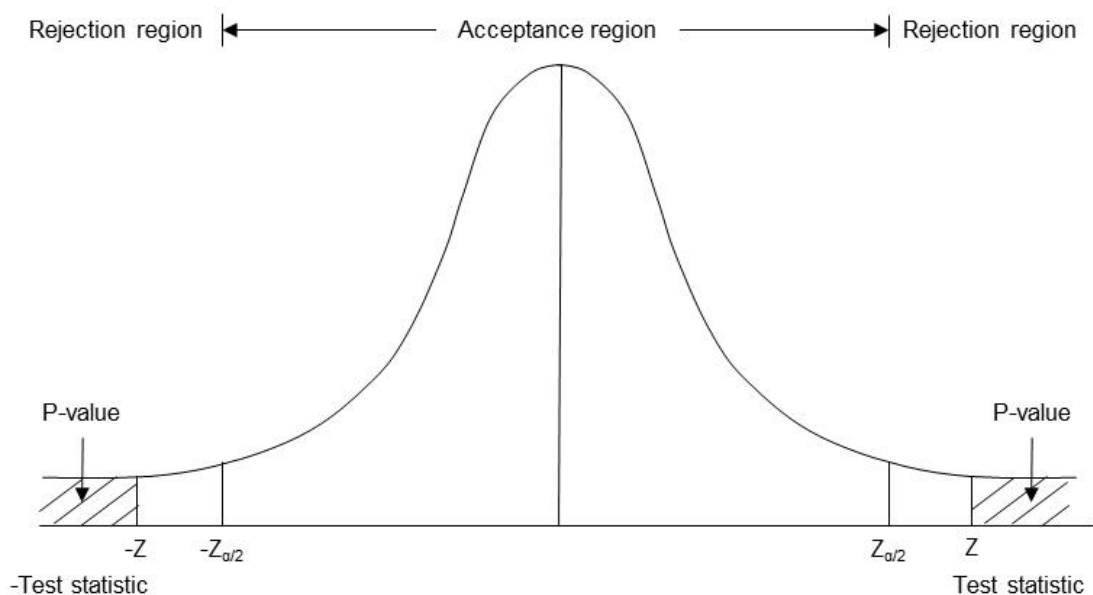


Figure 3.14 Two-tail test: Reject the null hypothesis

In the second step, the remaining independent variables are examined. The P-values of each independent variable are computed and the variable that generates the smallest P-value is added to the equation. When a new variable is added, the previous variable in the model may lose its predictive ability. Thus, the stepping criteria are also used to check the significance of the previous independent variable included in the model. If the variable is insignificant, it will be removed (i.e. backward deleting approach) from the model. Such forward adding and backward deleting approach is repeated until no variable is added or removed. The stepping procedure is terminated when the model is optimized, which is usually done by achieving the highest correlation coefficient (i.e. R^2)

(Cevik et al., 2010; Zhan et al., 2013), or when a maximum number of steps is reached. The following is an example showing the procedures of stepwise regression.

The user first identifies the output variable, y , and the set of potentially important k independent variables, x_1, x_2, \dots, x_k . The output variable and independent variables are then entered into a computer software, and the stepwise regression procedure begins.

Step 1- The software program fits all possible one-variable models of $E(y) = \beta_0 + \beta_1 x_1$ to the data, where x_i is the i^{th} independent variable, $i = 1, 2, \dots, k$. Then, test the null hypothesis $H_0: \beta_1 = 0$ against the alternative $H_a: \beta_1 \neq 0$. The independent variable that has the smallest P-value is declared the best one-variable predictor of y , i.e. x_1 (i.e. strong evidence against the null hypothesis).

Step 2 - The stepwise program now begins to search through the remaining $(k - 1)$ independent variables for the best two-variable model of $E(y) = \beta_0 + \beta_1 x_1 + \beta_2 x_2$. Again, the variable having the smallest P-value is retained, i.e. x_2

Step 3 - After a new variable x_2 is added, the previous variable x_1 in the model may lose its predictive ability. The aim of this step is to check the significance of x_1 in the model. If the P-value for $\beta_1 = 0$ has become insignificant, i.e. $P \geq 0.05$, x_1 has to be removed from the model.

The above step will be repeatedly applied to the remaining independent variables. The result is a model containing only those variables with a P-value that is smaller or equals the threshold value.

The stepwise regression analysis in this study was performed by a statistical program named SAS (i.e. Statistical Analysis System), which is an integrated system that enables the user to perform different types of data analysis. By using this stepwise regression approach, the normalized power demand of constant speed chillers, $w_{ch,const}$, can be expressed by [Equation 3.33](#).

$$\begin{aligned}
w_{ch,const} = & 0.17979 + 0.67551 (PLR) + 0.00018456 (T_{con}^2) - 0.05587 (T_{ch,s} \cdot PLR) \\
& + 0.01628 (PLR^2 \cdot T_{ch,s}) + 0.00976 (PLR^2 \cdot T_{con})
\end{aligned} \tag{3.33}$$

Stepwise regression can help to eliminate variables that are not significant in the regression equations. The number of regression variables of constant speed chillers was significantly reduced from 16 to 6 and the determination coefficient R^2 was maintained at a higher value, i.e. 0.9936, indicating that the predicted values of normalized power in Equation 3.33 are in agreement with the data provided by the manufacturers.

3.7.2 Variable Speed Chillers

Based on the chiller modelling approach developed in Section 3.7.1, part load performance data of 1,000 RT (3,517 kW) and a 800 RT (2,814 kW) variable speed chillers at different condenser water entering temperatures, i.e. 20°C, 25°C and 30°C and different chilled water supply temperatures, i.e. 4°C, 5°C, 6°C and 7°C was obtained from the manufacturers to develop a model for the variable speed chillers.

Based on this chiller performance data, the statistical program SAS was used to perform a stepwise regression to screen out the best regression variables from all possible combination of the variables, i.e. $T_{ch,s}$, T_{con} and PLR .

The normalized power demand of the variable speed chiller, $w_{ch,var}$, can be expressed by Equation 3.34. There are five regression variables and the determination coefficient R^2 is 0.9898, indicating that the predicted normalized power of variable speed chillers in Equation 3.34 are in agreement with the data provided by the manufacturers.

$$\begin{aligned}
w_{ch,var} = & -0.17264 + 0.01801 (T_{con}) + 0.51707 (PLR^2) + 0.00054573 \\
& (T_{con}^2 \cdot PLR) - 0.00158 (T_{ch,s} \cdot T_{con} \cdot PLR)
\end{aligned} \tag{3.34}$$

3.8 Primary Chilled Water and Seawater Pump Model

Besides chillers, the DCS plant also consists of primary chilled water pumps, seawater pumps, pipework and associated control devices such as valves and sensors. The power

demand of a constant speed chilled water or seawater pump is influenced by the volume flow of the fluid and the pressure difference between the inlet and the outlet.

3.8.1 Flow rate

For each chiller unit, there will be one primary chilled water pump and one seawater pump, which are rated for the chilled water and seawater flow rates that match the respective flow rates through the evaporator and condenser of the chiller.

In this regard, the flow rate, M_{cwp} , of the chilled water to be handled by the primary chilled water pump is determined on the basis of the rated cooling capacity of chillers, and the design temperature difference between the supply and return chilled water.

For the seawater pump, its flow rate, M_{swp} , is determined on the basis of the heat rejection rate of the chiller. It can be taken as the sum of the cooling capacity and the rated power demand of the chiller, evaluated from the rated COP of the chiller, as shown in [Equation 2.1](#) in [Chapter 2](#). The design condenser inlet and outlet temperatures are 27°C and 32°C respectively.

3.8.2 Pump Head

The Building Energy Evaluation Program (V.1.0) developed by [Yik \(2012\)](#) makes use of a method for estimating the total pipe run of chilled water pipe in a chiller plant which is used to estimate the pumping pressure required by each primary chilled water pump. [Equation 3.35](#) shows the method for estimating the total pipe run, L_p .

$$L_p = 2 \times (Wd \times Dd) \times (1 + F_f) \quad (3.35)$$

where

Wd and Dd = floor plate width and depth of the DCS plant room respectively
 F_f = the allowance factor for pipe fittings

Pumping pressure required by the primary chilled water pump, P_{cwp} , is determined by Equation 3.36.

$$P_{cwp} = \Delta P_L \times L_P + \Delta P_{ch} \quad (3.36)$$

where

ΔP_L = pressure drop per unit length of the pipe run

ΔP_{ch} = water pressure drop across the chiller

Equation 3.36 can also be applied to estimate the pumping pressure of the seawater pump, P_{swp} .

Hence, power demand of the primary chilled water pump and seawater pump, i.e. W_{cwp} and W_{swp} , can be determined by Equations 3.37 and 3.38.

$$W_{cwp} = \frac{P_{cwp} M_{cwp}}{\eta_{cwp}} \quad (3.37)$$

$$W_{swp} = \frac{P_{swp} M_{swp}}{\eta_{swp}} \quad (3.38)$$

3.9 Chiller Plant Model

To determine an optimum number of chillers to be operated, an optimization program was developed using Excel VBA to search for the optimum combination of chillers according to the algorithm presented in Figure 3.15. The primary objective was to look for the best combination of chillers so that the sum of the hourly power demand of all running equipment in the chiller plant, i.e. chillers, primary chilled water pumps and seawater water pumps, should be kept to a minimum.

The chiller plant control strategy and the determination of PLR of the equally-sized or unequally-sized chillers in a chiller plant will be discussed in the following sections.

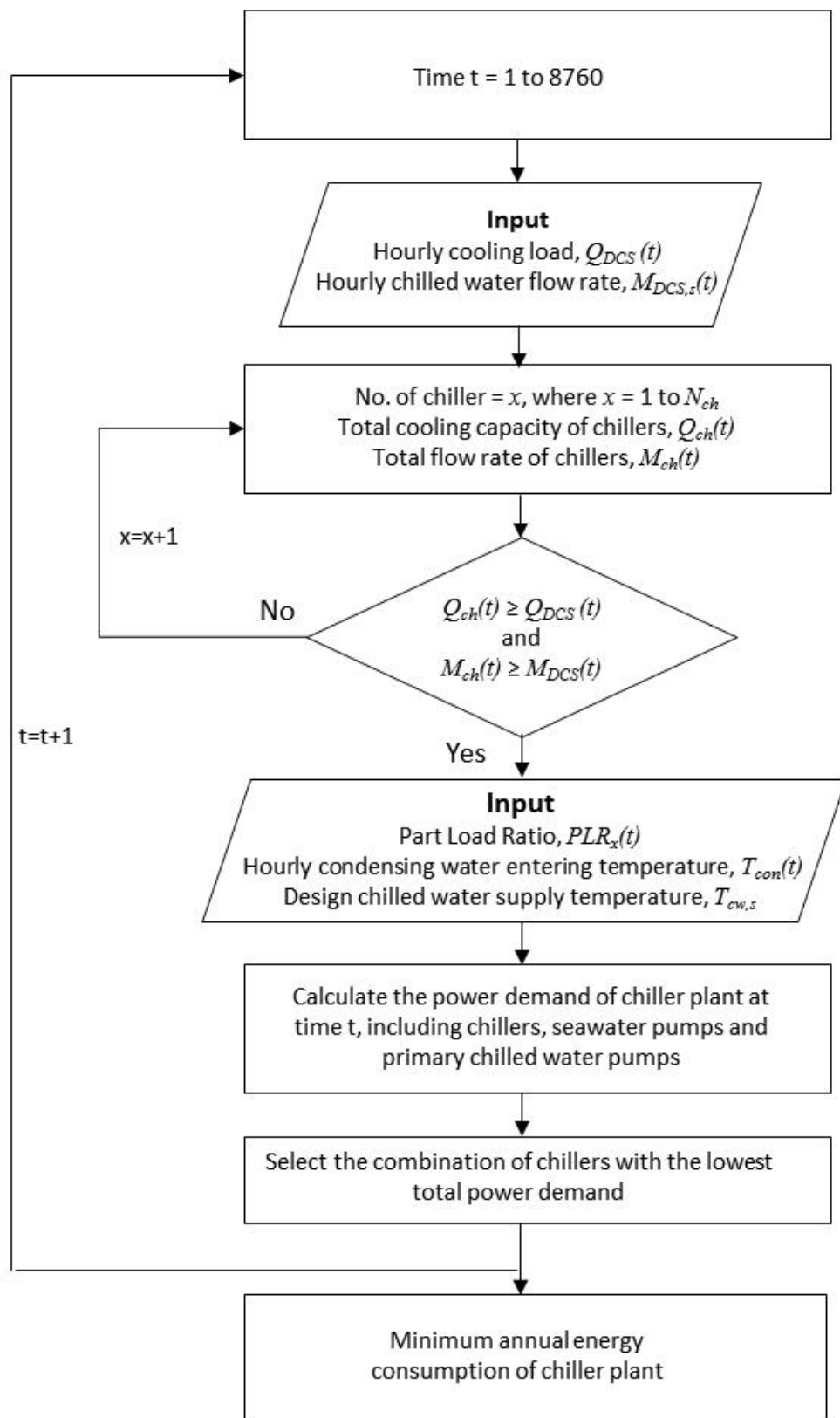


Figure 3.15 Algorithm for determining the minimum annual electricity consumption of the chiller plant

3.9.1 Chiller Plant Control Strategy

There are two basic chiller start or stop control strategies. One is based on system chilled water flow rate and the other is based on cooling load.

- i. Load based control strategy – compares the cooling capacity of the operating chillers with the calculated cooling load. The district total cooling load is determined by measuring the chilled water flow rate and the difference between the supply and return chilled water temperatures. An additional chiller is staged on when the operating chillers have insufficient capacity to meet the current cooling load. One of the operating chillers is switched off when the current cooling load can be met by the remaining chillers.
- ii. Flow based control strategy – compares the chilled water flow rate in the primary loop with that in the secondary loop. When the flow rate of the chilled water being circulated in the primary loop exceeds the water flow rate in the secondary loop, there will be a surplus flow through the decoupler bypass line. One of the operating chillers together with its primary chilled water pump and seawater pump will be stopped. On the other hand, when the chilled water flow rate of the secondary loop exceeds the flow rate of the water being circulated in the primary loop, deficit flow will occur, and the chilled water flows through the decoupler bypass line in a reverse direction. When deficit flow occurs, one more chiller together with its primary pump and seawater pump must be turned on immediately.

Ideally, the two strategies would be effectively the same since flow and load should track in a variable-flow system. However, flow and load do not track, i.e. the chilled water flow is not proportional to the cooling load when delta-T falls. In this case, neither strategy works ideally.

In this regard, to address the low delta-T issue, both the load based and flow based control strategies have to be applied to ensure that cooling load and chilled water flow can be met. A flow meter has to be installed in the chilled water supply line downstream

of the decoupler for staging chillers. This is to ensure that the secondary system flow to the building is adequate and that the primary system flow is equal to or greater than the secondary flow. Moreover, the operating chillers and pumps can meet both the load demand and chilled water demand.

3.9.2 Part Load Ratio of Chillers

Equal percentage load strategy was applied to determine the PLR of the operating chiller and the power consumption of the constant speed and variable speed chillers by [Equations 3.32](#) and [3.33](#) respectively. This is to ensure that the chillers carry an equal percentage of load and each of them operates in parallel with one primary chilled water pump and one seawater pump. This allows more flexibility for matching chiller capacity with system demand. Moreover, this can help to optimize the capacity of the chillers.

For a multiple chiller system consisting of N_{ch} number of equally- or unequally-sized chillers, the basic chiller sequencing control is to select the minimum number of evenly loaded chiller to offset the instantaneous cooling load at time t , $q(t)$. At part load, the PLR of x operating chillers, $PLR_x(t)$, at time t can be defined by [Equation 3.38](#).

$$PLR_x(t) = \frac{q(t)}{\sum_{x=1}^{N_{ch}} CC_x} \quad (3.38)$$

where

x = number of operating chillers to offset the instantaneous cooling load

CC_x = cooling capacity of the individual chiller

It is noted that hunting or surging will occur when the chiller is operated at low load. In surging, considerable vibration and eventual damage may occur in the compressor. To prevent the surge, one way is to maintain a minimum operating cooling capacity, i.e. 30% ([Chang et al., 2009](#); [Taylor Engineering, 2009](#)). To achieve this, the minimum value of the PLR will be set at 0.3 in the simulation of energy consumption of the chillers.

3.10 Summary

In this chapter, mathematical models were established for all the major components in DCS₀. To build a cooling coil model that can well represent the operating situation of the DCS, a systematic design approach was adopted. This model can simulate the operation of over thousands of cooling coils in a district in normal conditions. Moreover, field data of the chilled water systems of two commercial buildings with the low delta-T syndrome was obtained. This provided a reference for building a cooling coil model that had incorporated the low delta-T issue. These cooling coil models for DCS can be regarded as the first-of-its-kind.

Moreover, a model was tailor-designed for the heat exchanger serving as an interface between the chilled water distribution loop of the DCS and the chilled water circuit in the building. It was created to simulate the chilled water flow rate and temperature of the chilled water returning from each building to the centralized chiller plant via the chilled water distribution network.

To facilitate a quantitative evaluation of the dynamic change in pressure head corresponding to the change in chilled water flow rate, a hydraulic distribution network model was set up to couple pressure-flow relationships with the dynamic thermal loads of the buildings in the district. With the hourly chilled water flow rate and pressure head, the hourly demand and hence the electricity consumption of the secondary variable speed pumps can be determined.

The predicted power demand of the two major electricity consuming equipment in this study, i.e. chillers and variable speed pumps, well agreed with the data given by the manufacturers. This demonstrated that both models could exhibit acceptable performance in prediction. With the use of a stepwise multiple regression, a mathematical model in the form of polynomial with only five and six regressors (independent variables) was developed for the constant and variable speed chillers respectively. The few regressors in the polynomial regression model not only make the model structurally simple but also maintain a higher value of the determination coefficient R^2 .

Moreover, two simulation programs were developed to simulate the electricity consumption of various combinations of pumping station in the distribution loop and the electricity consumption of various chiller plant configurations. The mathematical models and simulation programs developed in this chapter provide a vital simulation platform for evaluation of the energy efficiency enhancement measures as shown in [Chapters 6 to 8](#).

Chapter 4

Impacts of Degrading Delta-T on the Energy Performance of DCS_o

4.1 Overview

As discussed in [Chapter 1](#), some researchers ([Kirsner, 1996](#); [Avery, 1998](#); [Hartman, 2001](#)) and manufacturers ([Schwedler and Bradley, 2000](#)) have advocated the use of variable primary flow (VPF) systems to replace constant primary–variable secondary flow (P-S) systems to resolve the low delta-T problem in chilled water systems.

As explained in [Chapter 1](#), the use of variable chilled water flow chillers in the VPF system does not bring any benefit in energy consumption as compared to using constant chilled water flow chillers in the P-S system ([Schwedler and Bradley, 2000](#); [Bahnfleth and Peyer, 2006](#); [Bullet, 2007](#)).

Moreover, chillers in P-S systems have a constant chilled water flow rate through the evaporator. It guarantees an optimum water-side heat transfer and prevents excessive fouling of the tubes. On the other hand, the VPF chiller allows chilled water flow rate to be reduced to 50% to 60% at low loads ([Brasz and Tetu, 2008](#); [Yang and Lin, 2012](#); [Trane Hong Kong, 2013](#)). Building owners, however, have reservation on this minimum flow rate as the VPF chillers cannot operate below a minimum percentage of rated

chilled water flow rate, as otherwise they will result in nuisance shutdowns and perhaps even freezing, ruptured evaporator tubes and costly equipment downtime. In this regard, some building owners would set the minimum flow rate at a level about 5% to 10% higher than the minimum flow rate recommended by the manufacturers in order to prevent the chillers from being shut down and affecting business operation. This practice, however, may reduce the energy saving potential of the variable speed pumps (VSP) of the VPF system.

For the chilled water distribution pumps, [Taylor \(2002b\)](#) and [Rishel \(2000\)](#) pointed out that the P-S system consumed more pumping energy than the VPF system because the primary constant speed pumps (CSP) selected for a lower pressure head in the P-S system were generally less energy efficient. The efficiency of CSP was about 70%, which was 10% less than that of the secondary VSP ([Bahnfleth and Peyer, 2004](#)). This inherently less efficient characteristic made the comparison of the two systems unfair. Nowadays, with the advancement in technology, the efficiency of the primary pump with a lower pressure head can be designed as high as 85% ([PACO, 2014](#)), which is comparable to the efficiency of the pump with a higher pressure head at the same design chilled water flow rate.

Consequently, the VPF system may not be a good choice for DCS. Currently, there is a lack of detailed quantitative research to compare the energy performance of the chilled water pumps of P-S systems against the VPF system in a DCS. This chapter shows the results of a comparative analysis of the pumping energy performance of the P-S and VPF systems with degrading delta-T. Moreover, the impacts of low delta-T on the energy performance of the baseline DCS_O will also be discussed.

4.2 A Comparison of the Energy Performance of P-S and VPF Systems

4.2.1 Design Considerations

A P-S system model was constructed based on the baseline DCS_O described in [Chapter 2](#). For the VPF system model, it was created by replacing the constant speed primary and variable speed secondary chilled water pumps in the P-S system with one set of

variable speed chilled water pumps with a high enough pressure head to distribute chilled water through the piping network as in the production and distribution loops of the P-S system. The following are the design considerations for the simulation study.

- i. As advised by several large pump manufacturers, the efficiency of a primary pump with a low pressure head in DCS_O can be selected to be over 85%, which is comparable to the secondary pump designed with a high pressure head. This can help to tackle the issue that [Taylor \(2002b\)](#) and [Rishel \(2000\)](#) have raised, as mentioned in [Section 4.1](#). To ensure a fair comparison of both systems, the efficiency of the CSP and VSP in both systems was assumed to be the same, i.e. 80%. Almost all manufacturers are able to provide pumps with this level of efficiency.
- ii. The main difference between constant and variable speed pumps is the introduction of a variable frequency drive, which has an impact on the power input of VSP. The power required by the VSP to run at nearly full speed is larger than the power required by a CSP because energy loss in the variable frequency drive will lower the overall efficiency of the VSP ([Marchi et al., 2012](#)). The efficiency of a variable frequency drive ranges from 80% to 95%, depending on the speed of rotation and hence the pump's flow rate ([Eaton, 2011](#)). To be on the safe side, the efficiency of the variable frequency drive was assumed to be 90% in this study.
- iii. According to a study conducted by [Doty \(2011\)](#) regarding the energy performance of the variable chilled water flow chiller, a minimum chilled water flow rate of 50% is prudent to ensure that the chilled water can stay solidly in the turbulent zone of fluid movement through the evaporator tubes.
- iv. The energy consumption of seawater pumps were not included in the comparative analysis of the P-S and VPF systems as these systems do not have any impact on the energy consumption of the seawater pumps.

[Table 4.1](#) shows a summary of the design conditions of the chilled water pumps in the P-S and VPF systems.

Table 4.1 Design conditions of the chilled water pumps in P-S and VPF systems

	P-S System		VPF System
	CSP	VSP	VSP
No. of pump	10	10	10
Design flow rate, l/s	718	718	718
Design pump head, m	16.8	56.9	73.7
Rated power, kW	164.4	618.5	801.2

4.2.2 Results Discussion

4.2.2.1 With reference to the mathematical model developed in [Chapter 3](#), the annual electricity consumption of the constant and variable speed pumps in the P-S and VPF systems with a low delta-T syndrome was simulated based on the year-round operating flow rate, pressure head and running hour of the pumps. [Table 4.2](#) lists out the annual electricity consumption of the pumps for comparison. It was found that the electricity consumption of the pumps in the P-S system would be slightly less than that of the pumps in the VPF system, e.g. by 0.5%.

Table 4.2 Comparison of the annual electricity consumption of chilled water pumps in the P-S and VPF systems

Annual electricity consumption, kWh			Difference between P-S and VPF systems, %
P-S System		VPF System	
CSP	VSP	VSP	
5,022,380	14,964,166	20,078,161	0.5

The energy consumption of the CSP and VSP in the P-S and VPF systems is determined by the power demand of the pumps and their operating hours, which are explained in detail in the following sections.

4.2.2.2 Regarding power demand, a VSP is equipped with motors that are able to be linked to a variable frequency drive. This drive is able to modify the frequency of power supply so that the pump can run at different levels of speed. Under

part load operation, the VSP will reduce its speed and power according to the operating flow rate. On the contrary, the power demand of CSP remains unchanged with varying flow requirements.

4.2.2.3 In addition to power demand, the energy consumption of pumps also depends on their operating frequency, i.e. the total hours in which the pumps are operated, denoted as “pump hours” in this study. To take an example, if ten pumps have operated for eight hours, they are regarded as having operated for 80 pump hours.

Figure 4.1 shows the operating frequency profile of the VSP in the P-S and VPF systems at different pump flow ratios. It was envisaged that the pumps would frequently operate at a flow ratio higher than 80% for over 80% of the annual pump hours.

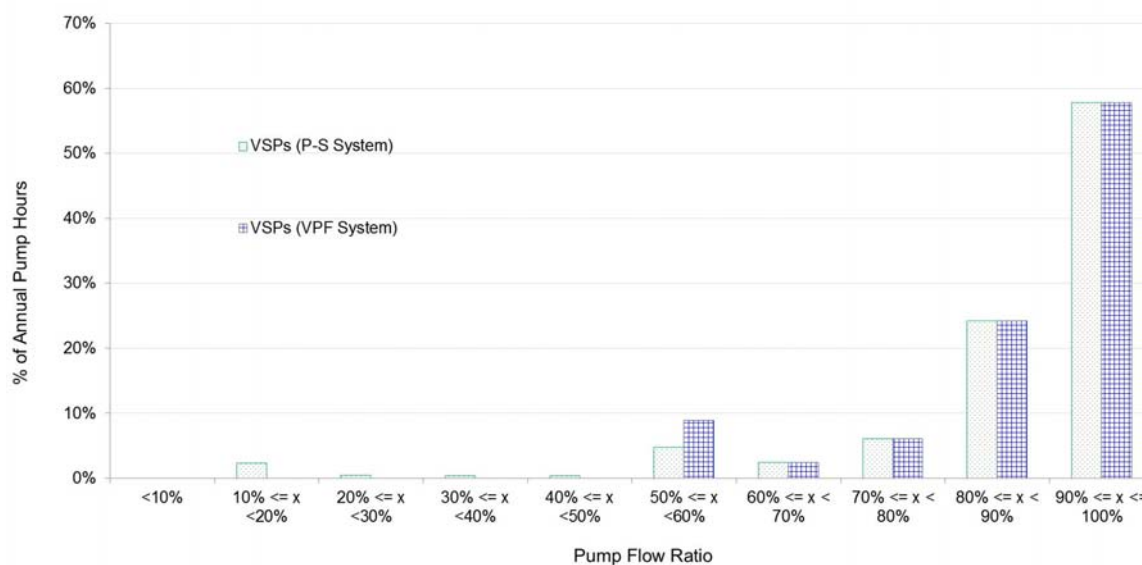


Figure 4.1 Operating frequency profile of the pumps in P-S and VPF systems at different flow ratios

4.2.2.4 Figure 4.2 shows the annual energy consumption of the pumps in the P-S and VPF systems at different flow ratios. The energy consumption of the VPF system was slightly lower than that of the P-S system when the pump’s flow ratio was below 80%. When the ratio was over 80%, the energy consumption

of the P-S system was higher than that of the VPF system. As the pumps are operated at a flow ratio greater than 80% for over 80% of the total annual pump hours, the energy saving of the P-S system is sufficient for compensating the additional energy consumption at a low flow ratio. Consequently, the overall electricity consumption of the pumps in the P-S system is slightly less than that of the pumps in the VPF system.

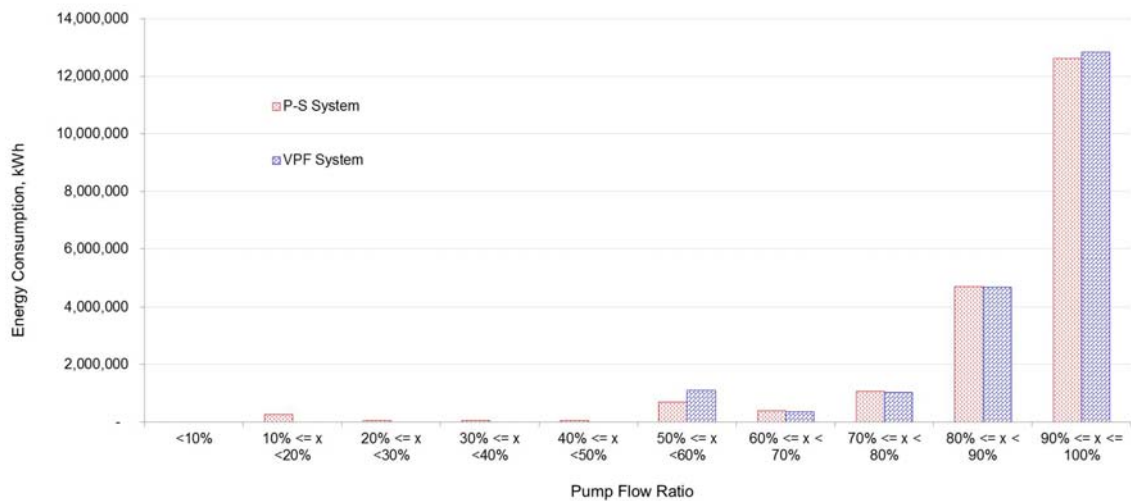


Figure 4.2 Annual energy consumption profile of the P-S and VPF systems at different flow ratios

4.2.2.5 In this section, different energy consumption patterns are discussed in situations where pumps are operated at low or high flow ratios.

Pumps operating at a low flow ratio

- i. When pumps run at a low flow ratio, the flow demand and pressure head of the VSP in the P-S and VPF systems will also drop. Accordingly, the power demand of the VSP in both systems will decrease.
- ii. However, the power demand of the primary CSP in the P-S system remains unchanged even when the chilled water flow demand decreases further. There is no energy saving potential for the primary pumps in the P-S system under such low flow condition.

- iii. Nevertheless, for the VPF system, the chilled water flow rate of the chillers and the corresponding VSP have to maintain a minimum of 50% of the rated flow rate to avoid causing damage to the evaporator. This limits the allowable decrease in pump speed and hence the energy saving potential of the VSP when the pump's flow ratio is below 50%.
- iv. On the contrary, the VSP in the P-S system do not suffer from the minimum flow rate requirement. The energy saving of the VSP in the P-S system can help compensate the energy consumption of the CSP operated at low flow ratio. This can help minimize the difference in the energy consumption between the P-S and VPF systems.
- v. Moreover, there were only 18% of the annual pump hours in which the pumps were operated at a flow ratio below 80%. The energy saving potential of the VSP in the VPF system is less significant, causing the electricity consumption of the VPF system to be slightly (i.e. 0.5% of the total energy consumption of the P-S system) higher than that of the P-S system.

Pumps operating at a high flow ratio

- i. For a VSP, the equipment efficiency, that is the wire to water efficiency (Rishel, 2001) η_{ww} , is often used to characterize how much energy is required for a VSP to deliver water. The general expression of this wire to water efficiency is represented by Equation 4.1, where η_{VFD} , η_{motor} , and η_{pump} are the efficiency values of the variable frequency drive, the motor and the pump respectively. For a CSP, as there is no frequency drive, η_{VFD} therefore equals 1.

$$\eta_{ww} = \eta_{VFD} \times \eta_{motor} \times \eta_{pump} \quad (4.1)$$

Hence, the main difference between the VSP and the CSP is in the variable frequency drive, which can help reduce the speed and hence the power required for the VSP running at a lower flow rate.

However, the variable frequency drive will have an impact on the overall wire to water efficiency of the VSP, particularly when the VSP runs nearly at its full speed. It is because under such circumstances, the efficiency of the drive decreases the efficiency of the pump running at nearly full speed. It causes the VSP to consume more power than the CSP when the pump runs at nearly full speed.

- ii. In this study, when the pump's flow ratio was greater than 80%, the power required for the VSP in VPF system was slightly higher than that of the VSP and CSP the in P-S system, as shown in [Figure 4.2](#).
- iii. Moreover, there were over 80% of the annual pump hours in which the pumps in both systems were operated at a flow ratio greater than 80%. This enables the P-S system to consume less electricity (i.e. 1% of the total energy consumption of the P-S system) than the VPF system. This energy saving under such operating condition is sufficient to compensate the additional energy consumption of the pump at low flow ratio.

Hence, the overall energy consumption of the P-S system was slightly lower than that of the pumps in the VPF system, i.e. by 0.5%.

4.2.2.6 Moreover, in a P-S system, there is an opportunity of lowering the energy consumption of the secondary pumps in the distribution loop by adopting a multiple pumping station design. This will be further discussed in [Chapter 6](#).

4.3 Energy Performance of DCS_0 under Normal or Low Delta-T Conditions

4.3.1 Delta-T of Chilled Water

Improving the chilled water system's operating efficiency to minimize its energy consumption is a big challenge for plant operators and researchers. Under normal delta-T condition, i.e. with no impact from low delta-T, one of the most effective energy efficiency measures is to maximize the chilled water return and supply temperature difference, or delta-T, of the system loop. The benefit of a high delta-T is that it can help to reduce the chilled water's flow rate and hence pump energy usage. As explained in [Chapter 1](#), however, almost every chilled water system is affected by the low delta-T problem, particularly at low cooling loads ([Taylor, 2002](#)).

In this regard, the cooling coil models (under normal or low delta-T conditions) and heat exchanger model developed in [Chapter 3](#) were used to simulate the hourly chilled water flow rate and temperature of chilled water returning from each building to the distribution loop according to their respective hourly cooling load profile under normal and low delta-T conditions. Then, a mixed-flow approach was used to calculate the average chilled water return temperature and hence the temperature difference in the distribution loop.

[Figure 4.3](#) shows the variation in delta-T under normal or low delta-T conditions, as a function of the percentage of the design cooling load of the hypothetical district.

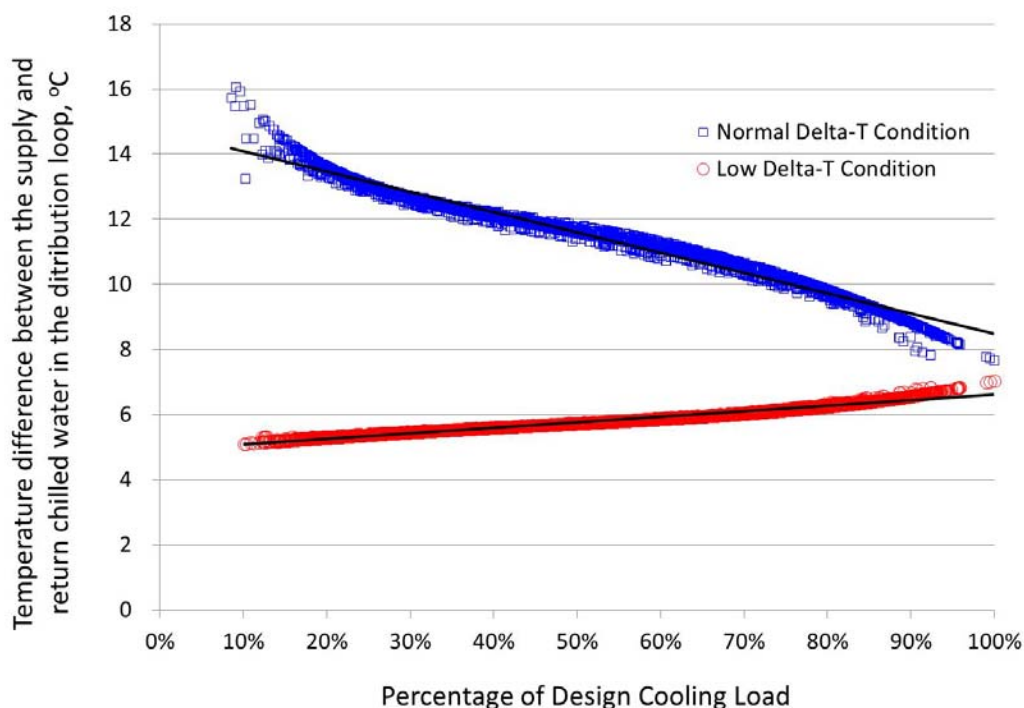


Figure 4.3 Variation of the temperature difference between supply and return chilled water under normal or low delta-T conditions

Under normal conditions, the temperature difference decreases when the cooling load increases from a low load to a full load. Eventually, it decreases to a level close to the design value, i.e. 7°C. On the contrary, low delta-T occurs when the temperature difference falls short of the design level at low cooling loads. It then gradually increases to a level close to the design value when the cooling load increases to a full load. Based on these values, delta-T curves were plotted with the respective trend lines, showing patterns similar to the “favourable” and “unfavourable” delta-T curves modelled by [Bahnfleth and Peyer \(2006\)](#). A favourable delta-T indicates that delta-T increases in a linear direction as the load decreases, whereas an unfavourable delta-T indicates that delta-T decreases in a linear direction as the load increases ([Figure 4.4](#)).

4.3.2 Chilled Water Flow Rate

[Figure 4.5](#) shows the distribution of the hourly chilled water flow rates simulated in [Section 4.3.1](#). These rates were plotted against different percentages of the design cooling loads under normal and low delta-T conditions. At low delta-T, flow rate exceeds the design value. This is because the difference between the chilled water

supply and return temperatures is far lower than that of a DCS without the low delta-T problem.

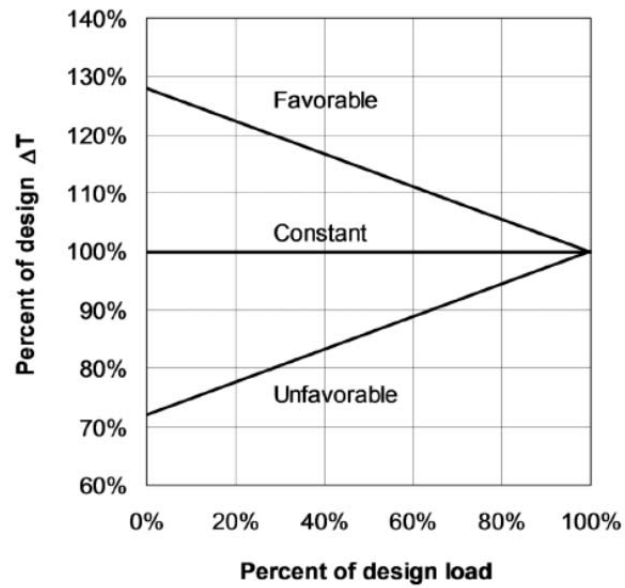


Figure 4.4 Modelled variation of chilled water delta-T
(Source: Bahnfleth and Peyer, 2006)

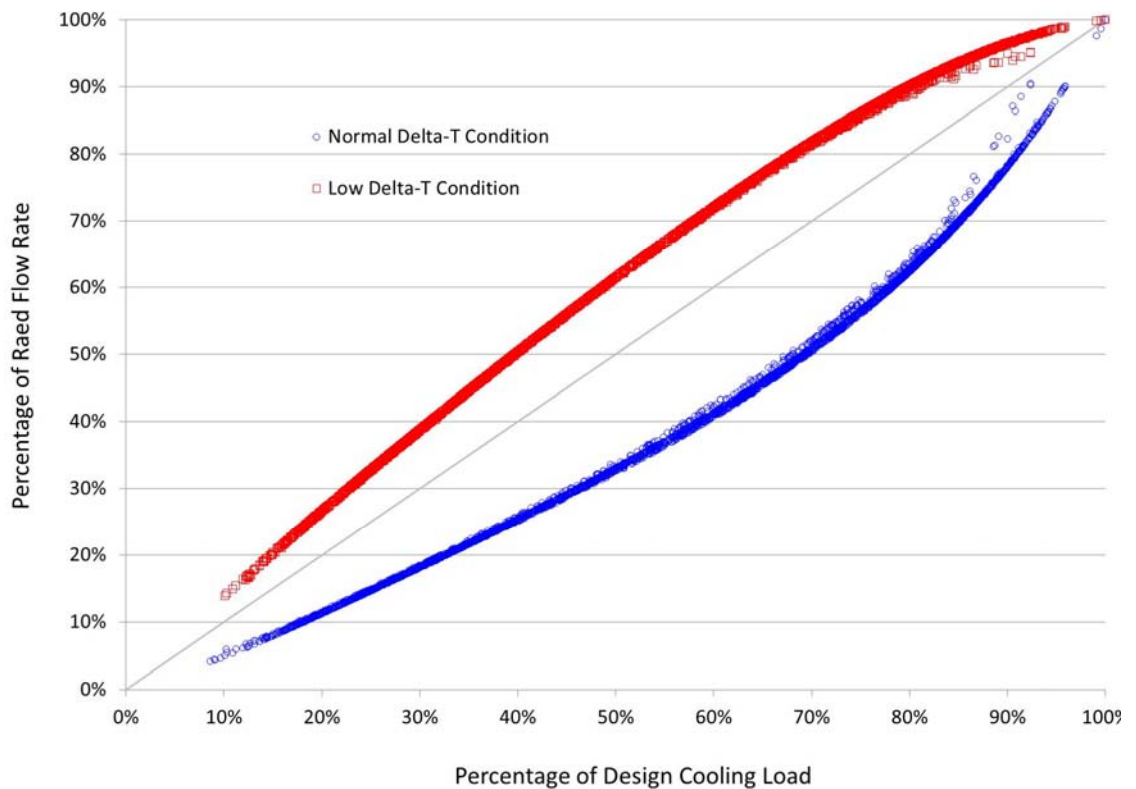


Figure 4.5 Chilled water flow rate of different cooling load percentages

[Table 4.3](#) shows the annual average chilled water flow rates required for distributing chilled water from the chiller plant. These rates were calculated by averaging the hourly chilled water flow rates around a year, as simulated by the cooling coil and heat exchanger models developed in [Chapter 3](#). It can be seen that the flow rate required at low delta-T was 77% higher than that in design condition.

Table 4.3 Annual average chilled water flow rate with different delta-T

	Normal delta-T	Low delta-T	Difference, %
Annual average chilled water flow rate, m ³ /s	1.35	2.38	77

As mentioned in [Chapter 3](#), two basic chiller staging control strategies can be used for designing a DCS, i.e. system flow rate control and load based control. The flow based control strategy continuously monitors cooling loads to see if they are met by starting additional chillers and pumps to ensure that the primary chilled water flow in the production loop is larger than the secondary flow in the distribution loop. This means that chillers are not fully loaded when delta-T is below the design value. This would degrade the energy performance of the chillers because they are operated at lower PLR, which is lower than the optimum range of 65% and 85% ([Wang et al., 2012b](#)), where efficiency is typically at the maximum level for constant speed chillers.

4.3.3 Operating Frequency of Chillers

As shown in [Figure 4.5](#), for a given cooling load, the chilled water flow rate with a low delta-T is relatively higher than that with a normal delta-T. The chiller plant was designed to meet both the chilled water flow rate and cooling load requirements. [Figure 4.6](#) shows the number of chillers to be operated in both conditions at different cooling loads. The annual chiller hours (the total number of hours in which the chillers are operated) at low delta-T were 33,952, which was 16.4% higher than those of the chillers operating under a normal delta-T condition, i.e. 29,158 hours.

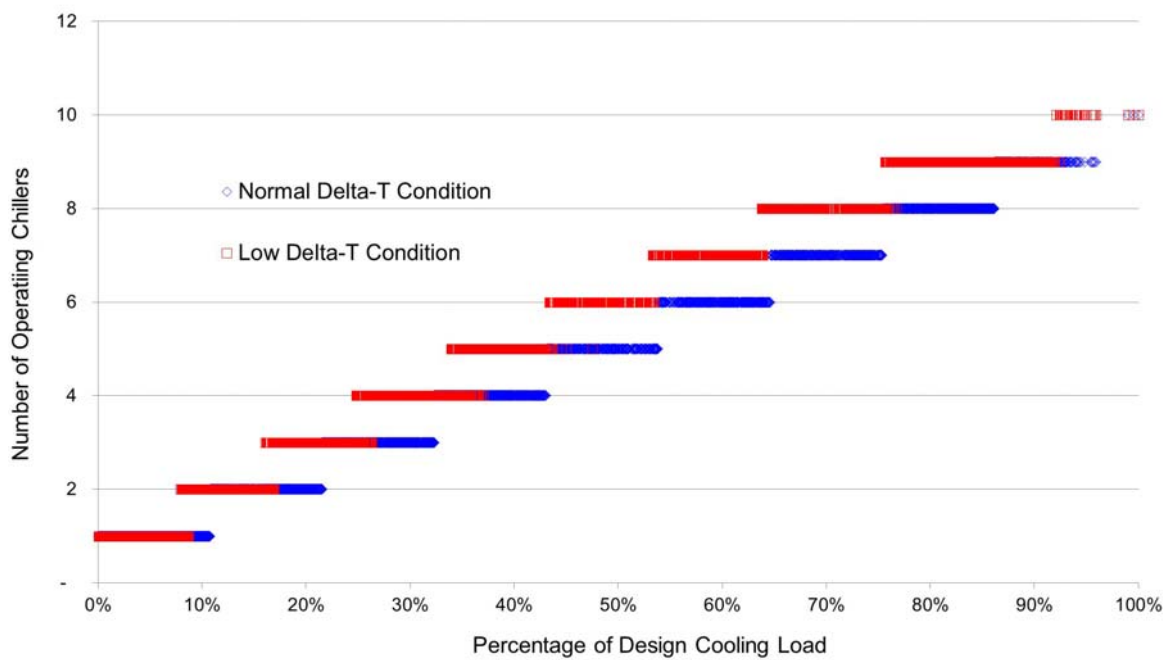


Figure 4.6 Number of operating chillers at different percentages of design cooling load

Throughout the year, no additional chiller was required to be operated at low delta-T for 46% of the annual operating hours (i.e. 8,760 hours). It is because the increased chilled water flow rate under this circumstance does not exceed the design level of chillers that are operated in design conditions. Therefore, there is no need to operate more chillers. In this regard, there is no significant difference in the number of chillers to be operated under both conditions and there is no difference in energy consumption.

On the other hand, additional chillers had to be staged on for about 54% of the annual operating hours in order to increase the primary flow rate at low delta-T. [Figure 4.7](#) shows the frequency of operating one or two additional chillers at low delta-T in comparison with those in design conditions throughout the year. There were 4,670 hours (53% of the total 8,760 hours) in which one additional chiller was required to be operated and 62 hours (1% of the total 8,760 hours) in which two additional chillers were required. It is because the increased chilled water flow rate has exceeded the design value of the chillers that are operated under design conditions. The number of chillers being operated in design conditions is unable to meet the increased chilled water flow rate in the distribution loop. To overcome the deficiency in cooling capacity

inherent with these problems, additional chillers are required to be operated to provide the required capacity and achieve a higher primary chilled water flow rate so as to meet not only the cooling load but also the excessive secondary chilled water flow in the distribution loop.

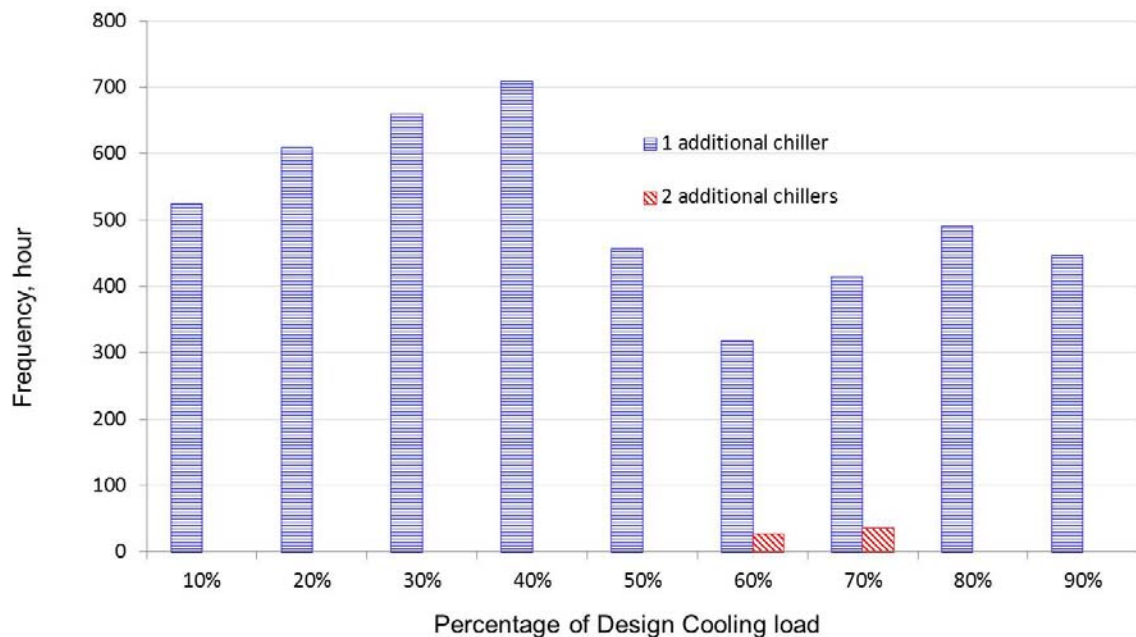


Figure 4.7 Frequency of operating additional chillers at low delta-T

4.4 Comparison of the Electricity Consumption of DCS_O under Normal and Low Delta-T Conditions

Table 4.4 lists out the annual electricity consumption of the chillers, seawater pumps, and primary and secondary pumps in DCS_O. Chillers accounted for a major portion of the DCS' annual electricity consumption, i.e. 82% and 76% under design and low delta-T conditions respectively. They were then followed by secondary chilled water pumps. Primary chilled water pumps and seawater pumps attributed only a small percentage in the overall annual electricity consumption of DCS_O.

When delta-T falls far short of the design level, a higher chilled water flow rate occurs in the distribution loop. Additional chillers and hence primary chilled water pumps and seawater pumps have to be brought into operation to maintain the flow requirements even though the total cooling capacity of all chillers is far below the cooling demand.

This leads to an increase in the electricity consumption of the chillers. Moreover, as flow rate increases significantly, the electricity consumption of secondary chilled water pumps increases accordingly. Specifically, the annual electricity consumption of DCS_O had increased by 9.3% at low delta-T.

Table 4.4 Annual electricity consumption of DCS_O under normal and low delta-T conditions

	Annual electricity consumption, kWh (% of overall electricity consumption)				Additional electricity consumption at low delta-T, kWh (% of difference)	
	Normal delta-T		Low delta-T		kWh	%
	kWh	%	kWh	%		
(a) Chiller plant						
i. Chiller	87,362,967	82	88,827,472	76	1,464,505	1.7
ii. Pri. ch. w. pumps	4,794,871	4	5,583,218	5	788,347	16.4
iii. Seawater pump	6,511,953	6	7,582,613	6	1,070,660	16.4
Sub-total [i + ii + iii]	98,669,791	92	101,993,303	87	3,323,512	3.4
(b) Sec. ch. w. pumps						
	8,251,900	8	14,911,696	13	6,659,796	80.7
Total [items (a) + (b)]	106,921,691		116,904,999		9,983,308	9.3

4.4.1 Electricity Consumption of Secondary Chilled Water Pumps

Among the four major components in [Table 4.4](#), secondary pumps were responsible for 8% of the total energy consumption of DCS_O at normal delta-T. However, when low delta-T occurs, its impact on the DCS' energy consumption became prominent, as it had led to an increase of 80.7% in the energy consumed. It is because the energy consumption of the secondary pumps varies with the chilled water flow rate in the distribution loop. As discussed in [Section 4.3.2](#), the annual average chilled water flow rates increased by 77% as a result of degrading temperature difference. This has caused a much higher increase in the pump energy consumed.

4.4.2 Electricity Consumption of Chillers

Chillers are the dominant electricity consuming equipment in the DCS. [Table 4.4](#) shows that for DCS₀, low delta-T could lead to an increase of 1.7% in the annual electricity consumption of chillers. Given the same cooling load, additional chillers are required to cater for the additional chilled water flow rate at low delta-T. In this regard, the PLR of chillers is significantly reduced because it is balanced to carry an equal percentage of the cooling load. As the COP of a constant speed chiller decreases when the PLR decreases, this has lowered the COP of the chiller.

As discussed in [Section 4.3.3](#), there were 4,670 hours (53% of the total 8,760 hours) in which one additional chiller was required to be operated and 62 hours (1% of the total 8,760 hours) in which two additional chillers were required at low delta-T in comparison with those under normal delta-T conditions throughout the year. For the period in which one additional chiller was required, the average hourly PLR and COP of the chillers operated under both conditions were simulated based on the chiller model developed in [Chapter 3](#). The same simulation was performed for the period where two additional chillers were required.

Table 4.5 Average PLR and COP when one or two additional chillers are operated under normal or low delta-T conditions

	One additional chiller		Two additional chillers	
	Normal delta-T	Low delta-T	Normal delta-T	Low delta-T
Average PLR	0.908	0.687	0.993	0.730
Average COP	6.149	5.864	6.173	6.042

It can be seen in [Table 4.5](#) that the average PLR at low delta-T was relatively lower comparing to that at normal delta-T. Furthermore, the average COP of chillers was also relatively lower at low delta-T, as compared to the COP in design condition. This explains why the electricity consumption of chillers operating at low delta-T is relatively higher in comparison with that of the chillers under normal delta-T condition.

Nevertheless, the impact of the low delta-T syndrome on the energy consumption of chillers is moderate in comparison with the secondary pumps. It is because the capacity of the chillers is sufficiently large enough to cater for the increase in the chilled water flow rate at low delta-T. In this case, one additional chiller was required to be on for only 53% of the annual total operating hours.

4.4.3 Electricity Consumption of Primary Chilled Water and Seawater Pumps

In DCS_O, constant speed primary chilled water pumps and seawater pumps were interlocked with dedicated chillers so that they could be switched on and off together. As discussed in [Section 4.3.3](#), the total operating hours of chillers at low delta-T were 16.4% higher than those of the chillers operating at normal delta-T. This explains why the annual electricity consumption of the primary chilled water and seawater pumps also increased proportionally by 16.4%, as shown in [Table 4.4](#).

4.5 Summary

A comparative analysis of the energy performance of P-S and VPF systems was conducted with reference to the baseline DCS_O. The results indicate that the VPF system was unable to yield any significant saving in the electricity of a large scale DCS such as DCS_O. The main reason is that there were over 80% of the annual pump hours in which the pumps in both systems were operated at a flow ratio greater than 80%. Under such circumstances, the variable frequency drive decreases the efficiency of the VSP running at nearly full speed. It causes the VSP to consume more power than the CSP. This enables the VSP and CSP in the P-S system to consume less electricity than the VSP in the VPF system. This has resulted in a slightly lower electricity consumption of the P-S system, which was 0.5% less than that of the pumps in the VPF system.

Moreover, a comparative analysis of the energy performance of DCS_O with a P-S system under normal or low delta-T conditions was performed. The simulation results show that chillers represent a major portion of the total electricity consumption of the DCS. They are then followed by distribution pumps. Primary chilled water pumps and seawater pumps attribute the least proportion. Compared to a normal delta-T situation,

the flow rate required to distribute chilled water from the chiller plant was 77% higher and the annual total electricity consumption of the DCS was increased by 9.3% at low delta-T.

Under such circumstances, additional chillers have to be staged on to meet the excessive chilled water flow. More electricity is needed for operating additional chillers to overcome the cooling capacity deficiency inherent with the degrading temperature issue. It is because the average hourly PLR and COP of the chillers at low delta-T are relatively lower than those in design conditions. It is interesting to note that the percentage of electricity consumption increased by 1.7% as no additional chiller was required to be operated at low delta-T for about 46% of the total operating hours. Nevertheless, as chillers were the major energy consuming equipment (76% of the total electricity consumption) in DCS_O, it was worth investigating an optimum chiller system configuration that could enhance its overall energy efficiency and accommodate the low delta-T issue.

Secondary pumps were the second largest electricity consuming equipment in DCS_O. Although their proportion of electricity consumption was relatively less as compared to chillers, their electricity consumption still increased massively by 81% due to the increase in the chilled water flow rate with degrading temperature difference. Potential energy saving measures associated with the use of various pumping station configurations will be studied in the chapters to follow.

Chapter 5

Effects of Chiller System Configuration on the Energy Performance of DCS_O

5.1 Overview

As it seems inevitable that almost every chiller plant is affected by the low delta-T syndrome, particularly at low cooling loads, additional chillers and pumps would be necessary for maintaining a primary flow in the production loop larger than the secondary flow in the distribution loop. As a result, chillers would operate at a part load ratio (PLR) smaller than the optimum range where efficiency or COP is maximized. According to the study in [Chapter 4](#) regarding the energy consumption of the base DCS_O at low delta-T, the chilled water plant was responsible for 87% of the total electricity consumption of a DCS at low delta-T ([Table 4.5](#)). Secondary chilled water pumps accounted for the remaining 13%. It is therefore imperative to explore ways of designing a chiller system configuration that can accommodate the low delta-T syndrome with little loss of efficiency.

As mentioned in [Chapter 2](#), five alternative configurations of chiller system - C_A, C_B, C_C, C_D and C_E - were defined (see [Table 2.8](#) in [Chapter 2](#)) by varying the influential design parameters of the chiller system C_O in DCS_O. These parameters included the number, cooling capacity and type of chillers. In this chapter, an evaluation of the

effectiveness of these five configurations in improving the energy performance of DCS_O, with C_O taken as the base chiller system configuration is summarized and discussed.

Using the mathematical models developed in [Chapter 3](#), the energy consumption of these five chiller system configurations was evaluated by simulation for comparison. The results are shown in [Section 5.2](#). Moreover, a detailed evaluation of the effectiveness of each design parameter can be found in [Sections 5.3, 5.4 and 5.5](#). [Section 5.6](#) gives a summary of the comparative analysis.

5.2 Comparison of Annual Total Electricity Consumption of DCS_O in Different Chiller System Configuration Designs

With all other design conditions of DCS_O held constant, its chiller system C_O was replaced by five alternative configurations, i.e. C_A to C_E, in turn, in the study. A comparison of the annual total electricity consumption of DCS_O when incorporated with each of these five configurations and operating with the low delta-T condition in place, is given in [Table 5.1](#).

The results show that all the five alternative configurations could lead to positive savings to different degrees in the annual total electricity consumption of DCS_O.

Among these five configurations, use of C_B had the smallest reduction in electricity consumption, i.e. 1.6%. In this case, the number of equally-sized constant speed chillers was increased from 10 in C_O to 15. For C_C, its configuration is similar to C_B's except that the chillers of the former are different in size. This change could help achieve a 2.9% saving in the DCS' annual electricity consumption, which would be higher when C_B was used. The adoption of variable speed chillers in C_A, C_D and C_E provided a significant improvement to the DCS' energy performance. A significant reduction was achieved by adopting C_E, which had led to the highest saving of 11.6%.

Table 5.1 Comparison of the annual total electricity consumption of DCS_O using various chiller system configurations at low delta-T

	C _O	C _A	C _B	C _C	C _D	C _E
Design parameter						
No. of chiller	10	10	15	15	15	15
Size	Equal	Equal	Equal	Unequal	Equal	Unequal
Type	Constant speed	Variable speed	Constant speed	Constant speed	Variable speed	Variable speed
Total chiller hours	33,952	33,952	48,279	37,127	48,279	37,746
Annual electricity consumption, kWh (% of total consumption)						
(a) Chiller plant						
i. Chiller	88,827,472 (76)	77,216,917 (74)	87,605,334 (76)	86,686,293 (77)	76,705,719 (74)	76,339,990 (75)
ii. Pri. ch. w. pump	5,583,218 (5)	5,583,218 (5)	5,289,233 (5)	5,040,671 (4)	5,289,233 (5)	5,107,501 (5)
iii. Seawater pump	7,582,613 (6)	7,582,613 (7)	7,198,935 (6)	6,845,941 (6)	7,198,935 (7)	6,936,400 (7)
Total [i + ii + iii]	101,993,303 (87)	90,382,748 (86)	100,093,502 (87)	98,572,905 (87)	89,193,887 (86)	88,383,890 (86)
(b) Sec. ch. w. pump	14,911,696 (13)	14,911,696 (14)	14,911,696 (13)	14,911,696 (13)	14,911,696 (14)	14,911,696 (14)
Total [(a) + (b)]	116,904,999	105,294,444	115,005,198	113,484,601	104,105,583	103,295,586
Difference in electricity consumption w.r.t. C _O , kWh (% of total saving)						
(a) Chiller plant						
i. Chiller	-	11,610,555 (-13.1)	1,222,139 (-1.4)	2,141,179 (-2.4)	12,121,753 (-13.6)	12,487,482 (-14.1)
ii. Pri. ch. w. pump	-	- (0.0)	293,985 (-5.3)	542,547 (-9.7)	293,985 (-5.3)	475,717 (-8.5)
iii. Seawater pump	-	- (0.0)	383,678 (-5.1)	736,672 (-9.7)	383,678 (-5.1)	646,214 (-8.5)
Total [i + ii + iii]	-	11,610,555 (-11.4)	1,899,802 (-1.9)	3,420,398 (-3.4)	12,799,417 (-12.5)	13,609,413 (-13.3)
(b) Sec. ch. w. pump	-	- (0.0)	- (0.0)	- (0.0)	- (0.0)	- (0.0)
Total difference [(a) + (b)]	-	11,610,555 (-9.9)	1,899,802 (-1.6)	3,420,398 (-2.9)	12,799,417 (-10.9)	13,609,413 (-11.6)

Impacts of each chiller system configuration parameter such as the number, cooling capacity and type of chillers on the energy performance of the DCS were then examined. [Table 5.2](#) shows a matrix of the cases selected for a more detailed comparison.

Table 5.2 Selection of cases for comparing the energy impact of each design parameter

	C _O	C _A	C _B	C _C	C _D	C _E
Design parameter						
No. of chiller	10	10	15	15	15	15
Size	Equal	Equal	Equal	Unequal	Equal	Unequal
Type	Constant speed	Variable speed	Constant speed	Constant speed	Variable speed	Variable speed
Comparison based on no. of chiller:						
Case O-B	✓		✓			
Case A-D		✓			✓	
Comparison based on size uniformity:						
Case B-C			✓	✓		
Case D-E					✓	✓
Comparison based on chiller type:						
Case O-A	✓	✓				
Case B-D			✓		✓	
Case C-E				✓		✓

Remark:

“✓” – configuration selected for evaluating the impact of the respective design parameter

- i. Case O-B was formed to compare C_O and C_B, and case A-D was formed to compare C_A and C_D with regard to an increase in the number of chillers.
- ii. Case B-C was formed to compare C_B and C_C, and case D-E was formed to compare C_D and C_E with regard to the chiller’s cooling capacity.
- iii. Cases O-A, B-D and C-E were formed to compare C_O with C_A, C_B with C_D, and C_C with C_E respectively with regard to the use of constant and variable speed chillers.

5.3 Effects of Increasing the Number of Chillers – Case O-B and Case A-D

Case O-B and case A-D were selected for a study of the effects of increasing the number of chillers in the system. The configurations of C_O and C_B in case O-B, and that of C_A and C_D in case A-D were as shown in [Table 5.3](#). A comparison of the annual total

electricity consumption of DCS_O , when configured with the different number of chillers represented by these cases, is given in Tables 5.4 and 5.5.

Table 5.3 Configuration of chiller systems in cases O-B and A-D

Chiller system configuration	Case O-B		Case A-D	
	C_O	C_B	C_A	C_D
No. of chiller	10	15	10	15
Size	Equal	Equal	Equal	Equal
Cooling capacity	10 x 6,000 RT (10 x 21,102 kW)	15 x 4,000 RT (15 x 14,068 kW)	10 x 6,000 RT (10 x 21,102 kW)	15 x 4,000 RT (15 x 14,068 kW)
Type	Constant speed	Constant speed	Variable speed	Variable speed

Table 5.4 Case O-B: Percentage of electricity saving after addition of chillers in C_B

	Annual electricity consumption, kWh		Annual electricity saving [C_B minus C_O]	
	C_O	C_B	kWh	%
(a) Chiller plant				
i. Chiller	88,827,472	87,605,334	-1,222,139	-1.4
ii. Pri. ch. w. pump	5,583,218	5,289,233	-293,985	-5.3
iii. Seawater pump	7,582,613	7,198,935	-383,678	-5.1
Total [i + ii + iii]	101,993,303	100,093,502	-1,899,802	-1.9
(b) Sec. ch. w. pump	14,911,696	14,911,696	0	0.0
Total [(a) + (b)]	116,904,999	115,005,198	-1,899,802	-1.6

Table 5.5 Case A-D: Percentage of electricity saving after addition of chillers in C_D

	Annual electricity consumption, kWh		Annual electricity saving [C_D minus C_A]	
	C_A	C_D	kWh	%
(a) Chiller plant				
i. Chiller	77,216,917	76,705,719	-511,198	-0.7
ii. Pri. ch. w. pump	5,583,218	5,289,233	-293,985	-5.3
iii. Seawater pump	7,582,613	7,198,935	-383,678	-5.1
Total [i + ii + iii]	90,382,748	89,193,887	-1,188,861	-1.3
(b) Sec. ch. w. pump	14,911,696	14,911,696	0	0.0
Total [(a) + (b)]	105,294,444	104,105,583	-1,188,861	-1.1

In case O-B, a comparison was made of the effects of increasing the number of equally-sized constant speed chillers from 10 in C_O to 15 in C_B . It shows a 1.6%

reduction in the electricity consumption of DCS_O after adopting C_B instead of C_O . For case A-D, more equally-sized variable speed chillers were used in C_D and this led to a saving of 1.1% in electricity consumption as compared to using C_A .

This indicates that the use of a greater number of equally-sized chillers with a smaller cooling capacity (i.e. 15 x 4,000 RT (14,068 kW)), as in C_B and C_D , can contribute to a reduction in the electricity consumption of DCS_O at low delta-T.

5.3.1 Electricity Consumption of Chillers

C_O and C_B comprised 10 x 6,000 RT (21,102 kW) and 15 x 4,000 RT (14,068 kW) equally-sized constant speed chillers, respectively. While a chiller plant is running, one additional chiller will be staged on when the cooling load exceeds the total cooling capacity of the operating chillers. The number of available steps of total cooling output capacity equals the total number of equally-sized chillers installed. Hence, the number of steps of C_B is higher, i.e. 15. There is then a greater freedom to adjust the number of chillers in C_B to achieve a higher COP while meeting the variable cooling demand. As Figure 5.1 shows, the average COP values of the constant speed chillers in C_B at different PLR were slightly higher than those of C_O . This explains why the annual electricity consumption of the chillers in C_B was 1.4% less than that of C_O .

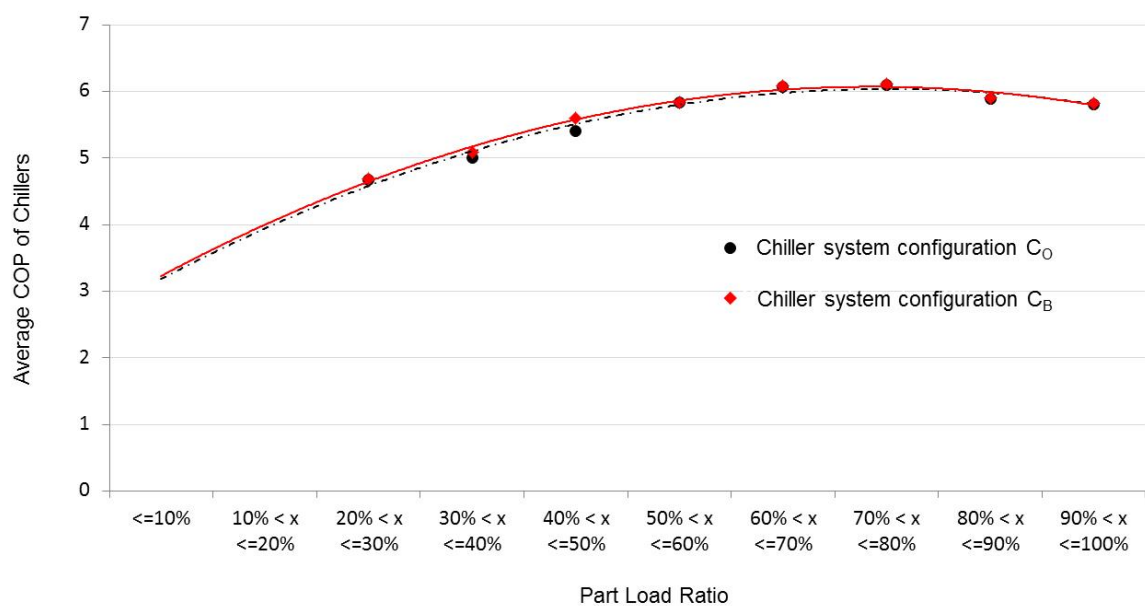


Figure 5.1 Average COP of constant speed chillers in C_O and C_B at different PLR

For case A-D where variable speed chillers were used, the saving in electricity consumption of the chillers after increasing their number from 10, as in C_A to 15, as in C_D , was only 0.7%. This percentage is relatively small when compared to case O-B (1.4%) where constant speed chillers were adopted. This is because of the higher part-load COP of variable speed chillers compared to constant speed chillers, as shown in Figure 5.2. As shown in Table 2.5 in Chapter 2, the cooling load on the DCS was below 50% for 77% of the total 8,760 operating hours in a year. Since the chillers were operated at part load for most of the time, the use of variable speed chillers could help significantly reduce the electricity consumption of the DCS, as in case C_A or C_D . Figure 5.3 shows that the average COP of the chillers in C_A and C_D were higher at low load in comparison with those in C_O and C_B (Figure 5.1). This had led to a smaller difference in the electricity consumption between C_A and C_D .

Moreover, this illustrates that the effect of using a greater number of chillers could be insignificant in reducing electricity consumption if the plant is already using variable speed chillers.

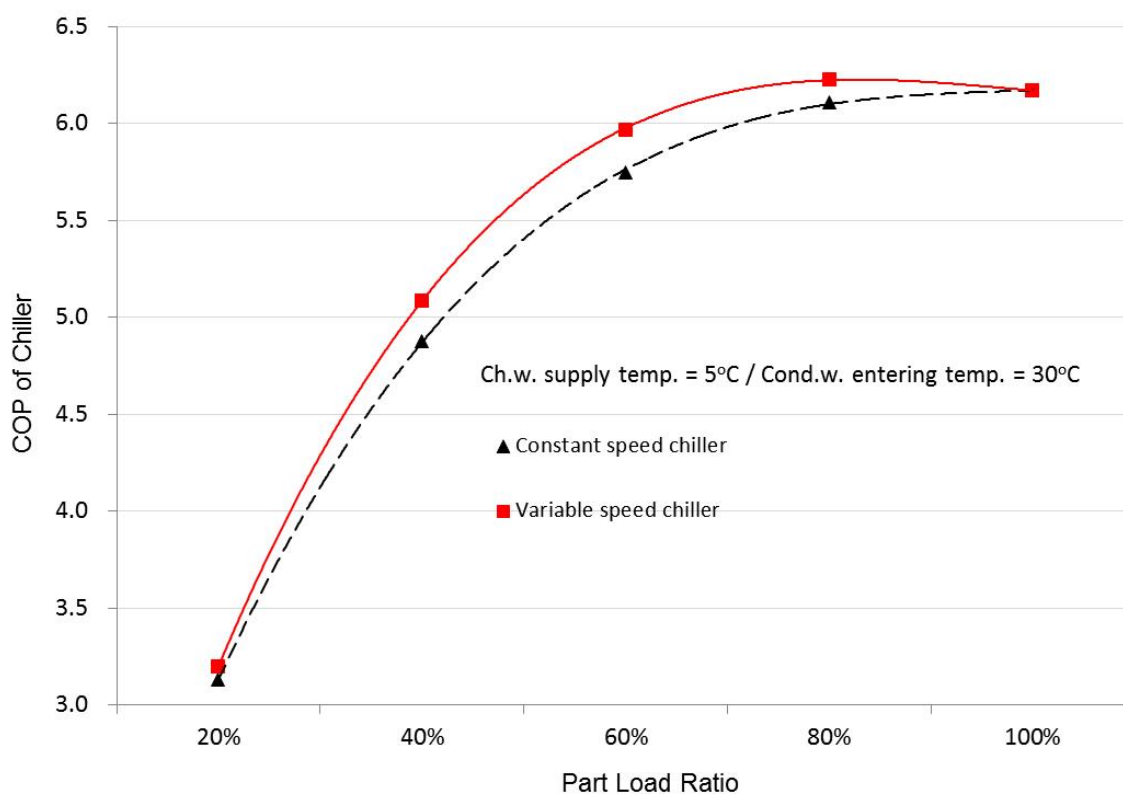


Figure 5.2 COP of constant and variable speed chillers with a cooling capacity of 4,000 RT (14,068 kW)

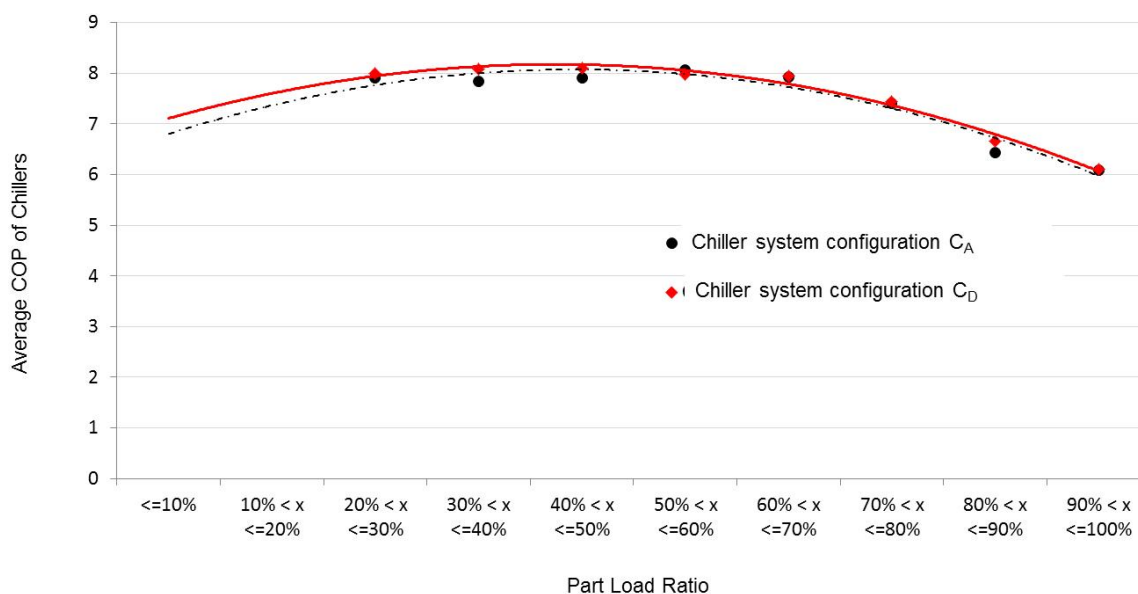


Figure 5.3 Average COP of variable speed chillers in C_A and C_D at different PLR

5.3.2 Electricity Consumption of Primary Chilled Water Pumps and Seawater Pumps

As primary chilled water pumps and seawater pumps are interlocked with their dedicated chillers during operation, their total pump hours are the same as the chiller's total chiller hours. With reference to [Tables 5.6](#) and [5.7](#), for cases O-B and A-D, the total pump hours of these pumps in cases C_B and C_D were longer, i.e. both were 42% more than those in C_O and C_A . However, in both cases, their electricity consumption was 5.3% and 5.1% less than that in C_O and C_A . The reason is that the power demand of the pumps in C_B and C_D was about 33% less than that in C_O and C_A . In other words, although the pumps in C_B and C_D had relatively longer pump hours, they consumed less electricity in comparison with those in C_O and C_A .

Having said that, however, it should be re-emphasized that primary chilled water pumps and seawater pumps constitute a much smaller portion of the annual total electricity consumption of the plant when compared to chillers. The electricity saving of these two types of pumps, therefore, would not significantly affect the annual total electricity consumption of the DCS.

Table 5.6 Operating chiller hours of chillers and electricity saving of the primary chilled water and seawater pumps in case O-B

	C_O	C_B	Difference (C_B minus C_O)	% difference
Total chiller hour	33,952	48,279	+14,327	+42
Primary chilled water pump				
Unit power demand, kW	164.6	109.6	-55	-33.4
Annual electricity consumption, kWh	5,583,218	5,289,223	-293,985	-5.3
Seawater pump				
Unit power demand, kW	223.3	149.1	-74.2	-33.2
Annual electricity consumption, kWh	7,582,613	7,198,935	-383,678	-5.1

Table 5.7 Operating chiller hours and electricity saving of the primary chilled water and seawater pumps in case A-D

	C_A	C_D	Difference (C_D minus C_A)	% difference
Total chiller hour	33,952	48,279	+14,327	+42
Primary chilled water pump				
Unit power demand, kW	164.6	109.6	-55	-33.4
Annual electricity consumption, kWh	5,583,218	5,289,223	-293,985	-5.3
Seawater pump				
Unit power demand, kW	223.3	149.1	-74.2	-33.2
Annual electricity consumption, kWh	7,582,613	7,198,935	-383,678	-5.1

5.4 Effects of Uniformity in Chiller Size – Case B-C and Case D-E

Cases B-C and D-E were selected for examining the effect of unequally-sized chillers on the total energy consumed. The configuration details of C_B and C_C in case B-C, and those of C_D and C_E in case D-E are given in [Table 5.8](#).

Table 5.8 Configuration of chiller systems in cases B-C and D-E

Chiller system configuration	Case B-C		Case D-E	
	C _B	C _C	C _D	C _E
No. of chiller	15	15	15	15
Size	Equal	Unequal	Equal	Unequal
Cooling capacity	15 x 4,000 RT (15 x 14,068 kW)	5 x 2,000 RT (5 x 7,034 kW)	15 x 4,000 RT (15 x 14,068 kW)	5 x 2,000 RT (5 x 7,034 kW)
		5 x 4,000 RT (5 x 14,068 kW)		5 x 4,000 RT (5 x 14,068 kW)
		5 x 6,000 RT (5 x 21,102 kW)		5 x 6,000 RT (5 x 21,102 kW)
Type	Constant speed	Constant speed	Variable speed	Variable speed

Case B-C represents a comparison of C_B and C_C, both of which consisted of 15 constant speed chillers. The only difference is that the chillers in C_B were of equal size, i.e. 15 x 4,000 RT (14,068 kW) and the chillers in C_C had three different cooling capacities, i.e. 5 x 2,000 RT (7,034 kW), 5 x 4,000 RT (14,068 kW) and 5 x 6,000 RT (21,102 kW).

The configurations of C_B and C_D were the same, except that the chillers in C_D were of variable speed. Similarly, C_C and C_E had the same configuration, as the only difference was in the chiller type (constant speed versus variable speed).

In case B-C, a comparison was made regarding the use of unequally-sized constant speed chillers in C_C. It was found that the adoption of C_C, instead of C_O, had resulted in a 1.3% reduction in the electricity consumption of DCS_O. For case D-E, unequally-sized variable speed chillers were used in C_E, which could lead to a saving of 0.8% in electricity as compared to using C_D.

As shown in [Tables 5.9](#) and [5.10](#), the annual total electricity consumptions of DCS_O designed with C_C and C_E and operating with low delta-T were 1.3% and 0.8% lower than those in C_B and C_D respectively.

Table 5.9 Case B-C: Percentage of annual electricity saving after using unequally-sized chillers in C_C

	Annual electricity consumption, kWh		Annual electricity saving [C_C minus C_B]	
	C_B	C_C	kWh	%
(a) Chiller plant				
i. Chiller	87,605,334	86,686,293	-919,040	-1.0
ii. Pri. ch. w. pump	5,289,233	5,040,671	-248,562	-4.7
iii. Seawater pump	7,198,935	6,845,941	-352,994	-4.9
Total [i + ii + iii]	100,093,502	98,572,905	-1,520,596	-1.5
(b) Sec. ch. w. pump	14,911,696	14,911,696	0	0.0
Total [(a) + (b)]	115,005,198	113,484,601	-1,520,596	-1.3

Table 5.10 Case D-E: Percentage of annual electricity saving after using unequally-sized chillers in C_E

	Annual electricity consumption, kWh		Annual electricity saving [C_E minus C_D]	
	C_D	C_E	kWh	%
(a) Chiller plant				
i. Chiller	76,705,719	76,339,990	-365,729	-0.5
ii. Pri. ch. w. pump	5,289,233	5,107,501	-181,732	-3.4
iii. Seawater pump	7,198,935	6,936,400	-262,536	-3.6
Total [i + ii + iii]	89,193,887	88,383,890	-809,996	-0.9
(b) Sec. ch. w. pump	14,911,696	14,911,696	0	0.0
Total [(a) + (b)]	104,105,583	103,295,586	-809,996	-0.8

5.4.1 Electricity Consumption of Chillers

C_C and C_E comprised unequally-sized chillers of three cooling capacities. A total of 215 steps or chiller combinations were involved in the simulation process to achieve different total cooling capacities. This increased the opportunity to optimize the operation of chillers by keeping their operation in the near full load and high COP region while meeting various cooling load requirements.

Table 5.11 lists out the distribution of average PLR of the chillers operating around the 8760 hours of a year in cases B-C and D-E. In case B-C, the 15 identical chillers in C_B operated at a near full load range, i.e. the PLR ranged from 0.8 to 1, for 22% (=20% + 2%) of the 8,760 operating hours in a year. This figure rose to 29% (=25% + 4%) in C_C with the use of 15 unequally-sized chillers. A similar increase can be found in case D-E

where the percentage increased from 22% (=20% + 2%) in C_D to 28% (=25% + 3%) in C_E .

Table 5.11 Distribution of average PLR of the chillers operating around the 8760 hours of a year in cases B-C and D-E

Part load ratio	Case B-C		Case D-E	
	C_B	C_C	C_D	C_E
≤ 0.1	0%	0%	0%	0%
$0.1 < \text{PLR} \leq 0.2$	0%	0%	0%	0%
$0.2 < \text{PLR} \leq 0.3$	11%	8%	11%	8%
$0.3 < \text{PLR} \leq 0.4$	3%	2%	3%	2%
$0.4 < \text{PLR} \leq 0.5$	6%	3%	6%	3%
$0.5 < \text{PLR} \leq 0.6$	7%	6%	7%	6%
$0.6 < \text{PLR} \leq 0.7$	18%	16%	18%	21%
$0.7 < \text{PLR} \leq 0.8$	32%	36%	32%	32%
$0.8 < \text{PLR} \leq 0.9$	20%	25%	20%	25%
$0.9 < \text{PLR} \leq 1.0$	2%	4%	2%	3%

As shown in [Figure 5.4](#), the average COP of the constant speed chillers in C_C at different PLR was slightly higher than that in C_B . This corresponds to the 1% reduction in the electricity consumption of chillers in C_C as compared to C_B (see [Table 5.9](#)).

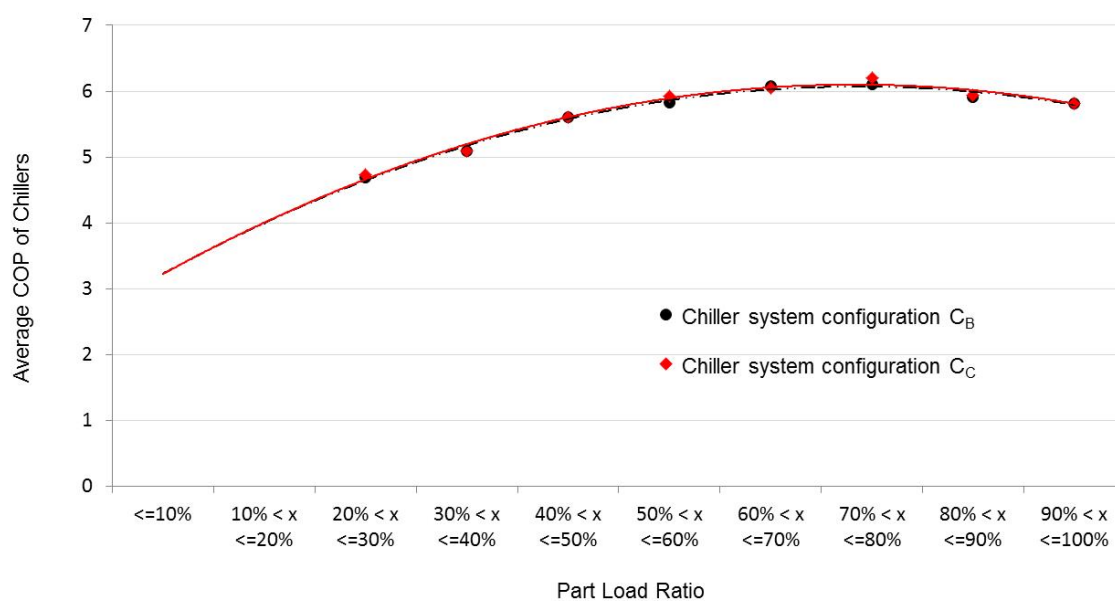


Figure 5.4 Average COP of constant speed chillers in C_B and C_C at different PLR

For case D-E, [Figure 5.5](#) shows that the average COP of the variable speed chillers in C_E at different PLR was higher than that in C_D . Unequally-sized chillers in C_E could reduce the electricity consumption of chillers by 0.5% in comparison with C_D .

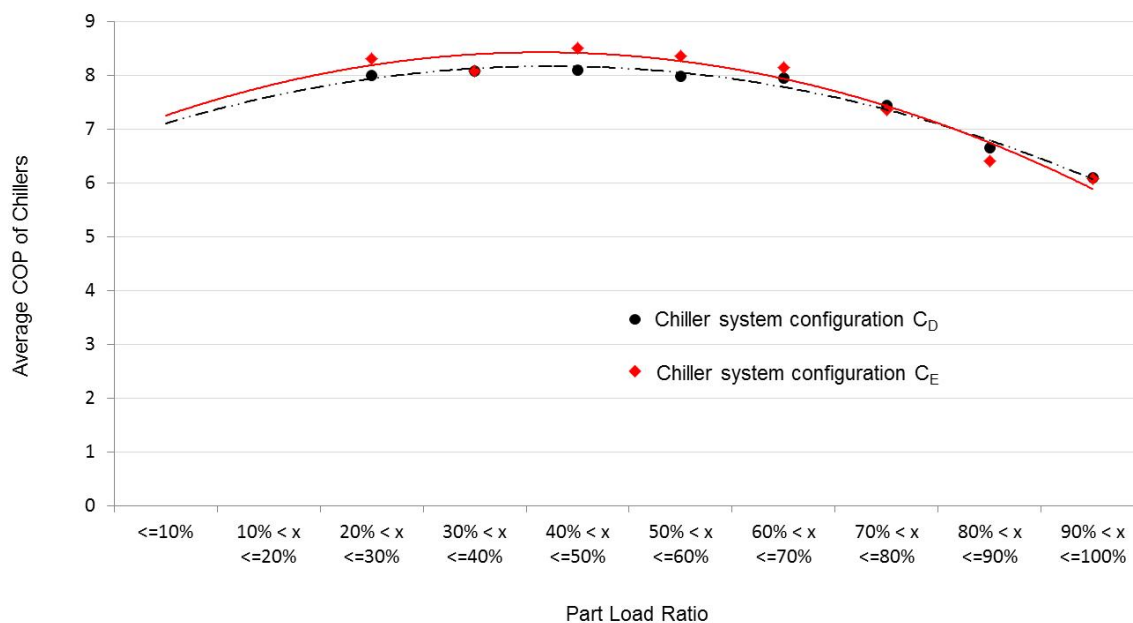


Figure 5.5 Average COP of variable speed chillers in C_D and C_E at different PLR

5.4.2 Electricity Consumption of Primary Chilled Water Pumps and Seawater Pumps

As shown in [Tables 5.12](#) and [5.13](#), the reduction in the annual electricity consumption of the primary chilled water pumps and seawater pumps in C_C and C_E ranged from 3.4% to 4.9% when compared to C_B and C_D . The reasons were as follows.

- i. Three sizes of primary chilled water pumps were selected for serving the chillers in C_C and C_E , which were with three different cooling capacities. There were five pumps of each size and the unit power demand values of the three pump sizes were 56.9 kW, 109.6 kW and 164.4 kW respectively. The weighted averages of the unit power demand in C_C and C_E were 110.3 kW (i.e. $(5 \times 56.9 \text{ kW} + 5 \times 109.6 \text{ kW} + 5 \times 164.4 \text{ kW})/15$) as shown in [Tables 5.12](#) and [5.13](#), which were slightly higher (i.e. 0.6%) than the unit power demand of 109.6 kW of the pumps in C_B and C_D . The difference was due to the small pumps selected

for lower chilled water flow rate as they are generally less efficient than the large pumps given that their pressure head is the same.

Each chiller was also equipped with a seawater pump of a matching size. There were five pumps of each size in C_C and C_E and the unit power demand values of the three pump sizes were 75.3 kW, 149.1 kW and 223.3 kW respectively. The weighted average of the unit power demand was 149.2 kW (i.e. $(5 \times 75.3 \text{ kW} + 5 \times 149.1 \text{ kW} + 5 \times 223.3 \text{ kW})/15$) as shown in [Tables 5.12](#) and [5.13](#), which was also slightly higher than the unit power demand of these pumps in C_B and C_D , i.e. 149.1 kW.

- ii. On the other hand, the chillers in C_C and C_E designed with unequal cooling capacities could allow more combinations of different total cooling capacities to meet the chilled water flow requirement. This is particularly useful when the low delta-T syndrome occurs as the chilled water flow rate becomes higher than the design value. The number of chillers required to meet the flow rate can also be reduced. The total chiller hours in C_C and C_E were 22% to 23% fewer in comparison with those in C_B and C_D respectively.

For example, to meet a required flow rate at $2.47\text{m}^3/\text{s}$, six sets of 4,000 RT (14,068 kW) chillers were required in C_B to be operated and the total design flow rate was $2.87\text{m}^3/\text{s}$ ($6 \times 0.4784\text{m}^3/\text{s}$), which was 16% higher than the required flow rate. However, for C_C , only four unequally-sized chillers (i.e. 1 x 4,000 RT (14,068 kW) and 3 x 6,000 RT (21,102 kW)) were required. The total design flow rate in C_C was $2.63\text{m}^3/\text{s}$, which was slightly higher, i.e. 6.5%, than the required flow rate.

- iii. As the total pump hours of the primary pumps correspond to the total chiller hours of the chillers, which they are dedicated to serve, the total pump hours of the pumps in C_C and C_E were far fewer than those in C_B and C_D , with a difference of 22-23% (see [Tables 5.12](#) and [5.13](#)). This could help to reduce their electricity consumption and offset the slight increase in power demand from the primary chilled water and seawater pumps.

Table 5.12 Chiller hours and electricity saving of the primary chilled water and seawater pumps in case B-C

	C_B	C_C	Difference (C_C minus C_B)	% Difference
Total chiller hour	48,279	37,127	-11,152	-23%
Primary chilled water pump				
Weighted average of unit power demand, kW	109.6	110.3	+0.7	+0.6%
Annual electricity consumption, kWh	5,289,233	5,040,671	-248,562	-4.7%
Seawater pump				
Weighted average of unit power demand, kW	149.1	149.2	~0	
Annual electricity consumption, kWh	7,198,935	6,845,941	-352,994	-4.9%

Table 5.13 Chiller hours and electricity saving of the primary chilled water and seawater pumps in case D-E

	C_D	C_E	Difference (C_E minus C_D)	% Difference
Total chiller hour	48,279	37,746	-10,533	-22%
Primary chilled water pump				
Weighted unit power demand, kW	109.6	110.3	+0.7	+0.6%
Annual electricity consumption, kWh	5,289,233	5,107,501	-181,732	-3.4%
Seawater pump				
Weighted unit power demand, kW	149.1	149.2	~0	
Annual electricity consumption, kWh	7,198,935	6,936,400	-262,536	-3.6%

5.5 Effects of Variable Speed Chillers

Cases O-A, B-D and C-E were set up for studying the effects of variable speed chillers. The configuration details of C_O and C_A in case O-A, C_B and C_D in case B-D, and C_C and C_E in case C-E were as shown in [Table 5.14](#).

Table 5.14 Configuration of the chiller systems in cases O-A, B-D, and C-E

Chiller system configuration	Case O-A		Case B-D		Case C-E	
	C _O	C _A	C _B	C _D	C _C	C _E
No. of chiller	10	10	15	15	15	15
Size	Equal	Equal	Equal	Equal	Unequal	Unequal
Cooling capacity	10 x 6,000 RT (10 x 21,102 kW)	10 x 6,000 RT (10 x 21,102 kW)	15 x 4,000 RT (15 x 14,068 kW)	15 x 4,000 RT (15 x 14,068 kW)	5 x 2,000 RT (5 x 7,034 kW) 5 x 4,000 RT (5 x 14,068 kW) 5 x 6,000 RT (5 x 21,102 kW)	5 x 2,000 RT (5 x 7,034 kW) 5 x 4,000 RT (5 x 14,068 kW) 5 x 6,000 RT (5 x 21,102 kW)
Type	Constant speed	Variable speed	Constant speed	Variable speed	Constant speed	Variable speed

In case O-A, C_O and C_A comprised 10 x 6,000 RT (21,102 kW) chillers. These chillers were constant speed in C_O and variable speed in C_A. The characteristics of case B-D were similar except for the number of chiller; 15 x 4,000 RT (14,068 kW) chillers were adopted for C_B and C_D. For case C-E, configurations C_C and C_E comprised 15 unequally-sized chillers, i.e. 5 x 2,000 RT (7,034 kW), 5 x 4,000 RT (14,068 kW) and 5 x 6,000 RT (21,102 kW) chillers. These chillers were constant speed in C_C and variable speed in C_E.

It can be seen from [Tables 5.15](#), [5.16](#) and [5.17](#) that application of variable speed chillers led to a significant reduction in the annual total electricity consumption of DCS_O, between 9% and 9.9% in comparison with the use of constant speed chillers across all the three cases.

Table 5.15 Electricity saving resulting from using variable speed chillers in case O-A

	Annual electricity consumption, kWh		Annual electricity saving [C _A minus C _O]	
	C _O	C _A	kWh	%
(a) Chiller plant				
i. Chiller	88,827,472	77,216,917	-11,610,555	-13.1
ii. Pri. ch. w. pump	5,583,218	5,583,218	0	0
iii. Seawater pump	7,582,613	7,582,613	0	0
Total [i + ii + iii]	101,993,303	90,382,748	-11,610,555	-11.4
(b) Sec. ch. w. pump	14,911,696	14,911,696	0	0
Total [(a) + (b)]	116,904,999	105,294,444	-11,610,555	-9.9

Table 5.16 Electricity saving resulting from using variable speed chillers in case B-D

	Annual electricity consumption, kWh		Annual electricity saving [C _D minus C _B]	
	C _B	C _D	kWh	%
(a) Chiller plant				
i. Chiller	87,605,334	76,705,719	-10,899,615	-12.4
ii. Pri. ch. w. pump	5,289,233	5,289,233	0	0
iii. Seawater pump	7,198,935	7,198,935	0	0
Total [i + ii + iii]	100,093,502	89,193,887	-10,899,615	-10.9
(b) Sec. ch. w. pump	14,911,696	14,911,696	0	0
Total [(a) + (b)]	115,005,198	104,105,583	-10,899,615	-9.5

Table 5.17 Electricity saving resulting from using variable speed chillers in case C-E

	Annual electricity consumption, kWh		Annual electricity saving [C _E minus C _C]	
	C _C	C _E	kWh	%
(a) Chiller plant				
i. Chiller	86,686,293	76,339,990	-10,346,303	-11.9
ii. Pri. ch. w. pump	5,040,671	5,107,501	+66,830	+1.3
iii. Seawater pump	6,845,941	6,936,400	+90,458	+1.3
Total [i + ii + iii]	98,572,905	88,383,890	-10,189,015	-10.3
(b) Sec. ch. w. pump	14,911,696	14,911,696	0	0
Total [(a) + (b)]	113,484,601	103,295,586	-10,189,015	-9

The application of variable speed chillers in C_A , C_D and C_E could lead to a significant reduction in the annual total electricity consumption of DCS_O by 9.9%, 9.5% and 9% compared respectively with C_O , C_B and C_C , which comprised constant speed chillers.

Variable speed chillers have better energy performance due to the following reasons.

- i. In a constant speed chiller, inlet guide vanes are traditionally used to throttle refrigerant at the inlet of the compressor to vary the compressor capacity at part load. As the vanes move from open to close, they become a restriction and reduce the compressor's capacity and efficiency.

For a variable speed chiller, a variable speed drive is adopted to vary the speed of the impeller of the compressor to meet various loads at part load. The power demand of the compressor can be significantly reduced when the speed of the impeller reduces at part load. The impeller must produce an adequate pressure differential (lift) to move the refrigerant from the low-pressure side (evaporator) to the high-pressure side (condenser). It is this lift that determines the minimum speed of the impeller. The lower the lift, i.e. the closer the temperature difference between the evaporator and the condenser, the slower the impeller can rotate. When the impeller is at the slowest possible speed, further reductions in capacity are obtained by using the inlet guide vanes.

- ii. [Figure 5.6](#) illustrates the part load performance curves of a constant and a variable speed chiller, each of which was rated for 2,000 RT (7,034 kW) output at the design chilled water supply temperature of 5°C. The curve in [Figure 5.6](#) shows the performance of these chillers when they operated at the condenser water entering temperature of 20°C, 25°C or 30°C.

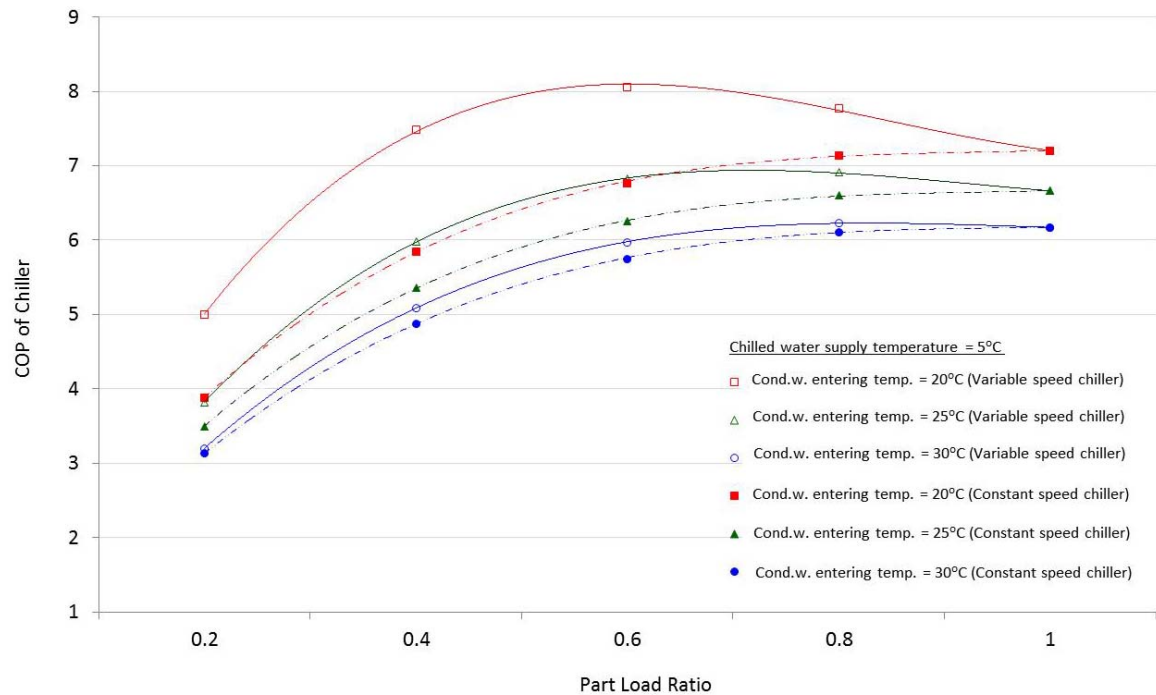


Figure 5.6 Part load performance of constant and variable speed chillers with different condenser water entering temperatures

It can be seen that the COP of the variable speed chiller is higher than that of the constant speed chiller, particularly when the condenser water entering temperature is at 20°C. The optimum COP of variable speed chillers occurs when the PLR is around 0.6. This characteristic can be utilized to enhance the energy performance of the chiller system operating at part load, to alleviate the low delta-T syndrome, particularly at low cooling loads.

Table 5.18 shows the difference in COP between the constant and variable speed chillers while operating under different condenser water entering temperatures. The COP difference at part load diminished as the condenser water entering temperature increased from 20°C to 30°C.

Table 5.18 Difference in COP between constant and variable speed chillers with different condenser water entering temperatures

Condenser water entering temp	Part load ratio				
	20%	40%	60%	80%	100%
20°C	29%	28%	19%	9%	0%
25°C	9%	12%	9%	5%	0%
30°C	2%	4%	4%	2%	0%

Figure 5.6 shows also that the increase in the COP of the variable speed chiller, as the condenser water entering temperature was reduced from 30°C to 20°C, was far more significant than that of the constant speed chiller. Since direct seawater cooling was used in DCS_O for heat rejection, the condenser water entering temperature was in fact the seawater temperature. As mentioned in Table 2.6 of Chapter 2, the seawater temperature of Hong Kong would stay below 25°C for over 50% of the total 8,760 operating hours in a year. Therefore, these conditions are conducive to achieving great energy saving by using variable speed chillers.

- iii. Figure 5.7 shows that the average COP of the variable speed chillers in C_A at different PLR was higher than that of the constant speed chillers in C_O, particularly at low load. This explains why C_A could help reduce the annual total electricity consumption of DCS_O by 10% in comparison with C_O. The same explanation applies to cases B-D and C-E.

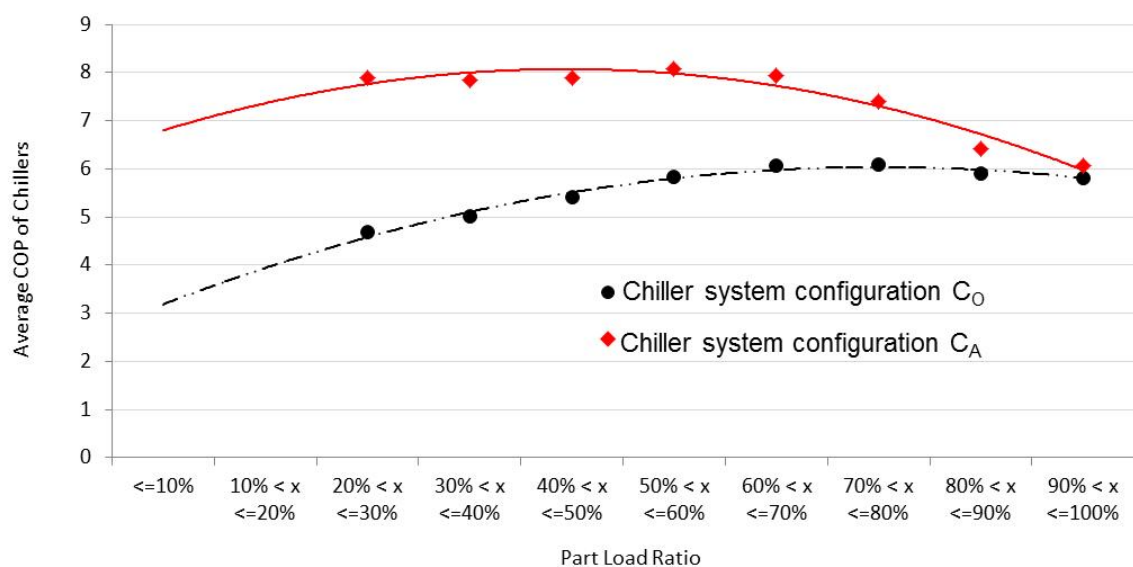


Figure 5.7 Average COP of the constant and variable speed chillers in C_O and C_A

For case C-E, both C_C and C_E were designed with chillers of unequal cooling capacities. The total chiller hours of the variable speed chillers in C_E were greater than those of the constant speed chillers in C_C (see Table 5.19). Energy simulation results indicate that it would be more energy efficient to operate more variable speed chillers as in C_E . This result may appear counterintuitive, as conventional wisdom is to run as few chillers as possible. This conception, however, is true for constant speed chillers only, because variable speed chillers can be more efficient at low load, particularly when the condenser entering water temperature is low (Taylor, 2012). In this regard, although the electricity consumption of primary chilled water and seawater pumps was slightly higher in C_E than that in C_C , this was offset by the substantial gain in electricity saving through the use of variable speed chillers in the former case.

Table 5.19 Operating hours of chillers in case C-E

	C_C	C_E	Difference (%) [C_E minus C_C]
Total chiller hour	37,127	37,746	+619 (+1.7%)

5.6 Summary

Optimization of chiller system configuration was one of the three energy efficiency enhancement measures evaluated in this study to improve the energy performance of DCS_O and accommodate the inevitable low delta-T issue. Initially, five different chiller system configurations were established by means of changing the design parameters such as the number, cooling capacity and type of chillers (constant or variable speed). Simulation was performed to evaluate the effectiveness of each type of configuration in enhancing the energy performance of DCS_O with reference to a base chiller system design C_O .

In a comparative analysis of the annual total electricity consumption of DCS_O when it was incorporated with one of the five proposed chiller system configurations, i.e. C_A to C_E , with low delta-T issue in place, it was found that chiller system configuration C_E , consisting of 15 unequally-sized variable speed chillers, i.e. 5 x 2,000 RT (7,034 kW), 5 x 4,000 RT (14,068 kW) and 5 x 6,000 RT (21,102 kW), performed the best in terms of

energy saving. It could reduce 11.7% of the annual total electricity consumption of DCS_O even when low delta-T occurred.

For cases O-B, A-D, B-C and D-E, the use of a larger number of or unequally-sized chillers would increase the flexibility of operating the chillers to cope with the variable cooling load requirements. The greater the number of chillers (or the number of chillers with different cooling capacities), the higher the average PLR and hence the COP of the operating chillers. However, the adoption of more or unequally-sized chillers could only lead to a limited saving in the annual total electricity consumption of DCS_O , as this saving was less than 2%, when compared to using the basic design C_O at low delta-T. There is also a limit in operation so that switching the chillers on and off cannot be done at a frequent pace.

On the other hand, for cases O-A, B-D and C-E, results indicate that the variable speed chillers could dramatically improve the part load performance of the chillers and save a substantial amount of electricity for DCS_O , i.e. between 9% and 9.9%. As a result, although the low delta-T issue is inevitable, particularly at low cooling loads, the high energy efficiency of the variable speed chillers at part load can help lessen the impacts caused by degrading delta-T.

The use of more variable speed chillers with different cooling capacities can lead to a higher initial capital and operating cost in comparison with the base design in C_O . Therefore, a financial analysis was performed to find out whether the total electricity cost saving could offset the higher initial costs. This issue is further explored in [Chapter 8](#).

Chapter 6

Effects of Pumping Station Configuration on the Energy Performance of DCS_O

6.1 Overview

As discussed in [Chapter 4](#), the annual average value of the hourly chilled water flow rate demand of the hypothetical district, when the DCS was suffering from the low delta-T problem, increased by 77% as compared to the normal delta-T condition. Consequently, the electricity consumption of the secondary chilled water pumps was significantly increased by 81%. Energy saving measures, in particular those related to pumping station configuration, are of critical importance in a study of DCS energy use.

In this chapter, the effects of different pumping station configurations on the energy performance of DCS_O are investigated. Moreover, a configuration that can mitigate the impacts of the low delta-T on the energy performance of DCS_O is discussed.

From [Chapter 3](#), the base pumping station system in DCS_O consisted of one main pumping station, denoted as PS₁₋₀, was located immediately downstream of the chiller plant. This pumping station was equipped with 10 equally-sized variable speed chilled water pumps. Two design schemes were examined in this chapter to evaluate their effectiveness in mitigating the impacts of low delta-T on the energy performance of

DCS_O. The first scheme was to adopt multiple pumping stations instead of a single pumping station, and the location of stations could be anywhere at the chilled water supply and return sides of the distribution loop. To further optimize the design of DCS_O, the second scheme was to adopt an unequal number of pumps in each pumping station.

Regarding the design of multiple pumping stations, the 1,024 combinations of pumping station could generate a total of 431,940 pumping station arrangements, based on the variation in the number of pumps, i.e. in groups of 5, 10 or 15, in each pumping station. As it would require a prohibitively large amount of time and effort in simulating the energy performance of each of the 431,940 pumping station arrangements, a hydraulic gradient approach was used to identify the combinations that were technically feasible for simulation. A detailed account of this approach is given in [Section 6.2](#). Another design scheme, that is to vary the number of pumps in each pumping station, is presented in [Section 6.3](#). Mathematically, calculation for an optimum pumping station design is a very complicated issue, as it involves over hundred thousands of pumping station arrangements for analysis. As a result, based on the mathematical models developed in [Chapter 3](#), an optimization program using Excel VBA was developed to calculate the annual electricity consumption of different pumping station combinations, as in [Section 6.4](#). Their energy performance is discussed in [Section 6.5](#).

6.2 Multiple Pumping Station Design

As shown in [Figure 2.7](#) of [Chapter 2](#), except that of the main pumping station, there were 11 possible locations at the chilled water supply and return sides for placing the booster pumping station to distribute chilled water to all buildings and return it to the central plant. Based on the calculation in [Table 2.10](#), a total of 1,024 “combinations” of pumping station location could be derived for the use of one to six pumping stations. In this chapter, the phrase “pumping station combination” refers specifically to the grouping of pumping stations according to their location in the distribution loop.

In view of the massive number of combinations to be involved in simulating the energy performance of each combination with different design parameters, a hydraulic gradient approach was adopted to identify only those technically feasible combinations.

6.2.1 Hydraulic Gradient Characteristics of Chilled Water Distribution Network

As discussed in [Section 3.4.2](#), the flow rate and pressure head of the secondary distribution pumps are consistently regulated by varying pump speed to match the changes in the chilled water demand. A differential pressure transmitter has to be installed in the critical branch, typically the furthest branch, so that any change in the flow rate demand, which is reflected by a change in the differential pressure across the critical branch, can be detected and used as a reference signal for controlling the secondary pump speed. As no previous research studies could be identified regarding the appropriate location for the differential pressure transmitters in a DCS, the transmitters in this study were located in all the intermediate branches in the chilled water distribution network model developed in [Chapter 3](#). The aim was to simulate the pressure difference across each branch so as to find out a critical branch. Results show that the critical branch was still located at the furthest end of the chilled water distribution network. The differential pressure across the critical branch was maintained at a constant level. Furthermore, pressure drop across all the intermediate branches should also be the same as the pressure drop across the critical branch.

In this regard, a screening strategy of using a hydraulic gradient approach ([Rishel et al, 2006](#)) was applied to calculate the pressure head and flow rate of each pumping station, and the differential pressure across the heat exchangers. Those combinations of location that could not meet the minimum pressure were removed from the analysis.

6.2.2 Identified Combinations of Pumping Station

Based on the chilled water distribution network model developed in [Chapter 3](#), the pressure difference across all the heat exchangers was simulated and checked against the minimum differential pressure, i.e. DP_{\min} . Taking the case of three pumping stations in the secondary chilled water network as an example, one of the pumping stations was a main station and there were 55 possible combinations, as shown in [Table 2.10](#), for locating the other two pumping stations in the network. [Figure 6.1](#) represents one of the 55 combinations that could meet the minimum differential pressure requirement. The

same simulation was performed for the other 54 combinations. It was found that only 38% (i.e. 21 of the 55) of the combinations could meet the requirement. The simulation results of the network designed with one, two, four, five or six pumping stations are shown in Table 6.1. Only 14% (i.e. 140 of the total 1,024) combinations were found to be technically feasible in maintaining the minimum differential pressure across the heat exchangers. A detailed illustration of the exact pumping station location using these 140 combinations is given in Table 6.2.

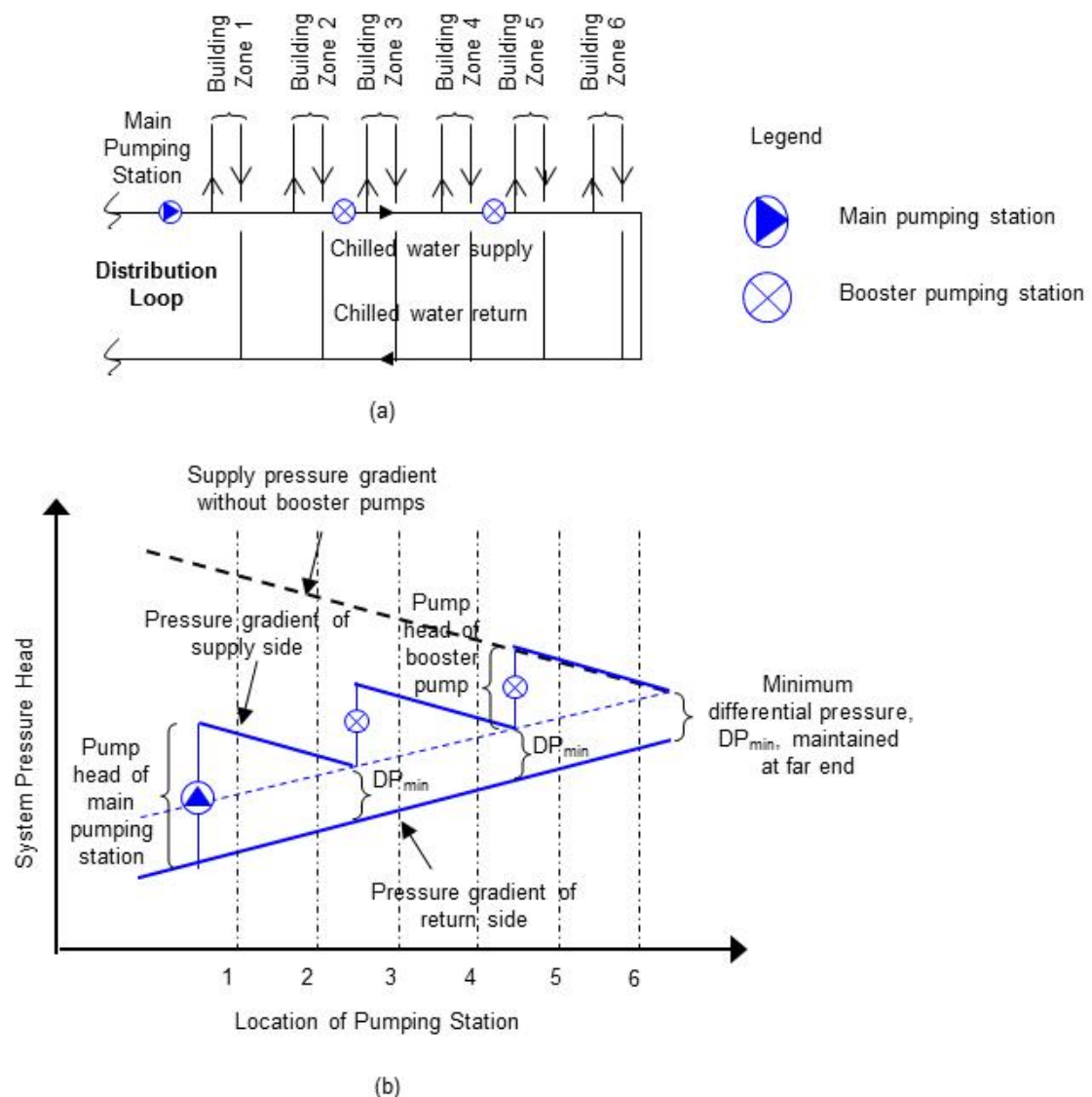


Figure 6.1 Examples of a pressure gradient diagram showing: (a) the location of one main pumping station and two booster pumping stations; and (b) their pressure gradient in the distribution loop

Table 6.1 Number of pumping station combinations that are technically feasible in meeting the minimum pressure differential requirement

No. of pumping station	No. of possible combination based on location	No. of combination that can meet the minimum pressure differential requirement (% of success)	
1	1	1	(100%)
2	11	7	(64%)
3	55	21	(38%)
4	165	37	(22%)
5	210	44	(13%)
6	462	30	(6%)
Total	1,024	140	(14%)

Table 6.1 shows that the rate of success in meeting the differential pressure requirement decreases when the number of pumping station increases. Failure cases often occurred when the pumping station was located at the far end of the centralized chiller plant. It is because the system's pressure head decreases as the distance from the central DCS plant increases. Meanwhile, the pumping station has to maintain a minimum pressure drop across the heat exchangers in each building. Therefore, there will be a situation in which system pressure decreases to a value in a location where the differential pressure between the chilled water supply and return cannot achieve the minimum value with a booster pumping station.

The hydraulic pressure diagrams in Figures 6.2, 6.3, 6.4 and 6.5 provide some examples of the successful and failure cases in the following four different situations, which have included all the possible location combinations.

Table 6.2 Combination of pumping station (PS) location that is technically feasible

No. of PS	Designation of PS combination	Location of pumping station											
		Chilled water supply side						Chilled water return side					
		PS _{1,s}	PS _{2,s}	PS _{3,s}	PS _{4,s}	PS _{5,s}	PS _{6,s}	PS _{1,r}	PS _{2,r}	PS _{3,r}	PS _{4,r}	PS _{5,r}	PS _{6,r}
1	PS 1-1	•											
2	PS 2-1	•	•										
	PS 2-2	•		•									
	PS 2-3	•			•								
	PS 2-4	•				•							
	PS 2-5	•					•						
	PS 2-6	•							•				
	PS 2-7	•								•			
3	PS 3-1	•	•	•									
	PS 3-2	•	•		•								
	PS 3-3	•	•			•							
	PS 3-4	•	•				•						
	PS 3-5	•		•	•								
	PS 3-6	•		•		•							
	PS 3-7	•		•			•						
	PS 3-8	•			•	•							
	PS 3-9	•			•		•						
	PS 3-10	•				•	•						
	PS 3-11	•							•	•			
	PS 3-12	•							•		•		
	PS 3-13	•								•	•		
	PS 3-14	•	•						•				
	PS 3-15	•	•							•			
	PS 3-16	•		•					•				
	PS 3-17	•		•						•			
	PS 3-18	•			•				•				
	PS 3-19	•				•			•				
	PS 3-20	•					•		•				
	PS 3-21	•					•			•			
4	PS 4-1	•	•	•	•								
	PS 4-2	•	•	•		•							
	PS 4-3	•	•	•			•						
	PS 4-4	•	•		•	•							
	PS 4-5	•	•		•		•						
	PS 4-6	•	•			•	•						
	PS 4-7	•		•	•	•							
	PS 4-8	•		•	•		•						
	PS 4-9	•		•		•	•						
	PS 4-10	•			•	•	•						
	PS 4-11	•							•	•	•		
	PS 4-12	•							•	•		•	
	PS 4-13	•							•		•	•	
	PS 4-14	•	•						•	•			
	PS 4-15	•	•						•		•		
	PS 4-16	•	•							•	•		
	PS 4-17	•		•					•	•			
	PS 4-18	•		•					•		•		
	PS 4-19	•		•						•	•		
	PS 4-20	•			•				•	•			

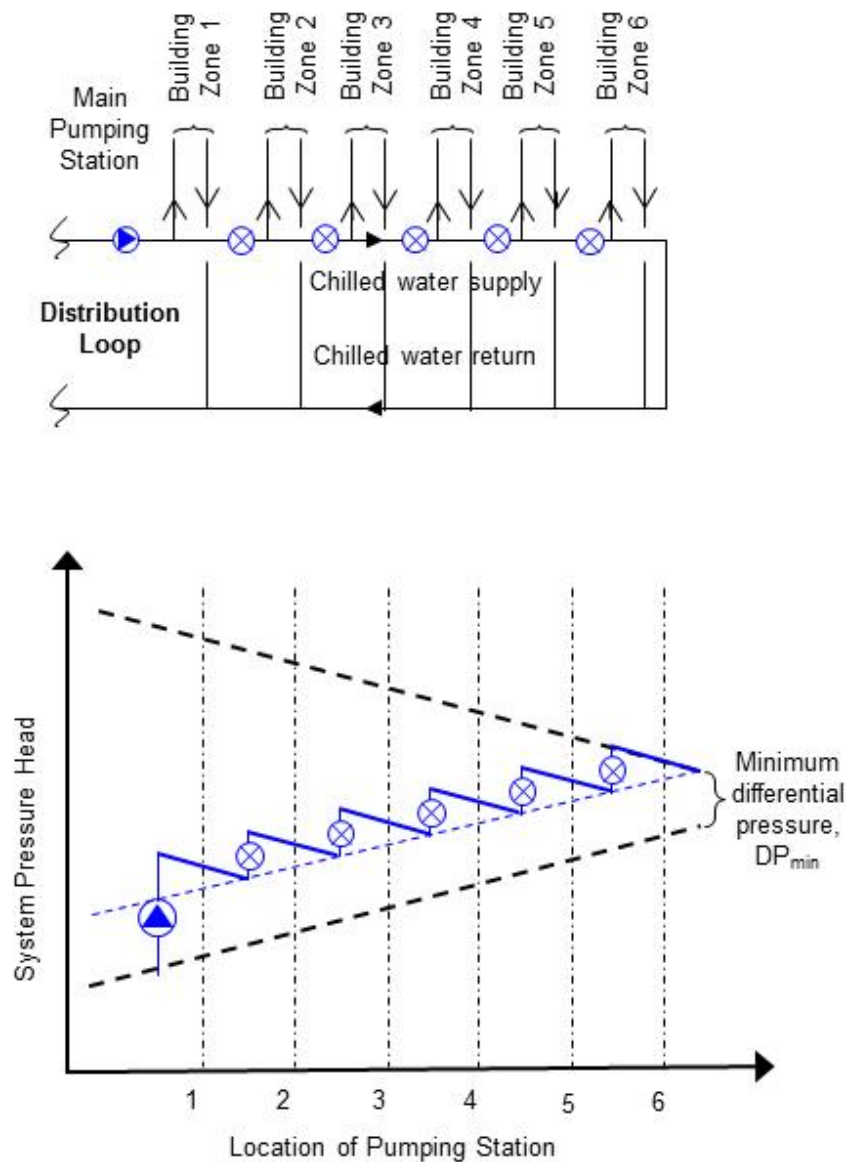
Table 6.2 Combination of pumping station (PS) location that is technically feasible (Con't)

No. of PS	Designation of PS combination	Location of pumping station											
		Chilled water supply side						Chilled water return side					
		PS _{1,s}	PS _{2,s}	PS _{3,s}	PS _{4,s}	PS _{5,s}	PS _{6,s}	PS _{1,r}	PS _{2,r}	PS _{3,r}	PS _{4,r}	PS _{5,r}	PS _{6,r}
4	PS 4-21	•			•				•		•		
	PS 4-22	•				•			•	•			
	PS 4-23	•					•		•	•			
	PS 4-24	•					•		•		•		
	PS 4-25	•	•	•					•				
	PS 4-26	•	•	•						•			
	PS 4-27	•	•		•				•				
	PS 4-28	•	•			•			•				
	PS 4-29	•	•				•		•				
	PS 4-30	•	•				•			•			
	PS 4-31	•		•	•				•				
	PS 4-32	•		•		•			•				
	PS 4-33	•		•			•		•				
	PS 4-34	•		•			•			•			
	PS 4-35	•			•	•			•				
	PS 4-36	•			•		•		•				
	PS 4-37	•				•	•		•				
5	PS 5-1	•	•	•	•	•							
	PS 5-2	•	•	•	•		•						
	PS 5-3	•	•	•		•	•						
	PS 5-4	•	•		•	•	•						
	PS 5-5	•		•	•	•	•						
	PS 5-6	•							•	•	•	•	
	PS 5-7	•	•						•	•	•		
	PS 5-8	•	•						•	•		•	
	PS 5-9	•	•						•		•	•	
	PS 5-10	•		•					•	•	•		
	PS 5-11	•		•					•	•		•	
	PS 5-12	•		•					•		•	•	
	PS 5-13	•			•				•	•	•		
	PS 5-14	•			•				•	•		•	
	PS 5-15	•			•				•		•	•	
	PS 5-16	•				•			•	•	•		
	PS 5-17	•				•			•	•		•	
	PS 5-18	•					•		•	•	•		
	PS 5-19	•	•	•					•	•			
	PS 5-20	•	•	•					•		•		
	PS 5-21	•	•	•						•	•		
	PS 5-22	•	•		•				•	•			
	PS 5-23	•	•				•		•	•			
	PS 5-24	•	•				•		•		•		
	PS 5-25	•		•	•				•	•			
	PS 5-26	•		•	•				•		•		
	PS 5-27	•		•		•			•	•			
	PS 5-28	•		•			•		•	•			
	PS 5-29	•		•			•		•		•		
	PS 5-30	•			•	•			•	•			
	PS 5-31	•			•		•		•	•			

Table 6.2 Combination of pumping station (PS) location that is technically feasible (Con't)

No. of PS	Designation of PS combination	Location of pumping station											
		Chilled water supply side						Chilled water return side					
		PS _{1,s}	PS _{2,s}	PS _{3,s}	PS _{4,s}	PS _{5,s}	PS _{6,s}	PS _{1,r}	PS _{2,r}	PS _{3,r}	PS _{4,r}	PS _{5,r}	PS _{6,r}
5	PS 5-32	•			•		•		•		•		
	PS 5-33	•				•	•		•	•			
	PS 5-34	•	•	•	•				•				
	PS 5-35	•	•	•		•			•				
	PS 5-36	•	•	•			•		•				
	PS 5-37	•	•	•			•			•			
	PS 5-38	•	•		•	•			•				
	PS 5-39	•	•		•		•		•				
	PS 5-40	•	•			•	•		•				
	PS 5-41	•		•	•	•			•				
	PS 5-42	•		•	•		•		•				
	PS 5-43	•		•		•	•		•				
	PS 5-44	•			•	•	•		•				
6	PS 6-1	•			•				•	•	•	•	
	PS 6-2	•				•			•	•	•	•	
	PS 6-3	•					•		•	•	•	•	
	PS 6-4	•	•	•					•	•		•	
	PS 6-5	•	•	•					•		•	•	
	PS 6-6	•	•		•				•		•	•	
	PS 6-7	•	•			•			•	•		•	
	PS 6-8	•	•				•		•	•	•		
	PS 6-9	•		•	•				•	•	•		
	PS 6-10	•		•	•				•	•		•	
	PS 6-11	•		•		•			•	•		•	
	PS 6-12	•			•	•			•	•	•		
	PS 6-13	•			•	•			•	•		•	
	PS 6-14	•			•		•		•	•	•		
	PS 6-15	•				•	•		•	•	•		
	PS 6-16	•	•	•	•				•	•			
	PS 6-17	•	•	•	•				•		•		
	PS 6-18	•	•	•			•		•		•		
	PS 6-19	•	•		•		•		•		•		
	PS 6-20	•	•			•	•		•	•			
PS 6-21	•		•	•	•			•	•				
PS 6-22	•		•	•		•		•	•				
PS 6-23	•		•		•	•		•	•				
PS 6-24	•			•	•	•		•	•				
PS 6-25	•	•	•	•	•			•					
PS 6-26	•	•	•	•		•		•					
PS 6-27	•	•	•		•	•		•					
PS 6-28	•	•		•	•	•		•					
PS 6-29	•		•	•	•	•		•					
PS 6-30	•	•	•	•	•	•							

Situation 1 - The pumping stations are located on the chilled water supply side only and the differential pressure of all combinations in this design can be maintained. Figure 6.2 shows an example of locating all the six pumping stations at the chilled water supply side while maintaining the minimum differential pressure across the heat exchangers in each branch.



Successful Case

Figure 6.2 Situation 1: all six pumping stations are located at the supply side and the minimum differential pressure across the heat exchangers in each branch can be maintained

Situation 2 - Equal number of pumping station at both the supply and return sides

Figures 6.3 (b) shows an example of locating two pumping stations at both the chilled water supply and return sides, while maintaining the minimum differential pressure across the heat exchangers in each branch. However, Figures 6.3 (a) and (c) show that when one pumping station at either the chilled water supply or return side was relocated to the farthest end of the distribution network, the minimum differential pressure could not be maintained.

Situation 3 - More pumping stations on the supply side

Figure 6.4 (b) shows an example of locating three pumping stations at the chilled water supply side and two pumping stations at the return side. The minimum differential pressure across the heat exchangers in each branch could be maintained. However, when one pumping station at either the supply or return side was relocated to the farthest end of the distribution network, the minimum differential pressure could not be maintained, as shown in Figures 6.4 (a) and (c).

Situation 4 - Fewer pumping stations at the supply side

Figures 6.5 (b) shows an example of locating two pumping stations at the chilled water supply side and three pumping stations at the return side. The minimum differential pressure across the heat exchangers in each branch could be maintained. However, when one pumping station at either the supply or return side was relocated to the farthest end of the distribution network, the minimum differential pressure could not be maintained, as illustrated in Figures 6.5 (a) and (c).

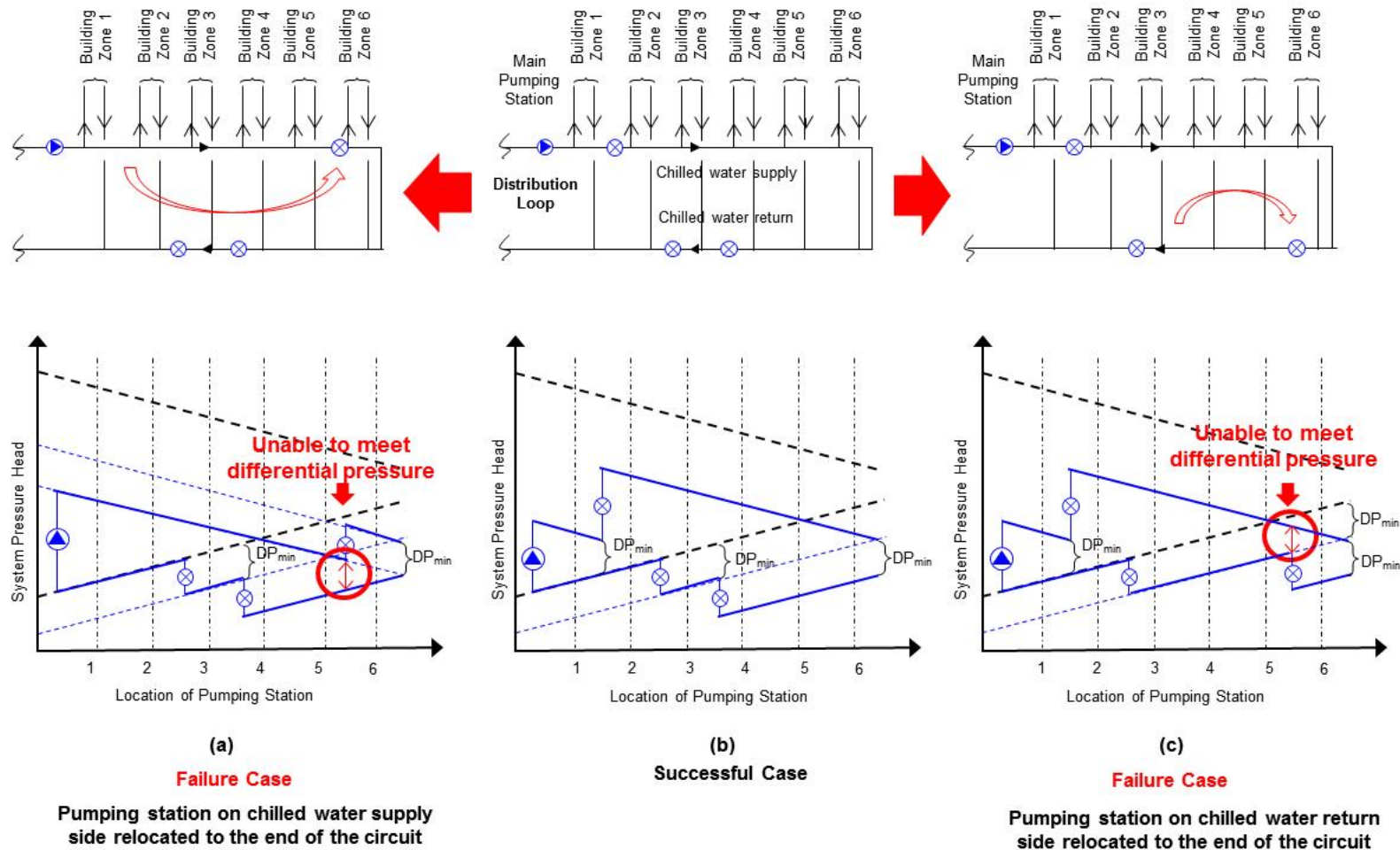


Figure 6.3 Situation 2: Equal number of pumping stations at both supply and return sides – (a) and (c) failure cases, (b) successful case in meeting the minimum differential pressure requirement

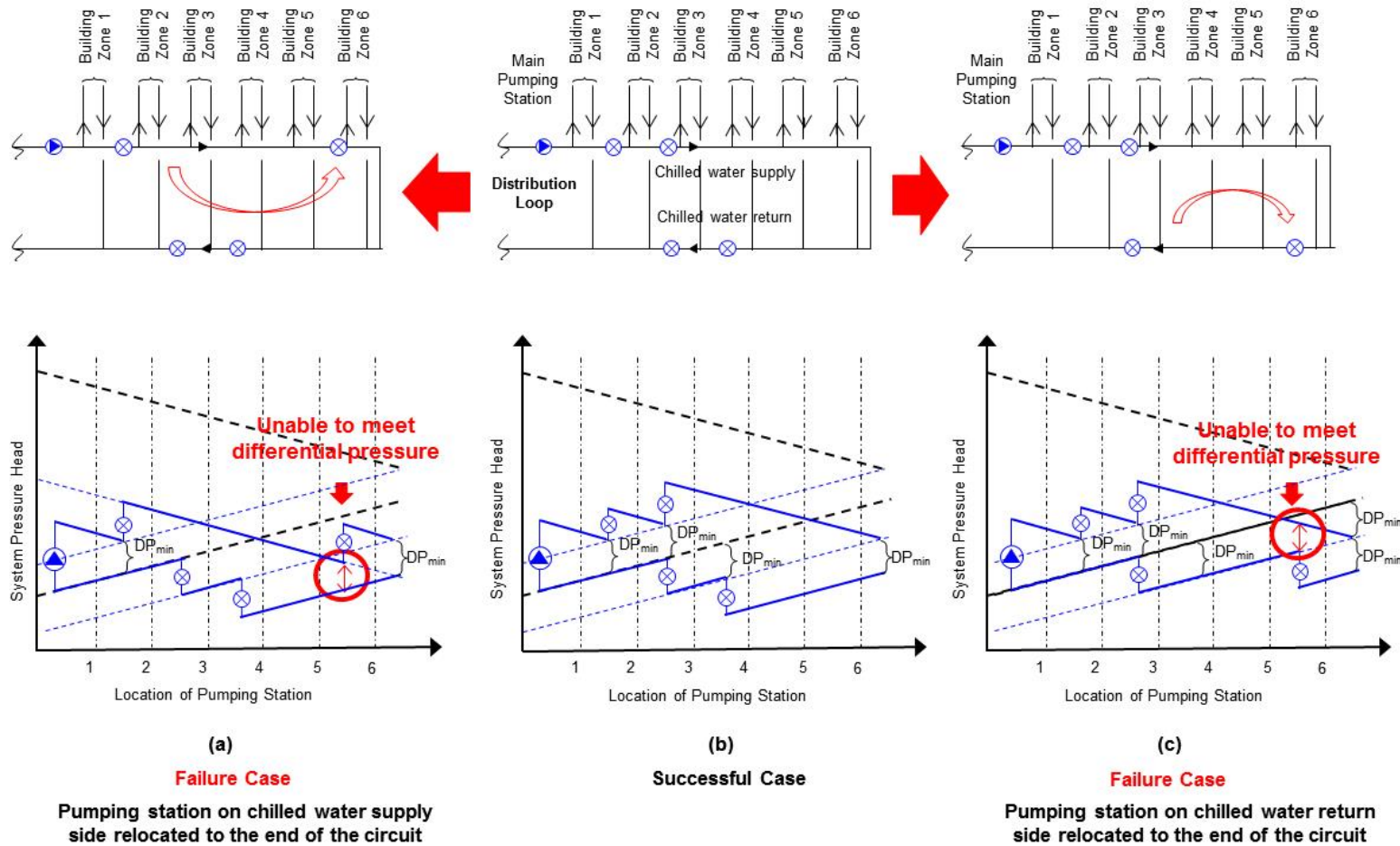


Figure 6.4 Situation 3: More pumping stations at the supply side – (a) and (c) failure cases, (b) successful case in meeting the minimum differential pressure requirement

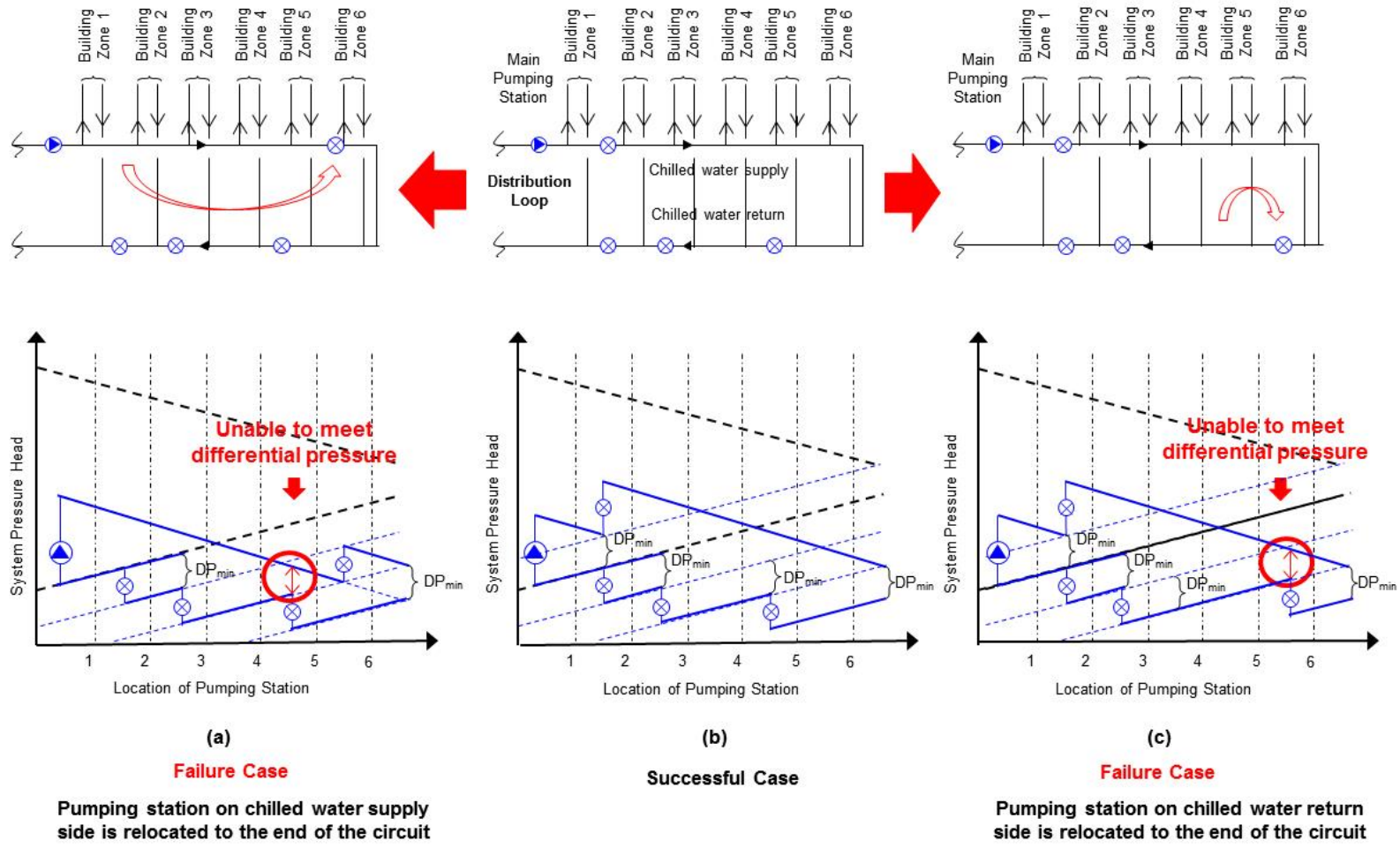


Figure 6.5 Situation 4: Fewer pumping stations at the supply side – (a) and (c) failure cases, (b) successful case in meeting the minimum differential pressure requirement

6.3 Impacts of Changing the Number of Pumps in Each Pumping Station

In addition to varying the location and number of pumping stations, variation in the number of pumps in each station, i.e. whether they are in groups of 5, 10 or 15, was also studied to evaluate its impacts on the electricity consumption of the pumping stations and find out an optimum combination of pumping stations.

According to the calculation explained in [Section 2.3 in Chapter 2](#), the pumping station arrangements for each combination of using one, two, three, four, five and six pumping stations were 3 ($=3^1$), 9 ($=3^2$), 27 ($=3^3$), 81 ($=3^4$), 243 ($=3^5$) and 729 ($=3^6$) respectively.

Using the hydraulic gradient approach, the number of combinations of using one, two, three, four, five and six pumping stations that could meet the minimum pressure differential requirement was reduced to 1, 7, 21, 37, 44 and 30 respectively ([Table 6.1](#)).

Subsequently, the number of pumping station arrangements of using one, two, three, four, five and six pumping stations were significantly reduced to 3 ($= 1 \times 3$), 63 ($= 7 \times 9$), 567 ($= 21 \times 27$), 2,997 ($= 37 \times 81$), 10,692 ($= 44 \times 243$) and 21,870 ($= 30 \times 729$), as shown in [Table 6.3](#). The total number of arrangement for all combinations of pumping stations was 36,192, which was significantly reduced by 92% from the original figure, i.e. 431,940 ($=1 \times 3 + 11 \times 9 + 55 \times 27 + 165 \times 81 + 210 \times 243 + 462 \times 729$).

Table 6.3 Total number of arrangements for the 140 combinations that are technically feasible in meeting the minimum pressure differential requirement

No. of pumping station	No. of combination that is technically feasible (a)	No. of arrangement for each pumping station combination (b)	Total no. of arrangement [= (a) x (b)]
1	1	3 ($=3^1$)	3 ($= 1 \times 3$)
2	7	9 ($=3^2$)	63 ($= 7 \times 9$)
3	21	27 ($=3^3$)	567 ($= 21 \times 27$)
4	37	81 ($=3^4$)	2,997 ($= 37 \times 81$)
5	44	243 ($=3^5$)	10,692 ($= 44 \times 243$)
6	30	729 ($=3^6$)	21,870 (30×729)
	140		36,192

6.4 Simulation of the Electricity Consumption of Pumping Stations

As 36,192 was still a huge figure to be involved in simulating the electricity consumption data of all these arrangements, a more efficient and systematic approach was adopted based on the following steps.

- Step 1: Determine the design chilled water flow rate of each pumping station, which equals the total chilled water flow rate of the building zones served by the pumping station, and the corresponding pressure head in the hydraulic distribution network.
- Step 2: Determine the rated power demand of the variable speed pumps in each pumping station.

Over thousands of variable speed pumps were involved in the simulation. A dataset was then developed based on the information obtained from the manufacturers on the rated power demand of 1,800 variable speed pumps at different operating flow rates and heads. This data was then plotted and shown in [Figure 6.6](#). Each line in the graph represents the power demand at different pressure heads in a range between 0.1 and 6 bar for a specific flow rate ranging from 0.1 to 3 m³/s in steps of 0.1m³/s.

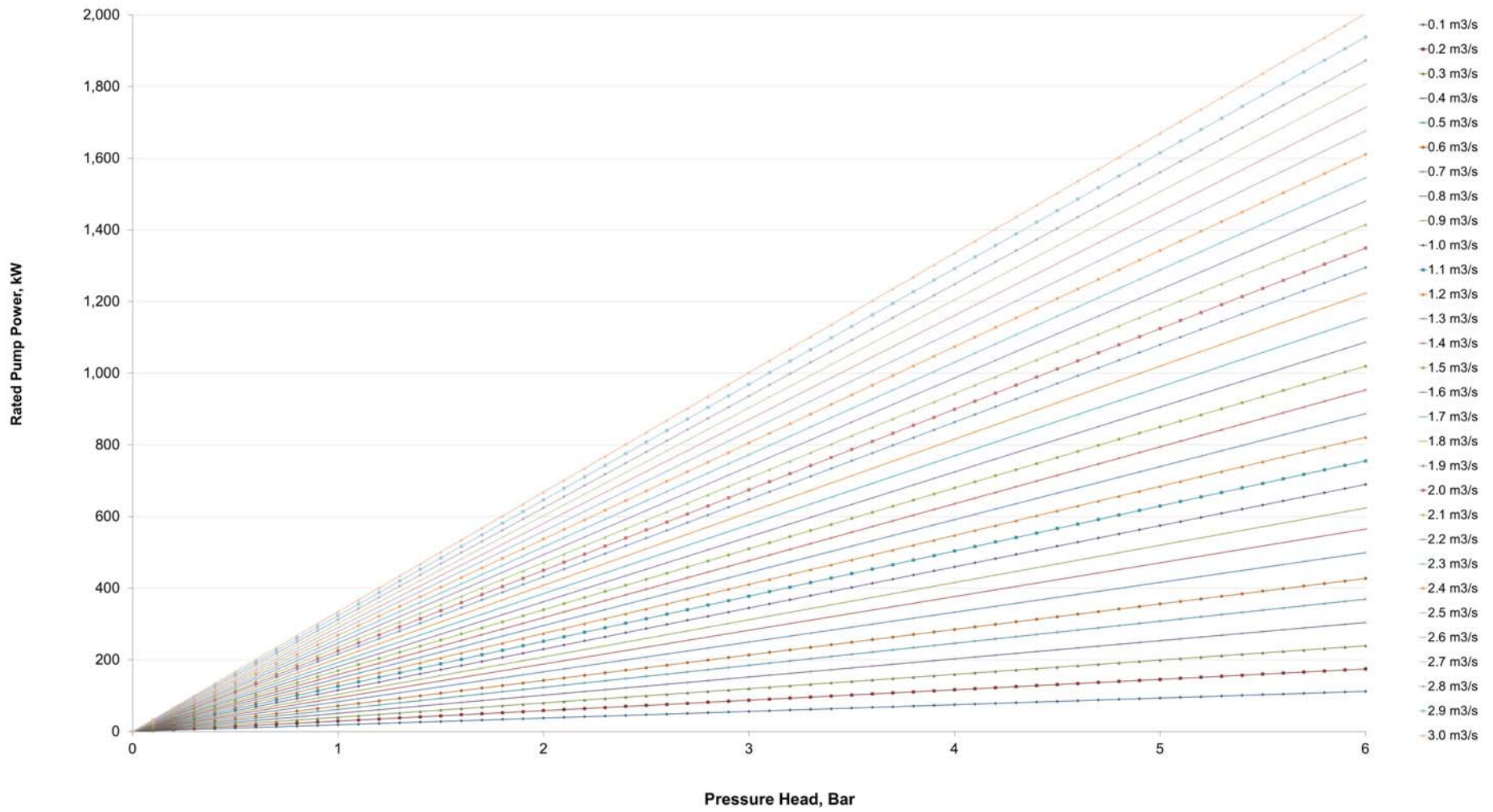


Figure 6.6 Rated power demand of variable speed pumps at different flow rates and pressure heads

Step 3: Determine the hourly operating flow rate and pressure head of the distribution pumps.

Based on the hourly cooling load profile simulated by HTB2 and BECON (c.f. [Chapter 3](#)), a time series of the year-round hourly cooling load and the corresponding chilled water flow rate of the four building models i , $M_{DCS,i}(t)$, were determined by [Equation 3.12](#) in [Chapter 3](#).

There were six building zones in the hypothetical district. Each zone consisted of different number of building model i , $N_{bldg,i,z}$, as shown in [Table 2.4](#) in [Chapter 2](#). The chilled water flow rate required by each building zone, $M_{DCS,z}(t)$ at a specific time t can be expressed by [Equation 6.1](#).

$$M_{DCS,z}(t) = \sum_{i=A}^D N_{bldg,i,z} M_{DCS,i}(t) \quad (6.1)$$

where

$$\begin{aligned} z &= \text{building zone number, 1 to 6} \\ i &= \text{building type, } i = A \text{ to D} \end{aligned}$$

The hourly chilled water flow rate of the pumping station, $M_{ps,z,s}(t)$, in building zone z at the chilled water supply side can be expressed by [Equation 6.2](#).

$$M_{ps,z,s}(t) = \sum_{z=j}^6 M_{DCS,z}(t) \quad (6.2)$$

where

$$\begin{aligned} s &= \text{chilled water supply side} \\ j &= \text{location of pumping station in building zone } z, \\ &\text{i.e. 1 to 6} \end{aligned}$$

The chilled water flow rates of the pumping stations installed in the same building zone at both chilled water supply and return sides were the same. Hence, the flow rate can be expressed by [Equation 6.3](#).

$$M_{PS,z,r}(t) = M_{PS,z,s}(t) \quad (6.3)$$

where

r = chilled water return side

Whereas the hourly operating flow rate of each pump in each pumping station in a building zone, $M_{pump,z}(t)$, depends on the number of pumps, N_{pump} , in the pumping station, i.e. 5, 10 or 15, the chilled water flow rate of pumps can be expressed by [Equation 6.4](#).

$$M_{pump,z}(t) = \frac{M_{ps,z,s}(t)}{N_{pump}} \quad (6.4)$$

A theoretical stochastic characterization of the pressure head required by each pumping station presented difficulties as it depends on the characterization of the chilled water flow. Hence, it would be more efficient to use the hydraulic distribution model developed in [Chapter 3](#) for simulating the corresponding system pressure head of each pumping station at time t .

Step 4: Determine the hourly power demand and electricity consumption of the pumps.

The hourly flow rate and pressure head requirements of the pump obtained in Step 3 were input into the variable speed chilled water pump model developed in [Section 3.5](#) of [Chapter 3](#). The hourly power demand of the variable speed pumps could then be determined and their summation equals the annual energy consumption.

Step 5: Design an optimization program to calculate the annual electricity consumption of the 36,192 pumping station arrangements.

To implement Steps 1 to 4, an algorithm depicted in [Figure 6.7](#) was developed. Based on this algorithm and the mathematical models developed for variable speed chilled water pumps, an optimization program using Excel VBA was established to calculate the annual electricity consumption of these 36,192 pumping station arrangements.

6.5 Results of Simulation

6.5.1 Electricity consumption of the pumping station arrangements with an equal number of pumps in each station

To evaluate the impacts of adopting an equal or unequal number of pumps in each pumping station, the electricity consumption data of those pumping station arrangements having an equal number of pumps in each pumping station was plotted and shown in [Figure 6.8](#).

Out of the total 36,192 pumping station arrangements, 140 arrangements with only five pumps, 140 arrangements with only 10 pumps and 140 arrangements with only 15 pumps were examined. Results show that their annual electricity consumption decreased as the number of pumping station increased. The 5-pump arrangement consumed less electricity in comparison with the 10-pump or 15-pump arrangement.

If the number of pumps in a pumping station was increased from 5 to 15, the discharge flow requirement for each pump reduced. When the pressure head of the pumping station was kept unchanged between 11 and 57 m, the efficiency of the pumps with a higher discharge flow rate was higher than those with a lower discharge flow rate. This explains why the pumping station arrangements with 5 pumps consumed less electricity in comparison with those equipped with 10 or 15 pumps.

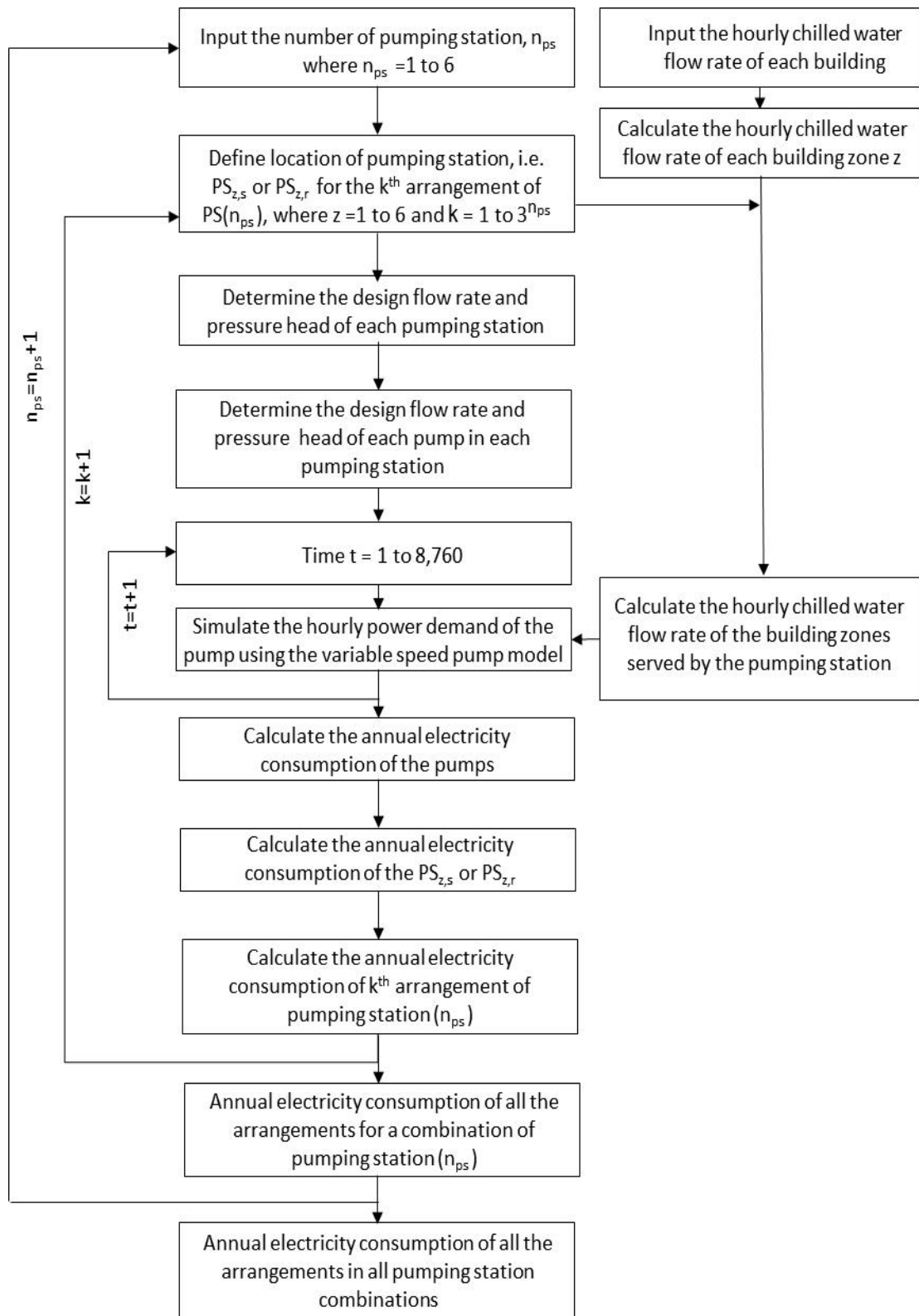


Figure 6.7 Algorithm for calculating the annual electricity consumption of different pumping station combinations

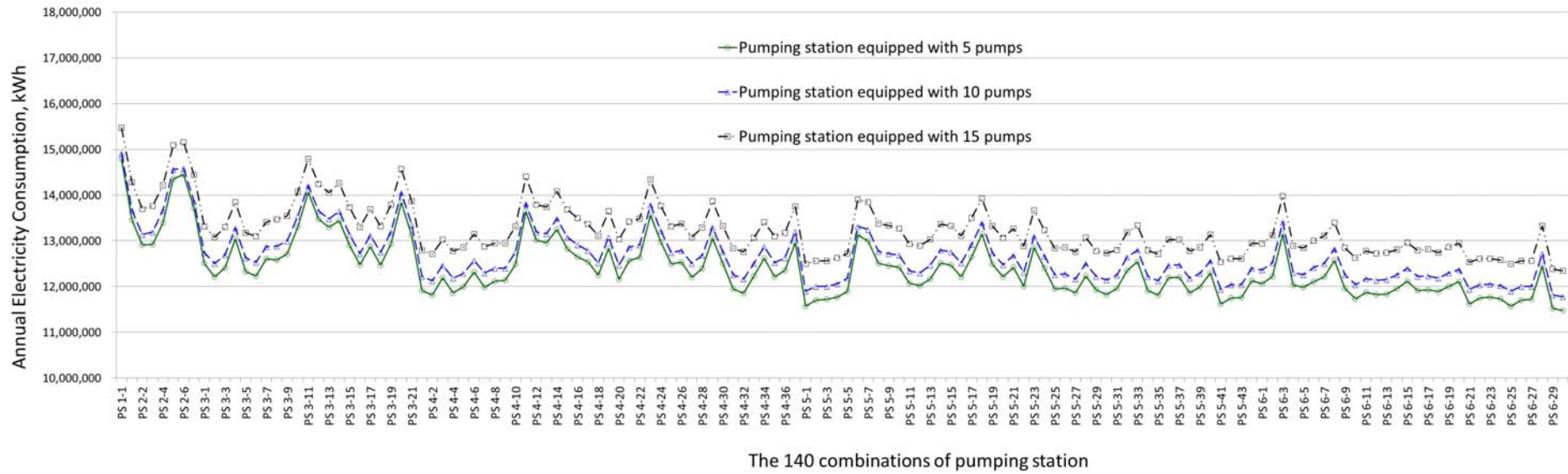


Figure 6.8 Annual electricity consumption of the pumping station arrangements with 5, 10 or 15 pumps in each station

6.5.2 Electricity consumption of the pumping station arrangements with an unequal number of pumps in each station

- i. A simulation of all the 36,192 arrangements shows that the 35464th arrangement with six pumping stations (i.e. “PS₆₋₃₅₄₆₄”) and five pumps in each station consumed the least electricity. The pumping stations in this “PS₆₋₃₅₄₆₄” were all located at the chilled water supply side.
- ii. [Table 6.4](#) gives a comparison of the base design PS₁₋₀ (i.e. one pumping station equipped with 10 pumps) and PS₆₋₃₅₄₆₄ in terms of the power demand and electricity consumption of the pumps. The following are the observations.

Table 6.4 Comparison of pump power and annual electricity consumption between PS₁₋₀ and PS₆₋₃₅₄₆₄

	Pumping station arrangement		Difference [PS ₆₋₃₅₄₆₄ minus PS ₁₋₀]	
	PS ₁₋₀	PS ₆₋₃₅₄₆₄	kW/kWh	%
No. of pumping station	1	6		
No. of pump per pumping station	10	5		
Location	Immediately downstream of the chiller plant	6 pumping stations at chilled water supply side		
Rated power, kW	576.0	577.4 / 132.6 / 68.5 / 45.1 / 27.7 / 6.4		
Total power, kW	5,760	4,288	-1,472	-25.6
Annual electricity consumption, kWh	14,911,696	11,478,917	-3,432,779	-23

When there is only one main pumping station for distributing chilled water to all the buildings in a district, the chilled water flow rate and pressure head are very high. Adding booster pumping stations can help to reduce the pressure head of the main pumping station. Moreover, the flow rate and pressure head requirements of the booster pumping station are further reduced if it is located further away from

the central plant. This can help to reduce the pump size and power demand of the main pumping station and the booster pumping stations.

More specifically, the total power demand and annual electricity consumption of the pumps in PS₆₋₃₅₄₆₄ was 25.6% and 23% less than those of the pumps in the base design PS₁₋₀ respectively.

- iii. Accordingly, the annual total electricity consumption of DCS_O could be reduced by 3% if its pumping station configuration (i.e. PS₁₋₀) was replaced by PS₆₋₃₅₄₆₄, which was a six-pumping station combination in nature (see [Table 6.5](#)).

Table 6.5 Difference in annual electricity consumption of DCS_O adopting the design of PS₁₋₀ or PS₆₋₃₅₄₆₄

	Annual electricity consumption, kWh		Difference [PS ₆₋₃₅₄₆₄ minus PS ₁₋₀]	
	PS ₁₋₀	PS ₆₋₃₅₄₆₄	kWh	%
Chiller plant	100,676,720	100,676,720	0	0
Pumping station	14,911,696	11,478,917	-3,432,779	-23.0
Total	115,588,416	112,155,637	-3,432,779	-3.0

6.6 Summary

The effectiveness of two pumping station design schemes, i.e. using multiple pumping stations and changing the number of pumps in each pumping station, was examined. A hydraulic gradient evaluation method was selected for conducting a quick assessment and identifying the combinations of pumping station that were technically feasible in meeting the minimum pressure differential requirement out of numerous possible combinations. The total number of pumping station combination was then significantly reduced by 86% from 1,024 to 140. Accordingly, the total number of pumping station

arrangement for each pumping station combination was also reduced by 92% from 431,940 to 36,192.

In view of the massive number of pumping station arrangements to be analyzed, a dataset of rated power of 1,800 pumps was developed to determine the rated pump power of the variable speed pumps designed with various flow rates and pump head requirements. To facilitate a simulation of the energy consumption of thousands of pumping station arrangements, an optimization program using a systematic approach was established to perform a more efficient calculation.

Results of simulation revealed that the adoption of six pumping stations, which were equipped with five pumps in each station, could lead to a 3% reduction in the annual total electricity consumption of DCS_O. However, this would imply higher initial capital cost, due to the greater number of pumps and accessories to be purchased, maintained and replaced, in comparison with the use of a single pumping station. This six-pumping station arrangement would only be financially viable when the achievable electricity cost saving could compensate for the higher initial and replacement costs of pumps. This issue will be further examined in [Chapter 8](#).

Chapter 7

Effects of Chilled Water Temperature on the Energy Performance of DCS_O

7.1 Overview

As mentioned in [Chapter 2](#), changing the design temperature of the supply and return chilled water can have a significant impact on two determining factors of the DCS' energy performance, i.e. the COP of chillers and the chilled water flow rate in the distribution network. As such, there would be a need to design an optimized chilled water temperature that could strike a good balance between the energy of chillers and pumps and minimize the overall electricity consumption of a DCS.

To the best of the author's knowledge, research literature has been lacking in this area to provide a useful guideline for engineers in designing a DCS. In this chapter, the impacts of changing the design chilled water supply and return temperatures of the chiller plant on the energy performance of DCS_O were investigated and the temperatures that can help optimize its energy performance were determined.

For the base design of the chiller system configuration C_O of DCS_O, the supply chilled water temperature was set at 5°C, whereas the chilled water return temperature was set at 12°C. To simulate the effects of changing the design temperatures, the chilled water

supply and return temperatures were each varied by $\pm 1^\circ\text{C}$. As a result, there are nine temperature regimes, including the base design, as shown in [Table 7.1](#).

The discussions in [Sections 7.2](#) and [7.3](#) to follow focus on the effects of changing the chilled water temperatures. Evaluation of the energy performance of DCS_0 and its major equipment under different temperature regimes is presented in [Section 7.4](#). The study results are summarized in [Section 7.5](#).

7.2 Effects of Changing the Chilled Water Temperature on the COP of Chillers

For a typical chiller, its COP improves with an increase in the design chilled water supply temperature, as the evaporator heat transfer may take place at a higher evaporating temperature and reduce the compressor work and hence the power demand of the chiller. The power consumption of the chiller will therefore decrease accordingly.

Based on the data obtained from the manufacturers, the part load performance of a constant speed chiller and a variable speed chiller are shown in [Figure 7.1](#).

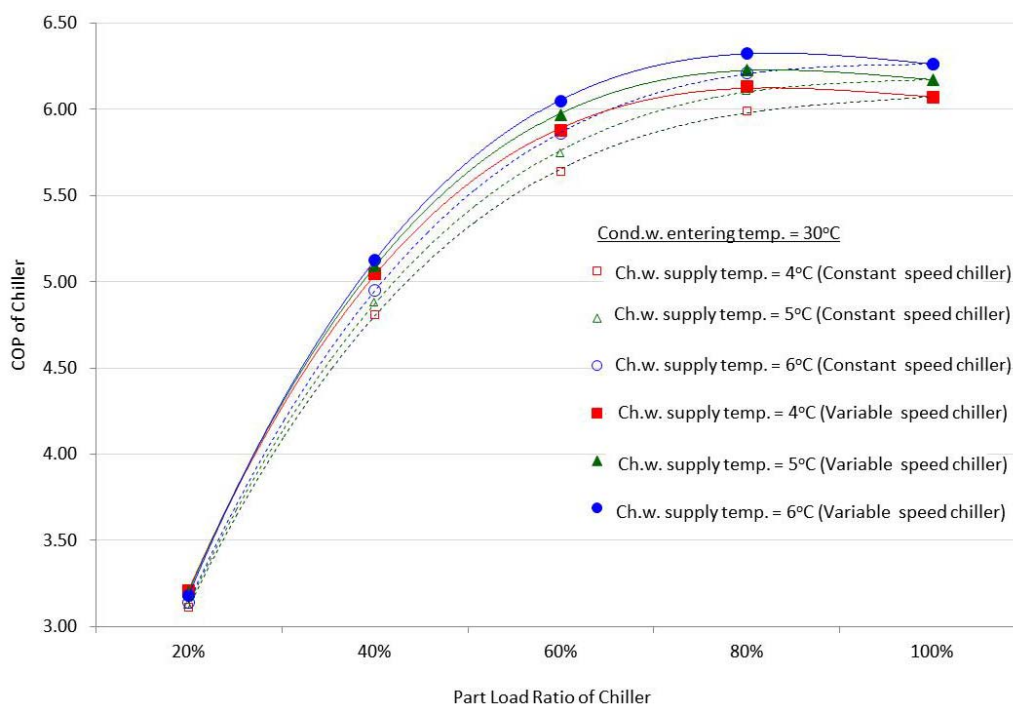


Figure 7.1 Part load performance of constant and variable speed chillers of different design chilled water supply temperatures

In this example, both chillers had the same capacity of 2,000 RT (7,034 kW). They were designed with the same condenser water entering temperature of 30°C and different chilled water supply temperatures, i.e. 4°C, 5°C and 6°C. From the graph, the chillers' COP increased as the chilled water supply temperature increased from 4°C to 6°C. In a situation where the PLR was greater than 40%, the average percentage of increment in the COP ranges from 1.3% to 2.0% for every °C of increase in the chilled water supply temperature. The percentage of improvement in the COP is not significant when the PLR was below 40%.

7.3 Effects of Changing the Chilled Water Temperature on the Chilled Water Flow Rate

If the difference between the design chilled water supply and return temperatures of the chiller plant (denoted as a “temperature difference” in this study) changes, it would affect the chilled water flow rate in a DCS. [Table 7.1](#) summarizes the annual average chilled water flow rate, which was calculated by averaging the hourly chilled water flow rate simulated by the cooling coil and heat exchanger models as developed in [Chapter 3](#) around a year, and was required in each temperature regime when the chilled water system was affected by the low delta-T syndrome.

Table 7.1 Annual average chilled water flow rate in different temperature regimes

Temp regime	Chilled water temp, °C			Annual average chilled water flow rate, m ³ /s
	Supply	Return	Temp difference	
T ₀ (base design)	5	12	7	2.38
T ₁	4	11	7	2.15
T ₂	4	12	8	2.03
T ₃	4	13	9	1.93
T ₄	5	11	6	2.53
T ₅	5	13	8	2.25
T ₆	6	11	5	2.92
T ₇	6	12	6	2.84
T ₈	6	13	7	2.69

The table shows that the annual average chilled water flow rate was the highest when the design temperature difference was at the lowest level, i.e. 5°C, in T_6 . Relatively less chilled water flow was required when the design temperature difference was at the highest level, i.e. T_3 (9°C). In the following section, the effects of changing the chilled water temperature on the chilled water flow rate are evaluated in detail for three types of situation.

- i. Situation 1 - The chilled water supply temperature is changed from 4°C to 6°C while the chilled water return temperature is maintained constant at 11°C, 12°C or 13°C.
- ii. Situation 2 - The chilled water return temperature is changed from 11°C to 13°C while the chilled water supply temperature is maintained constant at 4°C, 5°C or 6°C.
- iii. Situation 3 - The chilled water supply and return temperatures are changed from 4°C to 6°C and from 11°C to 13°C respectively.

7.3.1 Situation 1 – The design chilled water supply temperature is changed from 4°C to 6°C while the design chilled water return temperature is maintained constant at 11°C, 12°C or 13°C

Figure 7.2 (a) shows the connection between the chilled water circuit in a building and the distribution loop of DCS_O, with a heat exchanger serving as the interface. Figure 7.2 (b) shows the temperature profile of chilled water in the heat exchanger. When the design chilled water supply temperature at the primary side of the heat exchanger is increased from $T_{DCS,i,s}$ to $T_{DCS,i,s}'$, the design chilled water return temperature, $T_{DCS,i,r}$, remains unchanged. The chilled water temperature curves at the primary side are represented by Line 1 to Line 2, as shown in Figure 7.2 (b).

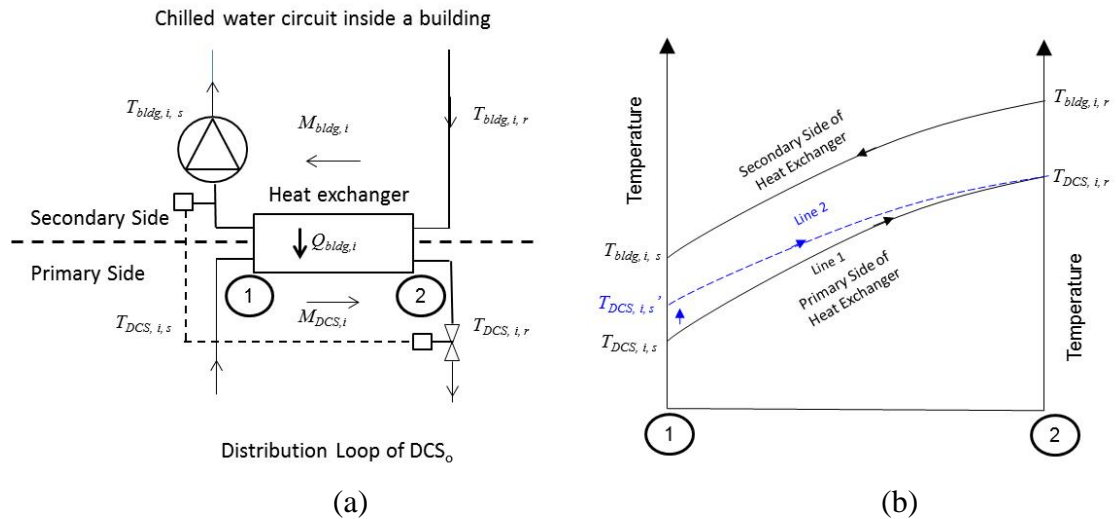


Figure 7.2 (a) Connection between the chilled water circuit and the distribution loop of DCS₀ via a heat exchanger
 (b) Temperature profile of chilled water in a heat exchanger when the design chilled water supply temperature increases from $T_{DCS, i, s}$ to $T_{DCS, i, s}'$

In a situation where the design chilled water return temperature was kept constant at, for example, 11°C, and when the chilled water supply temperature was increased from 4°C to 6°C, the design temperature difference would decrease. This had to be accomplished by increasing the chilled water flow rate at the primary side of the heat exchanger. Based on the annual average chilled water flow rate as shown in Table 7.1, the annual average chilled water flow rate increased from 2.15m³/s to 2.53 m³/s and then to 2.92m³/s, as shown in Table 7.2 (a). The same phenomenon occurred when the design chilled water return temperature was maintained at either 12°C or 13°C (Tables 7.2 (b) and (c)). The annual average of the chilled water flow rate increased as the design chilled water supply temperature was increased from 4°C to 6°C. Tables 7.2 (a) to (c) show that the percentage of increment ranges between 16.6% and 39.9%.

Table 7.2 Change in the annual average chilled water flow rate due to an increase in the design chilled water supply temperature:

(a) Return temperature is maintained at 11°C

Temp regime	Chilled water temp, °C			Annual average chilled water flow rate, m ³ /s	Difference in flow rate w.r.t. T ₁ , %
	Supply	Return	Temp difference		
T ₁	4	11	7	2.15	
T ₄	5	11	6	2.53	+17.7
T ₆	6	11	5	2.92	+35.8

(b) Return temperature is maintained at 12°C

Temp regime	Chilled water temp, °C			Annual average chilled water flow rate, m ³ /s	Difference in flow rate w.r.t. T ₂ , %
	Supply	Return	Temp difference		
T ₂	4	12	8	2.03	
T ₀	5	12	7	2.38	+17.2
T ₇	6	12	6	2.84	+39.9

(c) Return temperature is maintained at 13°C

Temp regime	Chilled water temp, °C			Annual average chilled water flow rate, m ³ /s	Difference in flow rate w.r.t. T ₃ , %
	Supply	Return	Temp difference		
T ₃	4	13	9	1.93	
T ₅	5	13	8	2.25	+16.6
T ₈	6	13	7	2.69	+39.4

To further investigate the impacts of increasing the design chilled water supply temperature on the chilled water flow rate at design or part load, temperature regimes T₁ and T₄ were selected as examples for comparing the hourly chilled water flow rates of a building affected by the low delta-T syndrome. As shown in [Figure 7.3](#), the design chilled water supply temperature was increased from 4°C in T₁ to 5°C in T₄ and the design chilled water return temperature remained constant at 11°C.

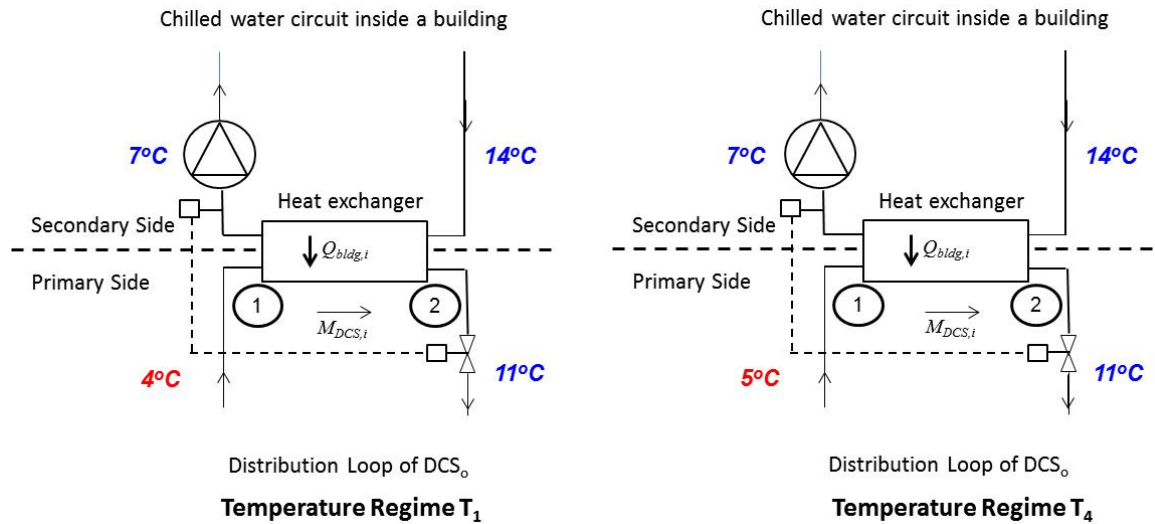


Figure 7.3 Design chilled water supply and return temperatures in T_1 and T_4

The design cooling load and part load of the building at a specific time $t=1,754$ hours were $Q_{bldg,i}$ (i.e. 10,065 kW) and $Q_{bldg,i}(t)$ (i.e. 7,092 kW) respectively (see Table 7.3).

Table 7.3 Comparison of the hourly chilled water flow rate of T_1 and T_4 in the distribution loop at design or part load

	T_1	vs	T_4
Design condition			
Building			
$Q_{bldg,i}$, kW	10,065	=	10,065
$T_{bldg,i,s}$, °C	7	=	7
$T_{bldg,i,r}$, °C	14	=	14
$T_{bldg,i,r} - T_{bldg,i,s}$, °C	7	=	7
DCS			
$T_{DCS,i,s}$, °C	4	<	5
$T_{DCS,i,r}$, °C	11	=	11
$T_{DCS,i,r} - T_{DCS,i,s}$, °C	7	>	6
M_{DCS} , l/s	342.4	<	399.4
Part load condition			
Building			
$Q_{bldg,i}(t)$, kW	7,072	=	7,072
DCS			
$T_{DCS,i,s}$, °C	4	<	5
$T_{DCS,i,r}(t)$, °C	10.6	>	10.5
$T_{DCS,i,r}(t) - T_{DCS,i,s}(t)$, °C	6.6	>	5.5
$M_{DCS}(t)$, l/s	254.9	<	304.6

Referring to the heat exchanger model in [Section 3.3](#) of [Chapter 3](#), with a design cooling load, the calculated chilled water flow rate, M_{DCS} , of T_4 was larger than that of T_1 . While at part load, it was also found that the temperature of the chilled water returning to the distribution loop of DCS_O, $T_{DCS,i,r}(t)$, in T_1 was relatively higher than that in T_4 . The chilled water supply temperature, $T_{DCS,i,s}$, in the distribution loop under T_1 was 4°C, which is relatively lower than that of T_4 , i.e. 5°C. This has resulted in a smaller temperature difference between the supply and return chilled water, $T_{DCS,i,r}(t) - T_{DCS,i,s}(t)$, and a higher chilled water flow rate, $M_{DCS}(t)$, in the distribution loop of DCS_O under T_4 .

7.3.2 Situation 2 – The design chilled water return temperature is changed from 11°C to 13°C while the design chilled water return temperature is maintained constant at 4°C, 5°C or 6°C

[Figure 7.4](#) shows the temperature profile of the chilled water in a heat exchanger where the design chilled water return temperature at the primary side of the heat exchanger increases from $T_{DCS,i,r}$ to $T_{DCS,i,r}'$, and the design chilled water supply temperature is kept constant at $T_{DCS,i,s}$. The chilled water temperature curves at the primary side are represented by Line 1 to Line 2, as shown in [Figure 7.4](#).

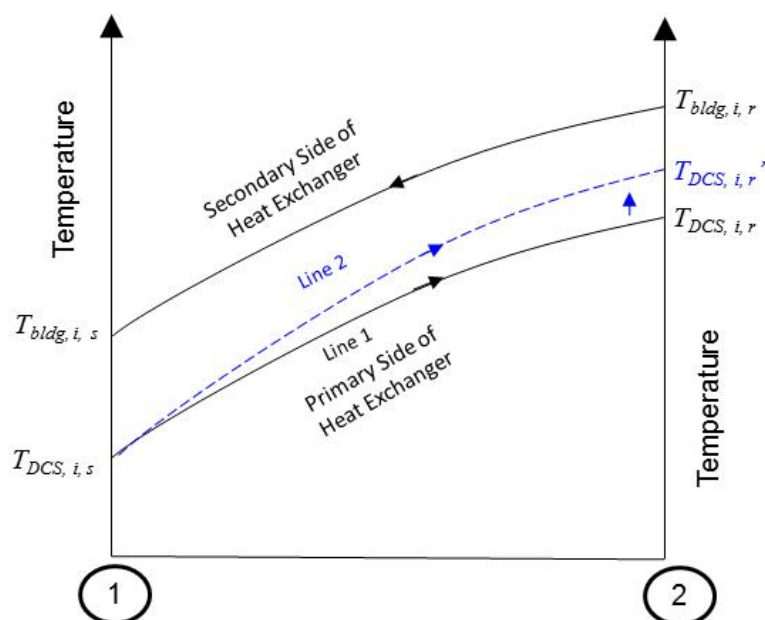


[Figure 7.4](#) Temperature profile of the chilled water in a heat exchanger where the design chilled water return temperature increases from $T_{DCS,i,r}$ to $T_{DCS,i,r}'$

In a situation where the design chilled water supply temperature was kept constant at, for example, 4°C, the design temperature difference increased when the chilled water return temperature was increased from 11°C to 13°C. This has resulted in decreasing the chilled water flow rate at the primary side of the heat exchanger accordingly. Table 7.4 (a) shows that the annual average chilled water flow rate decreased from 2.15 m³/s to 1.93 m³/s. The same phenomenon occurred when the design chilled water supply temperature remained unchanged at either 5°C or 6°C (Tables 7.4 (b) and (c)). The annual average chilled water flow rate decreased as the chilled water return temperature was increased from 11°C to 13°C. From Tables 7.4 (a) to (c), the percentage of flow rate decreased from 2.7% to 11.1%. The percentage of variation is relatively smaller in comparison with the result of changing the design chilled water supply temperature, as discussed in the previous section.

Table 7.4 Change in the annual average chilled water flow rate due to an increase in the design chilled water return temperature:

(a) Supply temperature is maintained at 4°C

Temp regime	Chilled water temp, °C			Annual average chilled water flow rate, m ³ /s	Difference in flow rate w.r.t. T ₁ , %
	Supply	Return	Temp difference		
T ₁	4	11	7	2.15	
T ₂	4	12	8	2.03	-5.6
T ₃	4	13	9	1.93	-10.2

(b) Supply temperature is maintained at 5°C

Temp regime	Chilled water temp, °C			Annual average chilled water flow rate, m ³ /s	Difference in flow rate w.r.t. T ₄ , %
	Supply	Return	Temp difference		
T ₄	5	11	6	2.53	
T ₀	5	12	7	2.38	-5.9
T ₅	5	13	8	2.25	-11.1

(c) Supply temperature is maintained at 6°C

Temp regime	Chilled water temp, °C			Annual average chilled water flow rate, m ³ /s	Difference in flow rate w.r.t. T ₆ , %
	Supply	Return	Temp difference		
T ₆	6	11	5	2.92	
T ₇	6	12	6	2.84	-2.7
T ₈	6	13	7	2.69	-7.9

Using the same design condition as stated in Section 7.3.1, T_1 and T_2 were selected as examples to further illustrate the impacts of increasing the design chilled water return temperature. In Figure 7.5, the design chilled water return temperature was increased from 11°C to 12°C and the design chilled water supply temperature remained unchanged at 4°C .

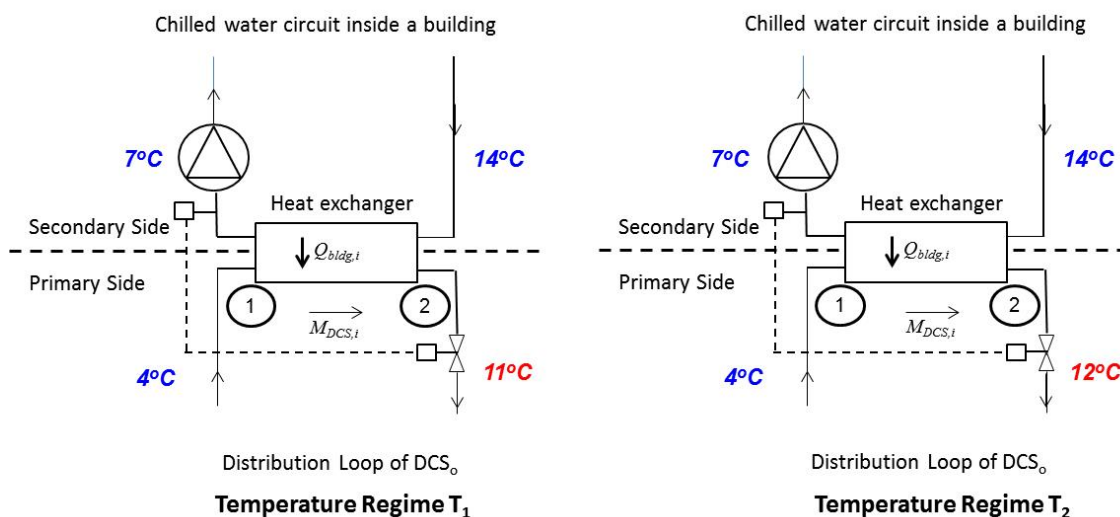


Figure 7.5 Design chilled water supply and return temperatures in T_1 and T_2

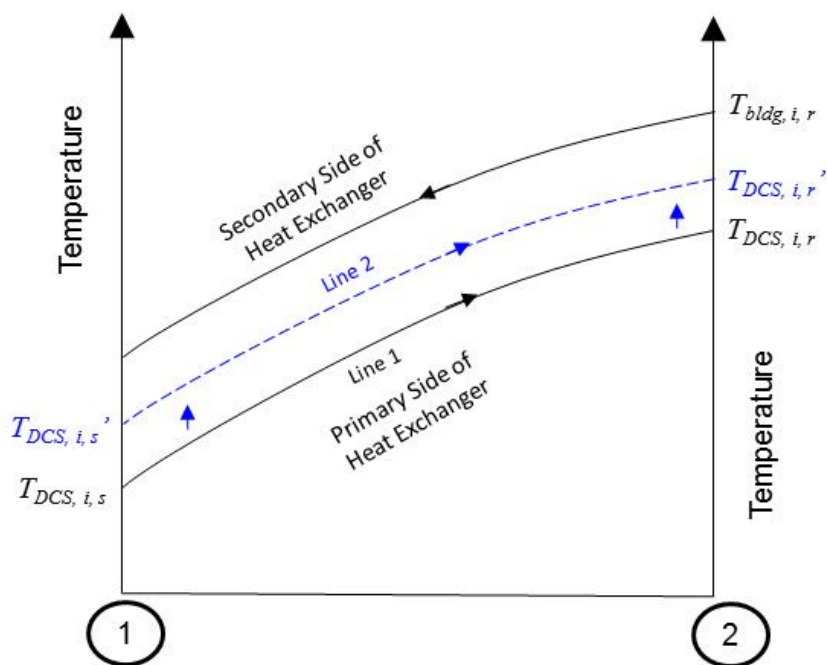
At part load, the simulation results in Table 7.5 revealed that the temperature of the chilled water returning to the distribution loop, $T_{DCS,i,r}(t)$, in T_1 was relatively lower than that in T_2 , while the chilled water supply temperatures, $T_{DCS,i,s}$, in the distribution loop in T_1 and T_2 were both at 4°C . This has resulted in a larger temperature difference, $T_{DCS,i,r}(t) - T_{DCS,i,s}(t)$, and a lower chilled water flow rate, $M_{DCS}(t)$, at the primary side of the heat exchanger under T_2 .

7.3.3 Situation 3 – The design chilled water supply and return temperatures are changed from 4°C to 6°C and from 11°C to 13°C respectively

Figure 7.6 shows the temperature profile of the chilled water in a heat exchanger where the design chilled water supply and return temperatures at the primary side are increased from $T_{DCS,i,s}$ and $T_{DCS,i,r}$ to $T_{DCS,i,s}'$ and $T_{DCS,i,r}'$ respectively, but their temperature differential is kept constant. The temperature curve moves uniformly from Line 1 to Line 2.

Table 7.5 Comparison of the hourly chilled water flow rate in T_1 and T_2 in the distribution loop at design or part load

		T_1	vs	T_2
Design condition				
Building				
	$Q_{bldg,i}$, kW	10,065	=	10,065
	$T_{bldg,i,s}$, °C	7	=	7
	$T_{bldg,i,r}$, °C	14	=	14
	$T_{bldg,i,r} - T_{bldg,i,s}$, °C	7	=	7
DCS				
	$T_{DCS,i,s}$, °C	4	=	4
	$T_{DCS,i,r}$, °C	11	<	12
	$T_{DCS,i,r} - T_{DCS,i,s}$, °C	7	<	8
	M_{DCS} , l/s	342.4	>	299.6
Part load condition				
Building				
	$Q_{bldg,i}(t)$, kW	7,072	=	7,072
DCS				
	$T_{DCS,i,s}(t)$, °C	4	=	4
	$T_{DCS,i,r}(t)$, °C	10.98	<	11.51
	$T_{DCS,i,r}(t) - T_{DCS,i,s}(t)$, °C	6.98	<	7.51
	$M_{DCS}(t)$, l/s	254.9	>	236.0

**Figure 7.6** Temperature profile of the chilled water in a heat exchanger where the design chilled water supply and return temperatures, i.e. $T_{DCS,i,s}$ and $T_{DCS,i,r}$, are increased to $T_{DCS,i,s}'$ and $T_{DCS,i,r}'$ but the temperature difference remains the same

From [Table 7.6](#), the annual average chilled water flow rate is in an increasing trend when the design chilled water supply and return temperatures were increased. Moreover, with the same design temperature differential at 7°C in T₁, T_O and T₈, this flow rate still increased in the order of 4°C-11°C, 5°C-12°C and 6°C-13°C respectively ([Table 7.6 \(b\)](#)). This is due to the combined effect of the results found in situations 1 and 2 above. When the design chilled water supply temperature was increased from 4°C to 6°C, the increase in the flow rate had far exceeded the decrease in the flow rate when the design chilled water return temperature was increased from 11°C to 13°C. The same phenomenon also occurred in T₄ and T₇ ([Table 7.6 \(a\)](#)), and in T₂ and T₅ ([Table 7.6 \(c\)](#)).

Table 7.6 Change in the annual average chilled water flow rate due to an increase in the chilled water supply and return temperature:

(a) Temperature difference remains at 6°C

Temp regime	Chilled water temp, °C			Annual average chilled water flow rate, m ³ /s	Difference in flow rate w.r.t. T ₄ , %
	Supply	Return	Temp difference		
T ₄	5	11	6	2.53	
T ₇	6	12	6	2.84	+12.3

(b) Temperature difference remains at 7°C

Temp regime	Chilled water temp, °C			Annual average chilled water flow rate, m ³ /s	Difference in flow rate w.r.t. T ₁ , %
	Supply	Return	Temp difference		
T ₁	4	11	7	2.15	
T _O	5	12	7	2.38	+10.7
T ₈	6	13	7	2.69	+25.1

(c) Temperature difference remains at 8°C

Temp regime	Chilled water temp, °C			Annual average chilled water flow rate, m ³ /s	Difference in flow rate w.r.t. T ₂ , %
	Supply	Return	Temp difference		
T ₂	4	12	8	2.03	
T ₅	5	13	8	2.25	+10.8

7.4 Simulation Results and Analysis

The electricity consumption of DCS_O under the nine temperature regimes (including that of the base case) has been simulated and summarized in [Table 7.7](#).

Table 7.7 Comparison of annual electricity consumption of DCS_O in nine different temperature regimes at low delta-T

Temp regime	Chilled water temp, °C			Annual electricity consumption, kWh						Difference in consumption w.r.t. T _O , %
	Supply	Return	Temp difference	Chiller plant				Pumping station	Total	
				Chiller [a]	Pri. ch. w. pump [b]	Seawater pump [c]	Sub-total [a] + [b] + [c]	Sec. ch. w. pump [d]	[a]+[b]+[c]+[d]	
T _O	5	12	7	88,827,472	5,583,218	7,582,613	101,993,303	14,911,696	116,904,999	
T ₁	4	11	7	92,833,355	5,065,218	6,896,226	104,794,798	13,333,416	118,128,214	+1.05
T ₂	4	12	8	93,686,540	4,784,789	7,410,722	105,882,051	12,342,376	118,224,427	+1.13
T ₃	4	13	9	94,601,544	4,505,142	7,859,620	106,966,306	11,857,991	118,824,297	+1.64
T ₄	5	11	6	87,896,958	6,001,400	7,001,053	100,899,411	15,944,134	116,843,545	-0.05
T ₅	5	13	8	89,794,320	5,224,382	8,071,490	103,090,192	13,766,463	116,856,655	-0.04
T ₆	6	11	5	83,248,379	7,219,174	6,975,753	97,443,307	18,367,820	115,811,127	-0.94
T ₇	6	12	6	84,329,686	6,674,711	7,771,021	98,775,418	18,065,505	116,840,923	-0.05
T ₈	6	13	7	85,499,888	6,206,791	8,412,718	100,119,397	17,054,325	117,173,722	+0.23

The results show that in T_6 (i.e. with the design chilled water supply and return temperatures set at 6°C and 11°C respectively), the annual total electricity consumption is the lowest, which was 0.94% less than that in T_0 of the base case where the design chilled water supply and return temperatures were 5°C and 12°C respectively.

The percentage of variation in the annual total electricity consumption of the eight temperature regimes, T_1 to T_8 , in comparison with the base T_0 , ranges from -0.94% to 1.64%, reflecting that the impact of changing the design chilled water temperatures was not significant.

In the following sections, the impacts of changing the design temperatures on the electricity consumption of chillers, primary chilled water pumps and seawater pumps in the chiller plant and the secondary chilled water distribution pumps in the pumping station are evaluated in detail.

7.4.1 Impacts of the Design Chilled Water Temperature on the Electricity Consumption of the Chiller Plant

7.4.1.1 Chillers

Based on [Table 7.8](#), the electricity consumption of chillers was the highest in T_3 , as these chillers consumed an additional 6.5% of electricity in comparison with those in other temperature regimes. On the other hand, the electricity consumption of the chillers in T_6 was the lowest and the percentage of electricity saving was the highest (i.e. 6.3%) in comparison with the base T_0 . The reasons are as follows.

- i. According to the comparison of the part load performance of chillers at different chilled water supply temperatures in [Figure 7.1](#), the COP of chillers increased when the chilled water supply temperature is increased from 4°C to 6°C . Therefore, comparing to other temperature regimes, the chillers in T_6 , T_7 and T_8 with a design supply temperature of 6°C consumed less electricity.

Table 7.8 Percentage of electricity saving of chillers in different temperature regimes

Temp regime	Chilled water temp, °C			Chiller hour, hr	Annual electricity consumption of chiller	
	Supply	Return	Temp difference		kWh	Difference w.r.t. T ₀ , %
T ₀	5	12	7	33,952	88,827,472	
T ₁	4	11	7	30,802	92,833,355	+4.5
T ₂	4	12	8	33,100	93,686,540	+5.5
T ₃	4	13	9	35,105	94,601,544	+6.5
T ₄	5	11	6	31,348	87,896,958	-1.0
T ₅	5	13	8	36,141	89,794,320	+1.0
T ₆	6	11	5	31,297	83,248,379	-6.3
T ₇	6	12	6	34,865	84,329,686	-5.1
T ₈	6	13	7	37,744	85,499,888	-3.7

- ii. As explained in [Chapter 2](#), provided that the chilled water supply temperature remains unchanged, changing the chilled water return temperature would have no significant impact on the COP and hence the power demand of chillers ([Taylor 2011](#)). However, the difference between the chilled water supply and return temperatures enlarged as the design chilled water return temperatures in T₆, T₇ and T₈ were increased from 11°C to 13°C. The rated chilled water flow rate of chillers in T₆ was thus the highest. This is then followed by the chillers in T₇. The rated chilled water flow rate of the chillers in T₈ was the lowest. Under such circumstances, comparing to the chillers in T₆, additional chillers had to be staged on in T₇ and T₈ to achieve the same chilled water flow requirement. The total operating chiller hour of chillers in T₆ was therefore the lowest ([Table 7.8](#)).

7.4.1.2 Primary Chilled Water Pumps

A summary of the design chilled water flow rate, power demand, pump hours and percentage of electricity saving of the primary chilled water pumps in the nine

temperature regimes is given in [Table 7.9](#). In T_6 , the electricity consumption of the primary chilled water pumps was the highest as it was 29.3% greater than that in the base T_0 . On the other hand, the pumps in T_3 had the lowest electricity consumption, leading to a saving of 19.3% in comparison with those in T_0 .

Table 7.9 Percentage of electricity saving of the primary chilled water pumps in different temperature regimes

Temp regime	Chilled water temp, °C			Design pump flow rate, l/s	Rated power, kW	Pump hour, hr	Annual electricity consumption of the pump	
	Supply	Return	Temp difference				kWh	Difference w.r.t. T_0 , %
T_0	5	12	7	718	164.4	33,952	5,583,218	
T_1	4	11	7	718	164.4	30,802	5,065,218	-9.3
T_2	4	12	8	628	144.6	33,100	4,784,789	-14.3
T_3	4	13	9	558	128.3	35,105	4,505,142	-19.3
T_4	5	11	6	837	191.4	31,348	6,001,400	+7.5
T_5	5	13	8	628	144.6	36,141	5,224,382	-6.4
T_6	6	11	5	1,005	230.7	31,297	7,219,174	+29.3
T_7	6	12	6	837	191.4	34,865	6,674,711	+19.5
T_8	6	13	7	718	164.4	37,744	6,206,791	+11.2

These consumption patterns are the results of the relationship between the operating frequency and the power demand of the pumps, which is explained below.

- i. Primary chilled water pumps are interlocked with chillers to distribute chilled water in the distribution loop. In this regard, the operating pump hours of the primary pumps in the nine temperature regimes as shown in [Table 7.9](#) were the same as the corresponding operating chiller hours as shown in [Table 7.8](#). As shown in [Table 7.9](#), despite of the long operating pump hours, the electricity consumption of the pumps would not necessarily increase as it is also affected by the power demand of the pumps.

- ii. The power demand of pumps also plays an important role in deciding the amount of electricity they consume. A pump's power demand depends on its design pressure head and chilled water flow rate. As the chilled water pump configurations were the same across all the temperature regimes, the pressure head of the pumps should be the same. Therefore, the power demand is mainly determined by the design chilled water flow rate, which is inversely proportional to the temperature difference.

T_3 was designed with the largest temperature difference, and hence the design chilled water flow rate was the lowest. Accordingly, the power demand of the pumps was the lowest in T_3 (i.e. 128.3 kW), as shown in [Table 7.9](#), but their operating pump hours were also the highest. The energy simulation results show that the pumps in T_3 had the lowest electricity consumption. This implies that the decrease in power demand could substantially offset the increase in the electricity consumed by pumps even with the highest operating frequency.

7.4.1.3 Seawater Pumps

A summary of the design seawater flow rate, power demand, operating pump hours and percentage of electricity saving of the seawater pumps is given in [Table 7.10](#). The electricity consumption of the seawater pumps in T_8 was the highest, which was 10.9% more than that in the base T_0 . On the contrary, the electricity consumption in T_1 was the lowest, as there was a saving of 9.1% in comparison with that in T_0 .

These consumption patterns reflect the relationship between the operating frequency and power demand of the pumps, which is explained below.

- i. Seawater pumps are also interlocked with chillers to circulate seawater for heat dissipation. In this regard, the electricity consumption of seawater pumps is determined by the operating frequency of chillers. In this study, the operating pump hours of the seawater pumps of the nine temperature regimes as shown in [Table 7.10](#) were the same as the operating chiller hours of the corresponding chillers as shown in [Table 7.8](#).

Table 7.10 Percentage of electricity saving of seawater pumps in different temperature regimes

Temp regime	Chilled water temp, °C			Design pump flow rate, l/s	Rated power, kW	Pump hour, hr	Annual electricity consumption of the pump	
	Supply	Return	Temp difference				kWh	Difference w.r.t. T ₀ , %
T ₀	5	12	7	973	223.3	33,952	7,582,613	
T ₁	4	11	7	975	223.9	30,802	6,896,226	-9.1
T ₂	4	12	8	975	223.9	33,100	7,410,722	-2.3
T ₃	4	13	9	975	223.9	35,105	7,859,620	+3.7
T ₄	5	11	6	973	223.3	31,348	7,001,053	-7.7
T ₅	5	13	8	973	223.3	36,141	8,071,490	+6.4
T ₆	6	11	5	971	222.9	31,297	6,975,753	-8.0
T ₇	6	12	6	971	222.9	34,865	7,771,021	+2.5
T ₈	6	13	7	971	222.9	37,744	8,412,718	+10.9

- ii. The power demand of the seawater pump depends on its design pressure head and seawater flow rate. As the seawater pumps' configurations were the same in all the temperature regimes, there was no change in the pressure head of the seawater pumps. According to [Equation 2.1](#) in [Chapter 2](#), seawater flow rate is proportional to the cooling capacity of chillers but is inversely proportional to the COP of chillers. With the same cooling capacity of the chiller, the seawater pump's design flow rate decreased slightly as the COP of the chiller increased moderately when the chilled water supply temperature was increased from 4°C to 6°C. In this regard, the seawater pump's power demand decreased accordingly.

Under such circumstances, it can be seen from [Table 7.10](#) that the lower the operating pump hours, the lower the electricity consumption of the seawater pumps. The electricity consumption of the seawater pumps in T₁ was the lowest. This reflects that the operating pump hours of the pumps had a greater impact on the seawater pump's electricity consumption than their power demand.

7.4.1.4 Overall Electricity Consumption of the Chiller Plant

Based on the electricity consumption data of the chillers, primary chilled water pumps and seawater pumps in the nine design temperature regimes, a comparison of the total electricity consumption of the chiller plant and the electricity savings in percentage is given in [Table 7.11](#).

Table 7.11 Percentage of electricity saving of the chiller plant in different temperature regimes

Temp regime	Chilled water temp, °C			Annual electricity consumption of chiller plant	
	Supply	Return	Temp difference	kWh	Difference w.r.t. T ₀ , %
T ₀	5	12	7	101,993,303	
T ₁	4	11	7	104,794,798	+2.7
T ₂	4	12	8	105,882,051	+3.8
T ₃	4	13	9	106,966,306	+4.8
T ₄	5	11	6	100,899,411	-1.1
T ₅	5	13	8	103,090,192	+1.1
T ₆	6	11	5	97,443,307	-4.6
T ₇	6	12	6	98,775,418	-3.2
T ₈	6	13	7	100,119,397	-1.8

The results indicate that the electricity consumption of the chiller plant was the highest in T₃ and the lowest in T₆. In other words, T₆ could save a maximum of 4.6% of electricity in comparison with the base design T₀.

7.4.2 Impacts of the Design Chilled Water Temperature on the Electricity Consumption of Secondary Chilled Water Distribution Pumps

Keeping all other design aspects unchanged, any change in the temperature difference between the design chilled water supply and return temperatures can lead to variations in the secondary chilled water distribution pump's design flow rates and hence the power demand. The higher the temperature difference, the lower the design chilled water flow rate.

The pump's design flow rate and power demand was the greatest when the design temperature difference was the smallest, i.e. 5°C, as in T₆. Moreover, the annual average chilled water flow rate in T₆ was also the highest. On the contrary, the least pump power was required and the annual average chilled water flow rate was the lowest when the design temperature difference was the greatest, i.e. 9°C, as in T₃ (Table 7.12).

The percentage change in the electricity consumption of the secondary distribution pumps in T₁ to T₈ exhibits the similar pattern of variation with that of the design pump power and the annual average chilled water flow rate (see Table 7.12). The electricity consumption of the pumps in T₃ could save 20% of electricity in comparison with the base case T₀ even though the operating pump hours were not the lowest.

Table 7.12 Percentage of electricity saving of the secondary chilled water distribution pumps in different temperature regimes

Temp regime	Chilled water temp, °C			Design pump flow rate, l/s	Rated power, kW	Annual average chilled water flow rate, m ³ /s	Pump hour, hr	Annual electricity consumption of the secondary pump	
	Supply	Return	Temp difference					kWh	Difference w.r.t. T ₀ , %
T ₀	5	12	7	718	576.0	2.38	33,952	14,911,696	
T ₁	4	11	7	718	576.0	2.15	30,802	13,333,416	-5.2
T ₂	4	12	8	628	481.2	2.03	33,100	12,342,376	-14.2
T ₃	4	13	9	558	423.7	1.93	35,105	11,857,991	-20.0
T ₄	5	11	6	837	709.4	2.53	31,348	15,944,134	+12.7
T ₅	5	13	8	628	481.2	2.25	36,141	13,766,463	-9.7
T ₆	6	11	5	1,005	920.2	2.92	31,297	18,367,820	+22.5
T ₇	6	12	6	837	709.4	2.84	34,865	18,065,505	+16.2
T ₈	6	13	7	718	576.0	2.69	37,744	17,054,325	+7.0

7.4.3 Overall Electricity Consumption of DCS₀

As discussed in the previous sections, chiller plants and pumping stations exhibit different electricity consumption patterns. With reference to Table 7.11, the chiller plant designed with T₆ had the lowest electricity consumption, which was 4.6% less than that

in the base case T_0 . On the contrary, the secondary distribution pumps in the pumping station designed with T_3 had the lowest electricity consumption and could save 20% of electricity with reference to T_0 (Table 7.12).

After summing up the electricity consumption figures of the chiller plant and the secondary distribution pumps (Table 7.7), it was found that DCS_0 designed with the chilled water supply and return temperatures of 6°C and 11°C respectively, i.e. in T_6 , had the lowest electricity consumption. Nevertheless, when compared to the base design T_0 , T_6 could only lead to a saving of electricity by about 1%. This is because the gain in electricity saving from the chiller plant was mostly offset by the increase in the electricity consumption of the pumping stations.

7.5 Summary

Eight different temperature regimes, i.e. T_1 to T_8 , were identified for comparing the energy performance of different components in DCS_0 , where the design chilled water supply and return temperatures were 5°C and 12°C respectively. It was found that in temperature regime T_6 , in which the design chilled water supply and return temperatures were 6°C and 11°C respectively, the annual total electricity consumption of DCS_0 was the lowest.

Results further revealed that the chiller plant and pumping stations in T_6 exhibited different electricity consumption patterns. The energy performance of the chiller plant in T_6 was the best, leading to a saving of 4.6% in electricity when compared with other temperature regimes. It is because the design chilled water supply temperature is on the high side at 6°C . The COP was thus relatively higher as compared to other temperature regimes with a design supply temperature of 4°C or 5°C .

On the other hand, it was found that the secondary distribution pumps in T_6 had the highest electricity consumption, as it was 22.5% higher with reference to the base design T_0 . The reason is that when the design temperature difference was at the lowest level, i.e. 5°C , this could lead to a higher annual average chilled water flow rate, and hence a higher design pump power and electricity consumption of the pumps.

Under such circumstances, the electricity saving of the chiller plant was nearly offset by the increase in the electricity consumption of the secondary pumps. The overall electricity consumption of DCS_O could only be reduced by about 1% in comparison with the base design T_O.

In view of this, it was desirable to perform a comprehensive analysis of all the three energy efficiency measures as mentioned in [Chapters 5, 6 and 7](#), so as to identify an integrated design solution for DCS_O that could achieve an optimum energy performance and the lowest life cycle cost.

Chapter 8

A Techno-Economic Analysis of the Integrated Design Solutions

8.1 Overview

Three energy efficiency enhancement measures were proposed in the preceding chapters for mitigating the impacts of the degrading temperature difference on the energy performance of DCS_O. These measures include optimization of: (a) the chiller system configuration; (b) the pumping station configuration; and (c) the chilled water temperature.

By combining these three measures, a total of 1,447,680 combinations (options) of design solutions could be generated. The present study focused on examining the energy performance, financial viability and environmental benefit of these design solutions. In view of the enormous number of combinations to be evaluated, a complete simulation of all these options would take a prohibitively large amount of time and effort. In this regard, a simple heuristic approach was developed to identify only those that possibly are the optimal for analysis.

After identifying these possible solutions, the next step was to predict their electricity consumptions by simulation for an evaluation of their energy performance. The results

were then used for a comparison with the base design of DCS_0 . Regarding financial viability, a life cycle cost (LCC) analysis of each possible solution was conducted to find out the most cost-effective combination of chiller system configuration, pumping station configuration and temperature regime. The environmental benefit, in respect of reducing greenhouse gas emissions, by adopting the optimal design solution was also estimated.

8.2 Simple Heuristic Strategy for Determining Possible Design Solutions

Based on the study results summarized in the preceding chapters, five combinations of chiller system configurations, 36,192 arrangements of pumping station, and eight temperature regimes were identified. The total number of combinations of these system design options ($= 5 \times 36,192 \times 8$) equals 1,447,680. In view of this huge number of options, a simple heuristic strategy was adopted to reduce the number for a detailed analysis.

In this heuristic approach, only those combinations or arrangements that could lead to the greatest reduction in the electricity consumption of DCS_0 were selected. These “selected combinations or arrangements” were then combined to form a group of “possible solutions”, which were then evaluated in terms of their energy performance, financial viability and environmental benefits. The ultimate outcome would be an “optimum design solution”, as illustrated in [Figure 8.1](#).

8.2.1 Selection of Combinations of Chiller System Configuration

The different combinations of chiller system configuration and the amount of annual total electricity saving with reference to the base design C_0 are shown in [Table 8.1](#). The results indicate that among the five combinations, C_A , C_D and C_E could lead to a 10%, 11% and 11.6% reduction in electricity consumption, respectively, which were significantly higher than those of C_B and C_C . Therefore, C_B and C_C were not further considered in the next stage of analysis.

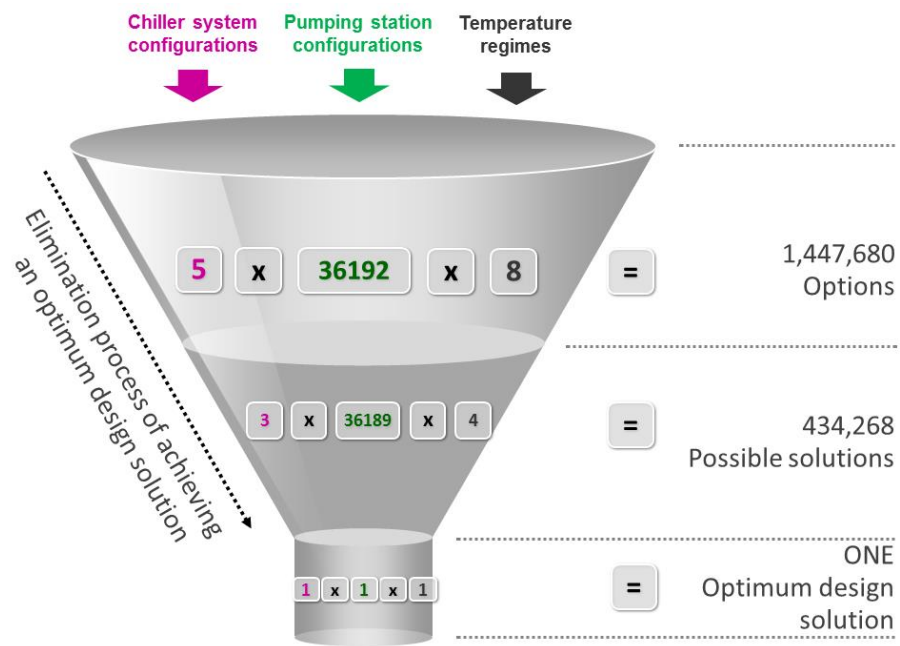


Figure 8.1 Elimination process of achieving an optimum design solution

Table 8.1 Percentage of annual electricity saving with different chiller system configurations

Chiller system configuration	No. of chiller	Size	Type	Annual electricity consumption of DCS _O	
				kWh	Difference w.r.t. C _O , %
C _O	10	Equal	Constant speed	116,904,999	
C _A	10	Equal	Variable speed	105,294,444	-9.9
C _B	15	Equal	Constant speed	115,005,198	-1.6
C _C	15	Unequal	Constant speed	113,484,601	-2.9
C _D	15	Equal	Variable speed	104,105,583	-10.9
C _E	15	Unequal	Variable speed	103,295,586	-11.6

8.2.2 Selection of Pumping Station Arrangement

For the 36,192 pumping station arrangements, their annual total electricity consumptions were compared with those of the base case PS₁₋₀ (Table 2.7 in Chapter 2). Table 8.2 shows the average percentage of the difference of the annual total electricity consumption. Only three arrangements where a single pumping station was used were

unable to reduce the electricity consumption of DCS_0 . As a result, a total of 36,189 arrangements were retained for analysis at the next stage.

Table 8.2 Percentage of annual total electricity saving with different pumping station arrangements

No. of pumping station	Total no. of arrangement	% of total no. of arrangement	Average % of difference w.r.t. base PS_{1-0}
1	3	0.01	+0.12
2	63	0.17	-0.85
3	567	1.57	-1.44
4	2,997	8.28	-1.78
5	10,692	29.54	-2.04
6	21,870	60.43	-2.22
	36,192	100	

8.2.3 Selection of Chilled Water Temperature Regime

Regarding chilled water temperature, only four temperature regimes, i.e. T_4 , T_5 , T_6 and T_7 , could lead to a reduction in the annual total electricity consumption of DCS_0 (see Table 8.3). Hence, these four temperature regimes were further analyzed in conjunction with the other selected options.

Table 8.3 Percentage of annual electricity saving in different temperature regimes

Temp regime	Chilled water temp, °C			Annual electricity consumption of DCS_0	
	Supply	Return	Delta-T	kWh	Difference w.r.t. T_0 , %
T_0	5	12	7	116,904,999	
T_1	4	11	7	118,128,214	+1.05
T_2	4	12	8	118,224,427	+1.13
T_3	4	13	9	118,824,297	+1.64
T_4	5	11	6	116,843,545	-0.05
T_5	5	13	8	116,856,655	-0.04
T_6	6	11	5	115,811,127	-0.94
T_7	6	12	6	116,840,923	-0.05
T_8	6	13	7	117,173,722	+0.23

After the elimination process, the number of possible solutions was substantially reduced by 70% from 1,447,680 (= 5 x 36,192 x 8) to 434,268 (= 3 x 36,189 x 4).

These 434,268 possible solutions can be expressed by the matrix $\mathbf{S}(C_i, T_j, \text{PS}_{n_{ps}-x})$ to represent a mixture of the three energy efficiency enhancement measures, where C_i represents one of the three selected combinations of chiller system configuration, T_j one of the four selected temperature regimes, and $\text{PS}_{n_{ps}-x}$ one of the 36,189 pumping station arrangements, where n_{ps} is the number of pumping station (i.e. 1 to 6) and x the number of arrangement from 1 to 36,189.

The following are the matrices of the 434,268 possible design solutions.

$\mathbf{S}(C_A, T_4, \text{PS}_{1-1}), \mathbf{S}(C_A, T_4, \text{PS}_{1-2}), \mathbf{S}(C_A, T_4, \text{PS}_{2-3}), \dots, \mathbf{S}(C_A, T_4, \text{PS}_{6-36189})$
 $\mathbf{S}(C_A, T_5, \text{PS}_{1-1}), \mathbf{S}(C_A, T_5, \text{PS}_{1-2}), \mathbf{S}(C_A, T_5, \text{PS}_{2-3}), \dots, \mathbf{S}(C_A, T_5, \text{PS}_{6-36189})$
 $\mathbf{S}(C_A, T_6, \text{PS}_{1-1}), \mathbf{S}(C_A, T_6, \text{PS}_{1-2}), \mathbf{S}(C_A, T_6, \text{PS}_{2-3}), \dots, \mathbf{S}(C_A, T_6, \text{PS}_{6-36189})$
 $\mathbf{S}(C_A, T_7, \text{PS}_{1-1}), \mathbf{S}(C_A, T_7, \text{PS}_{1-2}), \mathbf{S}(C_A, T_7, \text{PS}_{2-3}), \dots, \mathbf{S}(C_A, T_7, \text{PS}_{6-36189})$

$\mathbf{S}(C_D, T_4, \text{PS}_{1-1}), \mathbf{S}(C_D, T_4, \text{PS}_{1-2}), \mathbf{S}(C_D, T_4, \text{PS}_{2-3}), \dots, \mathbf{S}(C_D, T_4, \text{PS}_{6-36189})$
 $\mathbf{S}(C_D, T_5, \text{PS}_{1-1}), \mathbf{S}(C_D, T_5, \text{PS}_{1-2}), \mathbf{S}(C_D, T_5, \text{PS}_{2-3}), \dots, \mathbf{S}(C_D, T_5, \text{PS}_{6-36189})$
 $\mathbf{S}(C_D, T_6, \text{PS}_{1-1}), \mathbf{S}(C_D, T_6, \text{PS}_{1-2}), \mathbf{S}(C_D, T_6, \text{PS}_{2-3}), \dots, \mathbf{S}(C_D, T_6, \text{PS}_{6-36189})$
 $\mathbf{S}(C_D, T_7, \text{PS}_{1-1}), \mathbf{S}(C_D, T_7, \text{PS}_{1-2}), \mathbf{S}(C_D, T_7, \text{PS}_{2-3}), \dots, \mathbf{S}(C_D, T_7, \text{PS}_{6-36189})$

$\mathbf{S}(C_E, T_4, \text{PS}_{1-1}), \mathbf{S}(C_E, T_4, \text{PS}_{1-2}), \mathbf{S}(C_E, T_4, \text{PS}_{1-3}), \dots, \mathbf{S}(C_E, T_4, \text{PS}_{6-36189})$
 $\mathbf{S}(C_E, T_5, \text{PS}_{1-1}), \mathbf{S}(C_E, T_5, \text{PS}_{1-2}), \mathbf{S}(C_E, T_5, \text{PS}_{1-3}), \dots, \mathbf{S}(C_E, T_5, \text{PS}_{6-36189})$
 $\mathbf{S}(C_E, T_6, \text{PS}_{1-1}), \mathbf{S}(C_E, T_6, \text{PS}_{1-2}), \mathbf{S}(C_E, T_6, \text{PS}_{1-3}), \dots, \mathbf{S}(C_E, T_6, \text{PS}_{6-36189})$
 $\mathbf{S}(C_E, T_7, \text{PS}_{1-1}), \mathbf{S}(C_E, T_7, \text{PS}_{1-2}), \mathbf{S}(C_E, T_7, \text{PS}_{1-3}), \dots, \mathbf{S}(C_E, T_7, \text{PS}_{6-36189})$

8.3 Simulation of Energy, Financial and Environmental Performances

To evaluate the performance of these 434,268 possible solutions in the captioned three aspects, the first step was to simulate their electricity consumption patterns. Then it was necessary to collect their capital and operation cost data for calculating their LCC. This allowed a cost-optimal solution that could lead to the lowest LCC to be identified.

Based on the simulated electricity consumption figures, environmental benefits of the most cost-effective solution, in terms of reduction of CO₂ emissions, could be determined.

8.3.1 Simulation of Electricity Consumption and CO₂ Emissions

Figure 8.2 shows the algorithm used to predict the electricity consumption of the possible solutions. Before conducting the simulation, the first step was to define the temperature regime, T_j , as this would affect both the energy performance of the chiller system and pumps in a specific pumping station configuration. Then, the electricity consumption of chiller system configurations C_A , C_D and C_E , and the 36,189 pumping station arrangements under temperature regimes T_4 , T_5 , T_6 and T_7 were simulated according to the chiller plant model and pumping station model developed in Chapters 3 and 6 respectively.

The electricity consumption of any possible solution equals the summation of the electricity consumption of the chiller plant and pumping station under the same temperature regime.

In order to perform the simulation in a more efficient manner, a program written in VBA was established to integrate the mathematical models of the chiller plant and pumping station and calculate the annual total electricity consumption of all possible solutions.

Regarding CO₂ emissions, it could be estimated from the energy consumption of each possible solution, based on the CO₂ emissions factor of 197 tonnes of CO₂ (equivalent) emissions per TJ of electricity demand (Yik et al., 2012).

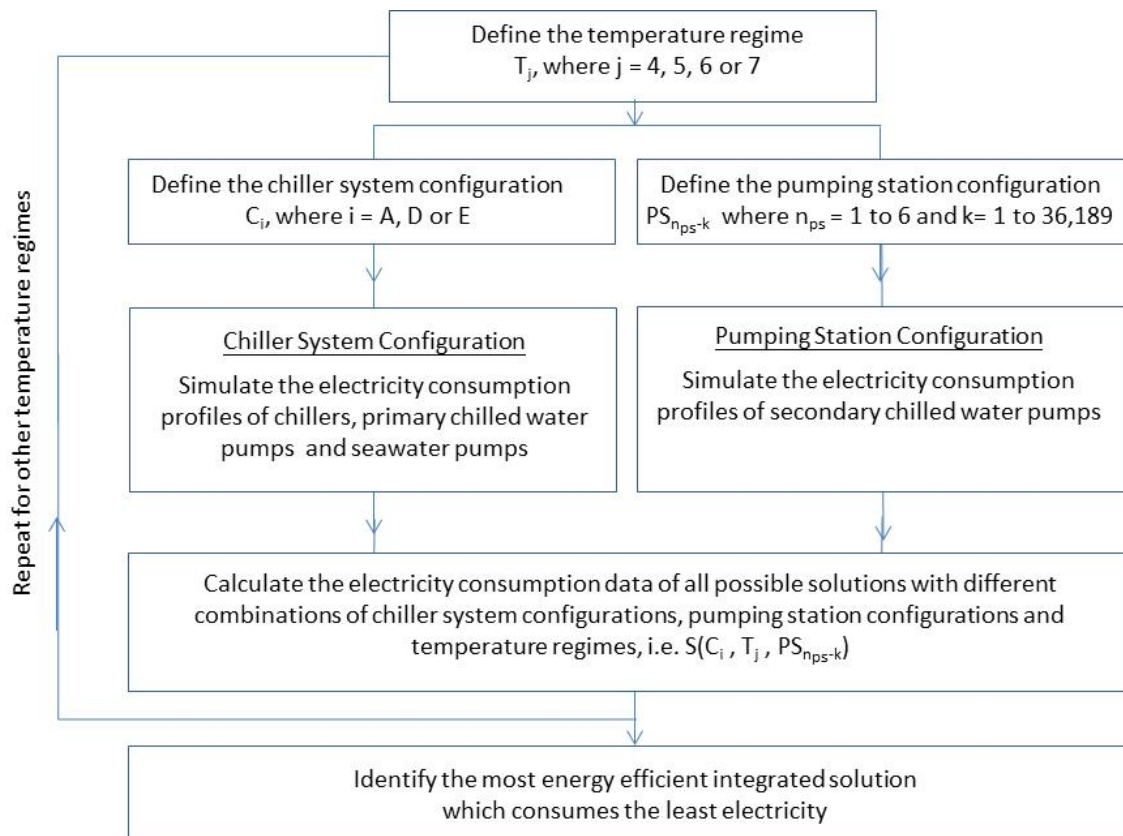


Figure 8.2 Algorithm of identifying an energy-optimal design solution with the lowest electricity consumption

8.3.2 The LCC Model

The life cycle cost analysis deployed in this thesis is built upon the LCC approach developed by Fuller and Petersen (1996), where is structured approach to address all the different costs of a project over a given study period with all the potential cost adjusted to reflect the time-value of money. An LCC analysis was performed to examine all the different costs of a DCS over a given study period. All potential costs were adjusted to reflect the time-value of money. After discounting or reducing all costs to current values or converting them into an annual cost, the LCC model was used to determine a cost-optimal design solution out of a set of possible design solutions as mentioned in Section 8.2. Within the range of possible design solutions, solutions with a lower LCC would be more financially favourable than those with a higher LCC. This information can provide a good reference for the DCS designers or owners in deciding whether or not to adopt a particular solution from a financial viability point of view.

8.3.2.1 LCC Analysis Estimation

In this study, the useful life span of a DCS was set to be 60 years. The life spans of chillers, chilled water and seawater pumps would be much shorter. The assumed life spans of all equipment and the number of times that they would require to be replaced within the life span of the DCS are summarized in [Table 8.4](#).

Table 8.4 Life span and number of replacement of equipment

	Life span, year	No. of replacement
Direct seawater-cooled chiller (constant/variable speed)	30	2
Primary chilled water pump (constant speed)	20	3
Secondary chilled water pump (variable speed)	20	3
Seawater pump (constant speed)	15	4

The reasons for adopting 60 years as the analysis period are as follows.

- i. The typical design service life for long life buildings, including offices and commercial buildings, is 50 to 99 years ([Hovde and Moser, 2004](#)). The 60-year life span of a DCS is within this range.
- ii. The various types of equipment, as listed in [Table 8.4](#), had different life spans, and their replacement would take place at different points in time within the life span of the DCS, whilst 60 years is the least common multiple of the life span of the equipment involved.

As a result, taking 60 years as the lifespan of a DCS could provide an equal basis for a fair comparison among the equipment. Otherwise, the LCC estimation could be unduly increased because the pumps would remain usable by the end of the life span covered by the analysis. In this case, such equipment would be regarded as being disposed of before they could be due for replacement.

The LCC of the DCS in this study was calculated based on the following assumptions.

-
- i. All the equipment is a new establishment.
 - ii. All monetary values are in constant Hong Kong dollars (i.e. already adjusted with inflation factor).
 - iii. The price of electricity is \$1/kWh, which was assumed to rise steadily at a real escalation rate of 2% per annum, and the real discount was taken to be 5% per annum (Yik et al., 2012).
 - iv. A DCS operator has to pay the annual licensing fee for laying chilled water distribution pipes on government land. According to a consultancy study conducted in 1999, the unit rate has been HK\$13 per 10 mm diameter per meter run (EMSD, 1999). It was anticipated that the government would adjust the unit rate periodically, but not frequently. For simplicity of estimation, the unit rate was assumed to increase with the inflation rate. As shown in Figure 8.3, the unit rate in 2013 was HK\$14.85 per 10 mm diameter per meter run.
 - v. The replacement cost of the equipment listed in Table 8.4 is the same as the initial cost in constant dollars. The life span of such equipment (Wong and Tang, 2010; Yik et al., 2012), as shown in Table 8.4, can be used to determine the present value of replacement cost.
 - vi. The annual maintenance cost is 1.5% of the initial capital cost (Anagnostopoulos and Papantonis, 2007).

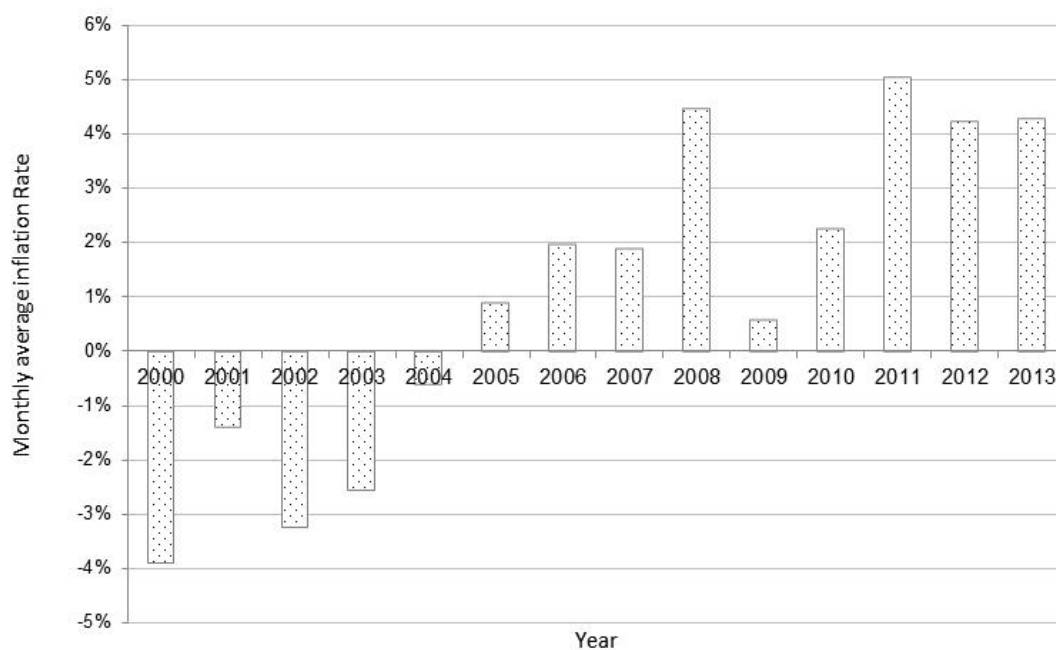


Figure 8.3 Monthly average inflation rate, 2000-2013
(Source: Trading Economics, 2013)

- vii. The land cost that the Hong Kong government calculated for the DCS plant or pump house at the Kai Tak Development was based on the accommodation value, which is defined as the land value per the gross floor area to be built on site for the plant or pump house, including the basement. The accommodation value for that DCS has been taken at HK\$1,500 per m² (EMSD, 2003c). This value is far below the market accommodation value because the land was restricted to be a government, institution or community site for new development. As no empirical data or formula was available for estimating or predicting this strategic land cost of DCS₀, the accommodation value used for the Kai Tak Development was adopted for the present study.

8.3.2.2 Capital Cost

Capital costs refer to the costs of the major equipment in this study. This major equipment included the constant and variable speed direct seawater-cooled chillers, primary constant speed chilled water and seawater pumps, and secondary variable speed chilled water distribution pumps. Their cost data was obtained from the local market.

i. Chillers

[Table 8.5](#) is a summary of the unit costs of the supply and installation of constant and variable speed chillers with different cooling capacities and associated accessories. Moreover, the land cost of installing the chiller in the chiller plant room is taken into account. Based on the accommodation value assumed in [Section 8.3.2.1](#), gross floor area (GFA) required for installing the chiller was estimated and the land cost per the cooling capacity of chiller was calculated, as shown in [Table 8.5](#).

Table 8.5 Different costs of the constant speed and variable speed chillers

	Constant speed chiller			Variable speed chiller		
	2,000 / 7,034	4,000 / 14,068	6,000 / 21,102	2,000 / 7,034	4,000 / 14,068	6,000 / 21,102
Cooling capacity, RT/kW						
Chiller and accessories cost, HK\$/RT	3,000	3,500	4,000	3,900	4,550	5,200
Installation cost, HK\$/RT	3,900	4,550	5,200	5,070	5,915	6,760
Land cost, HK\$/RT	12	9	8	12	9	8
Total unit cost, HK\$/RT	6,912	8,059	9,208	8,982	10,474	11,968

ii. Secondary variable speed chilled water distribution pumps

The capital cost of a chilled water distribution pump set consists of the cost of variable speed pumps, variable speed drives, motors, pipework, land and fittings and installation.

As presented in [Chapter 6](#), thousands of pumps could be involved in the simulation process and this would require a prohibitively large amount of time and effort to obtain the cost data of each pump. In this regard, the capital cost data of 16 chilled water distribution pump sets with different capacities was obtained from the manufacturers (see [Table 8.6](#)).

Table 8.6 Capital costs of variable speed chilled water pumps with different operational characteristics

	Flow rate, m ³ /s	Pressure head, bar	Rated Power, kW	Cost, HK\$					
				Pump and motor	Variable speed drive	Pipework	Land cost	Total cost	Unit cost per kW
1	0.36	0.70	36	450,000	12,750	18,860	9,186	490,796	13,752
2	0.29	1.03	41	480,000	17,400	16,000	9,891	523,291	12,627
3	0.27	1.21	46	480,000	17,400	16,000	9,891	523,291	11,485
4	0.58	0.55	54	500,000	22,680	28,000	13,154	563,834	10,438
5	0.40	1.21	68	550,000	22,680	22,000	13,721	608,401	8,937
6	0.36	2.25	116	650,000	26,600	18,860	14,765	710,225	6,142
7	0.80	1.21	138	700,000	42,100	36,000	18,118	796,218	5,760
8	0.54	2.25	173	780,000	48,100	24,460	16,173	868,733	5,028
9	1.09	1.70	261	1,000,000	66,970	60,000	19,737	1,146,707	4,398
10	0.46	4.42	291	1,250,000	88,200	22,000	16,173	1,376,373	4,735
11	0.46	6.10	410	1,600,000	95,900	22,000	18,450	1,736,350	4,231
12	1.09	2.73	420	1,800,000	150,000	60,000	19,737	2,029,737	4,832
13	0.69	4.42	431	1,600,000	155,760	32,340	20,032	1,808,132	4,200
14	0.69	6.10	589	1,900,000	212,800	32,340	19,500	2,164,640	3,675
15	1.38	4.42	862	2,500,000	320,000	100,000	20,158	2,940,158	3,410
16	1.38	6.10	1185	3,500,000	450,000	100,000	20,158	4,070,158	3,435

Figure 8.4 shows the relationship of their total capital costs over their pump power. A trend line was plotted. The unit cost is relatively high for a small scale pump set. It decreases to a minimum value with the increase in pump power, upholding the principle of economies of scale. The pump cost can be described by Equation 8.1.

$$Cost_{cwp, var} = 51,123 \times W_{cwp, var}^{-0.411} \quad (8.1)$$

where

$Cost_{cwp, var}$ = Unit cost of a variable speed chilled water pump (HK\$ per kW)

$W_{cwp, var}$ = Pump power of a variable speed chilled water pump (kW)

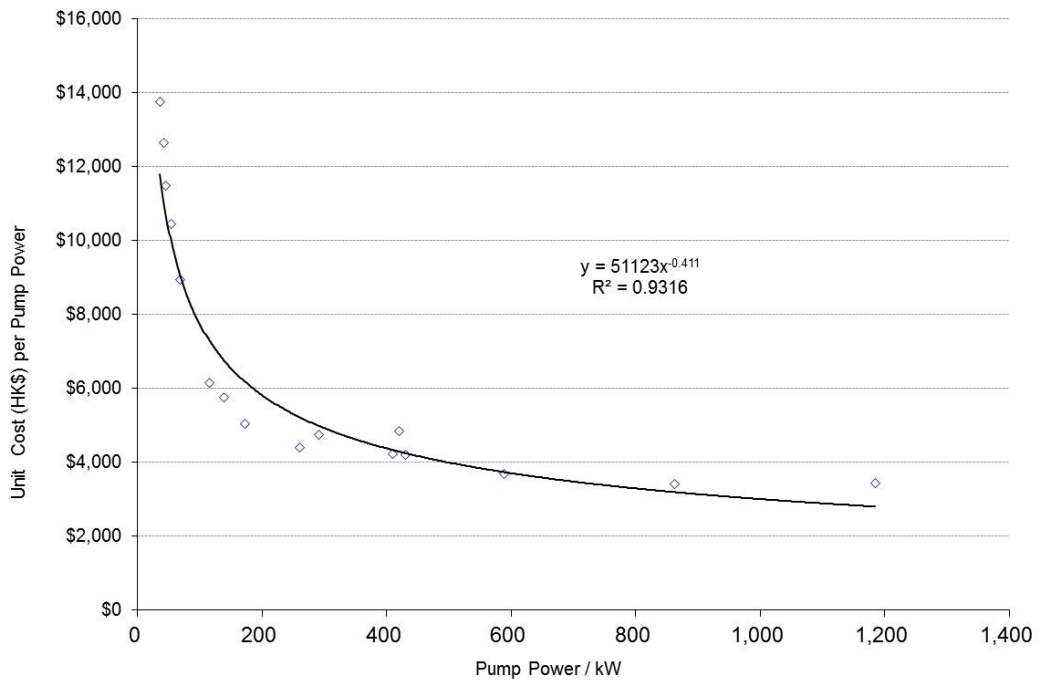


Figure 8.4 Unit cost of the variable speed pump set per pump power

iii. Primary constant speed chilled water and seawater pumps

The above methodology used for estimating the costs of the variable speed chilled water pump was applied for developing the cost models for the constant speed primary chilled water pumps and seawater pumps. Based on the cost data provided by the manufacturers and contractors, Equations 8.2 and 8.3 can be used for determining the costs of a constant speed chilled water pump set and a seawater pump set respectively.

$$Cost_{cwp, const} = 39,775 \times W_{cwp, const}^{-0.407} \quad (8.2)$$

$$Cost_{swp, const} = 59,138 \times W_{swp, const}^{-0.413} \quad (8.3)$$

where

$Cost_{cwp, const}$ = Unit cost of a constant speed chilled water pump, HK\$ per kW

$W_{cwp, const}$ = Pump power of a constant speed chilled water pump, kW

$Cost_{swp, const}$ = Unit cost of a constant speed seawater water pump, HK\$ per kW

$W_{swp, const}$ = Pump power of a constant speed seawater water pump, kW

8.3.2.3 Operating Expenses

Operating expenses include the replacement cost, the annual electricity cost, the annual license fee for laying chilled water distribution pipes on government land, and the annual maintenance cost.

i. Electricity Cost

The life-cycle electricity cost, $LCC(E)$, in present value is determined on the basis of the recurrent annual electricity cost, $C(E)$, using [Equation 8.4](#).

$$LCC(E) = C(E) \cdot USPWF_E \quad (8.4)$$

where

$$USPWF_E = \frac{(1+e)}{(d-e)} \left[1 - \left(\frac{1+e}{1+d} \right)^{LS_{DCS}} \right]$$

d = real discount rate, % per annum

e = real escalation rate of electricity price, % per annum

LS_{DCS} = useful life span of a DCS, in years

Remark: USPWF - Uniform series present worth factor

ii. License Fee

The life-cycle license cost, $LCC(L)$, in present value is determined on the basis of the recurrent annual license cost, $C(L)$, for laying the pipework, using [Equation 8.5](#).

$$LCC(L) = C(L) \cdot USPWF_L \quad (8.5)$$

where

$$USPWF_L = \frac{(1+d)^{LS_{DCS}} - 1}{d(1+d)^{LS_{DCS}}}$$

iii. Maintenance Cost

The maintenance cost covered the costs of regular check-up and system overhaul. The life-cycle maintenance cost, $LCC(M)$, in present value is derived from the recurrent annual maintenance cost, $C(M)$, using Equation 8.6.

$$LCC(M) = C(M) \cdot USPWF_M \quad (8.6)$$

where

$$USPWF_M = \frac{(1+d)^{LS_{DCS}} - 1}{d(1+d)^{LS_{DCS}}}$$

iv. Replacement Cost

The life cycle cost of replacement is the present value of the total replacement cost of equipment, $PV(Cost_{TR})$, throughout its life span in the DCS (Table 8.5). It can be determined by Equation 8.7.

$$PV(Cost_{TR}) = \sum_{i=1}^{N_R} \frac{Cost_R}{(1+d)^{i \cdot LS_e}} \quad (8.7)$$

where

$$\begin{aligned} N_R &= \text{number of times of replacement} \\ Cost_R &= \text{replacement cost of equipment} \\ LS_e &= \text{useful life of equipment, in years} \end{aligned}$$

8.3.2.4 Overall LCC

After each cost component was derived, the present values of electricity, license, maintenance, replacement and capital costs over the 60-year period were summed up to determine the total LCC of all the possible solutions by Equation 8.8.

$$LCC = Capital \text{ Cost} + LCC(E) + LCC(L) + LCC(M) + PV(Cost_{TR}) \quad (8.8)$$

8.4 An LCC Analysis of All Possible Solutions

8.4.1 Comparison of the LCC of all possible design solutions with DCS_0

In order to evaluate the cost-effectiveness of various possible solutions, it was necessary to predict the capital cost for investment and the total operating cost the solutions could save. This information was important because operating costs are typically greater than capital costs (Yates, 2011).

Tables 8.7, 8.8 and 8.9 show a comparison of the average LCC saving of all the 434,268 possible design solutions identified in Section 8.2 with reference to the LCC of the base case DCS_0 using the three energy efficiency enhancement measures selected in Section 8.2.

Among the three selected chiller system configuration options such as C_A , C_D and C_E , the average LCC saving of the solutions designed with C_D was the highest, i.e. 5.71%. The configuration of C_D consisted of 15 equally-sized variable speed chillers.

Regarding the use of two to six pumping station options as shown in Table 8.8, the solutions designed with six pumping stations as in P_6 had achieved the highest average LCC saving, i.e. 4.17%, in comparison with other options.

On the other hand, under temperature regime T_5 where the chilled water supply and return temperatures were at 5°C and 13°C respectively (Table 8.9), the highest average LCC saving of 4.92% was achieved.

Table 8.7 Percentage of average LCC saving of the solutions designed with chiller system configurations C_A , C_D and C_E with reference to DCS_0

Chiller system configuration	No. of design solution	Total % of LCC saving, HK\$	Average LCC saving w.r.t. to base DCS_0 , %
C_A	144,756	233,106	1.61
C_D	144,756	825,967	5.71
C_E	144,756	729,502	5.04

Table 8.8 Percentage of average LCC saving of the solutions designed with different number of pumping stations with reference to DCS_0

No. of pumping station	No. of design solution	Total % of LCC saving, HK\$	Average LCC saving w.r.t. to base DCS_0 , %
2 PS	756	2,600	3.44
3 PS	6,804	25,834	3.80
4 PS	35,964	142,475	3.96
5 PS	128,304	523,683	4.08
6 PS	262,440	1,093,883	4.17

Table 8.9 Percentage of average LCC saving of the solutions designed with temperature regimes T_4 , T_5 , T_6 and T_7 with reference to DCS_0

Temperature regime	No. of design solution	Total % of LCC saving, HK\$	Average LCC saving w.r.t. to base DCS_0 , %
T_4	108,567	355,969	3.28
T_5	108,567	534,435	4.92
T_6	108,567	406,516	3.74
T_7	108,567	491,556	4.53

8.4.2 A Cost-Optimal Design Solution

The LCC savings of the 434,268 design solutions as a result of adopting different combinations of the three energy efficiency measures were summarized in [Table 8.10](#). The solutions were ranked according to the percentage of LCC saving they could achieve in comparison with the base DCS_0 .

Table 8.10 Ranking of the 434,268 design solutions based on the LCC saving achieved in comparison with DCS₀

Ranking (from highest LCC saving achieved w.r.t to base DCS ₀)	No. of solution	Chiller system configuration (% in the ranking group)	Temperature regime (% in the ranking group)	No. of pumping station (PS) (% in the ranking group)	LCC saving (=S), %
1 (Solution C)	1	C _D (100%)	T ₅ (100%)	6 PS (100%)	S = 7.50
2 to 6	5	C _D (100%)	T ₅ (100%)	6 PS (100%)	7.46 ≤ S < 7.5
7 to 578	572	C _D (100%)	T ₅ (100%)	6 PS (68%) 5 PS (28%) 4 PS (4%)	7.21 ≤ S < 7.46
579 to 10,337	9,759	C _D (100%)	T ₅ (91%) T ₇ (9%)	6 PS (68%) 5 PS (26%) 4 PS (6%)	6.82 ≤ S < 7.21
10,338 to 289,168	278,831	C _D (48%) C _E (52%)	T ₄ (26%) T ₅ (22%) T ₆ (26%) T ₇ (26%)	6 PS (60%) 5 PS (30%) 4 PS (8%) 3 PS (2%)	3.15 ≤ S < 6.82
289,169 to 433,615	144,447	C _A (100%)	T ₄ (25%) T ₅ (25%) T ₆ (25%) T ₇ (25%)	6 PS (60%) 5 PS (30%) 4 PS (8%) 3 PS (2%)	0 < S < 3.15
433,616 to 434,268	653	C _A (100%)	T ₄ (86%) T ₆ (14%)	6 PS (42%) 5 PS (22%) 4 PS (22%) 3 PS (10%) 2 PS (4%)	-1 < S < 0

After comparing the LCC of all the 434,268 possible solutions with that of DCS₀, it was found that matrix S(C_D,T₅,PS₆₋₃₄₇₃₅) (henceforth referred to as “Solution C”) had the lowest LCC, i.e. HK\$4,108,032,442, which was about 7.5% lower than that of DCS₀. This cost-optimal design consisted of 15 x 4,000 RT (14,068 kW) variable speed chillers and six pumping stations with five pumps in each station. The design chilled water supply and return temperatures were 5°C and 13°C respectively. It was found that the system features of Solution C, i.e. the chiller system configuration, the number of pumping station and the temperature regime, were identical with the designs of the three solutions with the highest average LCC saving, as identified in [Section 8.4.1](#) where the comparison was based on each individual measure. [Table 8.11](#) provides a comparison of the system details of DCS₀ and Solution C.

Table 8.11 Comparison of the system details of DCS_O and Solution C

	DCS _O	Solution C
1. Chiller system configuration	C _O	C _D
Total no.	10	15
Nominal cooling capacity per chiller, RT/kW	6,000 / 21,102	4,000 / 14,068
Constant/variable speed	Constant	Variable
2. Pumping station configuration	PS ₁₋₀	PS ₆₋₃₄₇₃₅
No. of pumping station	1	6
No. of pump in each station	10	5
Location of pumping station	1 on supply side	5 on supply side 1 on return side
3. Temperature regime	T _O	T ₅
Chilled water supply temp, °C	5	5
Chilled water return temp, °C	12	13
Delta-T, °C	7	8

The LCC saving of five solutions (i.e. the 2nd to the 6th) was in the range of 7.46% to 7.5%, which was close to the LCC saving of Solution C. The matrices of these solutions were more or less the same as Solution C's except that the six pumping stations were arranged in different locations.

The third group was the 572 solutions (ranked 7th to 578th) that had an LCC saving between 7.21% and 7.46%. These solutions also adopted C_D and T₅ as the chiller system configuration and temperature regime respectively. However, their number of pumping station was not identical, as 68% of them were of a six-pumping station design while the remaining were designed with four or five pumping stations.

The fourth group consisted of 9,759 solutions that were also designed with chiller system configuration C_D. Concerning temperature regime and number of pumping station, the use of T₅ and six pumping stations was still a dominant feature.

As a result, it can be concluded that chiller system configuration C_D, temperature regime T₅ and the use of six pumping stations are the most critical factors for achieving a low LCC.

Despite of its lowest LCC, however, the total annual electricity consumption of Solution C was not the lowest. The most energy-optimal design solution that could lead to the lowest electricity consumption (henceforth referred to as “Solution E”) was matrix $S(C_E, T_7, PS_{6-35464})$. It consisted of 15 unequally-sized (i.e. 5 x 2,000 RT (7,034 kW), 5 x 4,000 RT (14,068 kW) and 5 x 6,000 RT (21,102 kW)) variable speed chillers and six pumping stations with five pumps in each station. The design chilled water supply and return temperatures were 6°C and 12°C, respectively. The annual electricity consumption of using the base design DCS_O was 116,904,999 kWh. After the adoption of Solution E, however, the annual electricity consumption was reduced by 15.3% to 99,035,646 kWh.

Compared to Solution E, the electricity consumption of Solution C was slightly higher, i.e. ~1%, as shown in [Table 8.12](#). This difference, however, is insignificant because it was mainly due to the relative high electricity consumption of chillers, which could not be compensated by the electricity saving of the secondary chilled water pumps.

Table 8.12 Comparison of the annual electricity consumption of Solutions C and E

	Annual electricity consumption, kWh		Difference [Solution C minus Solution E]	
	Solution C	Solution E	kWh	%
(a) Chiller plant				
i. Chiller	76,555,222	71,966,990	+4,588,233	+6.4
ii. Pri. ch. w. pumps	4,958,662	6,071,321	-1,112,659	-18.3
iii. Seawater pump	7,675,345	7,058,226	+617,119	+8.7
Total [i + ii + iii]	89,189,230	85,096,537	+4,092,692	+4.8
(b) Sec. ch. w. pumps				
	10,696,493	13,939,109	-3,242,616	-23.3
Total [(a) + (b)]	99,885,723	99,035,646	850,076	+0.9

[Table 8.13](#) is a summary of the LCC of capital investment, license, replacement, maintenance, and energy of both Solutions C and E. The result indicates that the LCC of Solution C was lower than that of Solution E and is hence more financially viable.

Table 8.13 Comparison of the LCC of Solutions C and E

	Solution C	Solution E
(a) Total initial capital investment, HK\$	676,894,270	713,379,294
(b) Life-cycle replacement cost, HK\$	357,645,409	376,439,378
(c) Life-cycle maintenance cost, HK\$	192,196,914	202,556,448
(d) Life-cycle license cost, HK\$	117,124,979	117,124,979
(e) Life-cycle energy cost, HK\$	2,764,170,870	2,738,956,176
Total LCC, HK\$	4,108,032,442	4,148,456,275

8.4.3 A Comparative Analysis of the LCC of DCS₀ and Solution C

A detailed comparison of the different costs and overall LCC of DCS₀ and Solution C is given in Table 8.14. It can be seen that the present value LCC of Solution C was HK\$332 million less than that of DCS₀, representing a saving of 7.5%.

For Solution C, the adoption of energy efficiency enhancement measures such as using variable speed chillers, and operating more chillers and pumps to achieve a higher energy performance could lead to a 13.2% increase in its LCC of capital investment. More specifically, the use of variable speed chillers accounted for the largest portion, i.e. ~96%, of the additional capital cost.

On the contrary, regarding pumping stations, the use of six pumping stations and less secondary pumps in each station could save 2.3% of the capital cost as compared to the use of a single pumping station and more pumps in each station in DCS₀. In the estimation, account had also been taken into about the associated higher maintenance and replacement costs, which were incurred by the greater amount of equipment to be maintained and replaced. The total LCC of Solution C in terms of the costs of capital investment, maintenance and replacement was 13.2% higher than that of DCS₀.

Table 8.14 Comparison of the LCC of DCS₀ and Solution C

	LCC, HK\$		Difference in LCC [Solution C minus DCS ₀]	
	DCS ₀	Solution C	HK\$	%
(a) Total initial capital investment				
i. Chiller	552,480,000	628,440,000	+75,960,000	+13.7
ii. Pri. ch. w. pumps	8,726,948	9,533,092	+806,144	+9.2
iii. Seawater pump	15,050,744	17,809,998	+2,759,254	+18.3
iv. Sec. ch. w. pumps	21,605,376	21,111,180	-494,196	-2.3
Sub-total	597,863,068	676,894,270	+79,031,202	+13.2
(b) Life-cycle replacement cost				
i. Chiller	286,701,300	326,119,615	+39,418,315	+13.7
ii. Pri. ch. w. pumps	4,528,720	4,947,057	+418,336	+9.2
iii. Seawater pump	13,202,913	15,623,404	+2,420,491	+18.3
iv. Sec. ch. w. pumps	11,211,789	10,955,334	-256,456	-2.3
Sub-total	315,644,723	357,645,409	+42,000,687	+13.3
(c) Life-cycle maintenance cost				
i. Chiller	156,870,808	178,438,841	+21,568,032	+13.7
ii. Pri. ch. w. pumps	2,477,924	2,706,820	+228,896	+9.2
iii. Seawater pump	4,273,498	5,056,959	+783,461	+18.3
iv. Sec. ch. w. pumps	6,134,616	5,994,295	-140,322	-2.3
Sub-total	169,756,847	192,196,914	+22,440,067	+13.2
(d) Life-cycle license cost	117,124,979	117,124,979	0	0
(e) Life-cycle energy cost				
i. Chiller	2,489,642,370	2,145,677,686	-343,964,684	-13.8
ii. Pri. ch. w. pumps	140,836,992	125,082,536	-15,754,456	-11.2
iii. Seawater pump	191,271,861	193,611,031	+2,339,170	+1.2
iv. Sec. ch. w. pumps	417,942,662	299,799,617	-118,143,044	-28.3
Sub-total	3,239,693,884	2,764,170,870	-475,523,014	-14.7
Total LCC	4,440,083,501	4,108,032,442	-332,051,058	-7.5

Despite of the higher capital investment, and life-cycle replacement and maintenance costs of Solution C, its total life-cycle energy cost was 14.7% less than that of DCS₀. 75% of the saving is attributed by the chiller plant, which used 15 x 4,000 RT (14,068 kW) equally-sized variable speed chillers. The remaining saving of 25% was generated

by the pumping stations. This revealed that although additional costs were required for the equipment and energy efficiency enhancement measures in Solution C, the life-cycle energy cost saving achieved is more than enough to offset the extra costs incurred.

8.5 A Comparative Analysis of the Electricity Consumption of DCS₀ and Solution C

Results from energy simulation (as in Table 8.15) show that when DCS₀ adopted the design of Solution C, its annual total electricity consumption could be reduced by 14.6%.

Over 72 % of this saving in electricity was generated by the chillers, i.e. the 15 x 4,000 RT (14,068 kW) chillers. It is then followed by the application of six pumping stations with five pumps in each station. These secondary chilled water pumps were responsible for 25% of the total reduction in electricity consumption. Some observations can be made about the simulation results.

Table 8.15 Comparison of the annual electricity consumption of DCS₀ and Solution C

	Annual electricity consumption, kWh		Difference [Solution C minus DCS ₀]		% of the total difference
	DCS ₀	Solution C	kWh	%	
(a) Chiller plant					
i. Chiller	88,827,472	76,555,222	-12,272,250	-13.8	72
ii. Pri. ch. w. pumps	5,583,218	4,958,662	-624,556	-11.2	3
iii. Seawater pump	7,582,613	7,675,345	+92,732	+1.2	0
Total [i + ii + iii]	101,993,303	89,189,230	-12,804,074	-12.6	75
(b) Sec. ch. w. pumps	14,911,696	10,696,493	-4,215,203	-28.3	25
Total [(a) + (b)]	116,904,999	99,885,723	-17,019,276	-14.6	

8.5.1 Electricity Consumption of Chillers

The adoption of additional and smaller sized variable speed chillers in Solution C could bring a significant reduction of 13.8% in electricity consumption in comparison with the use of less and larger sized constant speed chillers in DCS_O (see Table 8.15). The main reason is that the COP of variable speed chillers is relatively higher than that of constant speed chillers, particularly at low load. This has already been discussed in Chapter 6. Furthermore, as there were 77% of the system's total operating hours (c.f. Table 2.5 in Chapter 2) in which the system load was below 50%, it means that the chillers were operated at part load for most of the time. Under such circumstances, the variable speed chillers could help to significantly reduce the electricity consumption of DCS_O.

Figure 8.5 shows that the average COP of the variable speed chillers in C_D of Solution C was relatively high at low load when compared to that in C_O of DCS_O. The average COP of constant speed chillers decreased dramatically at low load. More specifically, the annual average COP of the chiller system configuration in Solution C was 7.43, which was relatively higher than that of DCS_O, i.e. 5.69.

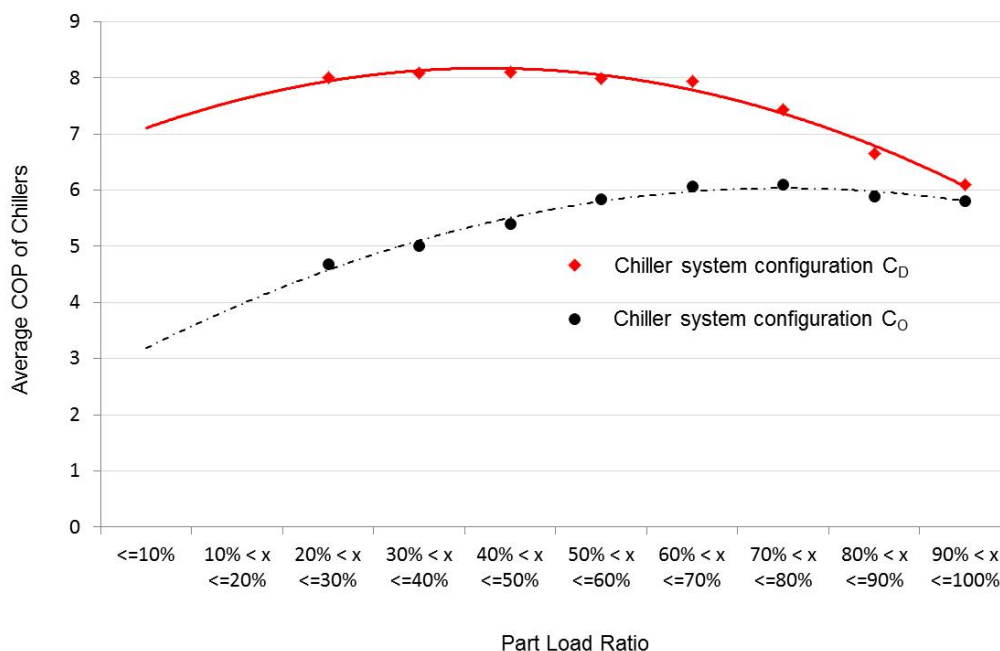


Figure 8.5 Average COP of the constant and variable speed chillers in C_O and C_D that are operating at different PLR

8.5.2 Electricity Consumption of Primary Chilled Water Pumps

Similar to chillers, the electricity consumption of the primary chilled water pumps in Solution C was also relatively lower than that in DCS_O, as there was a 11.2% difference between them (see [Table 8.16](#)).

Table 8.16 Comparison of the operating pump hour, power demand and electricity consumption of the primary chilled water pumps in DCS_O and Solution C

	DCS _O	Solution C
No. of chiller	10	15
Cooling capacity of chiller, RT/kW	6,000 / 21,102	4,000 / 14,068
Operating pump hour, hr	33,952	51,474
No. of pri. ch. w. pump	10	15
Rated power, kW	164.4	96.3
Total power demand, kW	1,644	1,445
Annual electricity consumption, kWh	5,583,218	4,958,662
Difference in annual electricity consumption w.r.t. DCS _O		
	kWh	-624,556
	%	-11.2

Their electricity consumptions depend on their power demand and operating pump hour, as in [Table 8.16](#). Under the same pressure head requirement, the design delta-T in Solution C (i.e. 8°C) was relatively higher than that of DCS_O (i.e. 7°C). This led to a lower design flow rate and power demand of the primary chilled water pumps in Solution C. Although the operating pump hours of the pumps in Solution C were relatively longer, the low power demand of the pumps there had led to a lower electricity consumption.

8.5.3 Electricity Consumption of Seawater Pumps

Same as the primary chilled water pumps, the electricity consumption of the seawater pumps also depends on the pump's power demand and operating pump hour. The electricity consumption of the seawater pumps in Solution C was 1.2% higher than that in DCS₀ (Table 8.17). However, as seawater pumps accounted for only a small portion of the total electricity consumption of DCS₀, this additional electricity consumption was offset by the significant savings derived from the chillers and secondary chilled water pumps.

Table 8.17 Comparison of power demand and electricity consumption of the seawater pumps in DCS₀ and Solution C

	DCS ₀	Solution C
No. of chiller	10	15
Cooling capacity of chiller, RT / kW	6,000 / 21,102	4,000 / 14,068
Operating pump hour, hr	33,952	51,474
No. of seawater pump	10	15
Rated pump power, kW	223.3	149.1
Total power demand, kW	2,233	2,237
Annual electricity consumption, kWh	7,582,613	7,675,345
Difference in annual electricity consumption w.r.t. DCS ₀		
	kWh	-
		+92,732
	%	-
		+1.2

8.5.4 Electricity Consumption of Secondary Chilled Water Pumps

Table 8.18 lists out the design information and electricity consumption of the pumping stations in DCS₀ and Solution C for comparison.

As mentioned earlier, the difference of the design chilled water supply and return temperatures in Solution C was 1°C slightly higher than that in DCS₀. In this regard, the annual average chilled water flow rate in Solution C, i.e. 2.25 m³/s, was 5.5% lower than that in DCS₀, i.e. 2.38 m³/s. The lower the chilled water flow rate, the lower the pressure drop and hence the power demanded by the pumps. Furthermore, using additional pumping stations can help to reduce the pressure head of each station in comparison with the adoption of a single pumping station. The flow rate and pressure head requirements of the additional pumping stations can be further reduced if the station is located far away from the central plant. The total power of the pumps in Solution C (i.e. 3,615 kW) was 37.2% lower than that in DCS₀, i.e. 5,760 kW.

Table 8.18 Comparison of power demand and electricity consumption of the secondary chilled water pumps in DCS₀ and Solution C

	DCS ₀	Solution C
Pumping station	PS ₁₋₀	PS ₆₋₃₄₇₃₅
No. of pumping station	1	6
No. of pump per station	10	5
Location of pumping station	1 on supply side	5 on supply side 1 on return side
Rated pump power, kW	576.0	499.9 / 95.4 / 57.7 / 39.5 / 24.6 / 5.9
Total pump power, kW	5,760	3,615
Annual electricity consumption, kWh	14,911,696	10,696,493
Difference in annual electricity consumption w.r.t. DCS ₀		
	kWh	-4,215,203
	%	-28.3

Based on the variable speed pump model developed in [Chapter 3](#), the results in [Table 8.18](#) show that the pumping stations in Solution C consumed less electricity (i.e. 28.3%) in comparison with using a single pumping station with 10 pumps in DCS₀.

8.6 Environmental Benefits of Solution C

Based on the predicted annual electricity consumption in [Table 8.15](#), the respective annual and life-cycle (for a life span of 60 years) equivalent CO₂ emissions incurred by generation of electricity for DCS₀ and Solution C were estimated, as shown in [Table 8.19](#). The CO₂ emissions were assumed to be 197 tonnes per TJ of electricity consumed ([Yik et al., 2012](#)). Results indicate that by adopting Solution C in lieu of base DCS₀, the greenhouse gas emissions over a life span of 60 years could be reduced by an equivalent amount of 721,941 tonnes (i.e. 14.7%).

If the emissions reduction ([Table 8.19](#)) is to be credited to the DCS operator for the purpose of a carbon trading scheme, the saving over a 60-year useful life cycle can represent a net present value of HK\$7 million (assessed against the base case). This value was based on the carbon value of €4 (~HK\$30) per tonne of carbon dioxide quoted by the [World Bank \(2013\)](#).

Table 8.19 Annual and life-cycle greenhouse gas emissions from DCS₀ and Solution C

	DCS ₀	Solution C	Difference [Solution C minus DCS ₀]	
			tonne	%
Annual CO ₂ (eqv.) emissions, tonne	82,909	70,839	-12,070	-14.6
Life-cycle (60 yrs) CO ₂ (eqv.) emissions, tonne	4,974,542	4,250,337	-724,204	-14.6

8.7 Summary

The effectiveness of each of the three energy efficiency enhancement measures in mitigating the impacts of a degrading temperature difference on the energy performance of the base case DCS₀ was discussed in the preceding chapters.

This chapter is to study the synergy effect of integrating different combinations of these three measures. A simple heuristic optimization-simulation algorithm was developed to reduce the 1,447,680 options into 434,268 possible solutions for an evaluation of their

energy, financial and environmental performance. The ultimate goal was to achieve a cost-optimal solution, emerging as having the lowest LCC and the best energy and environmental performance.

Results of energy simulation indicate that among the 434,268 possible solutions, matrix $S(C_E, T_7, PS_{6-35464})$ could lead to the greatest reduction in the electricity consumption of DCS_O . This energy-optimal design solution is referred to as Solution E.

On the other hand, based on the simulated energy consumption and cost data collected about the major equipment in the chiller plant and pumping station, an LCC model was developed to estimate the life-cycle cost-effectiveness of each possible solution. A cost-optimal design named as Solution C, i.e. matrix $S(C_D, T_5, PS_{6-34735})$, was successfully identified.

This cost-optimal design consisted of 15 equally-sized variable speed chillers and six pumping stations located at both the chilled water supply and return sides, and was equipped with five pumps in each station. The chilled water supply and return temperatures were set at 5 °C and 13°C, respectively.

As compared to Solution E, the electricity consumption of Solution C was about 1% higher. This difference, however, is insignificant because it was mainly due to the trade-off in electricity consumption associated with the chillers and the secondary chilled water pumps. Furthermore, the 14.6% life-cycle energy cost saving that Solution C could achieve is more than enough to offset the extra costs incurred by adopting the energy efficiency enhancement measures.

Results of the LCC analysis show that Solution C was the most financially favourable. After comparing the overall LCC of the base design, DCS_O and Solution C, it was found that the latter could generate an LCC saving of 7.5%, representing a reduction of HK\$322 million in present value.

In addition, the analysis illustrates that the cost-optimal solution could offer significant protection to the environment by reducing the DCS' carbon footprint by 14.6% in

comparison with the base case. This should be considered whenever possible in any LCC analysis in order to achieve a sustainable decision.

These findings are significant, as they can offer insights to the DCS designers and owners about the energy and financial trade-offs associated with the design of a large scale DCS. If an owner focuses only on the initial capital investment, the long-term energy costs and the associated environmental impacts may be overlooked.

Chapter 9

Conclusion and Suggestions for Future Research

9.1 Summary of Work Done and Key Findings

To promote energy efficiency and conservation, the Hong Kong government is planning to set up DCS in some new development areas, which are the Kai Tak Development, the West Kowloon Cultural District and the North East New Territories Development. The DCS will supply chilled water to buildings in these new areas for centralized air-conditioning. In 2010, the plan to build Hong Kong's first DCS that uses direct seawater-cooling for the Kai Tak Development area was confirmed. The project is divided into three phases. About 10% of the total installed capacity was completed in 2013 and the other two stages are expected to be finished in 2017 and 2021 respectively. The estimated maximum cooling demand would amount to 80,000 RT (about 280 MW) when all buildings served by the DCS are occupied. VPF chilled water systems and constant speed chillers were designed for this DCS.

As mentioned in [Chapter 1](#), low delta-T in the distribution loop of chilled water systems has been widely reported by many researchers over the last 25 years. There is no exception for the chilled water system in DCS. The resulting problem is the corresponding increase in the chilled water flow rate. Particularly at part load, the flow rate and cooling load do not correspond to each other, and hence additional chillers are

required to be on to maintain the flow requirements even though the maximum cooling capacity of the chillers has not been fully reached. Both high pumping energy consumption and reduced efficiency of the chillers operating at part load can lead to a dramatic decrease in the overall energy efficiency of the DCS.

There are many causes of the low delta-T syndrome. Many methods have been proposed in the areas of design, control and maintenance. Among them, the use of bypass check valves and VPF pumping schemes have received great attention. However, there is no universal conclusion of which solutions can absolutely help to mitigate the impacts of low delta-T on the energy performance of DCS. In reality, some of the causes cannot be avoided, such as the degradation of coil effectiveness.

A DCS should be designed to operate efficiently under low delta-T conditions. However, well-documented and detailed simulation work or case study in designing a DCS to accommodate the low delta-T has been lacking. In particular, regarding the VPF system in Hong Kong's first DCS under the Kai Tak Development project, there was a lack of quantitative analysis for comparing the amount of energy saving after applying either the P-S or VPF systems in the chilled water pumping system of a large scale DCS.

In this regard, all these have led to the need for a detailed investigation from a comprehensive system design perspective to find out a design solution that can mitigate the impacts of low delta-T on the energy performance of DCS. The findings can be useful for DCS designers as the DCS can operate in an efficient manner with the inevitable low delta-T. Furthermore, in view of the huge capital investment and lengthy payback period of such a large scale infrastructural development project, this research was geared towards finding a design solution that would be financially viable. It was hoped that this solution could help the DCS owner identify a system design that could strike a good balance between the initial costs and the long-term benefits.

9.1.1 Development of a Hypothetical District

As the first DCS in Hong Kong is still in an embryonic stage, it was more cost-effective to adopt a model-based approach for this study instead of performing field research. As

a result, a hypothetical district made up of office buildings, commercial complexes and hotels was established. These buildings encompassed a combination of offices, retail shops, restaurants and hotel guestrooms. The total design cooling capacity was about 200 MW, which was close to the scale of the biggest single DCS in Japan.

9.1.2 Design of a DCS

The comparative analysis results presented in [Chapter 4](#) indicate that the VPF system is unable to yield any significant saving in the electricity of a large scale DCS. The main reason is that there were over 80% of the total operating pump hours in which the pumps in the P-S and VPF systems were operated at a flow ratio greater than 80%. Under such circumstances, the variable frequency drive decreases the efficiency of the variable speed pump running at nearly full speed. It causes the variable speed pump to consume more power than the CSP. As a result, the variable speed pumps and CSP in the P-S system consume less electricity than the variable speed pumps in the VPF system, so that the overall electricity consumption of the P-S system was 0.5% slightly lower than that of the VPF system.

In this study, a P-S chilled water pumping scheme was designed for a baseline DCS - DCS_O. This DCS comprised a production loop, a distribution loop and building loops. In the primary loop, a centralized chiller system configuration C_O was designed with 10 constant speed chillers, which were equipped with dedicated primary chilled water pumps and seawater pumps. Once-through direct seawater was used for heat rejection. In the distribution loop, one pumping station, namely PS₁₋₀, equipped with 10 variable speed chilled water pumps was designed to distribute chilled water to each building in the building loop. The design chilled water supply and return temperatures were 5°C and 12°C respectively. Heat exchangers were used for the heat transfer of chilled water in the distribution loop and each building in the building loops. DCS_O was treated as a base case for comparing the various options of the following energy efficiency enhancement measures to improve the energy performance of the chiller plant and pumping stations at low delta-T, as these two components are responsible for the major portion of the total electricity consumption of the DCS.

The first measure was to change the configuration of the chiller system. This was done by altering the major influential design parameters such as the number, cooling capacity and type (i.e. constant or variable speed) of the chillers. The second measure was related to the pumping station. The variations included: application of multiple pumping stations in different locations of the chilled water supply and return network, and using different number of pumps in each pumping station. The third measure was to change the design temperature of the chilled water supplied by the chiller plant and the design temperature of the chilled water returning from the building. A sensitivity analysis of different temperature regimes was performed accordingly.

9.1.3 Development of Mathematical Models for Energy and Cost Simulation

Almost all published mathematical models of the major air-conditioning equipment such as chillers, cooling coils and heat exchangers have been developed for individual buildings only. The operating conditions of this equipment in a building are different from those in a DCS. Therefore, it was of a practical importance to develop a simple and accurate model, which could represent the design of a DCS. Moreover, mathematical models of a chilled water distribution network and variable speed pumps had to be specially developed for this study.

In this regard, mathematical models of the major equipment in the chiller plant and pumping station were tailor-built, as shown in [Chapter 3](#). They could facilitate an evaluation of the impacts of low delta-T and the assessment of the effectiveness of various options of the three energy efficiency enhancement measures. Moreover, a life cycle cost (LCC) model was developed in [Chapter 8](#) to evaluate the financial viability of various options of the measures over the 60-year operating life cycle of the DCS.

9.1.4 Impacts of Low Delta-T on the Energy Performance of DCS₀

In DCS₀, it was reported in [Chapter 4](#) that the delta-T under normal conditions was in a decreasing trend when the cooling load was increased to a full load. Eventually, it decreased to a level close to the design value of 7°C. However, delta-T fell short of the design level at low cooling loads and it gradually increased to a temperature close to the

design value when the cooling load was increased to a full load. Furthermore, the annual average chilled water flow rate required to distribute chilled water from the chiller plant with a low delta-T was 77% higher than that under normal conditions.

Under such circumstances, additional chillers had to be staged on for 54% of the annual operating hours to meet the excessive chilled water flow rate. There were 4,670 hours (53% of the 8,760 hours in a year) in which one additional chiller was required to be operated and 62 hours (1% of the 8,760 hours) in which two additional chillers were required. It is because the increased chilled water flow rate has exceeded the design value of chillers operating under normal conditions. This led to an increase in the annual total electricity consumption of DCS₀ by 9.3% when operating at low delta-T, in comparison with the normal condition. In this regard, it was worthwhile to study the energy efficiency measures mentioned above to enhance the energy efficiency of DCS₀.

9.1.5 Effects of Chiller System Configuration on the Energy Performance of DCS₀

Regarding chiller system configuration, it can be optimized by modifying the three influential design parameters: number, cooling capacity and type of chillers. With reference to the design of the baseline DCS₀, five alternative configurations were identified. The simulation results unveil that the chiller system configuration using more or unequally-sized chillers would provide more opportunities in meeting the available cooling capacity with the cooling load requirement. This can increase the average PLR of the chillers and hence the overall COP of the chiller plant. However, the adoption of additional or unequally-sized chillers could only lead to a limited saving in the annual total electricity consumption of DCS₀, as this saving was less than 2%, when compared to using the baseline configuration with a low delta-T. The main reason is that chillers in the DCS have a larger cooling capacity that ranges from 2,000 RT (7,034 kW) to 6,000 RT (21,102 kW). As a result, the adoption of more chillers with different cooling capacities does not have a significant impact on the chillers with a better COP under various part load conditions.

On the other hand, it was found that variable speed chillers could significantly reduce the total annual electricity consumption of DCS_O, as they could lead to a reduction of up to 9.9% in comparison with constant speed chillers. It is because the COP of variable speed chillers at part load is better than that of constant speed chillers. The energy efficiency of variable speed chillers is further improved when they are operated in a seawater temperature below 25°C. This can bring an additional benefit of reducing the electricity consumption of chillers. Therefore, although almost every chiller is affected by the low delta-T syndrome, particularly at low cooling loads, high energy performance of the variable speed chillers at part load can effectively lessen the problems incurred by degrading delta-T.

Among the five alternative configurations, it was found that the combination of 15 unequally-sized variable speed chillers, i.e. 5 x 2,000 RT (7,034 kW), 5 x 4,000 RT (14,068 kW) and 5 x 6,000 RT (21,102 kW), performed the best in terms of energy saving. It could reduce 11.6% of the total annual electricity consumption of DCS_O when low delta-T occurred.

9.1.6 Effects of Pumping Station Configuration on the Energy Performance of DCS_O

In [Chapter 6](#), two design initiatives related to pumping system configuration were examined. The first was to adopt a multiple pumping station approach instead of using a single pumping station, and the location of the stations could be anywhere at the chilled water supply and return sides of the distribution loop. To further optimize the design, the second initiative was to adopt an unequal number of pumps in each pumping station.

Mathematically, the search for an optimum pumping station design is a very complicated issue, as it involves 1,024 possible combinations in the analysis. As a result, a hydraulic gradient method was applied to conduct a quick assessment for identifying only those combinations that were technically feasible. The number of combinations was finally significantly reduced by 86% from 1,024 to 140. Failure cases often occurred when the pumping station was located at the far end of the central DCS plant. It is because the system's pressure head requirement decreases as the distance from the

central DCS plant increases. Meanwhile, the pumping station has to maintain a minimum pressure drop across the heat exchangers in each building. Therefore, there will be a situation in which the system pressure decreases to a value at a location where the differential pressure between the chilled water supply and return cannot achieve the minimum value with a booster pumping station.

The second initiative was to change the grouping of the pumping stations based on the number of pumps in each station, i.e. whether there were 5, 10 or 15 pumps in each pumping station. This would generate a total of 36,192 pumping station arrangements.

On the other hand, a dataset of rated power of 1,800 pumps was developed to determine the rated pump power of thousands of variable speed pumps designed with various flow rates and pump head requirements. To facilitate a simulation of the energy consumption of thousands of pumping station arrangements, an optimization program with a systematic approach was established to perform a more efficient calculation. Results of simulation reveal that the adoption of six pumping stations (i.e. PS₆₋₃₄₅₆₄), which were equipped with five pumps in each station, could lead to a 3% reduction in the annual total electricity consumption of DCS_O.

In DCS_O where there was only one main pumping station for distributing chilled water to all the buildings in the district, the chilled water flow rate and pressure head were very high. Adding booster pumping stations can help to reduce pressure head of the main pumping station. Moreover, the pressure head requirements of the booster pumping stations can be further reduced if the pumping stations are located further away from the central plant. This can help to reduce the pump size and power demand of the main pumping station and the booster pumping station. The total power demand and annual electricity consumption of the pumps in PS₆₋₃₅₄₆₄ were 25.6% and 23% less than those of the pumps in DCS_O respectively.

9.1.7 Effects of Chilled Water Supply and Return Temperature on the Energy Performance of DCS₀

Changing the temperature of the supply and return chilled water will have significant impacts on two determining factors of the DCS' energy performance, i.e. the COP of the chillers and the chilled water flow rate in the distribution network. In DCS₀, the supply chilled water temperature was set at 5°C and the chilled water return temperature was 12°C. To simulate the effects of changing the design temperature, eight different temperature regimes were identified. The energy performance of different components in DCS₀ was then compared.

As reported in [Chapter 7](#), the chiller's COP increased as the chilled water supply temperature was increased from 4°C to 6°C. In a situation where the PLR was greater than 40%, the average percentage of increment in the COP ranged from 1.3% to 2% for every °C of increase in the chilled water supply temperature. Regarding chilled water flow rate, results show that the annual average chilled water flow rate was the highest when the design temperature difference between the chilled water supply and return temperature was at the lowest level, i.e. 5°C. Relatively lower chilled water flow rate was required when the design temperature difference was at the highest level, i.e. 9°C. The resulting COP of the chillers and the chilled water flow rate would in turn affect the energy performance of the chiller plant and chilled water pumps in the DCS.

The simulation results also reveal that when the design chilled water supply and return temperatures were 6°C and 11°C respectively, the annual total electricity consumption of DCS₀ would be the lowest. Under this temperature regime, the chiller plant and the pumping station exhibited different electricity consumption patterns. The energy performance of the chiller plant was the best, due to a 4.6% of saving of electricity when compared to other temperature regimes. It was because the design chilled water supply temperature was on the high side of 6°C. The COP was thus relatively higher as compared to other temperature regimes with a design supply temperature of 4°C or 5°C.

On the other hand, it was found that the secondary distribution pumps under this temperature regime had the highest electricity consumption, i.e. 22.5% higher with

reference to the base design. The reason is that the design temperature difference was at the lowest level, i.e. 5°C. This can lead to a higher annual average chilled water flow rate, and hence the design pump power and electricity consumption of the pumps. Under such circumstances, the electricity saving of the chiller plant was nearly offset by the increase in the electricity consumption of the secondary pumps. The overall electricity consumption of DCS_O could be reduced by about 1% when compared to the baseline design.

9.1.8 A Cost-Optimal Integrated Design Solution

The simulation results presented in [Chapters 5, 6 and 7](#) provide valuable information in the design of a cost-optimal integrated solution for a DCS. By changing the design parameters of the three energy enhancement measures, five combinations of chiller plant configuration, and eight chiller water temperature regimes, 36,192 arrangements of pumping station were derived. This could result in generating 1,447,680 possible design solutions. A simple heuristic strategy was adopted to reduce this number by 70% to 434,268. The energy, financial and environmental performances of these possible solutions were then evaluated.

Based on the mathematical models developed in [Chapters 3 and 6](#) for chiller plants and pumping stations, an algorithm was formed in [Chapter 8](#) for conducting simulations of the electricity consumption of these possible solutions. The results show that the most energy-optimal design (i.e. Solution E) could save 15.5% of the annual total electricity consumption in comparison with that of DCS_O. This solution encompassed 15 variable speed chillers designed with three different cooling capacities. There were six pumping stations at the chilled water supply side and each pumping station was equipped with five pumps. The chilled water supply and return temperatures were 6°C and 12°C respectively.

Based on the simulated energy consumption data and the cost information collected for the major equipment in the chiller plant and pumping stations, an LCC analysis was performed to estimate the LCC of each possible solution, including that of Solution E, which had the best energy performance. It was found that instead of Solution E, another

design - Solution C - was the most cost-optimal. This latter design had the lowest LCC, which was 7.5% lower than that of the base case. The LCC saving in present value would be over HK\$332 million.

Solution C encompassed 15 equally-sized variable speed chillers. There were six pumping stations at both the chilled water supply and return sides and each was equipped with five pumps. The chilled water supply and return temperatures were 5 °C and 13°C respectively. This design could lead to a 14.6% reduction in the electricity consumption of DCS₀. Although this percentage was about 1% lower than that achieved by Solution E, the life-cycle energy cost saving from Solution C, which was 14.6%, was more than enough to offset the extra costs incurred by using additional equipment and other devices associated with the energy efficiency enhancing measures. Moreover, the LCC of this design was more financially favourable than that of Solution E, even though the latter outmatched the former in terms of energy performance.

There is always a budgetary constraint for the DCS designer or owner to select an optimum set of energy efficiency enhancement measures that can lead to the greatest benefits. The value of the current research lies in the way that it helps to provide a comprehensive review of the effectiveness of different energy efficiency measures. It also helps to point to a direction in the search for an integrated design solution that can mitigate the impacts of degrading delta-T on the energy performance of DCS. With all this information, the DCS owner can be in a better position to weigh between the energy benefits and the associated financial trade-offs. If a design decision is purely based on initial capital investment, the long-term energy costs that a large scale infrastructure development project can incur may be overlooked.

Moreover, the cost-optimal solution could offer a significant protection to the environment by reducing the DCS' carbon footprint by 14.6% in comparison with the base case. This should be considered whenever possible in an LCC analysis in order to achieve a sustainable future.

9.2 Original Contributions of this Study

To the best of the author's knowledge, this study is the first effort in conducting a comprehensive assessment of the low delta-T issue in DCS from a system design's perspective. It has yielded the following key findings, which are original contributions to knowledge in building services engineering.

9.2.1 One main contribution of this study is the development of a systematic approach for conducting a thorough assessment of the effectiveness of different possible design solutions so as to enhance the energy performance of the chiller plant and the pumping station in DCS.

A cost-optimal design solution was identified. It was able to mitigate the impacts of low delta-T on the DCS' electricity consumption. The results provide a guideline to the DCS designers with a considerable confidence when designing the chiller plant and pumping station of other DCS with a similar scale to accommodate the low delta-T issue in an energy efficient manner.

9.2.2 Major efforts have been exerted in developing a vast number of mathematical models for simulating the energy performance of all the major equipment in the chilled water plant and pumping stations of the DCS. The models were tailor-developed and could be applied for other DCS projects. Some new improvements were made in the following models. These are not found in any previous research literature.

i. Chiller Model

With the aid of a conventional bi-quadratic regression approach, the regression variables for the constant and variable speed chillers were 16 and 15 respectively. Stepwise multiple regressions were applied to simplify the mathematical models for these two types of chillers. This method could help to select an appropriate set of regression variables from all the possible items

and significantly reduce the number of regression variables to 6 and 5 for constant and variable speed chillers respectively, and maintain a higher value of determination of coefficient. This could help to simplify the structure of the chiller models with a certain physical significance of variables that could enable the model to make an accurate simulation of the chiller's performance.

Most of the chiller models developed in other research studies are constructed for applications in buildings rather than DCS. These models are always based on a chilled water supply temperature of about 7°C. The chiller models developed in this study were based on the part load performance data of chillers with a design chilled water supply temperature as low as 4°C. This chiller model can be widely used for other DCS research.

ii. Cooling Coil Model

There are tens of thousands of cooling coils of air supply equipment, i.e. AHU, PAU and FAU in the buildings within a district. It was not practical to study each of them. It is also not accurate to use a single cooling coil model developed by other researchers to simulate the chilled water flow rate and temperature of different types of buildings in a district. In this study, based on the hourly cooling load and chilled water flow rate predicted by BECON, the data was normalized and plotted to present the cooling coil characteristics of the four model buildings A, B, C and D. These buildings were an office, a low and a high rise commercial complex, and a hotel respectively. Polynomial regression curves were plotted to fit for the normalized data, and model the cooling coil output and the chilled water flow rate of each building under normal conditions.

iii. Hydraulic Chilled Water Distribution Model

Hydraulic chilled water distribution models of the pipe network topology of the DCS were built to simulate the dynamic and non-linear characteristic

between the hourly chilled water flow rate and the corresponding pressure drop along the distribution network.

- 9.2.3 There are over thousands of possible combinations of the number and location of the pumping stations in the distribution loop. The hydraulic gradient evaluation method was found to be an effective tool for designers to make a quick assessment of the technical feasibility of different combinations of pumping station design and identify the combinations that can meet the required minimum pressure across the chilled water supply and return pipework.
- 9.2.4 To facilitate a simulation of the power demand of ten thousand variable speed pumps under different pumping station combinations, a comprehensive dataset of the rated power of pumps with different sizes was obtained from the manufacturers for developing a simple pump power model. This model can help to provide an effective tool to designers in determining the power of pumps with different sizes.
- 9.2.5 To help the DCS owners and designers strike an optimum balance between the first costs and the energy benefits, an LCC model was developed to evaluate the financial performance of different DCS design solutions. This allows a more realistic determination of a cost- and energy-optimal design. This also provides them with a reasonable support in the decision-making process.
- 9.2.6 It has been proved in this study that variable speed chillers and multiple pumping stations play a vital role in mitigating the impacts of the low-delta T issue on the energy performance of DCS. The evaluation gives some useful guidelines for designers in reviewing the application of VPF systems and constant speed chillers for the DCS in the Kai Tak Development.

In the present study, a step-by-step and systematic approach was developed for evaluating and integrating different energy efficiency measures for identifying a

cost-optimal design solution that can mitigate the impact of low delta-T on the energy performance of DCS. This approach and the energy efficiency measures provide useful guidelines for DCS designers facing the inevitable low delta-T issue. Moreover, the models developed particularly for chillers and building cooling coils provide a useful basis for researchers in their future investigation. The chiller models is based on the part load performance data of chillers with a design chilled water supply temperature as low as 4°C. Moreover, the cooling coil model can well present the cooling coil characteristics of buildings comprising office, commercial complex and hotel. Moreover, the hydraulic gradient evaluation method was found to be an effective tool for designers to make a quick assessment of the technical feasibility of different combinations of pumping station design and identify the combinations that can meet the required minimum pressure across the chilled water supply and return pipework.

9.3 Limitations and Recommendations for Further Research

Although the objectives of this research have been reached and some original recommendations were made regarding the design of a DCS, this research has some limitations. These limitations, however, may be seen as potential areas for future research. It would be desirable and valuable to make further efforts in the following aspects related to the findings presented in this thesis.

Firstly, effort has been made in this study to model the cooling coil characteristics at low delta-T. However, most buildings did not have a comprehensive record of the chilled water temperature and flow rate. It was therefore difficult to collect sufficient information of the sample buildings operating under low delta-T conditions. Therefore, an extensive field work is desirable for finding out the operational characteristics of the cooling coils at low delta-T in different types of buildings. This can help to further develop more accurate mathematical models for the cooling coils suffering from the low delta-T problem.

Secondly, in the present study, a hypothetical district was developed based on the operational characteristics of the air-conditioning systems of existing buildings. Upon completion of the first phase of the DCS in the Kai Tak Development, even though the

scale is not large, it is still worthy to conduct a more extensive field test concerning the operational characteristics of the DCS so that a more comprehensive database can be obtained to facilitate the evaluation of the energy performance of chiller plants and pumping stations.

Last but not the least, a new type of water-cooled “oil-free” chillers has recently emerged in the market. The use of magnetic bearings for supporting the shaft that directly couples the motor with the compressor impeller and for fixing the axial position of the shaft offers an advantage that the shaft will be suspended in air by magnetic flux and so it makes no contact with any other parts in the chiller. As a result, the motor can run at a very high speed (e.g. up to 30,000 rpm). This eliminates the need for lubricant as well as a gear chain to step up the rotational speed of the motor to that of the impeller, and can also minimize the associated energy loss. The electricity consumption of these chillers at part load is relatively lower in comparison with the conventional water-cooled chillers. However, these chillers are relatively new and expensive, and their cooling capacity is limited to a maximum of 800 RT (2,814 kW). Extensive use of these chillers is, therefore, considered premature. Nevertheless, it would be worthwhile to investigate the potential of adopting these chillers in a DCS in the coming future and explore their effectiveness in accommodating the low delta-T issue, typically at low load.

∞ BIBLIOGRAPHY ∞

- Alexander D.K., 1996, HTB2 - A model for the thermal environment of building in operation (Release 2.0a), User Manual, Welsh School of Architecture R&D, University of Wales, Cardiff, UK.
- American Society of Heating, Refrigeration, and Air-conditioning Engineers (ASHRAE), 2001, ASHRAE Standard 62-2001: Ventilation for Acceptable Indoor Air Quality, Atlanta, GA.
- American Society of Heating, Refrigeration, and Air-conditioning Engineers (ASHRAE), 2009, ASHRAE Handbook: Fundamentals, ASHRAE, Atlanta, GA.
- American Society of Heating, Refrigeration, and Air-conditioning Engineers (ASHRAE), 2011, ASHRAE Handbook: Applications, ASHRAE, Atlanta, GA.
- Anagnostopoulos J.S. and Papantonis D.E., 2007, Pumping station design for a pumped-storage wind-hydro power plant, *Energy Conversion And Management*, 48(11): 3009-3017.
- Arup, 2014, The North East New Territories New Development Areas Planning and Engineering Study – Stage 3 Public Engagement Digest, Civil Engineering and Development Department, and Planning Department.
- Avery G., 1998, Controlling chillers in variable flow systems, *Heating/Piping/Air Conditioning Engineering*, 73(4):41-50.
- Bahnfleth W.P. and Peyer E.B., 2004, Variable Primary Flow Chilled Water Systems: Potential Benefits and Application Issues, Final Report to Air-Conditioning and Refrigeration Technology Institute.
- Bahnfleth W.P. and Peyer E.B., 2006, Energy use and economic comparison of chilled-water pumping system alternatives, *ASHRAE*, 112:198-208.
- Bhatia A., 2013, HVAC chilled water distribution schemes, *Continuing Education and Development Engineering*, retrieved on 15 Nov 2013, from <http://www.cedengineering.com>
- Brandemuehl M.J., 1993, A Toolkit for Secondary HVAC System Energy Calculations, ASHRAE, Atlanta.
- Brasz J.J. and Tetu L., 2008, Variable speed centrifugal chiller control for variable primary flow applications, *International Refrigeration and Air Conditioning Conference at Purdue*, July:1-12.

- Bullet J.D., 2007, Variable flow chiller plant design, presented in Technical Session no. 6 of ASHRAE Region XI CRC, Tuesday 15th May 2007.
- Cai H.W., 2009, Research on the Real Chilled Water System in Large-Scale Commercial Buildings, Master's thesis, Tsinghua University.
- Cai H.W., Chan C., Jiang Y., Wei Q.P. and Jean Q., 2012, Concise graphic-analytic method for chilled water system characteristics analysis, Proceedings of the 3rd Greater Pearl River Delta Conference on Building Operation and Maintenance - Green Building & Green Operation and Maintenance, China Science Literature Publishing House, 106-114.
- Campbell M.J., Statistics at square two: understanding modern statistical applications in medicine. London, GBR: BMJ Publishing Group; 2001.
- Cevik A., Gogus M.T., Guzelbey, I.H. and Filiz H., 2010, A new formulation for longitudinally stiffened webs subjected to patch loading using stepwise regression method, Advances in Engineering Software, 41:611-618.
- Chan A.L.S., Hanby V.I. and Chow T.T., 2007, Optimization of distribution piping network in district cooling system using genetic algorithm with local search, Energy Conversion and Management, 48(10):2622-2629.
- Chan C.W.H., 2006, Optimizing chiller plant control logic, ASHRAE Journal, 48(7):39-42.
- Chan K.T. and Yu F.W., 2004, How chillers react to building loads, ASHRAE Journal, August:52-57.
- Chang C., Wei Q.P. and Wang X., 2011, Assessing chilled water system retrofit through data-log-based simulation, Proceedings of Building Simulation 2011 - 12th Conference of International Building Performance Simulation Association, Sydney, 14-16 November.
- Chang Y.H., Lee C.Y., Chen C.R., Chan C.J., Chen W.H. and Chen W.H., 2009, Evolution strategy based optimal chiller loading for saving energy, Energy Conservation and Management, 50:132-139.
- Chow T.T., Au, W.H., Yau, R., Cheng V., Chan, A.L.S. and Fong K.F., 2004a, Applying district-cooling technology in Hong Kong, Applied Energy, 79(3):275-289.
- Chow T.T., Fong, K.F., Chan, A.L.S., Yau, R., Au, W.H. and Cheng V., 2004b, Energy modeling of district cooling system for new urban development, Energy and Building, 36(1):1153-1162.

- Clark S., Mardiat E.D., Swinson S.K., 2011, A Texas-sized district energy system: The energy behind what's next at the Texas Medical Center, District Energy, International District Energy Association, 3rd Quarter: 12-17.
- Dalin P., 2012, Free cooling/natural cooling is crucial for a successful district cooling development, paper presented in 2012 Annual Conference - Teaming up for renewable heating and cooling, Euroheat and Power.
- Dalkia, 2009, Creating energy progress, paper presented at 100th Annual Conference, International District Energy Association.
- Delbes J., 1999, District Cooling Handbook, European Marketing Group District Heating and Cooling.
- Dielman T.E., 2005, Applied Regression Analysis, Brooks/Cole Thomson Learning, USA.
- Doty S., 2011, Energy saving measure interactions in chilled water system, Energy Engineering, 108(5): 7-36.
- Douglas J.F., 1985, Fluid Mechanics, Pitman Publishing, London.
- Durkin T.H., 2005, Evolving design of chiller plants, ASHRAE Journal, Feb: 28-34.
- Eaton, 2011, Adjustable Frequency Drives, Eaton, USA.
- Electrical and Mechanical Services Department (EMSD), 1999, Preliminary phase consultancy on wider use of water cooled air conditioning system in Hong Kong – Final report, Consultancy Report, Electrical and Mechanical Services Department, Hong Kong.
- Electrical and Mechanical Services Department (EMSD), 2000, Pilot scheme for wider use of fresh water evaporative cooling towers for energy-efficient air conditioning systems, Electrical and Mechanical Services Department, Hong Kong.
- Electrical and Mechanical Services Department (EMSD), 2002, Implementation of district cooling system at SEKD, Legislative Council Panel on Environmental Affairs, Hong Kong.
- Electrical and Mechanical Services Department (EMSD), 2003a, Implementation study for a district cooling at South East Kowloon development – Executive Summary, Consultancy Report, Hong Kong.
- Electrical and Mechanical Services Department (EMSD), 2003b, Territory-wide implementation study for water cooled air conditioning systems in Hong Kong – Executive Summary, Hong Kong.

- Electrical and Mechanical Services Department (EMSD), 2003c, Territory-wide implementation study for water cooled air conditioning systems in Hong Kong – Final Report, Hong Kong.
- Electrical and Mechanical Services Department (EMSD), 2004, Pilot scheme for wider use of fresh water in evaporative cooling towers for energy efficient air conditioning system – 2004 Achievement Summary, Hong Kong.
- Electrical and Mechanical Services Department (EMSD), 2005, Implementation study for water-cooled air conditioning systems at Wan Chai and Causeway Bay – Investigation: Executive Summary, Hong Kong
- Electrical and Mechanical Services Department (EMSD), 2012a, EMSD code of practice for energy efficiency of building services installation, Hong Kong.
- Electrical and Mechanical Services Department (EMSD), 2012b, Hong Kong energy end-use data, Hong Kong.
- Electrical and Mechanical Services Department (EMSD), 2012c, Technical guidelines for connection to district cooling system (Draft), Hong Kong.
- Electrical and Mechanical Services Department (EMSD), 2013, District cooling system, retrieved on 15 Nov 2013, from http://www.energyland.emsd.gov.hk/en/building/district_cooling_sys/dcs.html
- Energy Market Authority (EMA), 2002, Price regulation for district cooling services, consultation document, Energy Market Authority of Singapore, Singapore.
- Energy Market Authority (EMA), 2009, District cooling services supply code, Energy Market Authority of Singapore, Singapore
- Environment Bureau, 2013, PWP Item No. 45CG - District Cooling System at the Kai Tak Development, Legislative Council Panel on Environmental Affairs, Hong Kong.
- Evans M., 2006, Possibilities with More District Cooling in Europe, Euroheat & Power, Belgium.
- Field B.C. and Field M., 2009, Environmental Economics: An Introduction, McGraw-Hill International, New York.
- Fiorino D.P., 1999, Achieving high chilled-water delta Ts, ASHRAE Journal, 41(11):24-30.

- Friotherm A.G., 2013, High demand for district cooling and heating in Stockholm, Stockholm, Sweden, retrieved on 15 Nov 2013, from http://www.friotherm.com/webautor-data/41/nimrod_e009_uk.pdf
- Fuller S.K. and Petersen S.T., 1996, Life-cycle costing manual for the federal energy management program, 1995th edition, Washington DC: U.S. Department Energy.
- Gordon J.M., Ng K.C. and Chui H.T., 1995, Centrifugal chillers: Thermodynamic modelling and a diagnostic case study, *International Journal of Refrigeration*, 18(4):253-257.
- Hartman T., 2001, Getting real about low delta T in variable-flow distribution systems, *Heating/Piping/Air Conditioning Engineering*, 73(4):17.
- Helsinki Energy, 2006, Prospects for district cooling, retrieved from <http://www.helsinginenergia.fi>
- Ho P.Y., 2003, *Weathering the Storm: Hong Kong Observatory and Social Development*, Hong Kong University Press, Hong Kong.
- Hovde P.J. and Moser K., 2004, Performance Based Methods for Service Life Prediction, State of Art Reports, CIB.
- Hydeman M., Sreedharan P., Webb N. and Blanc S., 2002, Development and testing of a reformulated regression-based electric chiller model, *ASHRAE Transactions*, 108(2):1118-27.
- Hyman L.B. and Little D., 2004, Overcoming low delta T, negative delta P - at large university campus, *ASHRAE Journal*, 46(2):28-34.
- International Energy Agency (IEA), 2002, *Optimization of Cool Thermal Storage and Distribution*, International Energy Agency, Novem, Netherlands.
- Japan for Sustainability, 2009, A key to urban comfort and efficiency - Japan's district heating and cooling systems, Newsletter, June, No. 82.
- Kirsner W., 1996, The demise of the primary-secondary pumping paradigm for chilled water plant design, *Heating/Piping/Air Conditioning Engineering*, 68(11):73-78.
- Kirsner W., 1998, Rectifying the primary-secondary paradigm for chilled water plant design to deal with low ΔT central plant syndrome, *Heating/Piping/Air Conditioning Engineering*, 70(1):128-31.
- Kuretich K.M., 2010, Large-campus district cooling, *Heating/Piping/Air Conditioning Engineering*, 82(5):26-33.

- Lam K.K., 1997, Performance Evaluation of Chiller System, Master's Thesis, Department of Building Services Engineering, Hong Kong Polytechnic University.
- Landman W., 1996, Off-design chiller performance, Trane Engineers Newsletter, 25(5).
- Lebrun J., 1999, A Toolkit for Primary HVAC System Energy Calculations, ASHRAE, Atlanta.
- Lee W.L. and Lee S.H., 2007, Developing a simplified model for evaluating chiller-system configurations, Applied Energy, 84:290-306.
- Leung Y.K., Wu M.C., Yeung K.K. and Leung W.M. 2007, Temperature projections for Hong Kong based on IPCC fourth assessment report, Hong Kong Meteorological Society Bulletin, Volume 17, HKO Reprint No. 764.
- Lo A.C.W., Yik F.W.H and Jones P., 2006, Techno-economic assessment and optimization of district cooling system in a mega-city, paper presented at the 2nd Mega Cities International Conference 2006, Guangzhou.
- Lomas K.J., Eppel H., Martin C.J. and Bloomfield D.P., 1997, Empirical validation of building energy simulation programs, Energy and Buildings, 26:253-275.
- Luther K., 2002, Chilled water system forensics, ASHRAE Transactions, 108(1):654-8.
- Ma S.W.Y., Kueh C.S.W., Chiu G.W.L., Wild S.R. and Yip J.Y., 1998, Environmental management of coastal cooling water discharges in Hong Kong, Water Science and Technology, 38(8-9):267-274.
- Ma Z.J. and Wang S.W., 2011, Enhancing the performance of large primary-secondary chilled water systems by using bypass check valve, Energy, 36:268-276.
- Majid M. A.A., Gilani S.I. and Rangkuti C., 2008, Gas District Cooling in Malaysia: Pioneering a new industry, District Energy, International District Energy Association, 3rd Quarter: 14-18.
- Marchi A., Simpson A.R., and Ertugrul N., 2012, Assessing variable speed pump efficiency in water distribution systems, Drinking Water Engineering and Science, 5: 15-21.
- Masters G.M. and Ela W.P., 1998, Introduction to Environmental Engineering and Science, Prentice-Hall, USA.
- McQuay, 2002, Chiller Plant Design - Application Guide, McQuay International, Minesota, USA.

- McQuay International, 2001, Parallel-Chiller Plants, McQuay International, Minnesota, USA.
- Moe E.M., 2005a, Building performance with district cooling, ASHRAE Journal, July: 46-53.
- Moe E.M., 2005b, Applying pressure independent control to achieve high delta-T, International District Energy Association (IDEA) Annual Conference, Nashville, TN.
- Montgomery D.C. and Runger G.C., 2010, Applied Statistics and Probability for Engineers, John Wiley & Sons, New York.
- NCSS, 2013, NCSS manual, NCSS Statistical Software, USA, Chapter 311:1-9.
- Nuon, 2013, District cooling in Amsterdam's Zuidas, retrieved on 15 Nov 2013, from http://www.web-logix.nl/CreativeEnergy/content/visits/folder_Zuidas.pdf
- Onyiah L.C., 2009, Design and Analysis of Experiments, CRC Press, USA.
- PACO, 2014, PACO Pump Catalogue.
- Qureshi T. Q. and Tassou S.A., 1996, Variable-speed control in refrigeration systems, Applied Thermal Engineering, 16(2):103-113.
- Rabehl R.J., Mitchell J.W. and Beckman W.A., 1999, Parameter estimation and the use of catalog data in modeling heat exchangers and coils, HVAC&R Research, 5(1):3-17.
- Rishel J. B., 2000, 40 years of fiddling with pumps, ASHRAE Journal, 42(3):43-49.
- Rishel J. B., 2001, Wire-to-Water Efficiency of Pumping System, ASHRAE Journal, 43(4):40-46.
- Rishel J., Durkin, T and Kincaid B., 2006, HVAC Pump Handbook, Second Edition, McGraw Hill Company, Inc., USA
- Sat P.S.K. and Yik F.W.H., 2003, Comparison of predictions of the building energy simulation programs HTB2 and BECON with metered building energy data, HKIE Transactions, 10(3):34-47.
- Schwedler M. and Bradley B., 2000, An idea for chilled water plants whose time has come... Variable-Primary-Flow Systems, Heating/Piping/Air Conditioning Engineering, 72(4):41-44.

- Severini S.C., 2004, Making them work: Primary-secondary chilled water systems, *ASHRAE Journal*, 46(7):27-33.
- Shiu K. S., 2000, Implementation of gas district cooling and cogeneration in Malaysia, *International Gas Engineering and Management*, 40:93-100.
- Siemens, 2006, Pressure-independent control valves vs. high performance control valves, Technology Report (Document No. 149-990), Siemens Industry Inc.
- Ssegane H., Tollner E.W., Mohamoud Y.M., Rasmussen T.C., Dowd J.F., 2012, Advances in variable selection methods I: Causal selection methods versus stepwise regression and principal component analysis on data of known and unknown functional relationships, *Journal of Hydrology*, 438–439:16-25.
- Skagestad B. and Mildenstein P., 1999, District Heating and Cooling Connection Handbook, The International Energy Agency, Novem, Netherlands.
- Stoecker W.F., 1975, Procedures for Simulating the Performance of Components and Systems for Energy Calculations, ASHRAE, Atlanta, GA.
- Tam A., 2014, Air-conditioning the target of district-wide scheme to reduce energy use, *Hong Kong Engineer*, 42:8-13.
- Taylor Engineering, 2009, Chilled Water Plant Design Guide, Taylor Engineering, Alameda.
- Taylor S.T., 2002a, Degrading chilled water plant delta-T: Causes and mitigation, *ASHRAE Transaction*, 108(1):641-53.
- Taylor S.T., 2002b, Primary-only vs primary-secondary variable flow systems, *ASHRAE Journal*, 44(2):25-29.
- Taylor S.T., 2003, Control of variable primary flow chilled water systems, presented at ASHRAE Annual Meeting.
- Taylor S.T., 2011, Optimizing design and control of chilled water plants – Part 3: Pipe sizing and optimizing delta T, *ASHRAE Journal*, 53(12):22-34.
- Taylor S.T., 2012, Optimizing design and control of chilled water plants – Part 5: Optimized control sequences, *ASHRAE Journal*, 54(6):56-74.
- Tey P.K., 2010, District cooling as an energy and economically efficient urban utility – Its implementation at Marina Bay business district in Singapore, presented in an evening talk organised by IES Power & Energy Interest Group, on 30 June 2010.

- Trading Economics, 2013, Hong Kong Inflation Rate, retrieved on 15 Nov 2013, from <http://www.tradingeconomics.com/hong-kong/inflation-cpi>
- Trane, 1989, Chiller plant system performance, Engineers Newsletter, 18(2).
- Trane Hong Kong, 2013, Variable Primary Water Flow Systems.
- Underwood C.P. and Yik F.W.H, 2004, Modelling Methods for Energy in Buildings, Blackwell Publishing, USA.
- Wan K.S.Y., 1998, Comparison of Predicted Cooling Load and Plant Performance with Measured Data from an Existing Building, MEng Dissertation, Department of Building Services Engineering, Hong Kong Polytechnic University.
- Wang L.P., Haves P and Buhl F., 2012a, An improved simple chilled water cooling coil model, paper presented at the SimBuild 2012 IBPSA Conference, Environmental energy and Technologies Division, Ernest Orlando Lawrence Berkeley National Laboratory, Berkeley, CA.
- Wang L., Watt J. and Zhao J., 2012b, Model based building chilled water loop delta-T fault diagnosis, paper presented at the Twelfth International Conference for Enhanced Building Operation, Manchester, UK, October 23-26.
- Wang S.W., Ma Z.J. and Gao D.C., 2010, Performance enhancement of a complex chilled water system using a check valve: Experimental validation, Applied Thermal Engineering, 30(17-18):2827-32.
- Wang Y.W., Cai W.J., Soh Y.C., Li S.J., Lu L. and Xie L.H., 2004, A simplified modeling of cooling coils for control and optimization of HVAC systems, Energy Conversion and Management, 45:2915-2930.
- Wei Z. and Zmeureanu R., 2009, Energy analysis of variable air volume systems for an office building, Energy Conversion and Management, 50(2):387-392.
- Wikipedia, 2013, District cooling, retrieved on 15 November 2013, from http://en.wikipedia.org/wiki/District_cooling
- Wong W.L. and Ngan K.H., 1993, Selection of an example weather year for Hong Kong, Energy & Buildings, 19:313- 316.
- Wong F.Y.H. and Tang Y. T., 2010, Comparative life-cycle carbon footprint study of a proposed district cooling system and conventional HVAC Systems for Hong Kong's new urban developments, paper presented in the 16th Annual International Sustainable Development Research Conference.

- Wong K.W., 1997, Design of Chilled Water System for High Rise Buildings, MSc Dissertation, Department of Building Services Engineering, Hong Kong Polytechnic University.
- World Bank, 2013, Mapping Carbon Pricing Initiatives – Development and Prospects 2013, World Bank Institute, Washington DC.
- Wu Y. and Rosen M.A., 1999, Assessing and optimizing the economic and environmental impacts of cogeneration/district energy system using an energy equilibrium model, Applied Energy, 62:141-154.
- Wulfinghoff D.R., 2004, Energy Efficiency Manual, Energy Institute Press, Wheaton, Maryland, United States.
- Yang, Jinming and Lin Yi, 2012, Control algorithms and control strategies for primary flow chilled water systems, The 2nd International Conference on Computer Application and System Modelling, pp. 634-637.
- Yang K.H. and Ting M.M., 2000, An innovative analysis and experimental investigation on energy savings of a VAV system in hot and humid climates, Building and Environment, 35(1):27-31.
- Yates A., 2001, Quantifying the business benefits of sustainable buildings – Summary of existing research findings (extracts), draft for discussion, February 16, 2001, extracted from <http://www.usgbc.org>
- Yik F.W.H., 1996, BECON – A Building Energy Consumption Estimation Program, User Manual, Department of Building Services Engineering, The Hong Kong Polytechnic University, Hong Kong.
- Yik F.W.H., 1999, Selection of control valves for air conditioning systems, the Hong Kong Institution of Engineers Transactions, 6(2):11-18.
- Yik F.W.H., 2012, Building Energy Evaluation Program - User Manual for BEEP (v.1.0), Department of Building Services Engineering, Hong Kong Polytechnic University, Hong Kong.
- Yik F.W.H., Burnett J. and Prescott I., 2001a, A study on the energy performance of three schemes for widening application of water-cooled air-conditioning systems in Hong Kong, Energy and Buildings, 33:167-182.
- Yik F.W.H., Burnett J. and Prescott I., 2001b, Predicting air conditioning energy consumption of a group of building using different heat rejection methods, Energy and Buildings, 33:151-16.

- Yik F.W.H., Burnett J., Lee W. L. and Prescott I., 1999, Chiller plant sizing by cooling load simulation as a means to avoid oversized plant, *HKIE Transactions*, 6(2):19-25.
- Yik F.W.H., Lai J., Leung P.H.M. and Yuen P.L., 2012, A case study on the application of air- and water-cooled oil-free chillers to hospitals in Hong Kong, *Building Services Engineering Research & Technology*, 33(3):263-279.
- Yik F.W.H. and Lam V.K.C., 1998, Chiller models for plant design studies, *Building Services Engineering Research and Technology*, 19(4):233-241.
- Yu F.W., 2009, Environmental performance and economic analysis of all-variable speed chiller systems with load-based speed control, *Applied Thermal Engineering*, 29:1721-1729.
- Yu P.C.H., 2001, A study of Energy Use for Ventilation and Air-conditioning System in Hong Kong, PhD Thesis, Department of Building Services Engineering, Hong Kong Polytechnic University.
- Zhan X., Liang, X., Xu G. and Zhou L., 2013, Influence of plant root morphology and tissue composition on phenanthrene uptake: Stepwise multiple linear regression analysis, *Environmental Pollution*, 179:294-300.
- Zhang Z.Q., Li, H. and Liu, J.J., 2012, Simulations of chilled water cooling coil delta-T characteristic, *ASHRAE Transactions*, 118(2):349-356.